香港中文大學理學院
FACULTY OF SCIENCE
THE CHINESE UNIVERSITY OF HONG KONG

International Conference on

Earth, Energy & Environmental Sciences for Carbon Neutrality (ICE3SCN)

Conference Abstract

1 – 5 December 2023

The Chinese University of Hong Kong

Shatin, Hong Kong SAR

Content

2 December 2023 (Saturday) 3
Plenary Session (2 December) 4
Energy Conversion Session (2 December) 7
Earth and Energy Transition Session (2 December) 25
Environment Session (2 December) 33
3 December 2023 (Sunday) 47
Plenary Session (3 December) 48
Energy Conversion Session (3 December) 51
Earth and Energy Transition Session (3 December) 69
Environment Session (3 December) 81
4 December 2023 (Monday) 88
Plenary Session (4 December) 89
Energy Conversion Session (4 December) 91
Earth and Energy Transition Session (4 December) 100
Environment Session (4 December) 107
5 December 2023 (Tuesday) 115
Energy Conversion Session (5 December) 116
Poster Presentation 123
Energy Conversion Session 124
Earth and Energy Transition Session 150
Environment Session 162

International Conference on Earth, Energy & Environmental Sciences for Carbon Neutrality (ICE3SCN)

Conference Abstract

2 December 2023 (Saturday)

Plenary Session (2 December)

Plenary Lecture 1:

From Nanometer-Sized Molecular Photovoltaics to Meter-Sized Printable Organic and Perovskite Solar Cells for Clean Energy

Alex Kwan Yue JEN (CityU, Hong Kong)
[a]Department of Materials Science &Engineering, [b]Department of Chemistry
[c]Hong Kong Institute for Clean Energy, City University of Hong Kong, Hong Kong
E-mail: alexjen@cityu.edu.hk

Minimizing energy loss and increasing the field factor are key aspects to transcend the current limitations on the performance of organic photovoltaics (OPV). However, an inherent limit has set for an organic bulk-heterojunction (BHJ) blends from prominent non-geminate recombination through non-radiative charge transfer states. Our recent study on charge recombination in BHJ and Planar-Mixed Heterojunction (PMHJ) blends comprising a crystalline polymer donor with Se-containing Y6-derived non-fullerene acceptors has shown both high photovoltaic internal quantum efficiencies and high external electroluminescence quantum efficiencies. Crystallographic and spectroscopic studies reveal that the pseudo-2D, fused-ring molecular acceptors are not only intrinsically highly luminescent but also meets the criteria in achieving intrinsically radiative recombination within the blend, by promoting delocalized excitons with much longer luminescent lifetime and reduced exciton binding energies. These results provide the important demonstration of radiative non-geminate charge recombination in efficient OPV blends to achieve PCEs close to 20%. Moreover, a new “Dilution Effect” concept is introduced to explain the commonly observed composition-dependent V_{oc} and reduced photovoltage loss in highly efficient ternary-based devices due to significantly reduced phonon-electron coupling. At the end, several novel interface/additive engineering approaches will be discussed to demonstrate high PCE (~26%) could be achieved in inverted perovskite solar cells and very efficient lead-capturing from decomposed perovskite devices. Their applications in various clean energy generation fields will also be discussed.

1. Y. Zhou, L. Herz, A. K-Y. Jen, and M. Saliba, *Nature Energy*, 2022, *7*, 794.
2. Y. Liu, F. Lin, F. Liu, D. S. Ginger, H-Z. Chen, A. K-Y. Jen, *Nature Nanotech*, 2022, *17*, 53.
3. K. Jiang, J, Zhang, C. Zhong, F. Lin, F. Qi, Q. Li, Z. Peng, W. Kaminsky, S. H. Jang, J. Yu, X. Deng, H. Hu, D. Shen, F. Gao, H. Ade, M. Xiao, C. Zhang, and A. K-Y. Jen, *Nature Energy*, 2022, *7*, 1076.
4. F. Li, X. Deng, Z. Shi, S. Wu, Z. Zeng, D. Wang, Y. Li, F. Qi, Z. Zhang, Z. Yang, S-H. Jang, F. R. Lin, S-W. Tsang, X. K. Chen, and A. K.-Y. Jen, *Nature Photonics*, 2023, *17*, 478.
5. S. Wu, Z. Li, M-Q. Li, Y. Diao, F. Lin, J. Zhang, P. Tieu, W. Gao, F. Qi, X. Pan, Z. Xu, Z. Zhu, A. K.-Y. Jen, *Nature Nanotech,* 2020, *15*, 934.
6. B. Fan, W. Gao, X. Wu, X. Xia, Y. Wu, F. R. Lin, Q. Fan, X. Lu, W. J. Li, W. Ma, A. K.-Y. Jen, *Nature Commun,* 2022, 13, 5946.
7. B. Fan, W. Gao, R. Zhang, W. Kaminsky, F. R. Lin, X. Xia, Q. Fan, Y. Li, Y. An, Y. Wu, M. Liu, X. Lu, W. J. Li, H.-L. Yip, F. Gao, A. K.-Y. Jen, *J. Am. Chem. Soc.,* 2023, 145, 5909.
8. L. Bi, Q. Fu, Z. Zeng, Y. Wang, F. R. Lin, Y. Cheng, H.-L. Yip, S. W. Tsang, A. K.-Y. Jen, *J. Am. Chem. Soc.,* 2023, 145, 5920.

Plenary Lecture 2:

Evolving Connections Between Minerals and Enhanced Carbon Storage in Soils

Satish Myneni, Jianshu Duan, William Atkinson

Department of Geosciences, Princeton University, Princeton, NJ 08544, USA

E-mail: smyneni@princeton.edu

As vast reservoils of organic carbon, soils play an important role in the global C-cycle, land-atmophere interactions, and thus the atmospheric CO_2 levels. The magnitude of organic carbon retention and the chemical forms of organic carbon retained by soils vary with the abundance and types of soil minerals. However, soil mineralogy evolves with rock type, prolonged weathering under different climates and biogeochemical conditions, and accordingly modulates the soil organic carbon storage. These interactions also modulate nutrient cycling, water quality, and pollutant retention and transport. To understand the role of minerals on the magnitude and quality of organic carbon retained, we examined the reactions of dissolved organic carbon with a variety of minerals (Fe-, Al-oxides, kaolinite, smectite, calcite, silica) representative of different soil types,. Time-dependent reactions (minutes to 6 months) showed that some minerals (Fe/Al-oxides) adsorb different types of carbon more rapidly when compared to slow and prolonged sorption by both types of clay minerals. In addition to sorption, we observed the organic carbon breakdown in the presence of minerals, and these reactions are likely caused by the mineral surface catalysis and radical mediated reactions involving redox-sensitive iron associated with the natural organic carbon. These laboratory findings are comparable with oxide-dominated versus clay-dominated soils from the tropical and temperate climate regions (Alaska, California, New Jersey of USA; Costa Rica), suggesting the transferability of laboratory microcosm studies to understand the complex biogeochemical reactions occurring at field scale. Our molecular findings allows the evaluation of how the long-term and short-term climate changes influence the organic carbon storage and carbon-cycle in different soil types. These findings are also crucial in understanding the effectiveness of widely considered enhanced rock weathering in different soils and associated carbon storage, and selection of suitable soil systems for atmospheric-carbon drawdown. A summary of these studies will be presented.

Plenary Lecture 3:

Understanding Triggered Seismicity and Permeability Evolution in the Subsurface – Key Needs in Pursuit of the Energy Transition

Derek Elsworth[a]

[a] Energy and Mineral Engineering & Geosciences, G^3 Center and EMS Energy Institute, Pennsylvania State University, University Park, USA

.

E-mail: elsworth@psu.edu

Contemporary methods of energy conversion that reduce carbon intensity and address the energy transition draw heavily on fluids in the subsurface. This includes sequestering CO_2, fuel switching to lower-carbon sources, such as from abundant gas shales, recovering deep geothermal energy *via* EGS, and diurnal and inter-seasonal storage of heat, H_2 and energized fluids (CAES). In all of these endeavors, either maintaining the low permeability and integrity of caprocks or in controlling the growth of permeability in initially very-low-permeability shales or geothermal reservoirs represent key desires. Injected volumes are necessarily enormous, anticipated overpressures large and the potential for hazardous triggered seismicity significant. We explore conditions controlling the linked evolution of seismicity and permeability in particular with respect to the (i) scaling of seismicity, (ii) controls on permeability evolution and the (iii) potential to recover permeability evolution from physics-based models of microearthquakes linked to permeability evolution.

Energy Conversion Session (2 December)

Keynote Lecture

Defective Layered Double Hydroxide Based Nanostructured Photocatalysts

Tierui Zhang

Technical Institute of Physics and Chemistry, Chinese Academy of Sciences, Beijing 10190, China.

E-mail: tierui@mail.ipc.ac.cn

On a double carbon background, photocatalysis is regarded as one of the effective means to solve the energy and environmental problems in the future. Developing low-cost and efficient photocatalysts is very critical for their practical applications. Layered double hydroxide (LDH) based nanostructured materials have been considered as very promising photocatalysts for chemical fuels and products. Recently, a series of LDH-based nanostructured photocatalysts have been designed and synthesized in my group for efficient CO_2 and N_2 reduction into high value-added heavy hydrocarbons, light olefins and ammonia, respectively, by introducing oxygen vacancies to activate reactants and intermediate species.[1-10]

References

[1] Zhang T, et al. *Adv. Mater.,* 2022, *34*, 2207793;

[2] Zhang T, et al. *Angew. Chem. Int. Ed.,* 2022, *61*, e202211469;

[3] Zhang T, et al. *Angew. Chem. Int. Ed.,* 2021, *60*, 21896;

[4] Zhang T, et al. *Angew. Chem. Int. Ed.,* 2021, *60*, 2554;

[5] Zhang T, et al. *Adv. Energy Mater.,* 2020, *10*, 2002199;

[6] Zhang T, et al. *Chem. Soc. Rev.,* 2019, *48*, 1375;

[7] Zhang T, et al. *Adv. Mater.,* 2019, *31*, 1806482;

[8] Zhang T, et al. *Adv. Mater.,* 2018, *30*, 1800527;

[9] Zhang T, et al. *Adv. Mater.,* 2018, *30*, 1704663;

[10] Zhang T, et al. *Adv. Mater.,* 2018, *30*, 1803127.

Keynote Lecture

Ferroelectric photocatalysts for overall water splitting

Gang Liu[a,b]

[a] Shenyang National Laboratory for Materials Science, Institute of Metal Research, Chinese Academy of Sciences, 72 Wenhua Road, Shenyang 110016, China.; [b] School of Materials Science and Engineering, University of Science and Technology of China, 72 Wenhua Road, Shenyang 110016, China.

E-mail: gangliu@imr.ac.cn

Ferroelectric materials hold great promise in the field of photocatalytic water splitting due to their spontaneous polarization that sets up an inherent internal field for the spatial separation of photogenerated charges. The ferroelectric polarization, however, is generally accompanied by some intrinsic defects, particularly oxygen vacancies, whose impact upon photocatalysis is far from being fully understood and modulated. Here, we have studied the role of oxygen vacancies over the photocatalytic behavior of single-domain $PbTiO_3$ through a combination of theoretical and experimental viewpoints. Our results indicate that the oxygen vacancies in the negatively polarized facet (001) are active sites for water oxidation into O_2, while the defect-free sites prefer H_2O_2 as the oxidation product. The apparent quantum yield at 435 nm for photocatalytic overall water splitting with $PbTiO_3$/Rh/Cr_2O_3 is determined to be 0.025%, which is remarkable for single undoped metal oxide-based photocatalysts. Furthermore, the strong correlation among oxygen vacancies, polarization strength, and photocatalytic activity is properly reflected by charge separation conditions in the single-domain $PbTiO_3$. Aurivillius-type compounds ($(Bi_2O_2)^{2+}(A_{n-1}B_nO_{3n+1})^{2-}$) with alternately stacked layers of bismuth oxide $(Bi_2O_2)^{2+}$ and perovskite $(A_{n-1}B_nO_{3n+1})^{2-}$ are promising photocatalysts for overall water splitting due to their suitable band structures and adjustable layered characteristics. Here, using Bi_3TiNbO_9 as a model photocatalyst, its surface termination was modulated by acid etching, which well suppressed the self-corrosion phenomenon. A combination of comprehensive experimental investigations together with theoretical calculations reveals the transition of material surface from the self-reduction sensitive $(Bi_2O_2)^{2+}$ layer to the robust $(BiTiNbO_7)^{2-}$ perovskite layer, enabling the efficient transfer of photogenerated electrons to the cocatalyst for greatly enhanced stable overall water splitting.

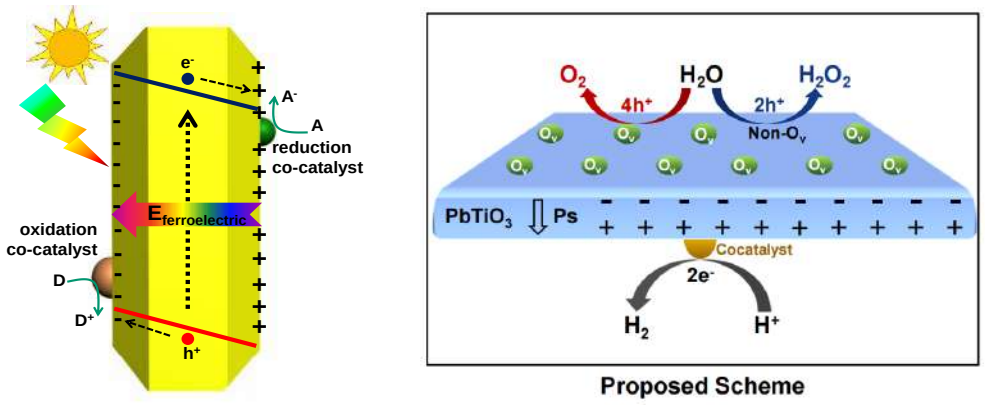

Proposed Scheme

References

[1] Huang J, Liu G, et al. *Nat. Commun.*, 2023, *accepted.*

[2] Huang J, Liu G, et al. *Adv. Sci.*, 2023, 2302206.

[3] C Zhen, Liu G, et al. *Acc. Mater. Res.* 2023, 591.

[4] Wan GD, Liu G, et al. *J. Am. Chem. Soc.*, 2022, 20342.

[5] Kang YY, Liu G, et al. *Joule*, 2022,1876.

Keynote Lecture

Efficient perovskite solar cells and light-emitting diodes

Jingbi You

Institute of Semiconductors, Chinese Academy of Sciences, Beijing, China

E-mail: *jyou@semi.ac.cn*

Halide perovskite materials own excellent semiconductor properties, which showed great potential in photovoltaic and emission display. In this talk, I will summarize our recent work in perovskite solar cells (PSCs) and light-emitting didoes (PeLEDs). 1). By charge transport layer and perovskite composition engineering, for the bandgap around 1.5 electron volt, we have achieved close to 25 percent efficiency with the FF around 85 percent of organic-inorganic PSCs; 2). By surface re-construction, we have pushed the PCE of inorganic perovskite CsPbI3 based solar cells to 20 percent efficiency; 3). According to several strategies, such as non-radiative recombination suppression, band structure modulation and charge injection balance, we have achieved over than 25 and 16 percent external quantum efficiency electroluminescence in red and blue region, respectively.

References

[1] Zhao Yet al., Science, 2022, 377, 531

[2] Chu XB et al., Nature Energy, 2023, 8, 372

[3] Chu Z et al., Nature Electronics, 2023, 6, 360

Invited Talk

Strategies for improving the performance of Sn-based perovskite solar cells

Feng YAN,[a]

[a] *Department of Applied Physics, The Hong Kong Polytechnic University, Hong Kong.*

E-mail: apafyan@polyu.edu.hk

Tin-based perovskites are promising candidate materials for efficient lead-free perovskite solar cells (PSCs) due to their excellent optoelectronic properties and suitable bandgaps. However, it is challenging to prepare highly stable and efficient tin-based PSCs because Sn^{2+} in perovskites can be easily oxidized to Sn^{4+} upon air exposure. Many effective approaches have been developed to improve the device performance and a power conversion efficiency of over 14% has been achieved. In this talk, I will introduce the fabrication of air-stable $FASnI_3$ PSCs by adding hydroxybenzene sulfonic acid or gallic acid as antioxidant agents into the perovskite precursor solution along with excess $SnCl_2$. The interaction between the additives and $SnCl_2$ promote their homogenous dispersion in the perovskite film. Moreover, the strong antioxidant capacity of the additives enables enhanced oxidation stability of $FASnI_3$. The corresponding PSCs can maintain 80% of the efficiency over 1000 h upon air exposure without encapsulation, which is over ten times longer than the best result reported before. Our results suggest a novel strategy for the design of efficient and stable tin-based PSCs.

References

1. J. Cao, H-L Loi, Y. Xu, X. Guo, N. Wang, C-K Liu, T. Wang, H. Cheng, Y. Zhu, M. Li, W. Wong, F. Yan, Adv. Mater. 34 (6), 2107729 (2022).
2. J. Cao, C. Liu, V. Piradi, H. Loi, T. Wang, H. Cheng, X. Zhu, F. Yan, ACS Energy Lett. 7, 3362-3369 (2022).
3. T. Wang, H. Loi, J. Cao, Z. Qin, Z. Guan, Y. Xu, H. Cheng, M. Li, C. Lee, X. Lu, F. Yan, Adv. Sci. 9, 2200242 (2022).
4. J. Cao, F. Yan, Energy & Environ. Sci. 14 (3), 1286-1325, (2021).
5. T. Wang, F. Zheng, G. Tang, J. Cao, P. You, J. Zhao, F. Yan, Adv. Sci., 2004315, (2021).
6. T Wang, Q. Tai, X. Guo, J. Cao, C. Liu, N. Wang, D. Shen, Y. Zhu, C. Lee, F. Yan, ACS Energy Lett. 5, 1741-1749 (2020).
7. Q. Tai, X. Guo, G. Tang, P. You, T. Ng, D. Shen, J. Cao, C. Liu, N. Wang, Y. Zhu, C. Lee, F. Yan, Angew. Chem.-Int. Edit. 58, 806-810 (2019).

Invited Talk

From UV to Near-Infrared light detection: next generation photodetectors for imaging and biometric applications

Nicola Gasparini

Department of Chemistry and Centre for Processable Electronics, Imperial College London, W120BZ, UK. n.gasparini@imperial.ac.uk

The current success of organic semiconductor technology is mainly driven by the development of organic light-emitting diodes (OLED), which are now routinely employed in display technologies. In the last decade, however, organic photovoltaics (OPV), leveraging the impressive improvement in device efficiency and stability, have gradually moved from a lab curiosity to a niche market. Their recent success has coincided with the rapid development of effective replacements for the fullerene-based materials that have been prevalent as electron acceptor materials until recently; namely the small molecule nonfullerene acceptors (NFAs). This relatively new class of materials offer a number of opportunities to develop new areas of research. Between those, organic photodetector (OPD), a technology based on organic photodiodes and thus closely related to OPV, is one of the most exciting. Recent efforts in the field of OPD have been focused on extending broadband detection into the near-infrared (NIR) region. The early absorption cut-off of solution processed organic semiconductors presents a challenge in achieving NIR detection, however, careful tuning of their chemical structures can help extend OPD responsivity into the infrared window. Here, we discuss how to design donor:acceptor blends and control charge carrier recombination in organic photodetectors for NIR light-to-current conversion for high efficiency and stable devices.

References

[1] Liang W, Xu H, Carraro F, et al. *J. Am. Chem. Soc*., 2020, *In Press*;

[2] Konkankit CC, Lovett J, Harris HH and Wilson JJ. *Chem. Commun.*, 2020, *56*, 6515-6518.

Invited Talk

Stable and efficient perovskite optoelectronic devices

Huanping Zhou

School of Materials Science and Engineering, Peking University, 100871

Recently, metal halide perovskites (ABX_3) emerge as promising materials for various applications, especially photovoltaics. However, the complex chemical landscape with respect to composition and phase in perovskites made it challenging to obtain efficient and stable devices simultaneously. Here, we show that the growth of halide perovskite can be substantially regulated by anion-π interaction with halide in AX component, which is independently conducted but works well together with BX_2 regulation, leads to dual-site regulation. The resultant $FAPbI_3$ films exhibit less defects, red-shifted absorption, and high phase purity without detectable nanoscale δ-phase. Consequently, we achieved the perovskite solar cells with power conversion efficiency (PCE) up to 26.07% for 0.08 cm^2 device (25.8% certified) and 24.63% for 1 cm^2 device. In terms of device stability, we developed methods such as "redox shuttle" and "multiple non-covalent bond synergistic effects", supramolecular bifunctional layers to inhibit perovskite ion migration and/or promote defect healing. The resulting device also kept 99% of its initial PCE after maximum power point (MPP) tracking for over 1000 h under AM 1.5G sunlight at 85 °C. Additionally, these findings and methodologies may be extended to other solution-processed compound materials and devices with soft lattice.

Invited Talk

Reducing the non-radiative charge recombination for high-performance organic solar cells with multi-functionalities

Lijian Zuo,[a]

[a] *Department of Polymer Science and Engineering, Zhejiang University, Hangzhou, China*

E-mail: zjuzlj@zju.edu.cn

Organic solar cells (OSCs) show promise as the next-generation renewable energy souce for sustainability and carbon neutrality of the world, due to their merits of low-cost, good flexibility, light weight, etc. The recent years has witnessed significant progress in OSCs, which shows a record efficiency over 20%. Nevertheless, further improving the device performance is still in need, and currently, the severe non-radiative charge recombination becomes the most important obstacle for further improving the device performance of OSCs. To resolve this issue, we identify that a third component with suitable physical and optoelectronic properties can significantly reduce the non-radiative charge recombination via suppressing the electron-vibration coupling, which we terms it as the "dilution effect".1 Following this, we have developed more diverse and efficient third compoents and successive make breakthroughs in the world-record certified effiency, which has greatly stimulated the progress of OSCs. Moreover, conforming to the potential and intrinsic merits of OPVs, we have developed high-performance OPV with multi-functionalities, e.g. semi-transparencey, supeir flexibility, good strechability, etc. These results should pave the way toward the commercialization of OSCs.

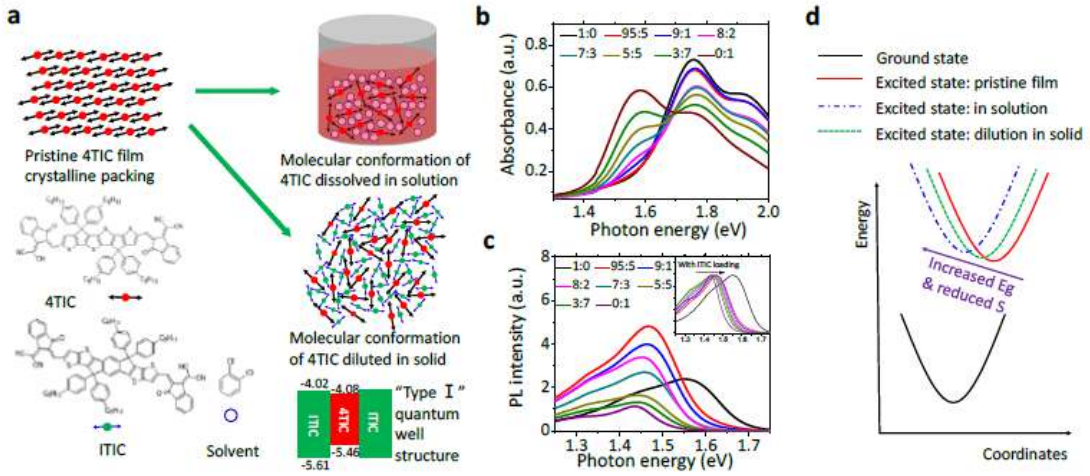

Figure 1. Schematic of dilution effect and optoelectronic properties light emitting species (4TIC) and diluent molecule (ITIC). a) schematic diagram of dilution effect, energy level diagrams (unit: eV), molecular structures of ITIC and 4TIC, dilution with solvent or solid, b) absorption spectra showing slight blue shifting upon blending, c) PL spectra of ITIC:4TIC blend with weight ratio 100:0, 95:5, 90:10, 80:20, 70:30, 50:50, 30:70, 0:100, inset shows the normalized PL spectra showing blue shifting upon blending. d) Frank-Condon schematic diagram of reduced S and increased band gap with dilution effect.

References

[1] Zuo L, Jo S, Li Y, Meng Y, et al. *Nat. Nanotechnol.*, 2022, *17*, 53–60.

Invited Talk

Heterogeneity in perovskite solar cells

Chen, Qi

School of Materials Science & Engineering,

Beijing Institute of Technology, Beijing 100081, China

The mixed halide perovskites have emerged as efficient light absorbers to construct perovskite solar cells which continually break the power conversion efficiency (PCE) records recently. Due to the unique compositional tunability, it reveals inhomogeneity in polycrystalline films, which often results in element/phase segregation in mixed cation/anion perovskites absorbers to hamper the efficiency and lifetime of corresponding devices. In this talk, we first investigate the evolution of residual strain over the mixed perovskite films by using the depth-dependent grazing incident X-ray diffraction measurement. We identify the gradient distribution of in-plane strain component perpendicular to the substrate. Moreover. we report a liquid medium annealing (LMA) technology which creates a robust micro-environment during film fabrication to allow fast bi-directional heat transfer. It leads to the films with higher crystallinity, lower defects concentration, ideal stoichiometric structure, and spatial homogeneity in composition/chemical environment. Resultant devices (PSC) yield a stabilized power conversion efficiency (PCE) of 25.3% (certified). It also maintains 95% of their initial PCE after 2000 h stabilized power output (SPO) tracking, showing the feasibility for scalable fabrication. Moreover, this strategy is also feasible for wide-band-gap perovskite absorbers, which leads to the perovskite/silicon tandem solar cells with certified PCE of 32.2% and improved stability.

Oral Presentation

Revealing and Regulating Crystallization Pathways for Efficient and Stable All-Inorganic Perovskite Solar Cells

Xiao Wu,[a] Xinhui Lu[a]

[a] *Department of Physics, The Chinese University of Hong Kong, Shatin, 999077, Hong Kong, China;*

E-mail: xiaowu@cuhk.edu.hk; xinhui.lu@cuhk.edu.hk

Halide perovskite solar cells (PSCs) have demonstrated remarkable photovoltaic properties, achieving a record efficiency of 26.1%. However, the inclusion of volatile organic cations like methylammonium and formamidinium in high-performance PSCs limits their applicability under intense thermal stress. To address this issue, all-inorganic perovskites with inorganic cationic (Cs^+) have been developed in recent years. Nonetheless, the relatively smaller size of Cs^+ imposes inherent phase instability, with the photo-inactive orthorhombic δ-phase being more stable than the desired photoactive black perovskite phases at lower temperatures. Therefore, fabricating high-quality all-inorganic perovskite films remains a grand challenge, demanding precise control over the thermal annealing process. In this presentation, I will discuss our recent findings on understanding and controlling the crystallization pathways of all-inorganic perovskites to fabricate uniform and defect-tolerant films with reduced lattice strain. We have uncovered a black γ-phase at low temperature (LT-γ-phase) that was temporarily stabilized by the presence of residue dimethyl sulfoxide (DMSO) solvent. Upon evaporating DMSO, the LT-γ-phase transformed into the unwanted δ-phase, only to be restored to γ-phase under high-temperature annealing (HT-γ-phase). Intriguingly, through additional methylammonium chloride (MACl) treatment, we have managed to regulate the crystallization pathways with a direct phase transition from the LT-γ-phase to the HT-γ-phase, bypassing the δ-phase. As a result, we have improved the efficiency to 20.1% and enhanced device stability under illumination and humidity conditions.

References

[1] Wu X, Wang SY, Zhu JY, Lu XH et al. *Nano Energy*, 2023, 117, 108907.

Keynote Lecture

Development of high performance and durable fuel cell electrocatalysts

Minhua Shao, Fei Xiao

Department of Chemical and Biological Engineering, Energy Institute, The Hong Kong University of Science and Technology, Clear Water Bay, Kowloon, Hong Kong, P.R. China

E-mail: kemshao@ust.hk

Low temperature fuel cells are electrochemical devices that convert chemical energy directly to electricity. They have great potential for both stationary and transportation applications and are expected to help address the energy and environmental problems that have become prevalent in our society. Despite their great promise, commercialization has been hindered by lower than predicted efficiencies and high loading of Pt-based electrocatalysts in the electrodes. For more than five decades, extensive work has being focused on the development of novel electrocatalysts for fuel cell reactions. In this talk, I will present recent progress in developing advanced electrocatalysts and their fuel cell performance in my group, with an emphasis on core-shell and non-previous metal materials.

Keynote Lecture

High-performance Organic Thermoelectric Materials and Devices

Chong-an Di

Beijing National Laboratory for Molecular Sciences, CAS Key Laboratory of Organic Solids, Institute of Chemistry, Chinese Academy of Sciences, China

E-mail: dicha@iccas.ac.cn

Organic semiconductors have gained significant attention as potential thermoelectric materials due to their inherently low thermal conductivity and the potential for low-cost production through low-temperature processing methods[1-3]. In the field of organic thermoelectrics (OTEs), substantial progress has been made in both material development and device fabrication. However, there are still significant challenges that need to be overcome in terms of designing rational molecular structures and precisely tuning molecular doping. In this presentation, we show our recent progress on the molecular assembly of organic semiconductors and the device fabrication for TE applications. These studies have enabled us to effectively screen and identify promising OTE materials, as well as construct photothermoelectric devices. Furthermore, we have achieved a figure of merit of up to 0.4 by manipulating the molecular orientation of the materials[4-6]. Finally, we will showcase the promising applications of OTE materials in self-powered sensing, Peltier cooling, and wearable electronic power generators. In summary, we highlight the potential of organic semiconductors in OTE fields and provides insights into the molecular design and device fabrication strategies to unlock their true benefits.

References

[1] Pijper, D.; Jongejan, M. G. M.; Meetsma, A.; Feringa, B. L. *J. Am. Chem. Soc.* 2008, *130*, 4541.
[2] Di, C. A.; Shen, H. G.; Zhang, F. J.; Zhu, D. B. *Acc. Chem. Res.* 2019, *52*, 1113.

[3] Wang, D. Y.; Liu, L. Y.; Gao, X. K.; Di, C. A.; Zhu, D. B. *CCS Chem*. 2021, *3*, 2212.

[4] Zhao, Y.; Liu, L.; Zhang, F.; Di, C. A; Zhu, D. *SmartMat* 2021, *2*, 426.

[5] Wang, D. Y.; Ding, J. M.; Dai, X. J.; Xiang, L.; Ye, D. K.; He, Z. H.; Zhang, F. J.; Jung, S. H.; Lee, J. K.; Di, C. A.; Zhu, D. B. *Adv. Mater. 2023*, *35*, e2208215.

[6] Zhu, D. B. *Organic Thermoelectrics*, WILEY-VCH: 2022.

Invited Talk

Electrochemical CO_2 reduction to liquid products

Sheng Zhang, Siyu Kuang, Jianlong Lin, Hai Liu, Tianxiang Yan, Xinbin Ma

School of Chemical Engineering and Technology, Tianjin University, Tianjin 300072, China.

E-mail: sheng.zhang@tju.edu.cn

Electrochemical CO_2 reduction is a promising strategy to store renewable electrical energy in the chemical bonds of carbon fuels. Currently, high performance has been reported for C1 products, like CO and formate, which are selectively produced by a number of catalysts through $2e^-/2H^+$ steps. Due to shared reaction pathways, ethanol is always produced competitively with ethylene. Copper is distinctive in electro-catalyzing reduction of CO_2 into various energy-dense forms, but it often suffers from limited product selectivity including ethanol in competition with ethylene. Here, we describe systematically designed, bimetallic electrocatalysts based on copper/gold heterojunctions with a faradaic efficiency toward ethanol of 60% at currents in excess of 500 mA cm^{-2}. In the modified catalyst, the ratio of ethanol to ethylene is enhanced by a factor of 200 compared to copper catalysts. Analysis by ATR-IR measurements under operating conditions, and by computational simulations, suggests that reduction of CO_2 at the copper/gold heterojunction is dominated by generation of the intermediate OCCOH*. The latter is a key contributor in the overall, asymmetrical electro-hydrogenation of CO_2 giving ethanol rather than ethylene.

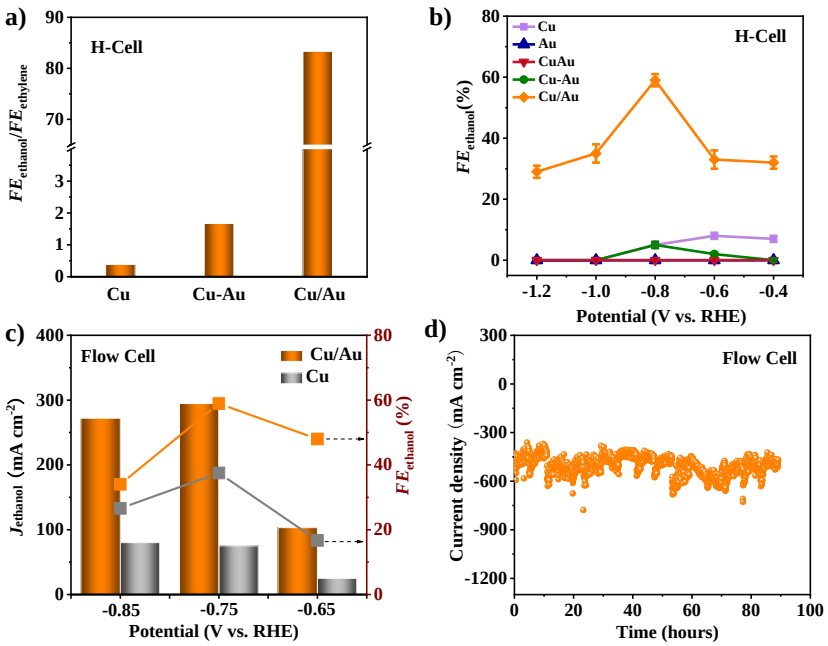

References

[1] Tianxiang Yan, Xiaoyi Chen, Sheng Zhang, et al. *Chemical Reviews*, 2023, *123*, 10530;

[2] Siyu Kuang, Yaqiong Su, Sheng Zhang, et al. *Proc. Natl. Acad. Sci.*, 2023, 120, *e2214175120*;

[3] Siyu Kuang, Minglu Li, Sheng Zhang, et al. *Chin Chem Lett.*, 2023, *34*, 108013.

Invited Talk

Tuning the Composition and Photophysical Properties of Silicon Quantum Dots

Zhenyu (Kevin) Yang

[a] *School of Chemistry, Sun Yat-sen University, Guangdong, China.*

E-mail: yangzhy63@mail.sysu.edu.cn

Nanostructured silicon, a widely utilized semiconductor, has garnered substantial attention owing to its natural abundance, optimal band gap for light absorption, adaptable photoluminescence, and excellent biocompatibility over the last few decades. Despite significant strides in refining synthetic approaches, surface modifications, and device applications, several pivotal inquiries persist in the realm of silicon research. Our research team has delved into comprehending the foundational aspects of silicon quantum dots (SiQDs), investigating their covalent atomic framework, surface bonding, and photophysical attributes. This presentation showcases our recent studies about the methods to tailor the compositions[1] and the photophysical properties[2,3] of SiQDs. The corresponding prototype applications of these materials, such as bioimaging, and photocatalytic reactions, will also be discussed.

References

[1] Chen H, Xiong Y, Li J, et al. *Nat. Commun.*, 2023, *14*, 1719;

[2] Chen H, Xu J, Wang Y,et al. *ACS Nano*, 2022, *16*, 15450-15459.

[3] Lai M, Zhang Y, Zhao L, et al. *Angew. Chem. Int. Ed.*, 2023, *62*, e202304056.

Oral Presentation

Layer Modulation of Aurivillius Compounds for Stable Photocatalytic Overall Water Splitting

Jie Huang, GangLiu*

Shenyang National Laboratory for Materials Science, Institute of Metal Research, Chinese Academy of Sciences, 72 Wenhua Road, Shenyang 110016, China.

E-mail: jhuang17s@imr.ac.cn

Photocatalytic overall water splitting for hydrogen production is one of the most effective ways to achieve carbon peak and carbon neutrality. However, traditional semiconductor materials face the challenges in simultaneously achieving a wide spectral response range and high photogenerated carrier separation efficiency, which limits the practical application of photocatalytic technology. Bi_3TiNbO_9, as a representative of Aurivillius compounds, possesses a flexible crystal structure and chemical composition. Rational modulation of its optical absorption properties, charge separation characteristics, and surface catalytic activity can be achieved based on band structure and crystal structure control, leading to high efficiency photocatalytic activity. As a result, it has attracted widespread attention and research. While numerous photocatalytic materials in this series have been utilized for hydrogen or oxygen production through strategies such as composition substitution and layer control, little attention has been paid to the stability of the materials in the overall water splitting process.

We found that when the surface of the material terminates with a $(Bi_2O_2)^{2+}$ layer (Bi_3TiNbO_9-BL, Figure 1a, c), the photogenerated electrons easily reduce the Bi^{3+} ions on the material surface, forming inactive metallic Bi sites. This results in the formation of carrier quenching centers and leads to the shedding of the cocatalyst, which greatly impair the water-splitting process and induce further self-reduction. However, when the surface of the material is transformed into a $(BiTiNbO_7)^{2-}$ layer termination (Bi_3TiNbO_9-PL, Figure 1b, d), the photoactive perovskite layer is directly in contact with the cocatalyst, increasing the charge transfer efficiency and the anchoring strength of the cocatalyst. This transformation significantly enhances the activity and stability of photocatalytic overall water splitting. In addition, this phenomenon is universal in other Aurivillius compounds, such as $SrBi_2Nb_2O_9$, $Bi_4Ti_3O_{12}$, and $SrBi_4Ti_4O_{15}$, all of which exhibit that compounds with perovskite layer termination have more stable photocatalytic water splitting activity[1].

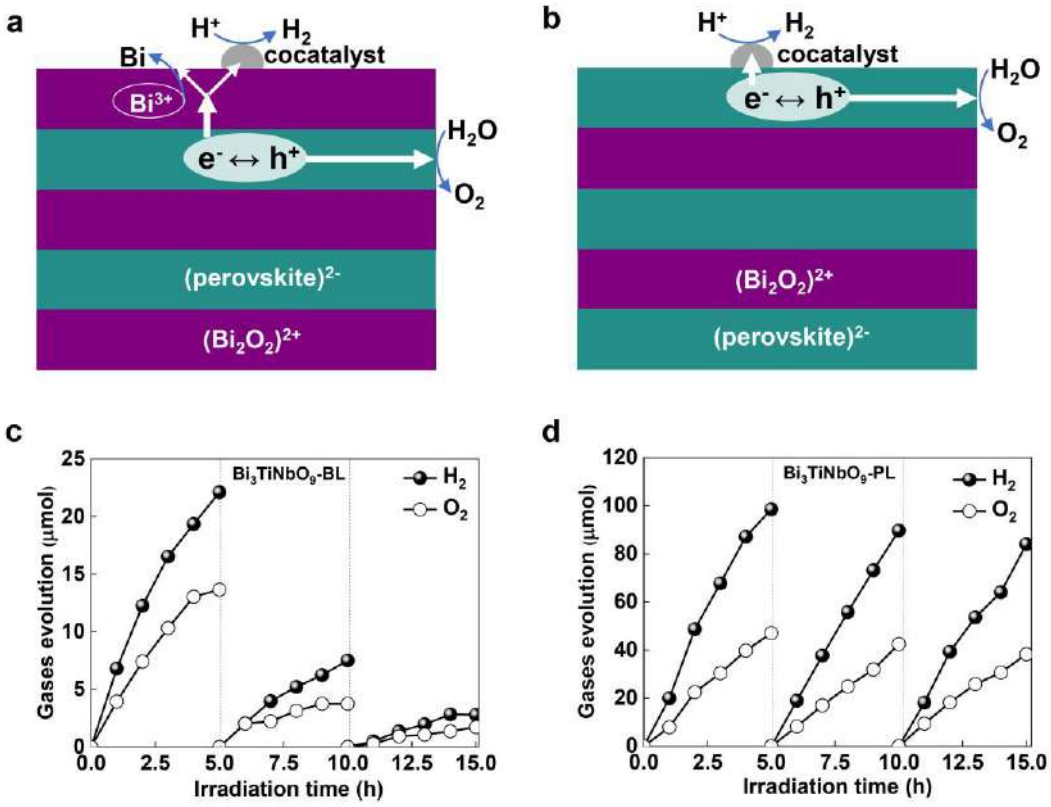

Figure 1. Schematic for photocatalytic water splitting processes over cocatalyst modified Bi_3TiNbO_9 with surface termination: a) $(Bi_2O_2)^{2+}$ layer (Bi_3TiNbO_9-BL) and b) $(BiTiNbO_7)^{2-}$ layer (Bi_3TiNbO_9-PL). Time courses of photocatalytic overall water splitting over c) Bi_3TiNbO_9-BL and d) Bi_3TiNbO_9-PL.

References

[1]Huang J, Kang Y, Liu J, et al. Adv. Sci., 2023, 10 (23), 2302206.

Oral Presentation

Semiconductor patterns steer directional charge transfer toward overall water splitting

Chao Zhen,[a,b] Gang Liu [a,b]

[a] *Shenyang National Laboratory for Materials Science, Institute of Metal Research, Chinese Academy of Sciences, Shenyang, China;* [b]*School of Materials Science and Engineering, University of Science and Technology of China (USTC), Shenyang, China.*

E-mail: czhen@imr.ac.cn

Medium mediated Z scheme charge transfer spikes a surge of solar driven water splitting systems by mimicking the nature photosynthesis process for efficient solar-to-hydrogen production. However, random distribution and contact of photoactive materials cause the conventional charge transfer competition in these systems. An inspiration from semiconductor integrated chips orderly assembled by the micro- and nanofabrication techniques for regulating charge transport signals towards artificial intelligence, we proposed a proof-of-concept for adopting the similar techniques to pattern semiconductor photocatalysts on a conductive substrate with well-modulated interfaces for the fabrication of artificial leaves towards water splitting. Specifically, we integrated parallel microstrips of n-type semiconductor and p-type semiconductor alternatively on the fluorine doped tine oxide (FTO) substrate with a tunable interspace, and then covered an atomic layer deposited TiO_2 film on top as an electron collection layer to selectively collect electrons from the p-type semiconductor and protect it from corrosion. The prolonged photoluminescent (PL) lifetimes, equivalent opposite surface photovoltage (SPV) signals, and selective depositions of oxidation and reduction products are observed on neighboring n-type semiconductor and p-type semiconductor strips, confirming the peculiar photocatalyst patterns steer directional Z-scheme transfer between neighboring semiconductor strips through the bottom FTO substrate. As a consequence, the patterned panel demonstrates the ability to split pure water into hydrogen and oxygen stoichiometrically under light irradiation after selectively decorating Pt co-catalyst on TiO_2 protected p-type semiconductor microstrips.

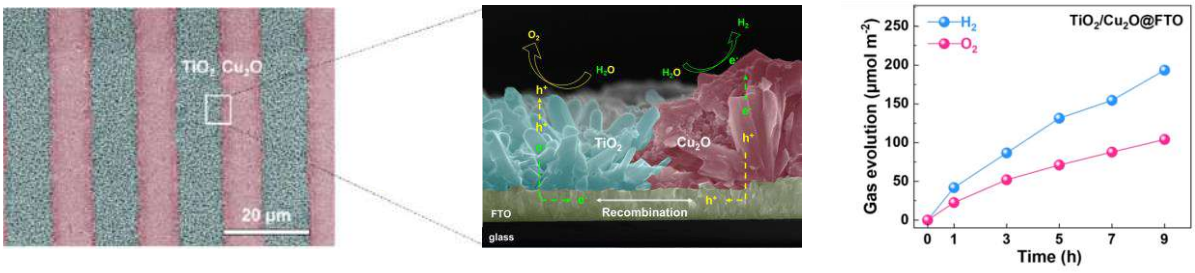

The patterned photocatalyst film with a directional charge transfer for solar driven overall water splitting

References

[1] Zhu HL, Zhen C, Liu G, et al. *Sci. Bull.* 2022, *67*, 2420–2427;

[2] Zhen C, Zhu HL, Liu G, et al. *in preparation*.

Earth and Energy Transition Session (2 December)

Keynote Lecture

The SEG and a changing world

Arthur Cheng

[a] *Earth Enviromental Sciences Programme, The Chinese University of Hong Kong, Shatin, Hong Kong.*

E-mail: arthurcheng@cuhk.edu.hk

This past September I took office as the President of the Society of Exploration Geophysicists, the primary professional organization for applied geophysicists. The SEG in the past has been viewed as an organization of geophysicists practicing mainly in the exploration of oil and gas, and to a less extent, minerals. However, we are much more than than. Over the past years, the world has changed, the environment has changed, and the SEG, like other professional socieites, has changed with it. In this talk, I will present SEG vision for the future geophysicists. It focuses on the three main stake holders: the members, the technology, and the society. We need to recruit more young geophysicists, our membership demographic tends way towards the older end of the spectrum. We need to offer more for the younger members and prospective members. On the technology front, the energy field is changing. Some of the more current research topics are carbon dioxide sequestration, hydrogen storage, aquifer monitoring, geothermal, near surface characterization, wind farm, and mineral exploration. SEG is a global society, over 60 percent of our members are located outside North America, however, our one main annual meeting has always been in North America. We intend to reach out more directly to our global members, especially in China given the interest in geophysics here, to conduct more events so that the global members can attend more easily. We also are, like CUHK, supporters of UN's 17 Sustainable Development Goals, and we plan our programs to specifically address a number of them. I will discuss some specific programs we have planned towards these objectives.

Keynote Lecture

Low-cost early-stage investigation of geothermal energy potential via seismic analysis: A case study in Singapore

Ping Tong,[a] Shojie Hao,[a] Yiming Bai[a]

[a] *School of Physical and Mathematical Sciences, Nanyang Technological University, Singapore.*

E-mail: tongping@ntu.edu.sg

The presence of the Sembawang hot spring in northern Singapore and recent findings of elevated underground temperatures during deep drilling have indicated a promising geothermal energy potential in this energy demanding country. In April 2022, the Energy Market Authority of Singapore initiated a Request for Information to assess the viability of geothermal energy throughout the country via geophysical investigations. However, Singapore has not previously undergone systematical geophysical investigation.

We have developed a comprehensive set of mathematical inversion and imaging methods that offer valuable insights into the intricate seismic structures beneath potential geothermal sites [1, 2, 3]. These methods involve joint inversion of various passive seismic observables with complementary sensitivities, enabling the detection and characterization of shear wave velocity and seismic anisotropy within the upper 10 km of the Earth's crust. Our team gathered high- quality data by deploying a dense, portable nodal seismic array near the Sembawang hot spring. The resultant subsurface images provide a detailed view of the geometry (e.g., location and volume) of Singapore's geothermal energy source(s) at depth. In general, this cost-effective early- stage investigation can be implemented in any potential geothermal energy location, demonstrating its affordability and broad applicability.

References

[1] Bai Y, Yao J, Wu S, et al. *Earth Planet. Sci. Lett*., 2023, 610, 118105;

[2] Hao S, Chen, J., Tong, P. *J. Geophys. Res. Solid Earth*, 2023, under review.

[3] Tong P. *J. Geophys. Res. Solid Earth*, 2021, 126, e2021JB021818.

Invited Talk

Understanding Volcanic Unrest Driven by Subsurface Fluid Processes Through Multiphysics Modeling

Yan Zhan[a], Patricia Gregg[b], Hélène Le Mével[c], Diana Roman[c]

[a]*Earth and Environmental Sciences Programme, The Chinese University of Hong Kong, Hong Kong SAR;*
[b]*Department of Earth Science & Environmental Change, University of Illinois Urbana-Champaign, IL, USA,*
[c]*Earth and Planets Laboratory, Carnegie Institution for Science, DC, USA.*

E-mail: yanzhan@cuhk.edu.hk

Subsurface fluid processes like magma movement, volcanic gas release, and hydrothermal activity can cause hazardous volcanic eruptions. However, these same processes also power geothermal energy production, which helps reduce carbon emissions. Geophysical observations recorded deformation, earthquakes, and other warnings before eruptions. Computer models coupling fluid flow, heat transfer, and rock movement help explain volcanic unrest mechanisms.

At Augustine volcano in the USA, a porous rock channel allowed gases escaping from deep underground to move heat toward the surface for over years before the eruption. But immediately before the 2006 eruption, gas flow increased ten times, speeding hydrothermal changes and lowering porosity. Overpressured gases then built up, causing uplift, quakes, and eventually cracks opening, leading to the eruption[1].

At Laguna del Maule in Chile, a large magma chamber inflated quickly since 2007, interacting with a regional fault. The volcanic swelling widened existing cracks in this fault, improving fluid transport and triggering earthquake swarms. The energy released from earthquakes may in return stabilize the volcanic system and delay eruption[2].

At Atka volcanic area in the USA, uplift of over 80 mm/yr measured by radar coincided with more seismic activity. Models combining these data revealed a magma chamber also caused fault widening, similar to Laguna del Maule. However, here increased fluid movement drained a crater lake at Korovin volcano 5 km north. The lower water level triggered a phreatic (steam-driven) eruption in 2006[3].

Overall, combining different geophysical data into models coupling fluids, heat and rock movement helps explain gas migration, rock-fluid interaction and processes making unrest signals and triggering eruptions in different volcanic systems. This improves understanding of eruption causes and also aids studies of subsurface fluid flows like geothermal energy and carbon storage.

Reference

1 Zhan, Y., Le Mével, H., Roman, D. C., Girona, T., & Gregg, P. M. (2022). Modeling deformation, seismicity, and thermal anomalies driven by degassing during the 2005-2006 pre-eruptive unrest of Augustine Volcano, Alaska. Earth and Planetary Science Letters, 585, 117524. https://doi.org/10.1016/j.epsl.2022.117524
2 Zhan, Y., Gregg, P. M., Mével, H. L., Miller, C. A., & Cardona, C. (2019). Integrating Reservoir Dynamics, Crustal Stress, and Geophysical Observations of the Laguna del Maule Magmatic System by FEM Models and Data Assimilation. Journal of Geophysical Research: Solid Earth, 124(12), 13547–13562. https://doi.org/10.1029/2019JB018681
3 Zhan, Y., Gregg, P. M., & Lu, Z. (2021). Modeling Magma System Evolution During 2006–2007 Volcanic Unrest of Atka Volcanic Center, Alaska. Journal of Geophysical Research: Solid Earth, 126(2), e2020JB020158. https://doi.org/10.1029/2020JB020158

Invited Talk

Seismic Imaging of Urban Faults and Ocean Subduction Zones using Earth's Ambient Vibrations

Xin Liu,[a] Gregory C. Beroza,[b] Yehuda Ben-Zion[c] Hongyi Li[d]

[a] *Department of Earth Sciences, University of Hong Kong, Hong Kong SAR, China;* [b] *Department of Geophysics, Stanford University, CA, USA.* [c] *Department of Earth Sciences, University of Southern California, CA, USA.* [d] *Key Laboratory of Intraplate Volcanoes and Earthquakes (China University of Geosciences, Beijing), Ministry of Education, Beijing, China.*

E-mail: liuxine@hku.hk

Seismic velocity and seismic attenuation are key characteristics that describe how seismic waves propagate within the earth. The former refers to the speed of wave propagation, while the latter is an inherent property of rocks that leads to energy dissipation as waves traverse the subsurface. We have developed new methods, specifically ambient noise differential adjoint/attenuation tomography using a linear triplet of stations, to examine the velocity/attenuation structure beneath linear seismic arrays. We first delve into the theory underpinning ambient noise tomography using a linear triplet of stations and validate it using finite-frequency sensitivity kernels. Then we demonstrate the application of this technique to various scenarios including urban faults in the Los Angeles basin, the Longmenshan fault, the San Jacinto fault in Southern California, and an Ocean-Bottom Seismometer (OBS) array off the Kii Peninsula across the Nankai Trough.

Our results from the ambient noise differential adjoint tomography reveal a slow S-wave velocity corresponding to fluid-bearing rocks[1] such as the Silverado Aquifer near the Newport-Inglewood Fault section in Long Beach, California. Additionally, S-wave velocity tomography for the OBS array uncovers a slow S-wave velocity associated with the Kumano forearc basin and subducting sediments at the Nankai Trench.

The attenuation tomography results for Southern California and the Longmenshan Fault Zone highlight a correlation between strong attenuation and fault damage zones[2]. This correlation is particularly useful for studies related to earthquake fault physics and earthquake hazard assessment.

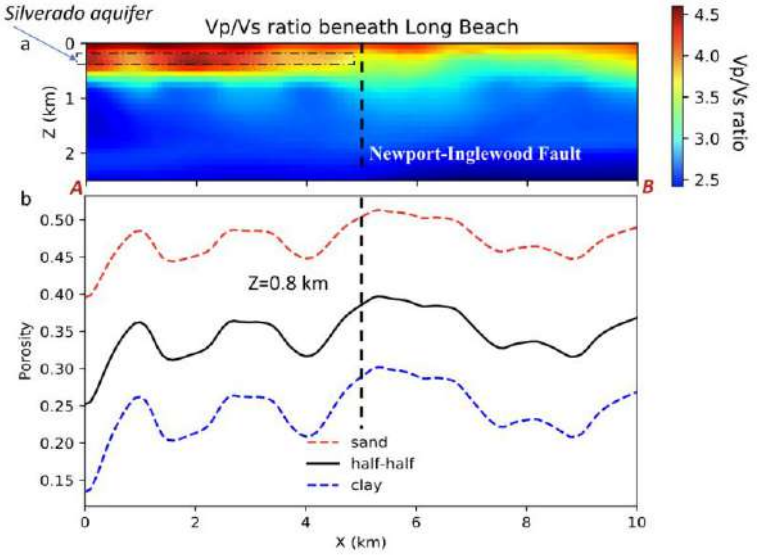

Figure 1. Velocity ratio and porosity estimation. a. P and S-wave velocity ratio in the Long Beach section[1]. b. Inferred porosity at 0.8 km depth converted from Vp/Vs ratio for pure sand (red dashed line), pure clay (blue dashed line), and half sand-half clay (black solid line), respectively. The dashed vertical black line represents the Newport-Inglewood Fault.

References

[1] Liu, X., Beroza, G. C., & Li, H. (2023). Ambient noise differential adjoint tomography reveals fluid-bearing rocks near active faults in Los Angeles. *Nature Communications*. https://doi.org/10.1038/s41467-023-42536-4

[2] Liu, X., Beroza, G. C., & Ben-Zion, Y. (2022). Ambient Noise Attenuation Tomography Reveals an Asymmetric Damage Zone Across San Jacinto Fault Near Anza, California. Geophysical Research Letters, 49(15). https://doi.org/10.1029/2022GL099562.

Invited Talk

Applied geophysical research for sustainable societies

Yunyue Elita Li

Sustainability Geophysics Project, Deparment of Earth, Atmospheric, and Planetary Sciences, Purdue University, West Lafayette, IN 47907 USA

E-mail: elitali@purdue.edu

As the global society focuses on combating climate change and embraces energy transition from fossil fuel to cleaner, renewable energy, applied geophysics research faces significant challenges in its own transition. At the Sustainability Geo- physics Project (SGP), our research group expands the horizon of “exploration” from the deep subsurface for energy resources to include all elements around the energy cycle. We demonstrate value of applied geophysical research for applications ranging from efficient energy recovery, optimal energy usage, to real- time monitoring and management, reclaim and recycle, and finally to carbon sequestration. With one case study in each category, we provide concrete examples on how applied geophysical research contributes broadly to the sustainable development of modern society. Finally, as a traditionally data-heavy discipline, we propose a new angle to perceive geophysics as a discipline of applied data science and point to the unprecedented opportunities for the applied geophysics community.

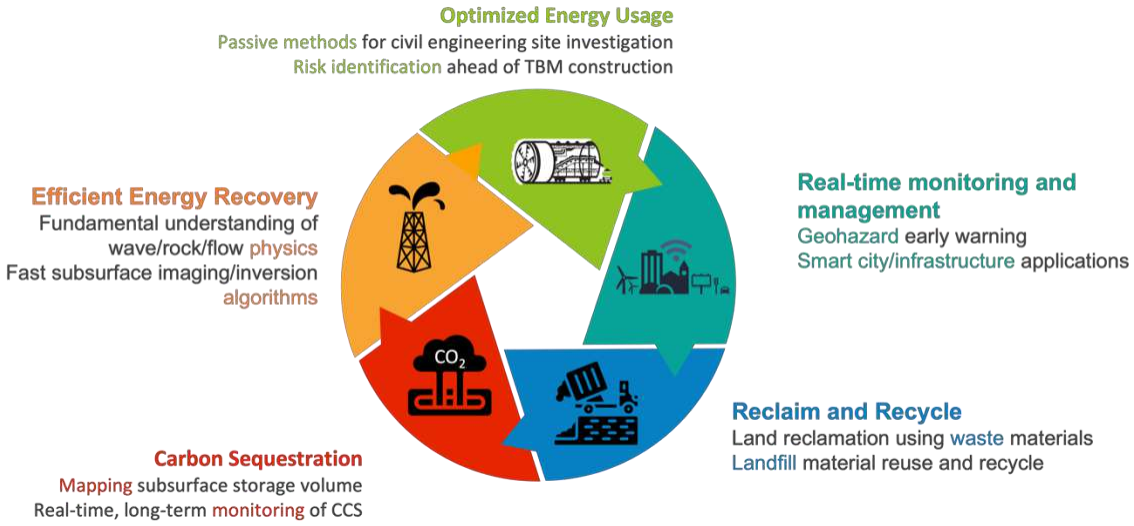

Invited Talk

Quantifying carbon emissions through satellite and surface measurements to support the transition to carbon neutrality in Hong Kong and the GBA

Hui Su[a], Yikang Zheng[a], Qiang Luo[a], Siwen Wang[a], Xu Chang, Rongshu Zeng[a]

[a] *Global STEM Professor, Department of Civil and Environmental Engineering,*

The Hong Kong University of Science and Technology, Clear Water Bay, Hong Kong SAR

E-mail: cehsu@ust.hk

The urgency to address climate change has become more pressing with the increasing frequency of extreme weather events. It is crucial to reduce anthropogenic greenhouse gases such as CO2 and CH4 to mitigate the impact of climate change. China has set a national goal to achieve carbon neutrality by 2060, while Hong Kong aims to achieve net-zero emissions by 2050. Accurately quantifying carbon sources and sinks is essential to defining and implementing strategies towards carbon neutrality. HKUST has taken a leading role in the research and development of satellite remote sensing technologies to measure atmospheric CO2 concentration. A carbon monitoring satellite is currently under planning and is expected to be launched in a year. This satellite will provide daily high-resolution observations of CO2 over the Greater Bay Area (GBA), significantly enhancing existing international satellite and ground-based observing networks. To convert satellite observations of CO2 concentration into carbon emission fluxes, a high-resolution carbon flux inversion modeling system is currently being developed at HKUST. In this talk, I will introduce our ongoing work to build the carbon flux inversion model and our plan to integrate satellite and surface measurements to develop a comprehensive carbon information system for the GBA. Our efforts aim to provide accurate and reliable data to support the transition towards a carbon-neutral future.

Invited Talk

Assessing the photosynthetic response of Amazon forests to climate change

Jin Wu,[a] Jing Wang,[c] Guangqin Song,[a] Xiaorong Wang,[a] Yuhao Pan,[a]

[a] *School of Biological Sciences, The University of Hong Kong, Pokfulam Road, Hong Kong, China;*

[b] *School of Ecology, Shenzhen Campus of Sun Yat-sen University, Shenzhen, Guangdong, China*

E-mail: jinwu@hku.hk

Main text in Arial 11 point font, single line spacing (or exactly 13 pt), 6 pt spacing before new paragraphs. Abstract must fit within this single page and end above footer line. [Maximum 400 Words]

Accurate understanding and modeling of Amazon forest responses to climate change are essential for assessing their fate under climate change and developing effective mitigation strategies. These responses depend on both external environmental factors and the ecosystems' inherent sensitivity, particularly through plant functional traits. Our limited knowledge and data on these traits hinder our comprehension of their role in regulating the sensitivity of Amazon forests to climate change. Using photosynthesis as an example—an essential process governing large-scale carbon and water cycles—we emphasize the importance of internal biotic factors in interpreting photosynthetic seasonality. Our findings indicate that fine-scale phenological diversity, specifically leaf quality phenology, drives high photosynthetic seasonality due to newly mature leaves having a greater photosynthetic capacity than older leaves[1,2]. Recognizing the significance of fine-scale phenological traits in regulating Amazonian tropical forest photosynthetic metabolism and climate change sensitivity, we investigate the potential of cutting-edge remote sensing techniques for improved monitoring across multiple scales. By combining newly emerging CubeSats technology with extensive proximate remote sensing data and sophisticated statistical modeling, we demonstrate its effectiveness and scalability as an alternative approach for mapping tropical phenology from individual tree crowns to entire forest ecosystems and regions[3,4]. This technical breakthrough not only addresses an important data gap in the scientific community, but also offers an unprecedented opportunity to comprehensively understand and model tropical forest photosynthetic responses to current and future climate change. In summary, we showcase how cutting-edge remote sensing technology significantly enhances tropical phenological trait characterizations across different scales and spatial extents, providing essential techniques, data, and insights for a better understanding of Amazon forests' sensitivity to climate change and pinpointing potential effective mitigation strategies.

References

[1] Wu J, Albert L, Lopes A, et al. *Science*, 2016, *351,* 972-976;

[2] Wu J, Guan K, Hayek M, et al. *Global Change Biology*, 2017, *3,* 1240-1257;

[3] Wang J, Yang D, Detto M, et al. *Remote Sensing of Environment*, 2020, 246*,* 111865;

[4] Wang J#, Song G#, Liddell M, et al. *Remote Sensing of Environment*, 2023, 286*,* 1113429.

Environment Session (2 December)

Keynote Lecture

Environmental intersection between net zero carbon and atmospheric mercury: Insights from mercury stable isotopes

Sae Yun Kwon[a]

[a] *Division of Environmental Science and Engineering, Pohang University of Science and Technology (POSTECH), Pohang, Sotuh Korea*

E-mail: saeyunk@postech..ac.kr

Mercury (Hg) is a global atmospheric pollutant, which can remain in the atmosphere for ~1 year prior to deposition to biosphere. The potential for its long-range transport and toxicity have called for a multilaterial agreement to mitigate anthropogenic Hg emissions and reduce ecosystem and human exposures via the UNEP's Minamata Convention on Mercury. While much of the scientific attention has been dedicated toward monitoring spatiotemporal Hg trends and understanding processes leading to atmospheric Hg deposition, we expect there to be substantial and complex environmental intersections between the objectives of carbon neutrality and the Minamata Convention on Mercury. This seminar is intended to show the importance of establishing baseline measurements on atmospheric Hg and constraining key predictors/indicators, which can be used to evaluate environmental intersections with carbon neutrality technologies and policies. To show this, I draw two case examples of 1) identifying climatic indicators that govern the extent of atmospheric Hg uptake and accumulation in forests, and 2) investigating baseline sources, transboundary transport, and chemical mechanisms leading to atmospheric Hg deposition in a nationally designated background site in South Korea. Both cases/systems suffer from significant uncertainties in predicting future outcomes on Hg due to natural climatic variability and policy-relevant issues under carbon neutrality. All my case examples rely heavily upon a state-of-art stable isotope technique for Hg, which provide multi-dimensional information regarding sources and complex atmospheric/biogeochemical procssses. By engaging in diverse scientific methodologies and coopertative effort, these complex intersections must be spoken, discussed, analyzed, and resolved to achieve carbon neutrality.

Oral Presentation

Variations of Methylmercury in a Mangrove Wetland Sediments: Insights from Subtropical Ecosystems in Hong Kong

Shaoyi Wang[a,b] Martin Tsz-Ki Tsui[a,b]

[a]*School of Life Sciences, Earth and Environmental Sciences Programme, The Chinese University of Hong Kong, Shatin, Hong Kong SAR, China*

[b]*State Key Laboratory of Marine Pollution, The City University of Hong Kong, Shatin, Hong Kong SAR, China*

E-mail: 1155168642@link.cuhk.edu.hk

Tropical and subtropical coastal wetland ecosystems serve vital bridging functions between offshore and inland environments. Most tropical and subtropical wetland areas, estimated to be between 60% and 75%, is mangrove forest. Mangroves are considered to have significant ecological and economic value, however, mangrove sediments with strong reducing conditions may play a potentially important, yet not well understood, role in converting inorganic mercury (Hg) into highly toxic methylmercury (MeHg). In this study, multiple 15-cm sediment cores were collected over different seasons from Mai Po Nature Reserve in Hong Kong along a transect: from within mangrove stands, water-land interface (margin), middle of the water channel to open water area. Sediment cores were sliced every centimeter for total mercury (THg), MeHg, and organic matter content analysis. We found that THg in sediments ranged narrowly between 90.32 and 225.81 ng/g and did not show a positive correlation with MeHg, which have been shown in many other aquatic studies. Interestingly, elevated MeHg concentrations were found at surface sediment near the root zones of mangrove trees. The percentage of THg as MeHg, i.e., %MeHg, was significantly correlated with loss-on-ignition (LOI), a proxy of organic matter content ($p<0.0001$), which suggests that sedimentary organic matter could serve as a crucial factor mediating Hg methylation in mangrove sediment. Over different seasons, a significantly higher MeHg ($p<0.05$) was observed during summertime, e.g., June & August. During summertime, the water would have lower salinity and higher temperature, which we suggest to be important factors promoting Hg methylation in sediments. All these results are now examined in other mangrove forests around Hong Kong, including one site at Futian Mangrove Reserve, Shenzhen), in which we will perform analyses for THg, MeHg, LOI, and Hg methylation related genes (*hgcAB* and *merAB*). Our current work will provide new insights into the key factors influencing Hg methylation in mangrove wetlands, where the resident food webs can extensively bioaccumulate and biomagnify.

Oral Presentation

Using Dairy Livestock Wastewater for Microalgae Production

Rui Xiao [1, 2], Huan Chen [2, 5], Pei-Lin Tan [5], Erika Carter [2], Austin Allen [2], Alex T. Chow [3], Clinton Williams [4]

[1] *Center for Synthetic Biochemistry, Institute of Synthetic Biology, Shenzhen Institutes of Advanced Technologies, Shenzhen, Guangdong 518055, China*

[2] *Department of Environmental Engineering and Earth Sciences, Clemson University, South Carolina 29634, United States*

[3] *The Earth and Environmental Science Programe, The Chinese University of Hong Kong, 999077, China*

[4] *USDA–ARS, US Arid Land Agricultural Research Center, Maricopa, Arizona 85138, United States*

[5] *Biogeochemistry & Environmental Quality Research Group, Clemson University, South Carolina 29442, United States*

E-mail: achow@cuhk.edu.hk

The increasing demand for animal products has triggered the scale-up from traditional household breeding to large-scale livestock farms with concentrated animal feeding operations (CAFOs), resulting in the production of a significant volume of livestock wastewater containing a large amount of nutrients and antibiotics. The improper management of this agricultural wastewater before discharge to surrounding freshwater ecosystems can easily deteriorate the natural environment. Here, in Clemson, US, we used dairy livestock wastewater to cultivate microalgae for nutrients recovery along with the surface water protection. We successfully cultivated three microalgae species of Chlamydomona reinhardtii, Chlorella protothecoides by using 100% dairy livestock wastewater [total organic carbon (TOC): 153 mg/L, total nitrogen (TN): 298 mg/L, total phosphorus (TP): 6.42 mg/L]. A variety of operating factors including light intensity, rainwater dilution and antibiotics concentration were investigated for cell growth, nutrients utilization and carbon neutralization. We observed the consumption of 12-28% of TOC, 88-95% of TN, and 58-74% of TP. Specifically, more than 99% of NH4+–N mass was used for microalgae growth. Moreover, we observed a significant decrease of SUVA254, indicating the aromaticity reduction of the wastewater after the microalgae cultivation. Total fatty acid content testing indicated C16:0, C18:1, C18:2 as the major fatty acids of C.reinhardtii and C. protothecoides, and their total fatty acid contents reached up to 13% and 17% by dry weight respectively. Meanwhile, in China, SIAT, aim to further decompose refractory organics in tertia treatment stage or/and replace the traditional active sludge process, the local microalgae, Chlorella sp. was acclimated and used for local livestock wastewater treatment (duck, piggery and cattle farms). Results indicated that Chlorella sp. can quickly utilize the nutrients from anaerobic digestion and active sludge oxidation process effluents for cell growth. The COD, TN as well as TP removal efficiency can reach to 80-95%. In addition, the crude protein content from Chlorella sp. can reach to 40-60%. Our studies concluded that the nutrients (C, N and P) from livestock wastewater were successfully used to cultivate three microalgae species of Chlamydomona reinhardtii, Chlorella protothecoides as well as Chlorella sp. for nutrients recovery, carbon neutralization as well as the potential biofuel production

Oral Presentation

Methylmercury biomagnification in subtropical forest food webs

Matthew Long-Hei Cheng [a], Martin Tsz-Ki Tsui [a, b], Ken Ming-Yin Yau [a], Jack Tsun-Hung Cheung [a]

[a] School of Life Sciences, The Chinese University of Hong Kong, Shatin, N.T., Hong Kong SAR, China; [b] Earth and Environmental Sciences Programme, The Chinese University of Hong Kong, Shatin, N.T., Hong Kong SAR, China

E-mail: matthewcheng@link.cuhk.edu.hk

Mercury (Hg), especially its organic form methylmercury (MeHg), is highly toxic and found to biomagnify in food webs, where its concentration increases with trophic position of organisms. Basal resources (e.g., litter) and terrestrial invertebrates were collected and their MeHg concentrations were determinated. Stable carbon ($\delta^{13}C$) and nitrogen ($\delta^{15}N$) isotope ratios were also used as indicators of energy flow and trophic structure respectively[1]. In contrast to aquatic ecoystems, such investigation is limited in terrestrial environment, particularly in subtropical biome.

Here we show that biomagnification exists in the three studied forests of Hong Kong as revealed by positive trophic magnification slopes (TMS) (0.1347 - 0.2383; $p < 0.05$), which is the slope of $\log_{10}$ [MeHg] vs $\delta^{15}N$. Such trend is consistent with relevant forset studies in other regions (e.g. USA[2] and Southwest China[3], etc.). The TMS value is similar to previous study on tropical freshwater and marine ecosystems (0.15 ± 0.07, n=9) under similar climatic conditions[4]. The percentage of total mercury (THg) as MeHg is found to have an significant increase with $\delta^{15}N$ ($p < 0.05$), confirming that MeHg mainly drives the Hg bioaccumulation within the food webs.

The three studied sites could be classified as mature secondary forests, fung shui wood and montane shrubland with a variety on elevation (~100m, ~200m and ~700m). Based on previous study[5] and official meteorological record[6], temperature is the lowest at the highest points. Our study suggests a warmer environment would facilate the productivity of organisms in the forest, therefore, the TMS value is lowered as a result of Hg dilution inside their faster growing biomass[4]. Previous studies on aquatic food webs also support such trend[4]. The current study emphasises the biomagnifying effect of MeHg in terrestrial ecosystems and how the TMS in various forest food webs were affected needs further investigation.

References

[1] Peterson, B. J., & Fry, B. (1987). Stable isotopes in ecosystem studies. *Annual review of ecology and systematics*, *18*(1), 293-320.
[2] Tsui, M. T. K., Liu, S., Brasso, R. L., Blum, J. D., Kwon, S. Y., Ulus, Y., ... & Finlay, J. C. (2019). Controls of methylmercury bioaccumulation in forest floor food webs. *Environmental science & technology*, *53*(5), 2434-2440.
[3] Li, C., Xu, Z., Luo, K., Chen, Z., Xu, X., Xu, C., & Qiu, G. (2021). Biomagnification and trophic transfer of total mercury and methylmercury in a sub-tropical montane forest food web, southwest China. *Chemosphere*, *277*, 130371.
[4] Lavoie, R. A., Jardine, T. D., Chumchal, M. M., Kidd, K. A., & Campbell, L. M. (2013). Biomagnification of mercury in aquatic food webs: a worldwide meta-analysis. *Environmental science & technology*, *47*(23), 13385-13394.
[5] Hao, J., & Chu, L. M. (2021). Vegetation Types Attributed to Deforestation and Secondary Succession Drive the Elevational Changes in Diversity and Distribution of Terrestrial Mosses in a Tropical Mountain Forest in Southern China. *Forests*, *12*(8), 961.
[6] Hong Kong Observatory, 2022: The Year's Weather 2022. *Monthly Weather Summary Dec 2022*.

Oral Presentation

Two new clades recovered at high temperatures provide new phylogenetic and genomic insights into Ca. Accumulibacter

Xiaojing Xie,[a] Xuhan Deng,[a] Jinling Chen[a], , Liping Chen[a], Jing Yuan[a], Hang Chen[a], Chaohai Wei [a,c], Xianghui Liu[b], Guanglei Qiu[a,b,c,d*]

[a] *School of Environment and Energy, South China University of Technology, Guangzhou 510006, China., ;* [b] Singapore *Centre for Environmental Life Sciences Engineering, Nanyang Technological University, Singapore 637551, Singapore.* [c] *Guangdong Provincial Key Laboratory of Solid Wastes Pollution Control and Recycling, Guangzhou 510006, China.* [d] *The Key Lab of Pollution Control and Ecosystem Restoration in Industry Clusters, Ministry of Education, Guangzhou 510006, China.*

E-mail: 1030472309@qq.com

Candidatus Accumulibacter, a key genus of polyphosphate-accumulating organisms playing key roles in enhanced biological phosphorus removal (EBPR) systems, can be divided into two major clades based on the gene polyphosphokinase 1. The genomic studies have deepened understanding of *Ca*. Accumulibacter over the years, but some metabolic aspects remain controversial. Controversies include P uptake coupled with nitrate/nitrite reduction and novel carbon source utilization. It is not clear if these capabilities are widely preserved within the genus, or clade/species specific. Additionally, in high-temperature EBPR systems, clade I members were scarcely detected while Clade IIF and IIC were observed as predominant community members, suggesting potential differences in their ability to survive in warmer environment. The genetic basis for this potential remains unexplored owing to the absence of high-quality genomes or limited genome integrity recovered at high-temperature systems.

A reliable phylogeny and clade classification is a prerequisite for understanding metabolic diversities of microorganisms. Some members, not adhere to ppk1-based population structure, highlight classification based on ppk1 may not sufficiently represent the evolutionary relationships. Modern evolutionary studies employ multiple genes and whole-genome data, aided by machine learning, for more accurate classification. Re-evaluating the phylogenetic structure through machine learning and pangenomics, in addition to ppk1-based classification, is necessary.

In this study, we used ten high-quality *Ca*. Accumulibacter genomes were recovered from high-temperatures reactors with available high-quality genomes in NCBI to perform a systematic pangenomic analysis. Clade IIF members SCELSE-3, SCELSE-4, and SCELSE-6 encoded a complete denitrification pathway, suggesting that Ca. Accumulibacter alone could achieve complete denitrification. All *Ca*. Accumulibacter likely has the potential to use dicarboxylic amino acids. AALB seemed to be the only one capable of glucose usage. A heat shock protein Hsp20 encoding gene was found exclusively in genomes recovered at high temperatures, which was absent in clades IA, IC, IIA, IIB, and IID members. High transcription of this gene in SCUT-2 suggested its role in surviving high temperatures. Ambiguous clade identity was observed for newly recovered genomes (SCELSE-9 and SCELSE-10). Five machine learning models, using orthogroups as input features, suggested that these two genomes belong to a new clade (IIJ). The phylogeny of *Ca*. Accumulibacter was re-evaluated based on the horizontally transferred polyphosphokinase 2 gene which showed effectiveness in differentiating and defining different clades.This study provide renovative understandings of nitrogen and carbon metabolisms, heat stress adaption and the phylogenic characteristics, resulting in an improved understanding of genomic differences within and among clades.

Oral Presentation

Candidatus Accumulibacter use fermentation products for enhanced biological phosphorus removal

Guanglei Qiu, Liping Chen, Gengrui Wei, Yushen Zhang, Kaiying Wang, Cenchao Wang, Xuhan Deng, Yaqian Li, Xiaojing Xie, Jinling Chen, Fu Huang, Hang Chen, Bin Zhang, Chaohai Wei.

School of Environment and Energy, South China University of Technology, Guangzhou 510006, China.

qiugl@scut.edu.cn

Abstract: Previous research suggested that two major groups of polyphosphate-accumulating organisms (PAOs), i.e., *Ca.* Accumulibacter and *Tetrasphaera*, play cooperative roles in enhanced biological phosphorus removal (EBPR). The fermentation of complex organic compounds by Tetrasphaera provides carbon sources for *Ca.* Accumulibacter. However, the viability of the fermentation products (e.g., lactate, succinate, alanine) as carbon sources for *Ca.* Accumulibacter and their potential effects on the metabolism of Ca. Accumulibacter were largely unknown. This work for the first time investigated the capability and metabolic details of *Ca.* Accumulibacter clade IIC strain SCUT-2 (enriched in a lab-scale reactor with a relative abundance of 42.8 %) in using these fermentation products for EBPR. *Ca.* Accumulibacter clade IIC strain SCUT-2 (with a relative abundance of 42.8 %) was enriched in a lab-scale reactor. The enrichment culture was able to assimilate lactate and succinate with the anaerobic P release to carbon uptake ratios of 0.28 and 0.36 P mol/C mol, respectively. In the co-presence of acetate, the uptake of lactate was strongly inhibited, since two substrates shared the same transporter as suggested by the carbon uptake bioenergetic analysis. When acetate and succinate were fed at the same time, *Ca.* Accumulibacter assimilated these two carbon sources simultaneously. Proton motive force (PMF) was the key driving force (up to 90%) for the uptake of lactate and succinate by *Ca.* Accumulibacter. Apart from the efflux of protons in symport with phosphate via the inorganic phosphate transport system, translocation of proton via the activity of fumarate reductase contributed to the generation of PMF, which agreed with the fact that PHV was a major component of PHA when lactate and succinate were used as carbon sources, involving the succinate-propionate pathway. Metabolic models for the usage of lactate and succinate by *Ca.* Accumulibacter for EBPR were built based on the combined physiological, biochemical, metagenomic, and metatranscriptomic analyses. Alanine was shown as an invalid carbon source for *Ca.* Accumulibacter. Instead, it significantly and adversely affected *Ca.* Accumulibacter-mediated EBPR. Phosphate release was observed without alanine uptake. Significant inhibitions on the aerobic phosphate uptake of *Ca.* Accumulibacter was also evident. Overall, this study suggested that there might not be a simply synergic relationship between *Ca.* Accumulibacter and *Tetrasphaera*. Their interactions would largely be determined by the kind of fermentation products released by the latter.

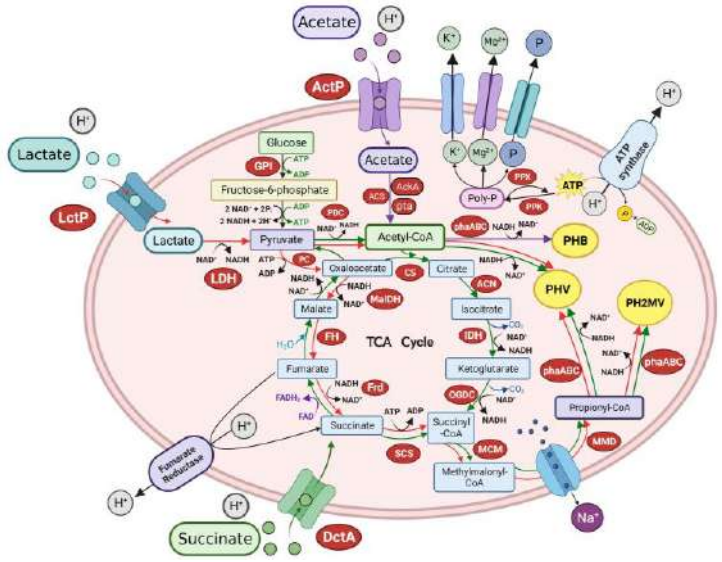

Fig. 1 Metabolic models for *Ca.* Accumulibacter with acetate, lactate, and succinate as carbon sources for EBPR.

Oral Presentation

Study on photocatalytic degradation to eliminate microplastic pollution in water environment under carbon neutral background

Huixue Ren,[a] Shengyun Jiang,[a] Yaping Qin [a]
[a] *School of Municipal and Environmental Engineering , Shandong Jianzhu University , Shandong Province ,P.R.China.*
E-mail: renhx138@163.com

Abstract: The microplastics (MPs) in the water system could easily enter the human body and pose potential threat, so finding a green and effective solution remains a great challenge[1]. At present, the advanced oxidation technology represented by photocatalysis has been proven to be effective in the removal of organic pollutants, making it a feasible method to solve the problem of MP pollution[2]. In this study, the photocatalytic degradation of typical MP polystyrene (PS) and polyethylene (PE) by a new quaternary layered double hydroxide composite photomaterial CuMgAlTi-R400 was tested under visible-light irradiation. After 300 h of visible-light irradiation, the average particle size of PS decreased by 54.2% compared with the initial average particle size. The smaller the particle size, the higher the degradation efficiency. The degradation pathway and mechanism of MPs were also studied by GC-MS, which showed that PS and PE produced hydroxyl and carbonyl intermediates in the process of photodegradation. This study demonstrated a green, economical, and effective strategy for the control of MPs in water.

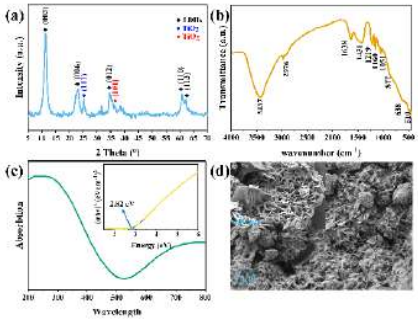

Fig. 1 (a)XRD patterns, (b)FTIR spectra, (c) Diffuse reflectance spectra and Tauc plot，and (d) SEM image of CuMgAlTi-R400.

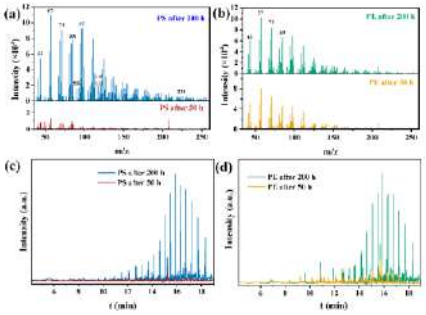

Fig. 2 GC/MS spectrum of PS(a,c) and PE(b,d).

References

[1]Shen M, Zhang Y, Zhu Y, et al. *Environ. Pollut.* 2019, *252*, 511–521.
[2]Xu Q, Huang Q.S, Luo T.Y,et al. *Chem. Eng. J.* 2021, *416*, 129123.

Oral Presentation

Influences of microplastics on mercury cycling in forested ecosystems

Ming Yin Yau[a], Martin Tsz-Ki Tsui[a], Aijun Miao[b]

[a] *School of Life Sciences, Earth and Environmental Sciences Programme, The Chinese University of Hong Kong, Hong Kong SAR, China*

[b] *School of the Environment, Nanjing University, Nanjing, Jiangsu Province 210023, China*

E-mail: kenyau0422@link.cuhk.edu.hk

Owing to the high toxicity and long-distance atmospheric transport, mercury (Hg) is widely considered as a global environmental pollutant, which is capable of being converted into highly toxic methylmercury (MeHg) by certain anaerobic microbes. Once produced, MeHg can be extensively bioaccumulated and biomagnified within natural food webs, resulting in elevated MeHg levels in top predators which can pose a health threat to wildlife and human[1]. There have already been plenty of studies regarding MeHg production in the aquatic environment. Both Hg methylation and demethylation processes determine the net MeHg concentrations, and potentially control the elevated MeHg contamination in forested ecosystems.

Global concerns of microplastic (MP) pollution are rising. Recent studies have found extensive MP contamination not just in aquatic ecosystems, but also terrestrial forested environments, and thus the roles of MP on transforming contaminant such as Hg/MeHg should be better clarified in the environments because MP can accumulate and interact with MeHgCl[2]. Some recent studies have already revealed that the ability of MP to reduce the agricultural soils' bioavailable MeHg concentration by modifying the soils' dissolved organic matter composition and microbial communities[3,4]. Meanwhile, a recent study has revealed the high Hg methylation potential in the plastisphere, leading to increasing MeHg production[5].

Therefore, this study is aimed to investigate the relationship between the presence of MP and the rate of MeHg production in forested environments, an experimental study demonstrating the process of litter decomposition with MP addition has been designed. Different types of MPs including polystyrene (PS) and polyvinyl chloride (PVC) of different sizes, i.e. 10, 100 and 1000 μm have been incubated with fresh streamwater and leaf litter from local forest over several weeks. Each bottle was kept sealed to provide an anaerobic environment which can elevate the MeHg production by Hg methylating micro-organisms. In this presentation, findings of the MP-litter incubation experiments will be shown regarding the MeHg levels. The preliminary data has provided us with insights into the suppression of MeHg production due to the presence of MPs, which may offer extra surface area to promote establishment of biofilm communities, which we hypothesize can adsorb MeHg or even degrade MeHg.

References

[1] Tsui MTK, Liu S, Brasso RL, et al. *Environ. Sci. Technol.*, 2019, *53*, 5, 2434–2440;

[2] Zhu J, Zhang Y, Xu Y, et al. *Mar. Environ. Res.*, 2022, *176*, 105615;

[3] Allouzi MMA, Tang DYY, Chew KW, et al. *Sci. Total Environ.*, 2021, *788*, 147815;

[4] Yang X, Li Z, Ma C, et al. *J. Hazard. Mater.*, 2022, *423*, 126895;

[5] Hao YY, Liu HW, Zhao J, et al. *J. Hazard. Mater.*, 2023, *457*, 131699.

Oral Presentation

Mercury in Human Health: Effects on Sperm Dysfunction and Maternal-Fetal Blood Systems

Mengwei Yuan, [a] Martin Tsz-Ki Tsui, [a] Chi-Chiu Wang, [b] David Yiu-Leung Chan, [b] Tak-Yeung Leung, [b]

[a] School of Life Science, The Chinese University of Hong Kong, Hong Kong, China; [b] Department of Obstetrics and Gynaecology, The Chinese University of Hong Kong & Prince of Wales Hospital,

Hong Kong, China

E-mail: mengweiyuan@link.cuhk.edu.hk

In recent decades, a global decline in birth rates has been observed, with notable instances such as Hong Kong recording fewer than 40,000 births last year for the first time in over half a century. Besides social and economic factors, an increasing concern has been raised about impact of environmental contaminant on the reproductive health in human.

As a prevalent environmental toxin, mercury (Hg) poses significant reproductive risks. Its detrimental effects encompass direct cellular injury, endocrine disruption, and neural modifications. Animal studies indicated that exposure to Hg can induce DNA rupture in sperm and leads to a decrement in sperm motility and their dysfunction[1]. However, the exact mechanisms by which various Hg forms influence sperm morphology and fertilizing capacity remain uncertain. Methylmercury (MeHg), an organic form of Hg, can readily cross placenta and blood-brain barrier[2], potentially harming the fetal brain during pregnancy, while the selective transport mechanisms at the placental barrier are still unidentified. Examining the impact of Hg on human reproductive health could offer valuable insights for medical interventions.

In our preliminary study, we analyzed 28 semen samples from patients undergoing semen analysis in Hong Kong. The average concentrations of total mercury (THg) and MeHg in the seminal plasma were 0.34±0.47 and 0.008±0.04 μg/L respectively. In sperm cells THg and MeHg were found to be 9.12±19.94 and 1.57±3.38 *p*g/10^6 cells, respectively. When grouped by median, it was observed that samples with higher THg had 12% and 11% higher sperm motility and progressive motility compared to the men with lower THg concentrations. Samples with higher THg displayed better normal morphology compared to those with lower THg concentration when grouped by the top 30% ($p < 0.03$). Additionally, we also test maternal blood from Hong Kong patients, the levels of THg and MeHg were 2.69 μg/L and 1.59 μg/L respectively. In cord blood, 4.59 μg/L of THg and 1.90 μg/L of MeHg were observed. The ratios of cord to maternal blood concentrations were 1.71 for THg and 1.19 for MeHg, our results are in agreement with earlier studies indicating active transport of Hg from mothers to fetuses[3], while the mechanism remains unclear. It's important to note while the current sample size is limited, and further investigation is required to validate our hypotheses.

References

[1] Henriques, Magda Carvalho et al. *Reproductive toxicology (Elmsford, N.Y.)* vol. 85 (2019): 93-103.

[2] Sakamoto M, Haraguchi K, Tatsuta N, et al. Environ Res. 2021;196:110896.

[3] Sakamoto M, Tatsuta N, Izumo K, et al. Toxics. 2018 Aug 3;6(3):45.

Oral Presentation

Agroecosystem Modeling of Reactive Nitrogen Emissions from U.S. Agricultural Soils with Biochar Amendments

Lina Luo,[a] Daniel S. Cohan,[b] Caroline A. Masiello,[c] Taras E. Lychuk,[d] Amos P. K. Tai[a]

[a]*Earth and Environmental Sciences Programme, The Chinese University of Hong Kong, Hong Kong SAR, China;* [b]*Department of Civil and Environmental Engineering, Rice University, Texas, United States;* [c]*Department of Earth, Environmental, and Planetary Sciences, Rice University, Texas, United States;* [d]*Agriculture and Agri-Food Canada, Manitoba, Canada*

E-mail: linaluo@cuhk.edu.hk

Fertilizer-intensive agriculture is a leading source of reactive nitrogen (Nr) emissions in the United States, including the potent greenhouse gas nitrous oxide (N_2O), and the air pollutants nitric oxide (NO) and ammonia (NH_3) which contribute to most health-damaging air pollution fine particulate matter (PM) and ozone (O_3). Biochar, a carbonaceous soil amendment produced from biomass, has potential for boosting crop yields, enabling carbon sequestration, and possibly reducing Nr emissions. However, the impacts of biochar on Nr emissions vary significantly with soil properties, climate conditions, and the properties of the biochar itself, ranging from positive to negative and even neutral. Previous studies have relied on field measurements or field-scale agroecosystem models, which are inadequate to characterize such complex variations across U.S. agricultural lands.

In this study, we incorporated biochar algorithms[1] into a regional-scale agroecosystem model, the Fertilizer Emission Scenario Tool for CMAQ (FEST-C)[2,3], to simulate changes in Nr emissions following biochar applications. Unlike typical field-scale process-based models, FEST-C, with its built-in databases for sites, soils, and crops, allows for simulations across U.S. agricultural lands at a fine-scale (12km by 12km) spatial resolution. Our previous work[2] enhanced FEST-C's nitrogen schemes to include emissions of NO and N_2O from nitrification, as well as NO from denitrification, enabling a consistent and mechanistic prediction of Nr emissions from U.S. agricultural soils. Model performance evaluations against published field studies in the United States showed that the enhanced FEST-C, with biochar algorithms, could capture the trends of Nr emission changes upon biochar applications. Scenario analyses were then performed with biochar application rates of 5 and 20 ton ha^{-1} on U.S. fertilized soils. Our results demonstrated that the responses of Nr emissions to biochar amendments vary significantly across different agricultural areas and are influenced by the amount of biochar applied. High-dose biochar applications in acidic soils with low organic carbon and inorganic nitrogen content exhibited the most favorable impacts on Nr emissions. Our analyses suggest that the net effects of biochar amendments on Nr emissions depend mostly on how nitrification rate is affected.

Our study is the first to model spatial variability in the impacts of biochar amendments on emissions of three crucial Nr species.[4] These simulations could inform the identification of field study sites where the application of soil carbon amendments would be most likely to mitigate emissions and their associated adverse impacts on air quality, human health, and climate.

Reference

[1] Lychuk TE, Izaurralde RC, Hill RL, McGill WB, Williams JR. *Mitig Adapt Strateg Glob Change* 2015, *20* (8), 1437–1458.

[2] Luo LL, Ran LM, Rasool QZ, Cohan DS. Integrated Modeling of U.S. *Environ. Sci. Technol.* 2022, acs.est.1c08660.

[3] Ran LM, Yuan YP, Cooter E, Benson V, Yang DM, Pleim J, Wang RY, Williams J. *J. Adv. Model. Earth Syst.* 2019, *11* (12), 4645–4668.

[4] Luo LL, Cohan DS, Masiello CA, Lychuk TE, Gao XD. *Biochar* 2023, *5* (1), 72.

Oral Presentation

Impacts of interannual climate variability on fire activities, biomass burning emissions and air quality in Amazon

NG, Leo T.H.,[a] Tai, Amos P. K.[a]

[a] *Graduation Division of Earth and Atmospheric Sciences, Faculty of Science, The Chinese University of Hong Kong, Sha Tin, Hong Kong SAR, China*

E-mail: leo_ngtsinhung@link.cuhk.edu.hk

Biomass burning in the Amazon region significantly affects regional climate, deteriorates regional air quality, posing a threat to human health.[1,2,3] Biomass burning in the Amazon has substantial influence on the surrounding regions where pollution worsens during the dry season (Jul to Nov).[4] Previous research has shown that wildfire occurrence in the Amazon is related to interannual climate variability, such as drought, and long-term changes in land use, such as deforestation.[5] To estimate the impacts of biomass burning and drought on fire emissions and regiuonal air quality, the Global Fire Emission Database Version 4 (GFED4)[6] was used to drive a global 3-D atmospheric chemical transport model, GEOS-Chem High Performance (GCHP)[7,8] with a resolution of ~50 km in the Amazon between 2010 to 2015. By comparing the “fire-on” and “fire-off” simulations, we find that biomass burning alone in normal year (2011 and 2013) contributes to the total concentrations of fine particulate matter ($PM_{2.5}$), carbon monoxide (CO), nitrogen oxide (NO_x) and ozone (O_3) by 5.7 μg m^{-3} (91%), 0.08 ppm (86%), 0.03 ppb (565%), and 9.5 ppb (70%), respectively. The study also find these number during drought years rises to 19.6 μg m^{-3} (296%), 0.20 ppm (203%), 0.19 ppb (3740%), and 15.6 ppb (108%), respectively. We find that the pollutants generated by biomass burning emissions mainly concentrate in the southeastern Amazon and advect southward, leading to stronger impact on public health in Brazil. Our study shows the significance of biomass emission in shaping the air quality in Amazon region, and highlights the impact of drought event on enhancing biomass emission, worsening regional air quality and causing public health issue. Therefore, it is important to address the underlying causes of biomass burning in the Amazon, such as deforestation and land use change, and drought, in order to protect the region's ecosystems and mitigate the impacts of climate change.

Reference

[1] Covey, K., Soper, F., Pangala, S., Bernardino, A., Pagliaro, Z., Basso, L., Cassol, H., Fearnside, P., Navarrete, D., Novoa, S., Sawakuchi, H., Lovejoy, T., Marengo, J., Peres, C. A., Baillie, J., Bernasconi, P., Camargo, J., Freitas, C., Hoffman, B., Nardoto, G. B., Nobre, I., Mayorga, J., Mesquita, R., Pavan, S., Pinto, F., Rocha, F., Mello., R. A., Thuault, A., Bahl, A. A., & Elmore, A. (2021, March 11). Carbon and Beyond: The Biogeochemistry of Climate in a Rapidly Changing Amazon. Frontiers in Forests and Global Change, 4. https://doi.org/10.3389/ffgc.2021.618401

[2] Werth, D., & Avissar, R. (2002). The local and global effects of Amazon deforestation. Journal of Geophysical Research: Atmospheres, 107(D20), LBA-55.

[3] Marlier, M. E., Bonilla, E. X., & Mickley, L. J. (2020). How do Brazilian fires affect air pollution and public health?. GeoHealth, 4(12), e2020GH000331.

[4] Aragão, L. E., Poulter, B., Barlow, J. B., Anderson, L. O., Malhi, Y., Saatchi, S., Phillips, O. L., & Gloor, E. (2014). Environmental change and the carbon balance of Amazonian forests. Biological Reviews, 89(4), 913–931. https://doi.org/10.1111/brv.12088

[5] Aragão, L. E., Anderson, L. O., Fonseca, M. G., Rosan, T. M., Vedovato, L. B., Wagner, F. H., Silva, C. V., Silva Junior, C. H., Arai, E., Aguiar, A. P., Barlow, J., Berenguer, E., Deeter, M. N., Domingues, L. G., Gatti, L., Gloor, M., Malhi, Y., Marengo, J. A., Miller, J. B., Phillips, O.L. & Saatchi, S. (2018). 21st century drought-related fires counteract the decline of Amazon deforestation carbon emissions. Nature Communications, 9(1). https://doi.org/10.1038/s41467-017-02771-y

[6] Randerson, J.T., G.R. van der Werf, L. Giglio, G.J. Collatz, and P.S. Kasibhatla. (2018). Global Fire Emissions Database, Version 4, (GFEDv4). ORNL DAAC, Oak Ridge, Tennessee, USA. https://doi.org/10.3334/ORNLDAAC/1293

[7] Bindle, L., Martin, R. V., Cooper, M. J., Lundgren, E. W., Eastham, S. D., Auer, B. M., Clune, T. L., Weng, H., Lin, J., Murray, L. T., Meng, J., Keller, C. A., Putman, W. M., Pawson, S., and Jacob, D. J. (2021). Grid-stretching capability for the GEOS-Chem 13.0.0 atmospheric chemistry model, Geosci. Model Dev., 14, 5977–5997.

[8] Martin, R. V., Eastham, S. D., Bindle, L., Lundgren, E. W., Clune, T. L., Keller, C. A., Downs, W., Zhang, D., Lucchesi, R. A., Sulprizio, M. P., Yantosca, R. M., Li, Y., Estrada, L., Putman, W. M., Auer, B. M., Trayanov, A. L., Pawson, S., & Jacob, D. J. (2022). Improved advection, resolution, performance, and community access in the New Generation (version 13) of the high-performance GEOS-Chem Global Atmospheric Chemistry model (GCHP). Geoscientific Model Development, 15(23), 8731–8748. https://doi.org/10.5194/gmd-15-8731-2022

International Conference on Earth, Energy & Environmental Sciences for Carbon Neutrality (ICE3SCN)

Conference Abstract

3 December 2023 (Sunday)

Plenary Session (3 December)

Plenary Lecture 4:

Reviving Manmade Seawalls: Enhancing Marine Biodiversity and Carbon Sequestration through Innovative Approaches

Kenneth M Y Leung [a]

[a] *State Key Laboratory of Marine Pollution and Department of Chemistry, City University of Hong Kong, Hong Kong, China*

E-mail: kmyleung@cityu.edu.hk

Coastal reclamation and marine infrastructure projects commonly rely on pragmatic designs of artificial vertical or sloped seawalls as defense against wave action, flooding, and land erosion. However, these structures lack microhabitats that can serve as refuges and feeding grounds for marine organisms. By leveraging knowledge from marine ecology and fostering collaboration among ecologists, architects, and engineers, we now have the ability to design ecologically friendly artificial structures. These structures serve dual purposes as coastal defenses while enhancing marine biodiversity and ecosystem services such as biofiltration and carbon sequestration. In this presentation, I will introduce the fundamental ecological principles behind the design of eco-engineered shorelines (i.e., eco-shorelines) and emphasize the importance of incorporating nature-based solutions such as oyster shell reefs and mangrove plantations. Additionally, I will showcase the results of recent trials on retrofitting various eco-engineered features on seawalls and highlight notable large-scale eco-shorelines in Hong Kong.

Planting mangrove trees on eco-engineered shorelines offers multiple benefits, including carbon sequestration and providing food (e.g., leaf litter and detritus) and habitats for marine organisms. Moreover, these plantations provide shade, reducing heat and desiccation stress for marine organisms, while enabling urban greening and creating habitats for animals like birds. However, successful plantation of mangrove trees and backshore plants on sloping seawalls heavily rely on consistent freshwater supply, which is often lacking in coastal areas. To address this challenge, an innovative approach is proposed, integrating natural-looking solar panels (e.g., solar pavement) with a reverse osmosis system. This system generates electricity to power pumps and convertion of seawater into freshwater for irrigation purposes. This innovation not only promotes marine biodiversity but also contributes to decarbonization efforts through eco-shorelines.

The creation of living seawalls and eco-shorelines aligns with the objectives of the UN Decade of Ecosystem Recovery (2021-2030) and China's National Master Plan for Major Projects to Protect and Restore Important Ecosystems (2021-2035). Implementing eco-engineered seawalls is a pivotal component of the National Master Plan's coastal ecosystem restoration strategy. This presentation will discuss the opportunities and challenges associated with their implementation, emphasizing their significance in restoring and revitalizing degraded coastal ecosystems.

Plenary Lecture 5:

Structural Design and Performance Regulation of Electrochemical Energy Materials

Shi-Gang Sun

State Key Laboratory of Physical Chemistry of Solid Surfaces, College of Chemistry and Chemical Engineering, Xiamen University, Xiamen 361005, China

E-mail: sgsun@xmu.edu.cn

The property of nanomaterials for electrochemical energy conversion (Fuel cells) and storage (lithium batteries) depends strongly on their structure. On the one hand, the platinum group metals (PGMs) and Pt-based catalysts are of vital importance for fuel molecule oxidation to promote the efficiency of energy conversion in polymer electrolyte membrane fuel cells (PEMFCs) and direct organic fuel cells (DOFCs); On the other hand, the performances of electrode materials are crucial for developing lithium ion batteries (LIBs) with high energy, high power and safety. We report in this communication our recent progresses on the structural design and performance regulation of both electrocatalysts for PEMFCs and electrode materials for LIBs.

Electrocatalysts for FCs. (1) Based on knowledge of the structure of electrocatalytic active centers gained by using single crystal electrode as model catalysts, we developed electrochemically shape-controlled synthesis, which produce well-defined nanocrystal catalysts enclosed with high-index facets and have high activity and stability for anode reactions of DOFCs; (2) As about 90% Pt loading required in the cathode of FCs due to the slow kinetics of oxygen reduction reaction (ORR), we developed high active and stable non-precious catalysts for ORR. Through design and preparation of efficient non-precious metal catalysts, constructing reaction interfaces and enhancing mass and charge processes and regulating transmission channels and strengthening transmission processes, we have achieved continuously refreshing the power density records of non-precious metal catalyst fuel cells

Electrode materials for LIBs. We have developed strategies to regulate the structure of electrode materials including metal oxide anode, li-rich layered and NCM cathodes, and improved effectively their performances. Though regulating the interface of solid electrolyte $LiCoO_2/Li_{10}GeP_2S_{12}$ by using ultra-thin $Li_2CoTi_3O_8$ layer, we demonstrated that the performance of all solid Li-ion battery could be boosted.

Acknowledgement. The study was supported by natural science foundation of China (22288102, 21621091) and the MOST (2016YFB0100202，2017YFA0206502).

References:

1. N Tian, ZY Zhou, SG Sun et al. *Science*, 2007, 316, 732.
2. ZY Zhou, SG Sun et al. *Chem Soc Rev* 2011, 40, 4167.
3. J Xiao, N Tian, SG Sun et al. *J Am Chem Soc* 2013, 135, 18754.
4. NF Yu, N Tian, SG Sun et al. Angew Chem Int Ed, 2014, 53, 12527.
5. C Xiao, N Tian, ZY Zhou, SG Sun et al, Joule 2020, 4, 2552
6. GZ Wei, SG Sun et al. *Adv Mater* 2010, 22, 4364.
7. F Fu AG Sun et al. *J Mater Chem A* 2013, 1, 3860.
8. YC Wang, ZY Zhou, SG Sun et al. *Angew Chem Int Ed* 2015, 54, 9907.
9. SH Yin, YX Jiang, Sun et al. *Angew Chem Int Ed* 2020, 59, 21976.
10. YC Wang, ZY Zhou, SG Sun et al. Sci Adv, 2022, 8, eadd8873.
11. SH Yin, YX Jiang, Sun et al. *Energy Environ Sci* 2022, 115, 3033
12. SH Yin, YX Jiang, SG Sun, et al. *Angew Chem Int Ed* 2023, 10.1002/anie.202306166

Plenary Lecture 6:

Photovoltaic Materials for Organic Solar Cells

Yongfang Li[a,b]

[a] *Institute of Chemistry, Chinese Academy of Science, Beijing 100190, China;* [b]*Soochow University, Suzhou, Jiangsu 215123, China.*

E-mail: liyf@iccas.ac.cn

Organic solar cells (OSCs) have attracted great attention in recent years, because of their advantages of simple device structure, light weight and capability to be fabricated into flexible and semitransparent devices. The key photovoltaic materials of OSCs are conjugated polymer donors and *n*-type organic semiconductor (*n*-OS) acceptors. Recently, the low bandgap *n*-OS small molecule acceptors (SMAs) (such as Y6)[1] have promoted the research progress of the OSCs significantly.

Here I will report our recent research progress on the photovoltaic materials of the polymer donors, new *n*-OS SMAs, polymerized SMAs and the giant molecule acceptors (GMAs) based on the SMAs. We synthesized Y6 derivative acceptors *m*-TEH, *o*-TEH and T2EH with thiophene upper side chains, power conversion efficiency (PCE) of the OSCs based PBQ6 as donor and *m*-TEH as acceptor reached 18.51%.[2] We developed a low cost medium bandgap D-A copolymer donor PTQ10 based on thiophene as D-unit and difluoroquinoxaline as A-unit in 2018.[3] And the OSCs with PTQ10 as donor showed high PCEs of 18.55% for the binary device with *m*-TEH as acceptor[4] and 19.34% for the ternary device. We proposed the strategy of polymerized small molecule acceptor (PSMA) for the design and synthesis of high performance polymer acceptors in 2017[5], and PCE of the all polymer solar cells (all-PSCs) with new PSMA as polymer acceptor reached the level of 16~18%[6,7]. The all-PSCs show high flexibility and good stability, while there are some problems on the photovoltaic performance reproducibility and cost of the all-PSCs due to the difficulty of the synthesis and molecular weight control of the PSMAs. To overcome these issues of the PSMAs, we recently developed GMAs by combining two or three SMAs through conjugated bridge.[8] The GMAs possess fixed molecular weight, and show the advantages of the PSMAs with good film-forming property and high stability and the SMAs with high PCE and good photovoltaic performance reproducibility.

References

[1] Yuan J, Zhang Y, Zhou L, et al. *Joule*, 2019, *3*(4), 1140-1151.
[2] Kong X, Zhu C, Zhang J, et al, *Energy Environ. Sci*., 2022, *15* (5), 2011–2020.
[3] Sun C, Pan F, Bin H, et al., *Nat. Commun*., 2018. *9*, 743.
[4] Kong X, Zhang J, Meng L, et al., *CCS Chemistry*, 2023, *5*, 841–850.
[5] Zhang Z, Yang Y, Yao J, et al., *Angew. Chem. Int. Ed*., 2017, *56*(43), 13503–13507.
[6] Du J, Hu K, Zhang J, et al., *Nat. Commun*. 2021, *12*, 5264.
[7] Guo J, Xia X, Qiu B, et al., *Adv. Mater*. 2023, *36*(16), 2211296.
[8] Zhuo H, Li X, Zhang J, et al., *Angew. Chem. Int. Ed*., 2023, *62*(26), e202303551.

Energy Conversion Session (3 December)

Keynote Lecture

Alkaline Polymer Electrolyte Based Technologies: Fuel Cells and Electrolysis

Lin Zhuang

College of Chemistry and Molecular Sciences, Wuhan University, Wuhan 430072, China

E-mail: lzhuang@whu.edu.cn

In this invited keynote lecture, I will first overview the development of a new class of electrochemical technology based on alkaline polymer electrolytes (APEs) in Wuhan University over the past decade, and then talk about our recent advances in the study of APE-based fuel cells and CO_2 electrolysis.

APE-based fuel cells (APEFCs) have witnessed a speedy development in recent years. The cell performance has been boosted from 1 W/cm^2 in 2015, to over 2 W/cm^2 in 2018, and now to over 3 W/cm^2, when the cells were operated with H_2 and O_2. The next target is to be able to operate with air containing CO_2, and with non-previous metal catalysts with long-term stability. Challenges in both electrocatalysis and materials will be presented.

CO_2 electrolysis (CO_2E) is an extremely hot topic in recent years. Unlike fuel cells and water electrolysis, where both acidic electrolytes and alkaline electrolytes can be used, CO2E can only make use of alkaline (poly)electrolytes, so as to suppressed the hydrogen evolution reaction (HER). APEs have been tested for CO_2E, the current density can reach industrial scales, such as 1 A/cm^2. Yet most reports on APE-CO_2E were still using KOH solutions as the anolyte, so as to maintain an alkaline environment at the cathode for the high efficient production of deep-reduction products, such as ethylene. Our recent study has demonstrated the feasibility of operation with pure water.

Details will be provided in the presentation.

Keynote Lecture

Catalytic Lignin Depolymerization and Aromatic Chemicals

Feng WANG

Dalian Institute of Chemical Physics, CAS, China

wangfeng@dicp.ac.cn

[Blank]

Invited Talk

Electrochemical Decarbonization Technology

Guoxiong Wang

Dalian Institute of Chemical Physics, Chinese Academy of Sciences, Dalian, China.

E-mail: wanggx@dicp.ac.cn

Development of electrochemical decarbonization technologies is critical to achieve carbon neutralization. One way is to electrochemically reduce CO_2 to valuable fuels and chemicals, and the other way is to replace traditional industrial process with electrochemical process for reducing CO_2 emission. In this talk, electrochemical CO_2 reduction and NH_3 synthesis will be presented.

CO/CO_2 co-electrolysis over Cu nanosheets was investigated in an alkaline membrane electrolyser[1]. With increasing CO pressure, the major product gradually switches from ethylene to acetate and the current density notably increases. The selectivity switch is ascribed to the increased CO coverage and local pH. The identification of reaction sites by operando Raman spectroscopy and the analysis of reaction pathways by density functional theory calculations indicate that CO preferentially adsorbs on the terrace sites and inclines to generate ethylene at low CO pressure/coverage, whereas the step sites are provided with more CO, resulting in favoured acetate production at high CO pressure/coverage. Under optimized conditions, the Faradaic efficiency and partial current density of C_{2+} products reach 90.0% and 3.1 A cm^{-2}, respectively, with the carbon selectivity and yield of C_{2+} products outperforming thermocatalytic CO hydrogenation. The scale-up demonstration using an electrolyser stack achieves the highest ethylene formation rate of 457.5 ml min^{-1} at 150 A and an acetate formation rate of 2.97 g min^{-1} at 250 A.

Alternative routes to the Haber–Bosch process are being sought to electrify ammonia synthesis. Nitric oxide can be electrocatalytically converted into ammonia, but the Faradaic efficiencies and rates of production are currently far below those needed for industrial application. We report a rationally designed copper–tin alloy that is highly active in the synthesis of ammonia from nitric oxide[2]. The rate of ammonia production in a flow cell reached 10 mmol cm^{-2} h^{-1} with a Faradaic efficiency of >96% at a current density >1,400 mA cm^{-2}, and it remained stable at >600 mA cm^{-2} with an ammonia Faradaic efficiency of ~90% for 135 h. The rate of ammonia production in a scaled-up electrolyser comprising a membrane electrode assembly reached ~2.5 mol h^{-1} with a current of 400 A at ~2.6 V. We attribute the high ammonia production rate to the enhanced intrinsic activity of the alloy; the kinetic barriers of protonation are invariably low over a range of Cu_6Sn_5-derived surface structures.

References

[1] Wei PF, Gao DF, Liu TF, Wang GX, Bao XH et al. *Nat. Nanotechnol.*, 2023, 18, 299.

[2] Shao JQ, Jing HJ, Wang GX, Xiao JP, et al. *Nat. Energy.*, 2023, DOI: 10.1038/s41560-023-01386-6.

Invited Talk

Promote Pd-catalyzed CO_2 to formate conversion via manipulation of the Pd valence state

Lei Wang[a]

[a] *Department of Chemical and Biomolecular Engineering, National University of Singapore, Singapore.*

E-mail: wanglei8@nus.edu.sg

Abstract

Electrochemical CO_2 reduction offers exciting opportunities in turning the waste carbon into value-added chemicals/fuels. Among different CO_2 reduction products, formate has attracted particular interest, as it shows promising near-term economic feasibility. Pd-based electrocatalysts have demonstrated excellent selectivity towards formate production, however, only within a narrow potential window of 0 V to −0.25 V vs. RHE. It has shown that Pd-based electrocatalysts suffer from the potential-dependent deactivation pathways (α-PdH to β-PdH phase transition, CO poisoning, *etc.*) and quickly loss their activity towards formate production. Thus, it is desirable to establish new strategies to enable Pd-based CO_2 reduction over a broader potential window to achieve both energy efficient and practical relevant formate production.

In this work [1], we discovered that polyvinylpyrrolidone (PVP) ligand decorated Pd surface exhibits an unexpected promotion effect on CO_2 electroreduction. Specifically, PVP decorated Pd can afford selective formate production at a much-extended potential window (beyond −0.7 V vs. RHE) with significantly improved activity (14-times enhancement at −0.4 V vs. RHE) compared to that of the pristine Pd surface (Fig. 1). Combined results from physical/electrochemical characterizations, kinetic analysis and first principal simulations suggest that the PVP capping ligand can effectively stabilize the Pd species with high valence state ($Pd^{\delta+}$) resulted from the catalyst synthesis and pretreatments, and these $Pd^{\delta+}$ species are responsible for the inhibited phase transition of α-PdH to β-PdH, as well as the suppression of CO and H_2 formation. Overall, our study confers a desired catalyst design principle: introducing positive charges into Pd-catalysts to enable efficient and stable CO_2 to formate conversion.

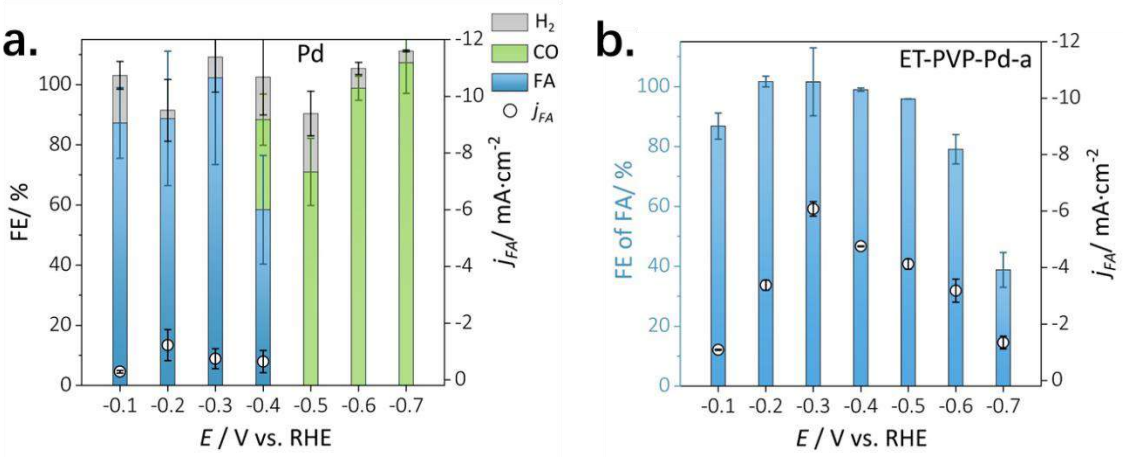

Fig. 1. CO_2 electroreduction performance. FE values (left) and partial current densities (right) for formate production on (a) prinstine Pd from −0.1 V to −0.7 V vs. RHE; (B) PVP treated-Pd from −0.4 V to −0.7 V vs. RHE.

References

[1] Y. Zhao, L. Wang* et al. *PNAS*, 2023, 120 (22) e2218040120.

Invited Talk

Tailoring the molecular interfaces for boosted CO_2 reduction

Ruquan Ye[a]

[a] *Department of Chemistry, City University of Hong Kong, Kowloon Tong, Hong Kong SAR.*

E-mail: ruquanye@cityu.edu.hk

Carbon dioxide reduction to produce various fuels and chemical products can simultaneously fix carbon dioxide and convert renewable electrical energy into chemical energy storage, making it an attractive route to achieve a closed-loop carbon cycle. Metal complexes are an important class of catalysts with the advantages of well-defined and controllable structures. However, due to the molecular aggregation and leaching effects in the catalytic process, the low conversion frequency, low electron transport rate and poor stability in the heterogeneous catalytic process are encountered. This talk will summarize our group's recent progress on carbon dioxide reduction based on metal-organic molecular catalysts, and mainly discuss the influence of catalyst interface aggregation effect on catalytic mechanism and product selectivity; this includes the in-depth understanding of interface electron transport and molecular configuration evolution, which change the product turnover and even selectivity. We demonstrate that interfacial aggregated state realizes efficient and controllable two-electron and multi-electron reduction.

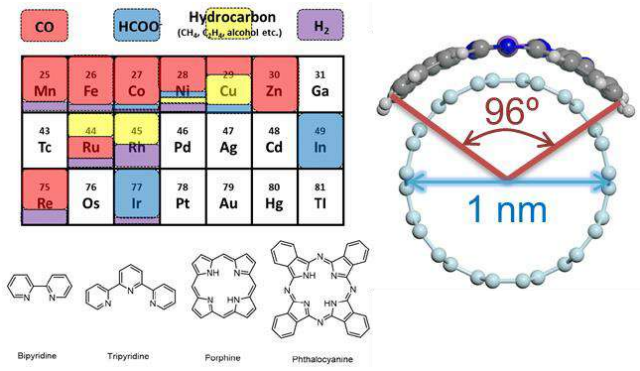

Fig 1. Molecular interfaces for controlled activity

References

[1]Su,# Charles B Musgrave III,# Yun Song, Libei Huang, Yong Liu, Geng Li, Yinger Xin, Pei Xiong, Molly Meng-Jung Li, Hao Ming Chen, Ben Zhong Tang, Marc Robert, William A Goddard III,* Ruquan Ye* *Nature Catalysis*, 2023 6, 818.

[2]Junlai Yu#, Libei Huang#, Qingxuan Tang, Shang-Bo Yu, Qiao-Yan Qi, Jiangshan Zhang, Danying Ma, Yifei Lei, Jianjun Su, Yun Song, Jean-Charles Eloi, Robert L Harniman, Ufuk Borucu, Long Zhang, Minghui Zhu, Feng Tian, Lili Du*, David Lee Phillips*, Ian Manners, Ruquan Ye*, Jia Tian* *Nature Catalysis*, 2023 6, 464

[3]Yun Song, Jun-jie Zhang, Yubing Dou, Zhaohua Zhu, Jianjun Su, Libei Huang, Weihua Guo, Xiaohu Cao, Le Cheng, Zonglong Zhu, Zhenhua Zhang, Xiaoyan Zhong, Dengtao Yang*, Zhaoyu Wang, Ben Zhong Tang, Boris I. Yakobson*, Ruquan Ye* *Advanced Materials* 2022 34 (42), 2110496

[4]J. Su, J.-J. Zhang, J. Chen, Y. Song, L. Huang, M. Zhu*, B. I. Yakobson, B. Z. Tang, R. Ye* *Energy & Environmental Science,* 2021 14, 483

[5]M. Zhu, J. Chen, L. Huang, R. Ye*, J. Xu, Y. Han. *Angewandte Chemie International Edition,* 2019 58, 6595-6599

Oral Presentation

Tailoring the selectivity for liquid products in plasma-enhanced catalytic conversion of CO_2 and CH_4

Pengxian Ye,[a] Debjyoti Ray,[a] Chunshan Song[a]

[a] *Department of Chemistry, Faculty of Science, The Chinese University of Hong Kong, Hong Kong SAR, China.*

E-mail: chunshansong@cuhk.edu.hk

CO_2 conversion to fuels and chemicals is one of the promising ways to reach the carbon neutrality and mitigate the climate change issues. However, efficient and selective conversion of CO_2 and CH_4 into value-added liquid oxygenates under mild conditions remains a challenge in the field of CO_2 utilization. In this work, we report a non-thermal plasma enhanced conversion of CO_2 and CH_4 to liquid oxygenates such as methanol, ethanol, and acetic acid by combining the plasma discharge with different metal-based catalysts. The main liquid products were successfully tailored between methanol and acetic acid by tuning catalyst surface, plasma discharge and process parameters.

Keynote Lecture

Fused-ring electron acceptors for organic photovoltaics

Xiaowei Zhan

School of Materials Science and Engineering, Peking University, Beijing 100871, China.
E-mail: xwzhan@pku.edu.cn

Organic photovoltaic cells (OPVs) possess some merits, such as facile fabrication, visual semitransparency, flexibility, low cost, high mass power density and short energy payback time, and attract considerable attention from both academia and industry. Fullerene derivatives showed higher power conversion efficiencies (PCEs) than other acceptor systems before 2015 and thus dominated as electron acceptor materials for 20 years. However, weak visible absorption of fullerenes and large energy loss in fullerene-based devices limit the theoretical PCE of fullerene-based OPVs to ~13%, and morphological instability of fullerenes leads to short device lifetime thus restricts the practical application of OPVs. Although some nonfullerene acceptors such as rylene diimides have achieved PCEs around 10-11%, the lack of optimal electron acceptors hinders further development of the OPV field.

In 2015 we invented the milestone molecule ITIC,[1] pioneered the conception of "fused-ring electron acceptor (FREA)",[2] and then built up a FREA family.[3-9] The FREAs present some advantages: 1) Their chemical structures are facile to tailor and synthesis is easy to scale up; 2) Their absorption and energy levels can be tuned and thus match with various high-performance electron donors; 3) Their crystallinity and film morphology can be regulated; 4) They exhibit strong and broad absorption, especially in the 700–1000 nm range, and can match with wide-bandgap donor materials to achieve panchromatic absorption; 5) They have high exciton diffusion coefficients and low exciton binding energy which are beneficial for exciton dissociation; 6) They show small energy losses in devices.[10] Single-junction OPVs based on these FREAs exhibit power conversion efficiencies of >19%, which far surpass fullerene acceptor counterparts (~12%). Moreover, the FREA-based OPVs exhibit good morphology stability and long device lifetime. Now FREAs invented by Zhan group are commercial available from >10 companies. Around 350 research groups in >20 countries have utilized these FREAs to fabricate high-efficiency OPVs. The emergence of high-performance FREAs has begun to marginalize previously predominant fullerene acceptors, and is inaugurating nonfullerene era of the OPV field.

References

1 Lin Y, Wang J, Zhang ZG, Bai H, Li Y, Zhu D and Zhan X. *Adv. Mater.*, 2015, *27*, 1170–1174.
2 Lin Y, He Q, Zhao F, Huo L, Mai J, Lu X, Su C, Li T, Wang J, Zhu J, Sun Y, Wang C and Zhan X. *J. Am. Chem. Soc.*, 2016, *138*, 2973-2976.
3 Lin Y, Zhao F, He Q, Huo L, Wu Y, Parker T, Ma W, Sun Y, Wang C, Zhu D, Heeger A, Marder S and Zhan X. *J. Am. Chem. Soc.*, 2016, *138*, 4955-4961.
4 Dai S, Zhao F, Zhang Q, Lau TZ, Li T, Liu K, Ling Q, Wang C, Lu X, You W and Zhan X. *J. Am. Chem. Soc.*, 2017, *139*, 1336-1343.
5 Yan C, Barlow S, Wang Z, Yan H, Jen AKY, Marder S and Zhan X. *Nat. Rev. Mater.*, 2018, *3*, 18003.
6 Wang J, Zhang J, Xiao Y, Xiao T, Zhu R, Yan C, Fu Y, Lu G, Lu X, Marder S and Zhan X. *J. Am. Chem. Soc.*, 2018, 140, 9140-9147.
7 Zhang M, Dai S, Chandrabose S, Chen K, Liu K, Qin M, Lu X, Hodgkiss J, Zhou H and Zhan X. *J. Am. Chem. Soc.*, 2018, 140, 14938-14944.
8 Jia B, Wang J, Wu Y, Zhang M, Jiang Y, Tang Z, Russell T and Zhan X. *J. Am. Chem. Soc.*, 2019, *141*, 19023-19031.
9 Li T, Wu Y, Zhou J, Li M, Wu J, Hu Q, Jia B, Pan X, Zhang M, Tang Z, Xie Z, Russell T and Zhan X. *J. Am. Chem. Soc.*, 2020, *142*, 20124-20133.
10 Wang J, Xue P, Jiang Y, Huo Y and Zhan X. *Nat. Rev. Chem.*, 2022, *6*, 614-634.

Keynote Lecture

Strategic Incorporation of Cleavable Side Chains Improves Thermal Stability of Polymer Solar Cells

Wei You,[a] Jordan Shanahan,[a] Jiyeon Oh,[a] Sungyun Son,[a] Selma Siddika,[b] Brendan T. O'Connor.[b]

[a] *Department of Chemistry, University of North Carolina at Chapel Hill, Chapel Hill, NC, 27599, USA.*

[b] *Department of Mechanical and Aerospace Engineering, North Carolina State University, Raleigh, NC, 27695, USA*

E-mail: wyou@unc.edu

Thermal degradation by intrinsic morphological change and extrinsic oxidation remain outstanding challenges for bulk heterojunction (BHJ) based polymer solar cells (PSCs). Post-processing thermocleavage of side chains on the donor conjugated polymers using ester pyrolysis is an emergeing method to kinetically trap morphology via increased glass transition temperature (T_g) and improved thermal oxidation resistance.[1] In this presentation, I will discuss our efforts in using thermoclevable side chains (TCS) incorporated into conjugated polymers to achieve high thermal stability to the BHJ devices. Particulary, I will discuss the most recent advances in our lab to expand the concept of using the copolymerized TCS monomer unit to balance the stability with efficiency into state-of-the-art PSC system PffBT-T4-OD:PCBM, where the original octyl-decyl (OD) branched sidechains are partially replaced with TCS in 50-70 mol% in the copolymers.[2] TCS content drastically increases the polymer resistance to oxidation. PSCs made with the fully cleavable PffBT-T4-TCS polymer only offer on a meager efficiency of 0.2%, while the copolymer with 60 mol% TCS can deliver a PCE of 3.2% with its BHJ device, double the previous highest reported efficiency for TCS containing polymer-based PSCs. Importantly, the copolymer with 60 mol% TCS based device is stable, retaining 80% of the initial performance after accelerated aging tests (100 ℃, 2 weeks). These new findings demonstrate that using partial cleavage of side chains could be a general strategy to gain both efficiency and stability for conjugated polymers-based PSCs.

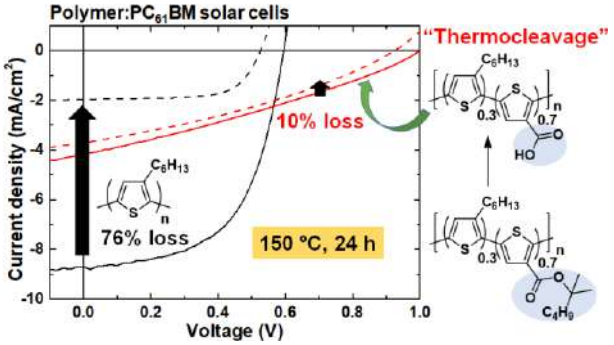

Figure 1. Applying TCS to P3HT

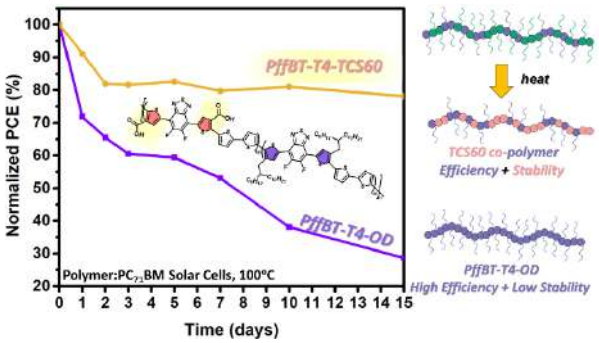

Figure 2. Extending TCS to PffBT-T4-OD

References

[1] Son, S.Y., Samson, S., Siddika, S., O'Connor, B.T., andYou, W. *Chem. Mater.* 2021*, 33 (12),* 4745–4756.

[2] Shanahan, J., Oh, J., Son, SY., Siddika S., Pendleton, D., O'Connor B.T., and You, W. submitted.

Invited Talk

Strategies for boosting the performance of organic photovoltaics

Thomas D. Anthopoulos,[a]

[a] *King Abdullah University of Science and Technology (KAUST), Thuwal 23955-6900, Saudi Arabia.*

E-mail: thomas.anthopoulos@kaust.edu.sa

The recent step change in power conversion efficiency (PCE) of organic photovoltaics (OPVs) has been primarily driven by significant advancements in the synthesis of new materials and the reduction of performance losses associated with traditional cell architectures. This presentation will discuss our most recent OPV research, focusing on practical strategies for boosting cell performance beyond the state-of-the-art. Firstly, I will describe our use of innovative charge-extracting interlayers and the multitude of benefits they offer for deployment in next-generation OPVs. Next, I will present our latest progress in utilizing molecular dopants to enhance PCE, and demonstrate how their combination with the aforementioned innovative interlayers and cell architectures can improve material utilization, device circularity, and maintain high performance and stability.

Invited Talk

Asymmetric design of electron acceptors for high performance organic solar cells

Hongzheng Chen

Department of Polymer Science & Engineering, Zhejiang University, Hangzhou 310027, P. R. China

E-mail: hzchenr@zju.edu.cn

Organic solar cells (OSCs) show great promise in renewable development, with the power conversion efficiency (PCE) over 19% for single cells. However, the efficiency is still a shortcoming for the future industrialization of OSCs, compared with other solar cells. In this presentation, I will share our strategies to solve this issue. I will introduce new design strategies to access small molecule electron acceptors with asymmetric structures for high performance OSC applications. The asymmetric design of the acceptor allows the simultaneous achievement of enhanced charge generation and reduced energy loss. As a result, high efficiency is obtained in the binary OSCs by carefully designing asymmetric terminals for acceptors. Efficiency over 19% is also realized in the ternary OSCs with the asymmetric electron acceptor as the third component.

References

[1] Li S, Zhan L, Jin Y, et al. *Adv. Mater.* 2020, *32*, 2001160;

[2] Zhan L, Li S, Xia X, et al. *Adv. Mater.* 2021, *33*, 2007231;

[3] He C, Bi Z, Chen Z, et al. *Adv. Funct. Mater*. 2022, 2112511

[4] Zhan L, Li S, Li Y, et al. *Joule* 2022, *6*: 662

[5] Chen T, Li S, Li Y, et al. *Adv. Mater.* 2023, *35*, 2300400

Invited Talk

Strategies for Engineering Performance Improvements in Perovskite Photovoltaics

Martyn A. McLachlan

Department of Materials, Imperial College London, Molecular Sciences Research Hub,

82 Wood Lane, London, UK.

E-mail: martyn.mclachlan@imperial.ac.uk

Metal halide perovskites (MHPs) continue to stimulate interest, generate significant research volume, and fuel scientific discussion and debate. The rapid evolution and deployment of MHPs to the commercial realm has been a remarkable journey. These materials, and their precursors, afford numerous synthetic pathways from a plethora of starting materials via a variety of processes – the sum of which are complex, multi-component functional materials around which numerous scientific questions remain unanswered. Here we investigate the role of additives and post-deposition processing and their influence of morphology and microstructure on photovoltaic device performance and MHP stability.

Many strategies have emerged for tuning the properties of MHPs from substitutional doping to influence bandgap and electronic properties to additive incorporation to tune lifetime and stability – collectively resulting in a diverse range of compositions or “flavours” of MHPs being reported. Here I will discuss strategies reliant on additive incorporation that result in improvements in photovoltaic device performance and stability. In parallel we consider the interaction such additive molecules have with the MHP films and by utilising a range of correlative characterisation techniques we probe the location where our additives reside and the influence they have on the microstructure and morphology. By carrying out systematic studies of isolated MHP films, films sandwiched with interlayers and complete devices we explain the key relationships between structure, composition, and performance of our additive engineered perovskite solar cells.

References

[1] Liang W, Xu H, Carraro F, et al. *J. Am. Chem. Soc*., 2020, *In Press*;

[2] Konkankit CC, Lovett J, Harris HH and Wilson JJ. *Chem. Commun.*, 2020, *56*, 6515-6518.

Keynote Lecture

Materials Development for Organic Solar Cells

Martin Heeney,[a]

[a] Physical Sciences and Engineering Division (PSE), King Abdullah University of Science and Technology (KAUST); [b] Department of Chemistry, Imperial College London

E-mail: martin.heeney@kaust.edu.sa

Organic solar cells are an emerging technology which can complement existing photovoltaic technologies. They are appealing because of their compatibility with high-throughput manufacture as well as their range of possible product forms. Their performance can be tuned through chemical design, and in this talk I will discuss our work to develop active materials and dopants for organic photovoltaic blends. I will show how device efficiency can be tuned via the development of novel fused aromatic building blocks. I will highlight how the efficiency of the photovoltaic blend is influenced by the aggregation of the component materials, which can be tuned by molecular design. Subtle changes to the solubilizing sidechains are shown to led to significant changes in device efficiencies, and given the difficulty in predicting the best sidechain to use, I will show how libraries of donor polymers can be readily fabricated with a variety of sidechains. This allows their influence on polymer properties, such as solubility, surface energy, self-assembly and device performance to be identified. Such approaches additionally allow for the identification of polymers which can be readily upscaled. Finally I will highlight our recent efforts to develop n-type dopants and their application in solar cell devices.

Invited Talk

Materials Design and Challenges for Non-fullerene Organic Solar Cells

He Yan

Hong Kong University of Science and Technology

Organic solar cells (OSCs) are flexible, semi-transparent and environmentally friendly devices which can be installed in areas where silicon panels are not suitable (such as glass windows on buildings). Conventional OSCs are based on fullerene acceptors as a key component. However, fullerene-based OSCs can only achieve modest efficiency of 12% at best, due to their large voltage loss (above 0.8V), and poor device stability.

Recently, there has been a major revolution in the OSC field, as researchers developed many high-performance non-fullerene acceptors that can overcome the limitation of traditional fullerene acceptors and open a new era for the OSC field. One of the unique features of non-emerging non-fullerene OSCs is the surprisingly small voltage losses of the devices (~ 0.5V). Since 2016, our team at HKUST has developed a range of non-fullerene systems that can simultaneously generate high photocurrent (near 100% yield) with small voltage losses (first published in Nature Energy). Moreover, we have recently achieved record-breaking OSCs based on a state-of-the-art non-fullerene acceptor, achieving an unprecedented efficiency of over 20% in single-junction OSC device. Our work clearly indicates that OSCs have the potential to reach the high efficiency of inorganic solar cells. Our results show that the key factor is the long charge transfer life-time that allows for efficient charge separation despite of a small energy offset. In the other aspect, we study structure-property relationship of high-performance donor and non-fullerene acceptor materials and reveal the key structure features that enable highly efficient non-fullerene organic solar cell devices.

Invited Talk

Revealing Solution Aggregate Structures of Polymers and Film Formation Kinetics on Film Morphology in Organic Solar Cells

Yanchun Han, Qiang Zhang, Ye Yan, Yading Liu

State Key Laboratory of Polymer Physics and Chemistry, Changchun Institute of Applied Chemistry, Chinese Academy of Sciences, 5625 Renmin Street, Changchun 130022, P. R. China

E-mail: ychan@ciac.ac.cn

Organic solar cells (OSCs) have emerged as a promising technology for next-generation photovoltaic applications due to their desirable features, such as flexibility, light weight, and solution-processability. In most organic materials, the short exciton diffusion length, which is typically only a few nanometers, is a critically limiting factor for achieving high efficiency OSCs. BHJ exhibiting nanoscale phase separation between the donor-acceptor (D-A) mixture has been recognized for its ability to overcome the limitation of short exciton diffusion lengths. However, the morphology of the solution-processed active layer is difficult to control because of thermodynamic and dynamics factors, i.e., different polymers solution aggregate structures and rapid solidification process of the active layer upon the fast removal of solvent. These result in a kinetically trapped state with undesired morphology. In this talk I will address our several strategies to change the liquid-solid phase transition and crystallization kinetics during film formation to optimize the phase-separated morphology and boost the photovoltaic performance.

Invited Talk

Monolithic Perovskite/Organic Tandem Solar Cells

Angus Hin-Lap Yip[1,2,3*]

1. Department of Materials Science and Engineering, City University of Hong Kong

2. School of Energy and Environment, City University of Hong Kong

3. Hong Kong Institute for Clean Energy, City University of Hong Kong

In this talk, I will discuss our work on developing high-performance monolithic perovskite/organic tandem solar cells comprising a wide bandgap perovskite (WBG) front cell and a narrow bandgap (NBG) organic rear cell connected through a recombination junction. The WBG (Eg: 1.7-1.85 eV) PSCs are chosen for the front cell due to their strong and broad absorption for visible light, smaller voltage loss, and higher photoresponse compared to their organic counterparts with approximate bandgap. While NBG (Eg: 1.1-1.25 eV) OSCs can offer better near-infrared absorption tunability and stability compared with the Sn-based NBG perovskites, making them favourable candidates for the rear cell.[1,2] Moreover, the advantage of the perovskite and organic light absorbing layers being processed from orthogonal solvents imposes fewer constraints on the choice of the materials for constructing the recombination junction and provides better flexibility on the device design of tandem solar cells. To demonstrate state-of-the-art perovskite/organic tandem cells, an integrated strategy combining materials, interface, optical, and process engineering was adopted to optimize the two subcells and the interconnect junction simultaneously.[3,4,5] In addition, a comprehensive optoelectronic model is being developed to simulate the electrical and optical properties of the tandem solar cells and to provide guidelines to optimize their device performance. The successful development of perovskite/organic tandem cells will have far-reaching impacts on producing high-efficiency, low-cost and scalable PV cells for clean energy production.

References

[1] Yip, H. L. et al, Monolithic perovskite/organic tandem solar cells: Developments, prospects, and challenges. *Nano Select* 2021, *2*, 1266-1276.
[2] Yip, H.-L. et al, Homogeneous grain boundary passivation in wide-bandgap perovskite films enables fabrication of monolithic perovskite/organic tandem solar cells with over 21% efficiency. *Adv. Funct. Mater.* 2022, *32*, 2112126.
[3] Yip H.-L. et al, Dual Sub-Cells Modification Enables High-Efficiency n–i–p Type Monolithic Perovskite/Organic Tandem Solar Cells. *Adv. Funct. Mater.* 2023, *33*, 2212599.
[4] Yip, H.-L et al, All-Inorganic Perovskite-Based Monolithic Perovskite/Organic Tandem Solar Cells with 23.21% Efficiency by Dual-Interface Engineering. *Adv. Energy. Mater.*, 2023, *13*, 2204347.
[5] Yip, H.-L et al, Optimizing Crystallization in Wide-Bandgap Mixed Halide Perovskites for High-Efficiency Solar Cells. *Adv. Mater.*, 2023, *35*,2306568

Invited Talk

Nanomaterials and Perovskites: A Joint Effort to Generate Sustainable Power

Thomas J. Macdonald[a]

[a] *School of Engineering and Materials Science, Queen Mary University of London, London E1 4NS, United Kingdom*

E-mail: t.j.macdonald@qmul.ac.uk

Emerging perovskite materials are routinely studied as nanostructures, polycrystalline films, or single crystals and have opened up new pathways for optoelectronic device designs (e.g. photovoltaics). Combining perovskite materials with other nanostructures or bespoke charge selective contact layers has also proven beneficial to both performance and building fundamental understandings of their operation in photovoltaics and beyond (Figure 1). Herein, we discuss a variety of perovskite structures and device architectures with an emphasis on understanding their surface chemistry as well as interfacial interactions between the light-absorbing materials and their contacts.[1-4] Additionally, experimental techniques that will facilitate the measurement of charge carrier dynamics at both the surface of the materials, as well as at the interface, will be discussed.

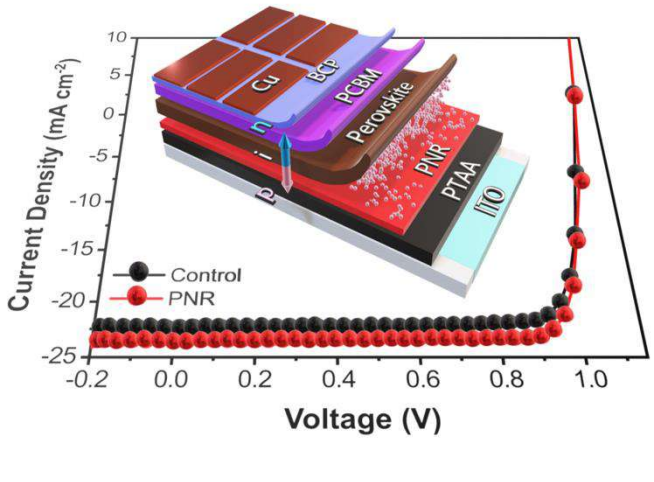

Figure 1: *J-V* characteristics and device stack for phosphorene nanoribbon loaded perovskite solar cell.

References

1. T.J. Macdonald, L. Lanzetta, X. Liang, et al. *Adv. Mater*. 2023. 2206684.

2. T.J. Macdonald, A.J. Clancy, R.R.C. Shutt, et al. *Joule*. 2022. 6, 11, 2441-2446.

3. T.J. Macdonald, A.J. Clancy, W. Xu, et al. *J. Am. Chem. Soc*. 2021. 143, 51, 21549–21559.

4. F.M. Rombach, S.A. Haque, T.J. Macdonald. *Energy Environ. Sci*. 2021. 14, 10, 5161-5190.

Invited Talk

Strategies toward high-performance polymer-based solar cells

Philip C.Y. Chow[a]

[a] *Department of Mechanical Engineering, The University of Hong Kong, HKSAR, China*

E-mail: pcyc@hku.hk

Solar photovoltaic (PV) technology is one of the most efficient ways to generate clean renewable energy. However, the current solar PV energy usage only occupies a very small fraction of the world's total energy portfolio. In Hong Kong, solar power is much lower than the 1% to 1.5% target set by the government by 2030. Today's solar PV panels are made of crystalline silicon, which are rigid, opaque, heavy and expensive to manufacture. These properties greatly limit the installation of solar panels in urban city environments (e.g. with buildings). Therefore, the development of an alternative solar PV technology suitable for large-scale building integration is urgently needed. In this talk, I will discuss the latest research developments in polymer-based solar energy harvesting technologies, which are suitable for urban applications thanks to their mechanical flexibility, lightweight, non-toxicity, low manufacturing costs and colour tunability. The prospects of these technologies and key challenges towards their large-scale application will also be discussed.

Earth and Energy Transition Session (3 December)

Keynote Lecture

Research on geophysical exploration and monitoring technologies in carbon dioxide geological sequestration

Yibo Wang[a], Yikang Zheng[a], Qiang Luo[a], Siwen Wang[a], Xu Chang, Rongshu Zeng[a]

[a] *Key Laboratory of Petroleum Resource Research, Institute of Geology and Geophysics, Chinese Academy of Sciences, Beijing, China*

E-mail: wangyibo@mail.iggcas.ac.cn

In pursuit of carbon reduction objectives, carbon dioxide geological sequestration will play a pivotal role. Despite current cost-related challenges, it remains a highly promising carbon mitigation technology. Addressing the full lifecycle of geological sequestration presents various geophysical exploration and monitoring challenges. In recent years, our research team have undertaken corresponding research in the identification of high-quality reservoirs for carbon dioxide storage, time-lapse seismic imaging/inversion, CO2 fluid transport simulation, and related aspects within the carbon dioxide geological sequestration.

Addressing the challenges of site selection and high-quality reservoir identification in carbon dioxide geological sequestration and construction, we propose a method for extracting seismic texture attributes based on a high-dimensional co-occurrence matrix. This approach encapsulates three-dimensional spatial orientation information within a high-dimensional co-occurrence matrix, reducing the dependency of attribute extraction on geological orientations and resolving the issues of directional distortion in traditional methods. Effective identification of the primary reservoir distribution in carbon dioxide geological sequestration areas is achieved through the application of this method.

In the monitoring of injected CO2 fluid in carbon dioxide geological sequestration, an improved method for time-lapse Vertical Seismic Profile (VSP) seismic imaging of multiples has been employed. This method extends the imaging coverage and enhances imaging resolution. The acquired primary and multiples imaging profiles can be used to analyze the underground structural changes. To invert the velocity changes caused by injected CO2 in the deeper reservoirs, we propose a frequency-dependent reflection wave-equation traveltime inversion method. It can effectively invert the P-wave velocity from the collected time-lapse walkaway VSP data. This process allows for the determination of the extent and trends of CO2 fluid migration based on the differences in P-wave velocity.

Regarding the safety assessment post-sequestration, a geological model of the area has been established with seismic constraints, and CO2 fluid transport simulations have been conducted. This study adds 3D seismic horizon information constraints to the spatial interpolation method to construct a geological model that is more suitable for the actual stratigraphy characteristics, thereby obtaining more reliable numerical simulation results. These simulations predict the maximum range of CO2 fluid transport over the next 50 years. The entire workflow provides a rational basis for assessing the safety of CO2 sequestration.

In future research, we plan to further refine these methods and, ultimately, establish a multidisciplinary system for geophysical exploration and monitoring technology in carbon dioxide geological sequestration, through a combination of geological interpretation, seismic imaging/inversion, and reservoir simulation.

References

[1] Wang S, Wang Y, Zheng Y, et al., Comparison of geological models for the simulation of CO2 migration a case study in Ordos, China, GGST, *Greenhouse Gas Science Technology*, 2021, 11, 277-296.

[2] Luo Q, Wang Y, Zheng Y, et al., High dimensional co-occurrence matrix A new tool for 3D seismic target visualization and interpretation, *Interpretation*, 2020, 8(4), T967–T979.

[3] Zheng Y, Wang Y, Chang X,VSP Imaging Using Free-Surface Multiples With Wavefield Decomposition: Synthetic and Field Data Examples, *Frontiers in Earth Science,* 2021, 9, 730184

[4] Zheng Y, Wang Y, Luo Q, et al., Frequency-dependent reflection wave-equation traveltime inversion from walkaway vertical seismic profile data, *Geophysics*, 2019, 84(6), R959–R973.

[5] Luo Q, Wang Y, Wang Y, et al., Time-lapse VSP monitoring for CO2 injection A case study in ordos, China, *International Journal of Greenhouse Gas Control*, 2018, 75, 41-51.

Invited Talk

Signatures of subsurface fluids in the earthquake waveforms

Hongfeng Yang,[a] Aqeel Abbas [a] Jinping Zi[a]

[a] *Earth and Environmental Sciences Programme, The Chinese University of Hong Kong, Shatin, Hong Kong;*

E-mail: hyang@cuhk.edu.hk

Hydraulic Fracturing (HF) often stimulates the local earthquake productivity which provides a unique opportunity to characterize the crustal heterogeneities, reservoir properties, and fluid injection effects. However, the velocity models acquired solely based on the arrival time records are often undermined due to the seismic network coverage and interpolation techniques. Instead, we adopt the waveform-based approach to apprehend; (1) structural heterogeneities, (2) reservoir distribution, and (3) signatures of the injected fluid in the Weiyuan shale gas field (WSGF). We categorize the waveforms into dominant high and low frequencies based on the qualitative inspection and frequency index analysis of the seismic waveforms. We first inspect the waveform to access the potential controlling mechanisms (source, site, and path effects) at both single and multiple stations in different azimuthal orientations. As a result, we find the path effect as a dominant factor to influence the waveform characteristics, especially S-waves amplitude, and frequency. Subsequently, to localize the path effect, we conduct an in-depth examination of events within 10 km of each seismic station and classify the waveform record into low and high frequency using the frequency index method. Notably, certain stations record a significant proportion of low-frequency waveforms (LFWs) (up to 20%), while others have limited occurrences (~1%) indicating suspected anomalous zones. Afterward, we identify two suspected anomalous zones based on LFWs intensity and ray tracing map. Both zones are in close proximity to fault zones and preserved reservoirs with no HF activities. Hence, we infer that these LFWs are not solely affected by structural variations but may also be associated with the reservoir. However, a comprehensive analysis that incorporates precise localization and characterization of these factors necessitates the deployment of a dense seismic network.

References

[1] Liang W, Xu H, Carraro F, et al. *J. Am. Chem. Soc*., 2020, *In Press*;

[2] Konkankit CC, Lovett J, Harris HH and Wilson JJ. *Chem. Commun.*, 2020, *56*, 6515-6518.

Invited Talk

Stability Analysis of Underground Storage Caverns for Energy Products using FDEM

Qi Zhao,[a] and Huanyu Wu,[a]

[a] *Department of Civil and Environmental Engineering, The Hong Kong Polytechnic University, Hong Kong SAR, China*

E-mail: qi.qz.zhao@polyu.edu.hk

Underground caverns have been increasingly exploited for the storage of energy products. They have better performance on safety, security, economy, and greater environmental acceptance compared with traditional storage infrastructures such as storage tanks and pipelines. In this study, we employ a 2D hydro-mechanical coupled hybrid finite-discrete element method (FDEM) to simulate the excavation and operation processes of an underground storage cavern. The performance of the water curtain system (WCS) is evaluated, and the influence of the natural discrete fracture network (DFN) is considered..

The simulation results captured the propagation and slipping of the pre-existing DFN during the excavation and operation process. We quantitatively evaluate the containment performance based on the water inflow and pore pressure distribution. Our results demonstrate that the injection pressure of WCS is essential in controlling the pore pressure distribution in the host rock, which affects the containment performance of the storage cavern. Both hydraulic gradient and water inflow are greatly promoted by rising the WCS pressure. However, our results suggest that injection of high-pressure water may reactivate frictional slipping on natural DFN. The hydraulically induced slip may cause additional weakening of the fractures and potential coalescence of them, which could raise unexpected risks to the stability of surrounding rock masses. Our study provides new insights into evaluating the stability of cavern-surrounding rock masses and the containment performance of underground storage caverns.

Oral Presentation

Stress Transfer Outpaces Injection-Induced Aseismic Slip and Triggers Seismicity[1]

Yuyun Yang,[a] Hongfeng Yang,[a,b,c] Jinping Zi[a]

[a] *Earth and Environmental Science Programme, The Chinese University of Hong Kong, Shatin, Hong Kong;* [b]*Shenzhen Research Institute, The Chinese University of Hong Kong, Shenzhen, China;* [c]*Institute of Environment, Energy and Sustainability, The Chinese University of Hong Kong, Shatin, Hong Kong.*

E-mail: yuyunyang@cuhk.edu.hk

As concerns rise over damaging earthquakes related to industrial activities such as hydraulic fracturing, geothermal energy extraction and wastewater disposal, it is essential to understand how subsurface fluid injection triggers seismicity even in distant regions where pore pressure diffusion cannot reach. Previous studies suggested long-range poroelastic stressing and aseismic slip as potential triggering mechanisms. In this study, we show that significant stress transfer far ahead of injection-induced aseismic slip can travel at much higher speeds and is a viable mechanism for distant earthquake triggering. It could also explain seismicity migration that is much faster than aseismic slip front propagation. We demonstrate the application of these concepts with seismicity triggered by hydraulic fracturing operations in Weiyuan Shale Gas Field, China. The speed of stress transfer is dependent on the background stress level and injection rate, and can be almost an order of magnitude higher than that of the aseismic slip front.

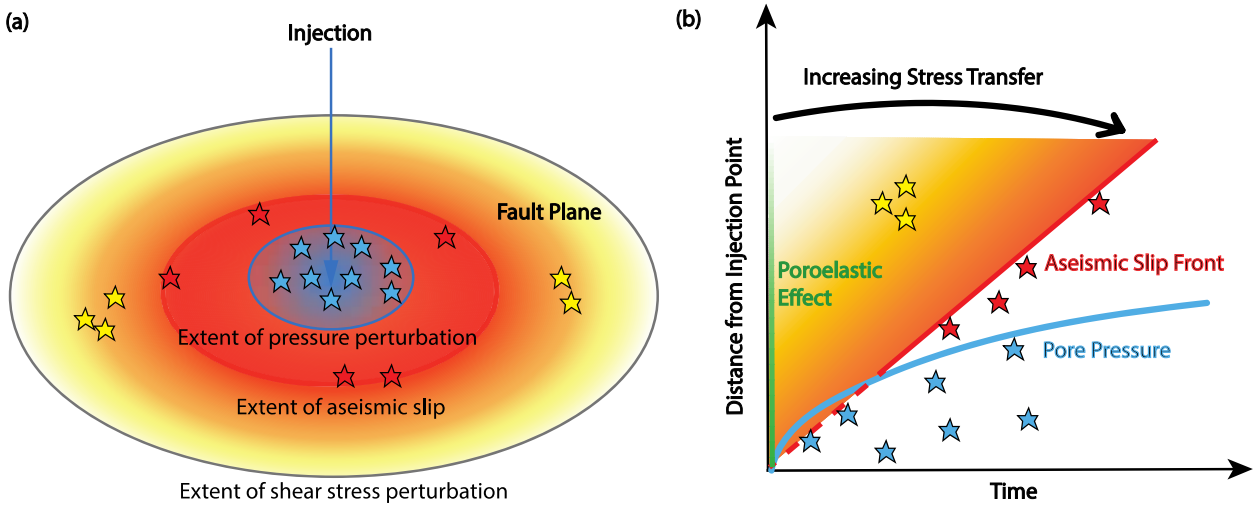

Figure 1. (a) Schematic diagram showing the extent of influence of pore pressure, aseismic slip and shear stress perturbations on a fault at a moment sometime after injection begins. Earthquakes caused by each factor are marked as stars in corresponding colours. (b) Migration speed of pore pressure (blue) and aseismic slip (red), and the influence of poroelastic effect (green). A range of Coulomb failure stress transfer of varying magnitudes is possible outside of the aseismic slip front, which can be considered as the front of maximum stress perturbation. Stress transfer increases as we get closer to the slip front, but even far ahead of the slip front, small magnitudes of stress transfer are already being radiated and could have an impact on distant triggering of seismicity. Representative earthquakes caused by each factor are marked as stars in corresponding colours. The yellow stars are characteristic of distant earthquakes that could be triggered by stress transfer ahead of the aseismic slip front.

References

[1] Yang Y, Yang H, Zi J. *Sci. Rep.*, 2023, *13,* 16626.

Oral Presentation

Least-squares reverse time migration of vertical seismic profile data for CO_2 storage monitoring

Jizhong Yang[a], Jingjing Zong[b], Arthur Cheng[c], and Yunyue Elita Li[d]

[a] *School of Ocean and Earth Science, Tongji University, Shanghai, China;* [b] *School of Resources and Environment, University of Electronic Science and Technology of China, Chengdu, China;* [c] *Earth Systems Science Programme, The Chinese University of Hong Kong, Shatin, Hong Kong, China;* [d] *Department of Earth, Atmospheric, and Planetary Sciences, Purdue University, West Lafayette, IN, USA*

E-mail: 10yangjizhong@tongji.edu.cn

Vertical seismic profile (VSP) survey has been frequently used for reservoir characterization and CO2 storage monitoring. Reverse time migration (RTM) of VSP data could provide much higher resolution images when compared with surface seismic data[1]. However, due to limited illumination of VSP survey, the resulting migration profile suffers from severe artifacts and imbalanced amplitude, and it may sensitively affected by errors present in the migration velocity model. In this study, we proposed a least-square RTM with subsurface offset extension (LSETM) method for VSP data. Our method could provide much better migration profile than conventional RTM with less migration artifacts and balanced amplitude. In particular, our method is less sensitive to the migration velocity errors. Field data application demonstrates the superior of the proposed method. We think this method will benefit the monitoring of CO2 sequetration, especially for dealing with time-lapse seismic data.

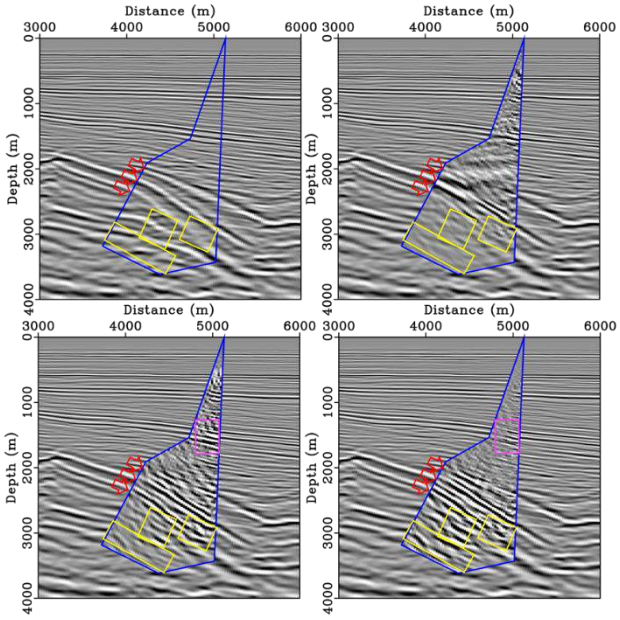

Figure 1: (a) The surface seismic image is overlaid by (b) the conventional RTM VSP image, (c) the stacked ERTM VSP image, and (d) the stacked LSERTM VSP image. The blue polygons separate the VSP images and the background surface seismic image.

References

[1] Zong J, Yang J, Cheng A, et al. *Geophysics*, 2022, 87, B1-B8.

Keynote Lecture

Systematic study of the induced seismicity in the Changning shale gas field in China

Junlun Li[a], Jian Xu[a], Wen Yang[a], Haijiang Zhang[a], Renqi Lu[b], Yuyang Tan[c], Yang Zang[d], Lingyuan Meng[d]

[a]*School of Earth and Space Sciences, University of Science and Technology of China, Hefei, China;*

[b]*Institute of Geology, China Earthquake Administration, Beijing, China*

[c]*College of Marine Geosciences, Ocean University of China, Qingdao, China;*

[d]*China Earthquake Networks Center, Beijing, China.*

E-mail: lijunlun@ustc.edu.cn

The Changning field is one of the largest shale gas fields in the world and has been under increasing production since 2013. However, 53 moderate to strong induced earthquakes[1] (*M*>3.5) have infested this area since then, including the damaging Xingwen *M*5.7 and the Gongxian *M*5.3 earthquakes occurring in Dec. 2018 and Jan. 2019. Until now, there still lacks a comprehensive study on the induced seismicity problem in this area. By compiling datasets monitored by several dense local monitoring networks relaying from 2016 to 2023, we obtained a very comprehensive, eight-year-long seismicity catalog with high location accuracy. In this talk, we will present a systematic study of the induced seismicity for the Changning field, by integrating high resolution velocity models from passive and active sources, stratigraphy and well data, fault characterization, stress analysis, as well as source attribute analysis for the hundreds of thousands of induced earthquakes ranging from *M*-1.0 to *M*5.7. We have noticed some intriguing remote or cascading triggering and rupturing behaviors that may not have been well observed in other shale gas fields in the world.

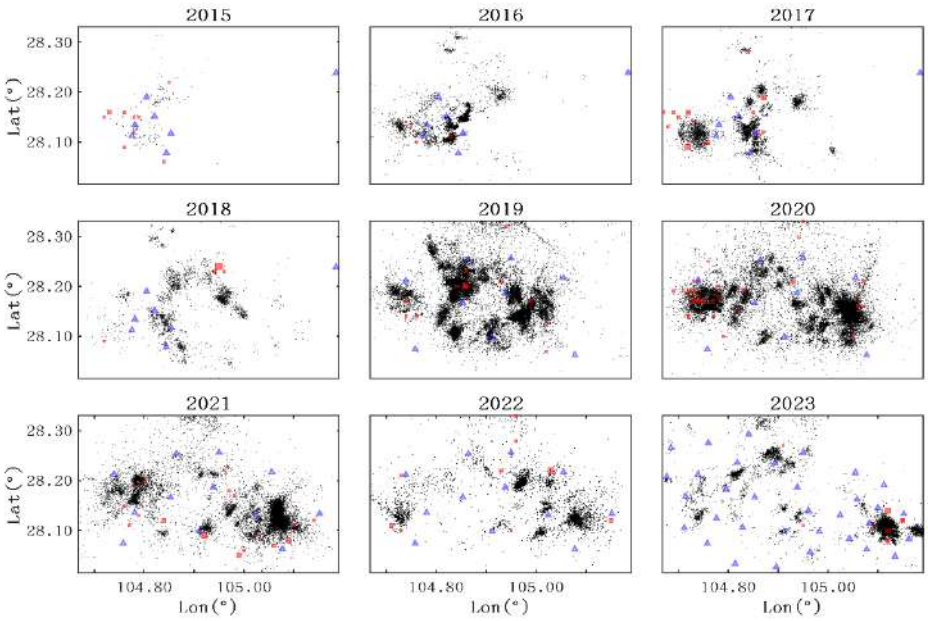

Figure 1. annual seismicity statistics for the Changning shale gas field from 2015 to 2023.

References

[1]Li J, Xu J, Zhang H, et al. *Comm. Earth and Environ.*, 2023;

Invited Talk

On the non-double-couple components of small-moderate magnitude earthquakes

Ruijia Wang,[a] Lichun Yang[a]

[a] *Department of Earth and Space Sciences, Southern University of Science and Technology*

E-mail: wangrj@sustech.edu.cn

Although most earthquakes occur on near-linear planes and generate shear motions, the small-moderate magnitude events may contain explosive or non-linear features, which translate into the "non-double-couple" components in the full moment tensors. However, constraining such secondary components remains challenging and often involves full-waveform based modelling, demanding high-resolution 3D velocity structures that are barely available at local scales. Alternatively, the recent boost of the dense nodal array provides an opportunity to resolve full moment tensors using only body waves.

In this study, we introduce an algorithm that joints different far-field observations, including the direct P-wave polarities, amplitudes, and the S/P amplitude ratios, to constrain and virtualize the non-double-couple components of small earthquakes. We first employ a grid search method to explore the 6-D space of the moment tensor, generating synthetic P- and S-wave amplitudes for each moment tensor. The optimal solution and corresponding uncertainties are then resolved by evaluating the misfit between observed and synthetic data. Finally, the resolved seismic source is decomposed and projected onto the state-of-the art source type plot (i.e., the lune plot) for virtualization.

The efficiency and accuracy of our metric are tested with both synthetic data and field observations near a hydraulic-fracturing well (i.e., ToC2ME in Western Canada), where both microseismicity and induced seismicity are present during fracking. We adopted the angular difference ω (i.e., range from 0 to 180°) to quantify the difference between two moment tensors and obtained averaged ω values below 2° during the synthetic test, indicating the robustness of our metric. For the application to ToC2ME, the inversion results for 167 M>1 events are consistent with the previous results from Zhang et al. (2019), wherein 93% of events displayed ω values less than 20°and more interpretable non-double-couple components. Our method can be easily applied to other contexts and assist the evaluation of local earthquake sources that may contain anthropogenic contributions (i.e., induced seismicity, mine blasts, and collapses), as well as natural events within complex systems (i.e., volcanic tremors).

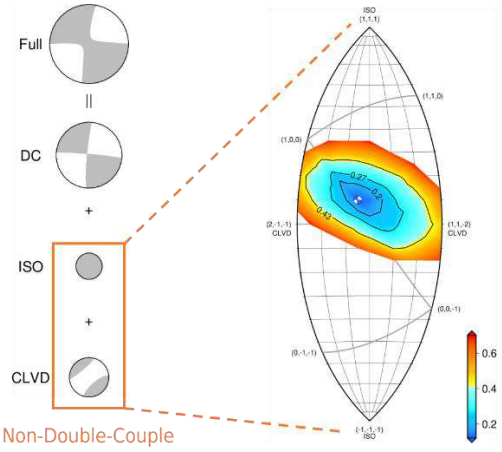

Figure 1. Example of moment tensor decomposition and the projection of its non-double-couple components with uncertainties on a Lune plot.

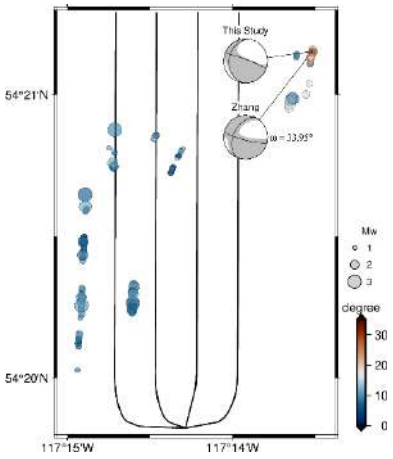

Figure 2. Comparison of the the inversion result between this study and Zhang et al., 2019. The M>1 event with the largest angular difference (33.95°) is located to the NE of the hydraulic well, as indicated by the two "beach-balls".

References

[1] Zhang H, Eation DW, Rodriguez G and Jia SQ. BSSA, 2019, 109, 636-651.

Invited Talk

Source characteristics of icequakes caused by surface crevasses on Urumqi Glacier No. 1, Tianshan, China

Risheng Chu,[a,b] Haichao Ma,[a,b]

[a] *State Key Laboratory of Geodesy and Earth's Dynamics, Innovation Academy for Precision Measurement Science and Technology, Chinese Academy of Sciences, Wuhan 430077, China;* [b] *College of Earth and Planetary Sciences, University of Chinese Academy of Sciences, Beijing 100049, China.*

E-mail: chur@apm.ac.cn

Icequakes associated with crevassing provide key information on stress fields and water flow pathways inside glaciers, conditions which are sensitive to temperature and precipitation. In this study, we analyse seismic data from 321 days recorded by 5 broadband seismometers on Urumqi Glacier No. 1, Tianshan, China, to investigate the source characteristics of icequakes. We first apply a multidimensional autoregressive maximum-likelihood algorithm to detect 12 template events from 62 days of continuous waveform data. The centroid locations of the 12 template events are located using a grid-search approach. We then obtain a catalogue of 41895 icequakes by compiling all seismic data through a template-matching method. The local magnitudes of all icequakes range between -3.3 and 0.5, with a completeness magnitude of -2.95 and Gutenberg-Richter b-value of 1.08. The particle motion and frequency contents of the 12 template events show that the dominant phases on the vertical component are Rayleigh waves at 5-40 Hz, suggesting that these icequakes were generated by near-surface crevasses. The average daily icequake number for each month and diurnal icequake variations show clear seasonal features. The icequakes may be related to growth of the surface crevasses due to additional melting water and precipitation in summer and to the thermal contraction of the ice body in winter.

References

[1] Ma HC, Chu RS, Sheng MH, Wei ZG, Zeng XF and Wang W. Source characteristics of icequakes caused by surface crevasses on Urumqi Glacier No. 1, Tianshan, China, *Geophys. J. Int.*, 2023, 234, 620-635.

Invited Talk

The 2022 M_w 7.3 Southwest Sumatra Tsunami Earthquake: Rupture Up-dip of the 2007 M_w 8.4 Bengkulu Event

Yangmin Hu[1], Tao Xia[1], Lingling Ye[1,#], Yefei Bai[2], Thorne Lay[3], Hiroo Kanamori[4], Luis Rivera[5], Sesar Prabu Dwi Sriyanto[6]

1. Department of Earth and Space Sciences, Southern University of Science and Technology, Shenzhen, 518055, China
2. Ocean College, Zhejiang University, Zhoushan, Zhejiang, China.
3. Department of Earth and Planetary Sciences, University of California Santa Cruz, Santa Cruz, CA 95064, USA
4. Seismological Laboratory, California Institute of Technology, Pasadena, CA 91125, USA
5. Institut Terre et Environnement Strasbourg, Université de Strasbourg/CNRS, Strasbourg, France.
6. Badan Meteorologi, Klimatologi, dan Geofisika (BMKG), Jakarta, Indonesia

Presenting author: Lingling Ye; E-mail address: yell@sustech.edu.cn

Tsunami earthquakes are shallow subduction zone events that occur near the trench, usually on the plate boundary, producing larger than typical tsunamis relative to their surface and body wave magnitudes. These events produce weak ground shaking, leaving coastal populations unaware of the event until a large tsunami arrives. They are also important indicators of the frictional state of the shallow megathrust fault. We use seismic and tsunami observations to determine the rupture process of the 18 November 2022 Sumatra event, which occurred up-dip of the 2007 magnitude 8.4 Bengkulu rupture. We find that the 2022 magnitude 7.3 event shares common rupture characteristics with other recognized tsunami earthquakes. We compare the tsunami earthquakes that have struck in different subduction zones globally (Figure 1), noting examples involving spontaneous failures of stress accumulations at shallow depths or triggering strain perturbation from great earthquakes at deeper depths. Additional endeavors to estimate the seismic coupling of shallow megathrusts are needed to evaluate the potential for tsunami earthquakes.

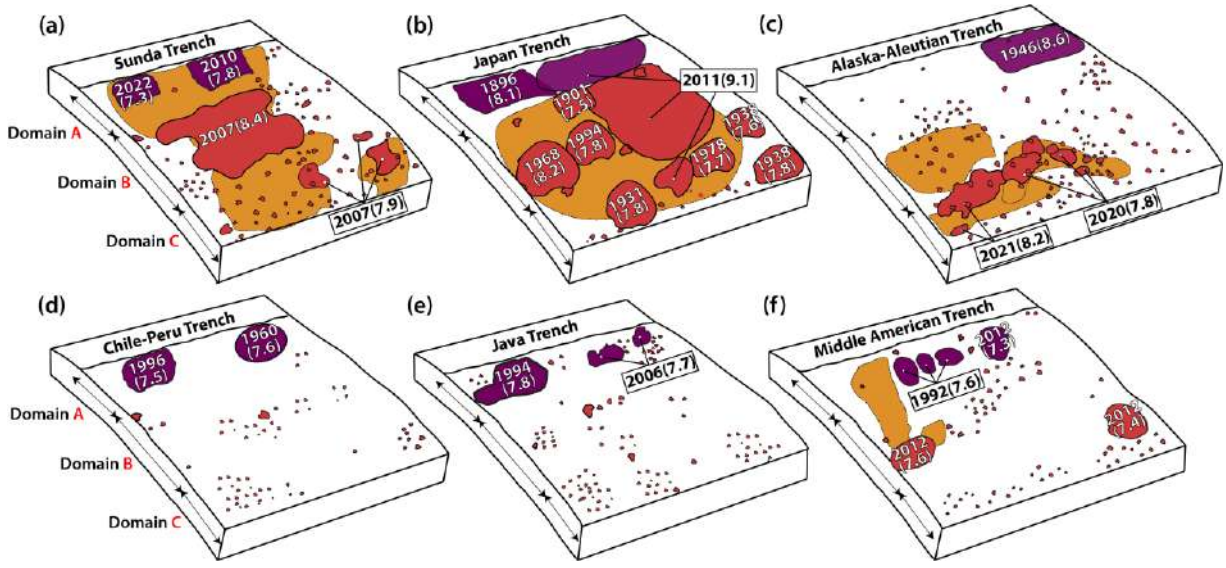

Figure 1. Schematics for subduction zones with major tsunami earthquakes.

Oral Presentation

The Long-term Fault Activation of the 2019 Weiyuan M_w 5.0 Earthquake in the Weiyuan Shale Gas Field, China

Jinping Zi,[a] Hongfeng Yang,[a,b]

[a] *Earth and Environmental Sciences Programme, Faculty of Science, Chinese University of Hong Kong, Shatin, Hong Kong;*

[b] *Shenzhen Research Institute, The Chinese University of Hong Kong, Shenzhen, China*

E-mail: zijinping@link.cuhk.edu.hk

The recent booming of shale gas development greatly improved global energy shortage and contributed to the climate change issue. However, the accompanying and consequent earthquakes, especially those unexpected destructive events, pose serious threats to residents and properties. Thus, understanding the triggering mechanism and identifying fault activation are crucial for hazard mitigation.

We present observations of the 2019 Weiyuan M_w 5.0 earthquake, which is one of the largest hydraulic fracturing (HF)-triggered earthquakes. The high-resolution earthquake catalog is first gained with the aid of close stations, waveform cross-correlation constraints, and velocity models from borehole measurements. Our results show that the M_w 5.0 event occurred at a depth of 3.95 km, which is 0.65 km below the fracking layer. We then conducted hierarchical clustering of events by waveform similarity, from which we gained 13 clusters. Analysis of the duration time and location of clusters separates them into HF-related clusters and fault-related clusters. Stress drop analysis shows HF-related clusters have smaller stress drop values than fault-related clusters.

We find that there is a large number of fault-related events before the M_w 5.0 and they started in September 2018, which is almost one year before the mainshock. These precursory events illuminated the fault plane before the M_w 5.0 earthquake. The unresting seismicity on the fault shows the fault experienced long-term fault activation. Combined with the fracking activities of nearby wells, we infer that multi-stage fracking activities contributed to the fault activation.

Environment Session (3 December)

Keynote Lecture

Interactions between carbon and nitrogen cycles in temperate forest ecosystems

Patrick Schleppi [a]

[a] *Forest Soils and Biogeochemistry, Swiss Federal Institute for Forest, Snow and Landscape Research (WSL), Switzerland*

The carbon cycle is attracting much attention because of the global changes linked to the accumulation of CO_2 in the atmosphere. Another chemical element has a cycle that is in multiple ways linked to that of carbon: nitrogen. As an essential nutrient, nitrogen naturally limits plant growth, particularly in terrestrial ecosystems. Since human activities now produce more reactive nitrogen than natural processes, this abundance inevitably has an impact on the carbon cycle. But more nitrogen does not necessarily mean that plants grow faster and fix more carbon. Too much nitrogen can have deleterious effects, particularly on biodiversity and water quality. In high doses, it can even cause trees to wither. So the main questions are: at which dose do the negative effects become dominant over the positive ones? And on which timescale? And how does this affect carbon fixation? In our experiments, we found clear effects of increased nitrogen deposition to forests[1,2] and these effects depend on both the history of the site and the deposition amounts themselves[3].

Conversely, global changes in the carbon cycle also influence nitrogen availability in forests and other terrestrial ecosystems. In particular, we could hypothesize that increased atmospheric CO_2 accelerates plant growth and that nitrogen becomes more limiting. But we know that experiments carried out on a small scale and over short periods are not always representative of the reality of forests. In mature forest stands, we were actually able to show the opposite effect, that nitrogen availability in the soil increases with atmospheric CO_2 concentration[4,5].

The interactions between carbon and nitrogen are complex, but our understanding of them continues to improve. This allowed us to propose some improvements to global models like Community Land Model 5 (CLM5)[6,7].

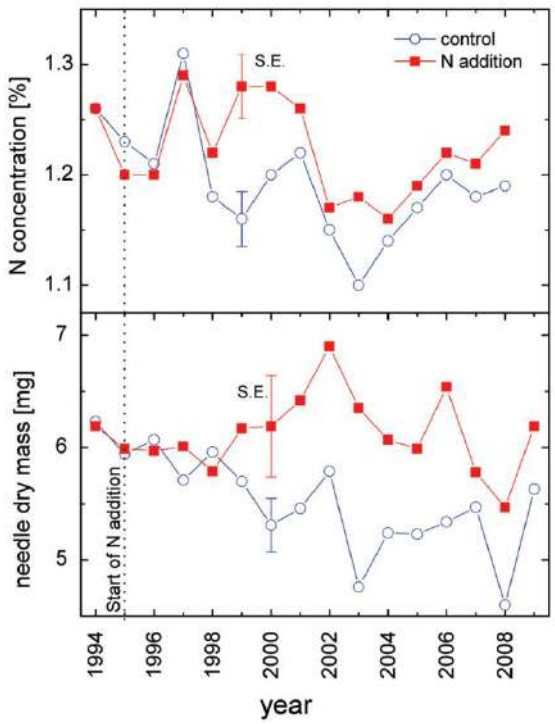

Fig. 2: Needle N concentration and dry mass of *Picea abies* at Alptal, Switzerland with or without N addition. n = 5.

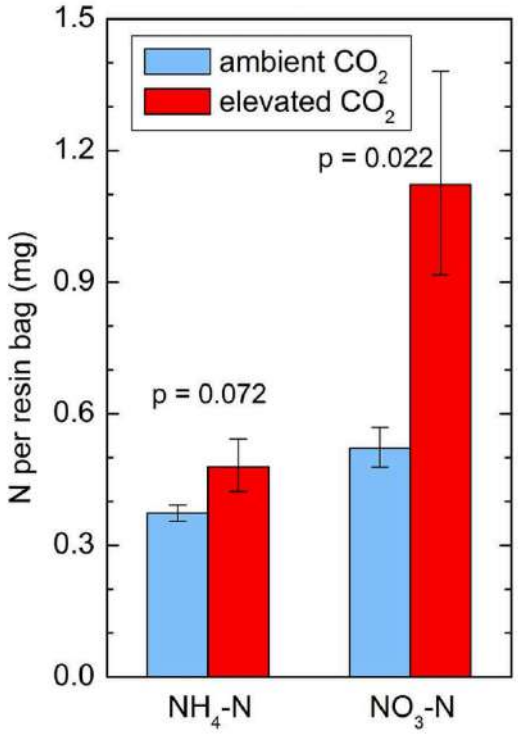

Fig. 3: NH_4^+ and NO_3^- captured during the growing season in resin bags under adult *Picea abies* trees with or without canoopy CO_2 enrichment. n = 5.

References

[1] Schleppi P, Curtaz F, Krause K, *Biogeochem.*, 2017, *134*, 319-335.

[2] Baer T, Furrer G, Zimmermann S, Schleppi P, *Biogeosci.*, 2023, *In Press.*

[3] Emmett BA, Boxman D, Bredemeier M et al., *Ecosystems*, 1998, *1*, 352-360.

[4] Schleppi P, Bucher-Wallin I, Hagedorn F, Körner C, *Glob. Change Biol.*, 2012, *18*, 757-768.

[5] Schleppi P, Körner C, Klein T, *Front. For. Glob. Change*, 2019, *2*, 59.

[6] Nadelhoffer KJ, Emmett BA, Gundersen P et al., *Nature*, 1999, *398*, 145-148.

[7] Cheng SJ, Hess PG, Wieder WR et al., *Biogeosci.*, 2019, *16*, 2771-2793.

Oral Presentation

Tracking circulation change in the western North Atlantic during the Little Ice Age using a multi-proxy approach

Wai Ching Chu [a], Anne de Vernal [b], Andre Poirier [b], Christelle Not [c], Benoit Thibodeau [a,d]

[a] *School of Life Sciences, The Chinese University of Hong Kong, Hong Kong SAR,*
[b] *Geotop, University of Quebec at Montreal, Quebec, Canada,*
[c] *Department of Earth Sciences, The University of Hong Kong, Hong Kong SAR,*
[d] *Earth and Environmental Sciences Programme,The Chinese University of Hong Kong, Hong Kong SAR.*
E-mail: wcrachel@link.cuhk.edu.hk

Atlantic Meridional Circulation is hypothesized to be at a weak state in present days and is predicted to be further weakened in the future[1]. While ocean circulation is often suggested to be a climate driver for past climatic events, there have been on-going debates on the role of a weakened circulation to the onset of the Little Ice Age (LIA). Previous studies have observed a weaker Labrador Current during LIA[2,3], suggesting a linkage between changes in the western North Atlantic circulation and the abnormal cooling during that period[3]. However, the mentioned shift in oxygen isotopic signals could infer to a change in circulation and/ or a change in water temperature. To deduce the actual cause of the shift, this study incorporates an additional temperature proxy, Mg/Ca ratio, to constrain the data from the oxygen isotopic analysis, such that a concise ocean circulation during LIA in the western North Atlantic can be reconstructed.

To acquire the Mg/Ca ratio in foraminifera, results acquired from a novel technique called Laser Ablation Inductively Coupled Plasma Mass Spectrometry (LA-ICPMS)[4] are compared against the results from the conventional solution-based ICPMS method. This comparison aims to verify both the accuracy of the results and the effectiveness of the method used.

Two cores from the Laurentian Channel are selected for this study: 1) CR02-23 (48°42.008'N, 68°38.894'W, water depth = 345cm), is used to establish a Mg/Ca calibration curve against instrumental temperature from 1903 to 2001 CE; 2) The sections covering the LIA are analysed in high-resolution in MD99-2220 (48°38.32'N, 68°37.93'W, water depth = 320m). The benthic foraminifera species, Globobulimina auriculata., is selected for the Mg/Ca ratio paleo-temperature reconstruction because of its high temperature sensitivity[5].

All in all, this study aims to provide new knowledge about the potential role of ocean circulation and its linkages with cooler condition during the LIA. Also, the use of a multi-proxy approach will be validated, enhancing the methodologies used in paleoceanography. With a better understanding of the mechanism of climate drivers in the past, better predictions and preparations for future climatic scenarios can be done.

References

1. Ditlevsen P and Ditlevsen S. *Nat. Commun.,* 2023*, 14*, 4254.
2. Thornalley DJR. *et al. Nature* 2018, *556*, 227–230.
3. Thibodeau, B. *et al. Geophys. Res. Lett.* 2018, *45*, 12,376-12,385.
4. Fehrenbacher, J., Marchitto, T. & Spero, H. J. *Geochem. Geophys. Geosystems* 2020, *21*.
5. Weldeab, S., Arce, A. & Kasten, S. *Earth Planet. Sci. Lett.* 2016, *438*, 95–102

Oral Presentation

A microcosm of nitrogen removal and carbon mineralization under salinity gradients: an insight into coastal salinity intrusion

Ziyan Wang[a], Benoit Thibodeau[a,b]

[a] *School of Life Sciences, the Chinese University of Hong Kong, Hong Kong, China;* [b] *Earth and Environmental Sciences Programme, the Chinese University of Hong Kong, Hong Kong, China.*

E-mail: 1155186101@link.cuhk.edu.hk

Nitrogen loading in aquatic environments has been identified as far exceeding the threshold for a stable Earth[1]. Human activities like agriculture and industrial processes majorly contribute to excessive nitrogen levels and ecological crises (e.g. eutrophication, hypoxia) in natural water. Coastal wetlands, as a transition between lands and seas, play a vital role in reducing this nitrogen overload through natural processes, including denitrification and anaerobic ammonium oxidation (anammox)[2,3]. Considering denitrification's potential risk of producing nitrous oxide—a potent greenhouse gas—and anammox's efficient co-removal of ammonium and nitrite, it's crucial to identify what controls the balance between these two processes. However, the mechanisms that determine the predominance of anammox and its interplay with carbon and sulfur cycles in coastal wetlands are not well-documented.

Herein, our study investigated salinity's role in anammox's contribution to nitrogen loss in response to coastal salinity intrusion. We hypothesized that higher salinity could enhance the ratio of anammox to denitrification. Slurry incubation of air-dried mangrove sediments and artificial seawater with different salinities is set for 28 days (n=80). Nitrogen transformation was monitored by NH_4^+, NO_2^-, and NO_3^- variance. Carbon mineralization was monitored by dissolved inorganic carbon (DIC) and total alkalinity. 15N-paring isotope technique was applied to quantify the potential of nitrogen loss pathways[4].

Results showed that effective nitrogen removal began after a week. Interestingly, while salt ions generally slowed the process, we observed faster nitrogen removal at higher salinities. The turnover rates of NH_4^+ and NO_3^- showed the same pattern, while the releasing rates of DIC were the reverse. The data suggests source differences between DIC and nitrogen species. Namely, autotrophic anammox could be more active than heterotrophic denitrification. The ratio of total alkalinity to DIC (~1) supports that sulfate reduction contributes more to carbon mineralization instead of denitrification[5]. Further isotope and molecular analysis will provide more information for intertwined nitrogen, carbon, and sulfur cycles.

References

[1] Richardson, K. et al. Earth beyond six of nine planetary boundaries. Sci. Adv., 2023, 9 (37), eadh2458.

[2] Cao, W., Guan, Q., Li, Y., Wang, M. & Liu, B. The contribution of denitrification and anaerobic ammonium oxidation to N2 production in mangrove sediments in Southeast China. J. Soils Sediments., 2017, 17 (6), 1767–1776.

[3] Salk, K. R., Erler, D. V., Eyre, B. D., Carlson-Perret, N. & Ostrom, N. E. Unexpectedly high degree of anammox and DNRA in seagrass sediments: Description and application of a revised isotope pairing technique. Geochim. Cosmochim. Acta., 2017, 211, 64–78.

[4] Thamdrup, B. & Dalsgaard, T. Production of N2 through Anaerobic Ammonium Oxidation Coupled to Nitrate Reduction in Marine Sediments. Appl. Environ. Microbiol. 2002, 68 (3), 1312–1318.

[5] Santos, I. R. et al. The renaissance of Odum's outwelling hypothesis in 'Blue Carbon' science. Estuar. Coast. Shelf Sci., 2021, 255, 107361.

Oral Presentation

Baseline lithium-ion concentrations in sediments and soils in a rural area of Hong Kong

Norah Muisa[a#], Tsz Ki Martin Tsui[b],

[ab]School of Life Sciences, Earth and Environmental Sciences Programme, The Chinese University of Hong Kong, Shatin, Hong Kong

E.mail: norahmuisa@gmail.com/mtktsui@cuhk.edu.hk

Lithium (Li) is possibly an environmental contaminant of elevating concern due to its increasing global use, while it is neither regulated nor monitored in the environment. The major driver of the increasing demand is the use of Li-ion batteries (LIBs) in electric vehicles since electric vehicles are regarded as a panacea to achieve carbon neutrality in the transport sector. However, spent Li-ion batteries may pose a potential source of Li and associated metals in the environment. To monitor and assess this potential future impact, reference levels of lithium in diverse environments are critical. Numerous studies have been conducted on metals in various environmental compartments in Hong Kong, but only one study performed between 2002 and 2003 on assessment of groundwater quality in and around the Mid-Levels area in Hong Kong examined twenty elements including lithium. Nevertheless, a more recent examination is warranted amid the increasing global use of Li. Outside Hong Kong, detailed studies on lithium distribution in diverse environmental compartments are still relatively scarce.

This study determined baseline lithium distribution in sediments and soils from a rural area in northeastern Hong Kong called Kuk Po Village, as a case study of unimpacted sites. Sediment samples were collected twice in each of four seasons from April to February 2022 in a freshwater stream and marshland at Kuk Po Village. Soil composite samples were collected from five accessible sites adjacent to sediment sampling sites along the stream and marshland, and the soil cores were separated as 0-10 cm, 10-20 cm and 20-30 cm depths. General water quality of the stream was also assessed.

All soil and sediment samples were microwave-digested at 180 ^{o}C using a modified aqua regia method, and analyzed using the Inductively Coupled Plasma-Mass Spectrometer (ICP-MS). In this presentation, lithium levels in Kuk Po Village will be reported. Our ongoing study is assessing the distribution of Li in other areas of Hong Kong and more diverse land uses to get a holistic view. Also, speciation and isotope studies are critical to establish the mobility, source, and potential for trophic transfer in the food chain

References

[1] Bolan, N., et. al. From mine to mind and mobiles- Lithium contamination and its risk management. Environ. Pollut., 2021, 290: 118067.

[2] Chow, A. T. Proactive approach to minimize lithium pollution. *J. Environ. Qual*., 2022.

[3] Leung, C.-M., & Jiao, J. J. Heavy metal and trace element distributions in groundwater in natural slopes and highly urbanized spaces in Mid-Levels area, Hong Kong. *Water Res.*, 2006, 40(4): 753-767.

[4]Robinson, B. H., Yalamanchali, R., Reiser, R., & Dickinson, N. M. Lithium as an emerging environmental contaminant: Mobility in the soil-plant system. *Chemosphere*, 2018,197: 1-6.

[5] Shakoor, N., Adeel, M., Azeem, I., Ahmad, M. A., Zain, M., Abbas, A., Hussain, M., Jiang, Y., Zhou, P., & Li, Y. Interplay of higher plants with lithium pollution: Global trends, meta-analysis, and perspectives. *Chemosphere*, 2022,136663.

[6] Thibon, F., Weppe, L., Vigier, N., Churlaud, C., Lacoue-Labarthe, T., Metian, M., Cherel, Y., & Bustamante, P. Large-scale survey of lithium concentrations in marine organisms. *Sci. Total Environ.*, 2021,751, 141453.

Oral Presentation

Mercury Biomagnification in Temperate Grassland Food Web (Kansas, USA)

Jack Tsun-Hung Cheung [a], Martin Tsz-Ki Tsui [a,b], Yener Ulus [b], Peijia Ku [b], Kristina Morales [b], Paul Nyarko [b], Hon-Ming Lam [a]

[a] *School of Life Sciences, Earth and Environmental Sciences Programme, State Key Laboratory of Agrobiotechnology, The Chinese University of Hong Kong, Hong Kong*

[b] *Department of Biology, University of North Carolina at Greensboro, Greensboro, North Carolina 27402, USA*

E-mail: 1155125230@link.cuhk.edu.hk

Mercury (Hg) is a pollutant of global concern, and Hg can be converted into methylmercury (MeHg), a highly toxic and persistent form risking the health of human and wildlife. Many studies on Hg cycling have been conducted in aquatic ecosystems, and to a lesser extent on forest ecosystems. To our knowledge, little is known regarding Hg cycling and bioaccumulation in grassland ecosystems. In this study, vegetation, animal and soil samples were collected in the Konza Prairie Biological Station (KPBS) dedicated to research in various locations in 2019. KPBS is a grassland divided into different zones, which are subject to different treatments, such as burning and cattle grazing. Analysis for total mercury (THg), MeHg and stable isotope ratios for carbon ($\delta^{13}C$) and nitrogen ($\delta^{15}N$) were performed on the biota samples. The mean THg concentration in the animal samples was 42.70±59.63 ng/g dry weight (n = 147) while the mean MeHg concentration was 15.55±31.96 ng/g dry weight (n = 155). By comparing $\delta^{15}N$, an indicator of trophic level [1] (n = 96) and $\log_{10}$MeHg, the evidence of MeHg biomagnification can be obtained when the slope of $\log_{10}$MeHg concentration against $\delta^{15}N$ was shown to be greater than 0 [1]. The slope of the terrestrial food web was found to be 0.201, which is similar to that in terrestrial forest food web in the temperate ecosystems [2]. The percentage of THg as MeHg, i.e., %MeHg, increased along trophic levels. Overall, %MeHg in vegetation had an average of 7.8% (THg concentration was 7.55±3.34 ng/g dry weight, MeHg concentration was 0.53±0.44 ng/g dry weight, n = 11), as compared to 18.0% in herbivore (n = 74), 29.8% in detritivore (n = 14), 50.4% in omnivore (n = 16), and 61.5% in carnivore (n = 32). Evidence shows that bioaccumulation and biomagnification occurs in a similar manner in terrestrial grassland and forest ecosystems.

References

[1] Rodenhouse NL, Lowe WH, Gebauer RLE et al. *Science of the Total Environment*, 2019, *665*, 1125 -1134.
[2] Tsui TK, Liu S, Brasso RL, et al. *Environ. Sci. Technol.,* 2019, *53*, 2434−2440.

International Conference on Earth, Energy & Environmental Sciences for Carbon Neutrality (ICE3SCN)

Conference Abstract

4 December 2023 (Monday)

Plenary Session (4 December)

Plenary Lecture 7:

Energy Conversion and Storage: Novel Materials and Operando Methods

Héctor D. Abruña

Department of Chemistry & Chemical Biology and
Center for Alkaline Based Energy Solutions (CABES)
Cornell University, Ithaca, New York, 14853 USA
E-mail: hda1@cornell.edu

This presentation will deal with the development of new materials and *operando* methods for energy systems with emphasis on fuel cells and battery materials and technologies. The presentation will begin with a brief overview of the methods employed with emphasis on the use of X-ray based methods and transmission electron microscopy (TEM) under active potential control and DEMS (Differential Electrochemical Mass Spectrometry). The utility of these methods will be illustrated by selected examples focusing on non-precious metal electrocatalysts for the oxygen reduction reaction (ORR), fuel cell testing and mechanistic studies of ethanol oxidation. Recent studies of the use of operando TEM for the study of copper deposition, cathodic corrosion of precious metals and the reduction of CO_2 will also be discussed. The presentation will conclude with an assessment of future directions.

Plenary Lecture 8:

Wildfire Impacts on Soil Carbon Cycling

Thomas Borch,[a]
[a] *Department of Soil and Crop Sciences and Department of Chemistry, Colorado State University, Colorado, USA.*
E-mail: borch@colostate.edu

Wildfires are ecosystem disturbances that burn millions of acres each year. While beneficial within fire-adapted environments, the length of the global fire-weather season has increased by 27% and extreme fire weather events have increased by 54% since 1979. This augmented wildfire activity impacts global carbon cycling and greenhouse gas emissions. For instance, in 2020, wildfires were the second largest contributor of carbon emissions in California, only behind the transportation sector.[1] However, beyond just emissions, wildfires impact carbon pools within soil. Soil organic carbon in particular contains approximately two times the amount of carbon present in the atmosphere.[2] Thus, understanding how wildfires influence carbon cycling within soils is essential. My lab specifically investigates changes in the quantity and composition of soil organic carbon following wildfires across varying spatial and temporal scales. Using state of the art chemical analyses, we analyze the carbon content of burned soil samples from small-scale, prescribed fires to some of the largest wildfires in the United States. We conduct CO_2 soil respiration incubations to evaluate potential carbon emissions from burned soils. By utilizing ultrahigh resolution mass spectrometry, we also assess soil organic carbon composition to determine what labile molecules are in burned soils that remaining microbes could metabolize and mineralize[3] [4] [5] [6]. Our mass spectrometry data are coupled with microbial community and function analyses, shining light on the carbon-cycling interplay between post-fire soil carbon and soil microbiology. Through this research, we strive to better understand how increased wildfire activity will impact soil carbon stocks and ultimately influence global carbon cycling.

Reference

[1] Jerrett, M.; Jina, A. S.; Marlier, M. E. Up in smoke: California's greenhouse gas reductions could be wiped out by 2020 wildfires. *Environmental Pollution* 2022, *310*, 119888.

[2] Simpson, M. J.; Simpson, A. J. The Chemical Ecology of Soil Organic Matter Molecular Constituents. *Journal of Chemical Ecology* 2012, *38* (6), 768-784.

[3] Bahureksa, W.; Young, R. B.; McKenna, A. M.; Chen, H.; Thorn, K. A.; Rosario-Ortiz, F. L.; Borch, T. Nitrogen Enrichment during Soil Organic Matter Burning and Molecular Evidence of Maillard Reactions. *Environmental Science & Technology* 2022, *56* (7), 4597-4609.

[4] Nelson, A. R.; Narrowe, A. B.; Rhoades, C. C.; Fegel, T. S.; Daly, R. A.; Roth, H. K.; Chu, R. K.; Amundson, K. K.; Young, R. B.; Steindorff, A. S.; Borch, T. et al. Wildfire-dependent changes in soil microbiome diversity and function. *Nat Microbiol* 2022, *7* (9).

[5] Roth, H. K.; McKenna, A. M.; Simpson, M. J.; Chen, H.; Srikanthan, N.; Fegel, T. S.; Nelson, A. R.; Rhoades, C. C.; Wilkins, M. J.; Borch, T. Effects of burn severity on organic nitrogen and carbon chemistry in high-elevation forest soils. *Soil & Environmental Health* 2023, *1* (3).

[6] Roth, H. K.; Nelson, A. R.; McKenna, A. M.; Fegel, T. S.; Young, R. B.; Rhoades, C. C.; Wilkins, M. J.; Borch, T. Impact of beaver ponds on biogeochemistry of organic carbon and nitrogen along a fire-impacted stream. *Environmental Science: Processes & Impacts* 2022, *24* (10), 1661-1677.

Energy Conversion Session (4 December)

Keynote Lecture

Working towards a comprehensive analysis of CO_2 and CO electrolysis devices

Brian Seger,[a] Ming Ma,[b] Gaston Larrazabal,[a] Asger Moss,[a] Sahil Garg,[a] Qiucheng Xu,[a] Ib Chorkendorff,[a] Jakub Drnec[c]

[a]*Department of Physics, Technical University of Denmark (DTU), Denmark;* [b] *Xi'an, Jiaotong University China,* [c] *European Synchrotron Radiation Facility (ESRF), France*

E-mail: brse@dtu.dk

This talk will analyze CO_2 electrolysis from a device perspective to provide perspective into what are the bottlenecks in the field and how to resolve them. While we show CO_2 can effectively be converted into CO, ethanol and ethylene, this electrochemical reduction process produces hydroxyl groups, which can additionally convert CO_2 to carbonates. Via a device mass balance, we show these carbonates transfer through a membrane, get acidified at the anode, and are released as CO_2 along with O_2.[1] The CO_2 released anodically is more than the CO_2 converted to products at the anode entailing this is a substantial issue.

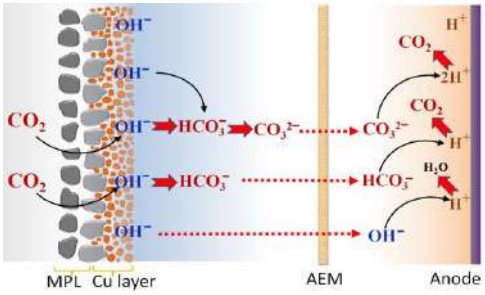

Figure 1: Cartoon of CO_2 crossover in CO_2 electrolysis devices. From Ref 1.

An additional issue is that during higher current density (>100 mA/cm^2) CO_2 electrolysis devices are prone to cathodic 'flooding' leading to greatly enhanced hydrogen production. We show that during this degradatory issue there is chaotic oscillatory fluctuations in potential, and product distribution.[2] By analyzing these fluctuations in the presence of a synchrotron, we monitor salt deposition and even electrolyte penetration by a shift in the background scattering signal. From the comprehensive analysis we have developed a hypothesis of why we both see the oscillations as well as flooding. Interestingly, salt solubility and precipitation has a strong role in flooding issues. We then analyzed various salts (Li, Na, K, Cs) of differing solubility while doing CO_2 electrolysis.[3]

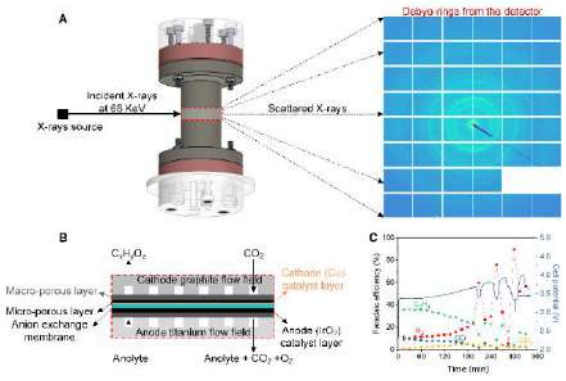

Figure 2: Synchrotron cell and the oscillatory degradation we analyze with it.From Ref 2.

The synchrotron analysis clearly demonstrates the importance of salt solubility on stable operation. We then switched to CO electrolysis as this resolve CO2 crossover issues and allows for

more soluble hydroxides compared to the carbonates used during CO_2 electrolysis. While CO electrolysis allowed for more stable hydration management, it did corrode the anode, as evidenced by IrO_2 appearing on the cathode. This was resolved by switching to a Ni anode, though long term acetate build-up caused pH issues. The acetate issues was resolved by simply removing the acetate from the anolyte during testing. This allowed for multiple tests with over 100 hour stability.[4]

References

[1] Ma, M.; Clark, E. L.; et al. *Energy & Environmental Science* 2020 13 ,3, 977-985

[2] Moss, AB, Garg, S, et al. *Joule* 2023. 7,2, 350-365

[3] Garg, S. Xu, Q, et al. *Energy & Environmental Science*, 2023 16, 1631-1643

[3] Xu, Q, Garg, S, et al. *Nat. Cat.* 2023 *In Press*

Invited Talk

Electrocatalysis on Structure Ordered Intermetallics

Deli Wang

[a] *School/Department, Institution, State, Country;* [b]*School/Department, Institution, State, Country.*

Key Laboratory of Material Chemistry for Energy Conversion and Storage (Ministry of Education), School of Chemistry and Chemical Engineering, Huazhong University of Science and Technology, Wuhan, 430074, P.R. China

Email: wangdl81125@hust.edu.cn

The performance of fuel cells is largely affected by the property of catalysts. However, the commonly used electrocatalysts in fuel cells are still platinum (Pt) based materials. Due to the shortage of Pt and its high price, the high cost of fuel cells greatly limits their large-scale commercial application. Therefore, it is necessary and meaningful to carry out in-depth research on the catalysts. There are two ways to solve this problem: one is to improve the utilization rate of platinum based catalysts; the other is to develop non-platinum based catalysts. In terms of improving the utilization rate of Pt, our group mainly aims to build a novel series of Pt based ordered intermetallic compounds. Changing the types, proportions and post-treatment temperatures of Pt and transition metal atoms is applied to optimize the surface structure, alloy degree and electronic structure of Pt based catalyst, resulting in regulating their electrocatalytic performance. On the other hand, the morphology regulation of ordered intermetallic compounds has always been a major challenge in this field. We have made preliminary attempts in morphology regulation.

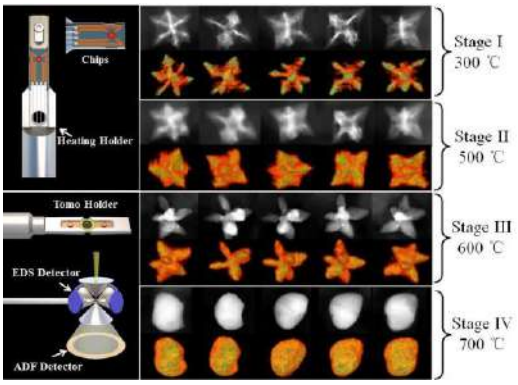

Fig 1. In-situ observation of the formation of ordered intermetallic structure and morphology change during heating.

References

1. Shen T, Gong M, Xiao D, Wang D, et al. *Adv. Funct Mater.*, 2022, 2203921.
2. Gong M, Xiao D, Wang D, et al. *Appl. Catal. B: Environ.*, 2021, 282, 119617.

Invited Talk

Rational Catalyst Design for CO_2 Electrochemical Reduction Reaction

Ziyun Wang[a]

[a] *School of Chemical Sciences, The University of Auckland, Auckland 1010, New Zealand*

E-mail: ziyun.wang@auckland.ac.nz

Selectivity is very important in electrochemical reduction of CO_2 (CO_2RR) both scientifically and industrially. Recently, C_2 selectivity has exceeded 80% on Cu-based catalyst using the flow cell[1], and ethylene and ethanol are the main two products. Understanding the mechanism branching the ethylene and ethanol is the key to achieve high selectivity of CO_2RR.

In this work, we first used density functional theory (DFT) calculations to understand the reaction pathways of CO_2RR to ethylene and ethanol. The reaction barriers and enthalpy changes are calculated for the elementary steps considered in the two pathways on Cu(100). Based on the DFT results, we investigated two factors that could affect the ratio between ethylene and ethanol, namely CO coverage[2] and surface decoration[3]. Using DFT calculation, we found that CO coverage could affect the relative energies of intermediates along ethylene and ethanol pathways, thus favoring one product over the other. With the decrease of CO coverage, the ethylene pathway becomes more favorable. Experiment results suggest the same trend and the highest ethylene selectivity is achieved with low CO partial pressure in CORR experiment. We also investigated the effect of surface decoration and found metal oxide and surface condiment favors ethanol.

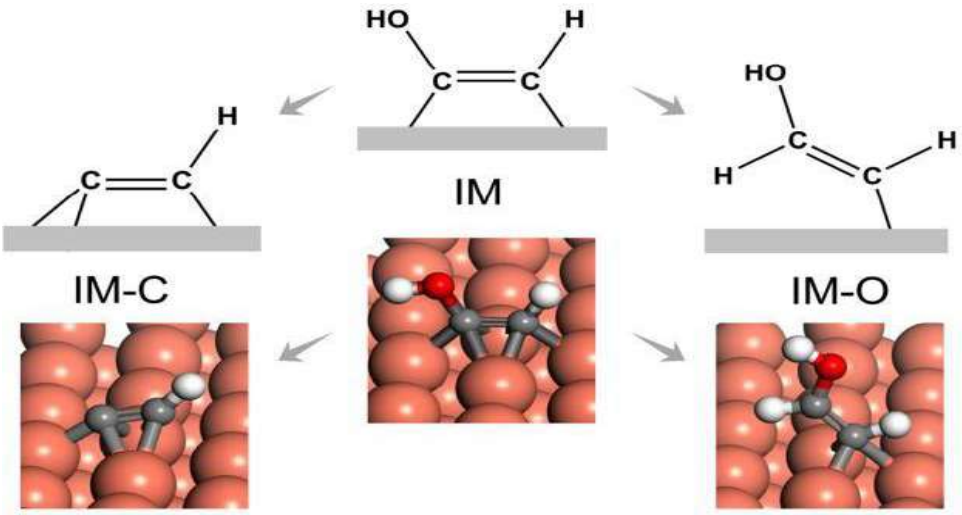

References

1 Li, F.; Thevenon, A.; Rosas-Hernandez, A.; Wang, Z.; Li, Y.; Gabardo, C. M.; Ozden, A.; Dinh, C. T.; Li, J.; Wang, Y.; et al., Nature 2020, 577, 509-513.
2 Li, J.; Wang, Z. Y.; McCallum, C.; Xu, Y.; Li, F. W.; Wang, Y. H.; Gabardo, C. M.; Dinh, C. T.; Zhuang, T. T.; Wang, L.; et al., Nat. Catal. 2019, 2, 1124-1131.
3 Luo, M.; Wang, Z.; Li, Y. C.; Li, J.; Li, F.; Lum, Y.; Nam, D.-H.; Chen, B.; Wicks, J.; Xu, A.; et al, Nat. Commun. 2019, 10, 5814.

Invited Talk

Cu-Co dual-atom catalysts supported on hierarchical USY zeolites for efficient cross-coupling reactions

Tianxiang Chen[1], Taoyuan Liang[2], Bolong Huang[1], Benedict Tsz Woon Lo*[1]
[1] State Key Laboratory of Chemical Biology and Drug Discovery, Department of Applied Biology and Chemical Technology, The Hong Kong Polytechnic University, Hong Kong, China
[2] Guangxi Key Laboratory of Electrochemical Energy Materials, School of Chemistry and Chemical Engineering, Guangxi University, Nanning, Guangxi 530004, China
*benedict.tw.lo@polyu.edu.hk

Introduction

Cross-coupling reaction over heterogeneous solid atomic catalysts offers practical solutions toward economical and sustainable elaboration of simple organic substrates.[1] Current utilization of this technology is, however, hampered by limited molecular definition of many solid catalysts.

Here, we report the development of Cu-M dual-atom catalysts (where M = Co, Ni, Cu, and Zn) supported on hierarchical USY zeolite to mediate a series of cross-coupling reactions.[2] The highest yields have been attained over Cu-Co-USY, which shows much superior reactivity when compared with our Cu_1 and other Cu-M analogs. The superior reactivity on a series of cross-coupling reactions can be attributed to (1) the specifically designed bimetallic Cu-Co active sites within the micropore for 'co-adsorption-co-activation' of the reaction substrates, and (2) the facile intracrystalline (meso/micropore) diffusion of the heterocyclic organic substrates. This study offers critical insights into the engineering of next-generation solid atomic catalysts where complex reaction steps.

Materials and Method

The Cu-M dual-atom catalysts were synthesized over a specifically chosen hierarchical USY zeolite (SiO_2:Al_2O_3 = 12) by a modular assembly approach by utilizing the underlying principles of coordination (*via* formation of acid-base adducts) chemistry and solid-state (*via* steric confinement) chemistry. In a molecular manner, di-basic 2-methylimidazolate was used as a linker to connect multiple cationic metal M^{2+} (M = Co, Ni, Cu, and Zn) nuclei in the micropore of USY to form dual-atomic Cu-M-USY.

The detailed atomic and structural parameters of these dual-atom catalysts have been determined by our multi-modal characterization, including X-ray absorption spectroscopy (XAS), synchrotron X-ray powder diffraction (SXRD), resonant X-ray diffraction, and so forth.

Results and Discussion

The Rietveld refinement of the SXRD and quantitative analysis of XAS to elucidate the crystal structures of Cu-M-USY. Two crystallographic metal sites are located around 5.8 Å apart in the micropores of the USY zeolites. This atomic separation suggests the presence of a bridging 2-methylimidazolate between the two metal motifs. Taking the unique structural property of the hierarchical USY into account, these Cu-M dual-atoms are primarily located in the micropores of USY, but larger dimension access is also given to reaction substrates at the micro-mesopores junctions. This can be verified by that nil product has been collected from the coupling involving large organic macromolecules, e.g., estrone, but smaller substrates (2) were converted effectively. It can be attributed to the active sites being mainly located at the micropores, instead of the mesopores, based on our porosity analysis. Hence, the Cu-M dual-atoms supported on this hierarchical USY zeolite,

with the dual-atoms predominantly immobilized in the micropores, would not only offer substrate activation within a reasonable molecular separation but also provides a quasi-isolated domain within esopore for effective coupling reaction between the activated substrates to proceed, as well as enhanced intracrystalline (meso/micropore) diffusion of substrates and products.

By employing probe-assisted SXRD and probe-assisted pulse electron paramagnetic resonance spectroscopy, we discovered a ‘co-adsorption-co-activation’ model for dual-atom Cu-M-USY for the cross-coupling reactions, where the synergy between the Cu and M metal motifs in Cu-M-USY can greatly promote the adsorption and electron transformation, which is in great agreement with our catalytic and computational findings.

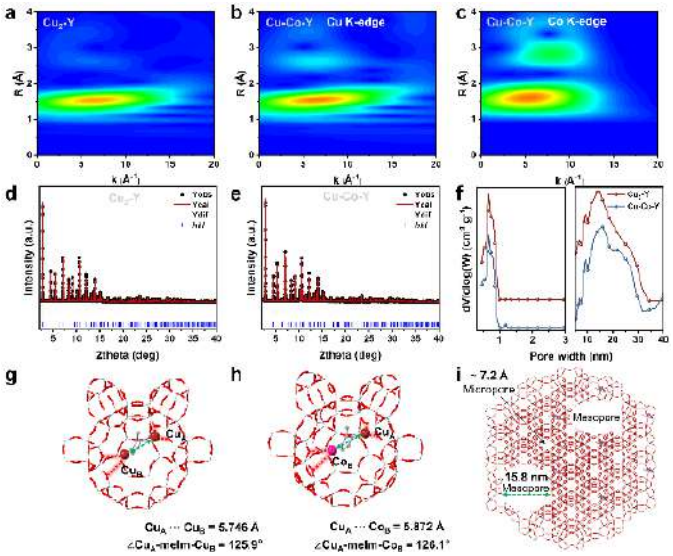

Figure 1. Atomic and structural elucidation of the catalysts. (a-c) Wavelet transforms for k^3 weighted EXAFS signal of Cu_2-USY and Cu-Co-USY. The Rietveld refinement profiles of SXRD. (f) Pore size distribution profiles. (g–h) The corresponding Rietveld refined crystal structures. (i) Schematic illustration of Cu-M dual-atoms supported on hierarchical USY zeolites.

Significance

The manipulation and control of materials and phenomena of atom-precise metal clusters can be achieved. This work will pave solid foundations for developing a widely transferable research platform for the precise engineering of new-generation solid atomic catalysts which will ultimately reach the molecular homogeneous frontier.

References

X. Hai, Y. Zheng, Q. Yu, N. Guo, S. Xi, X. Zhao, S. Mitchell, X. Luo, V. Tulus, M. Wang, X. Sheng, L. Ren, X. Long, J. Li, P. He, H. Lin, Y. Cui, X. Peng, J. Shi, J. Wu, C. Zhang, R. Zou, G. Guillen-Gosalbez, J. Perez-Ramirez, J. Lu, *Nature* 2023, DOI /10.1038/s41586-023-06529-z.

T. Chen, W. Yu, C. Kit, T. Wun, T. Wu, M. Sun, S. J. Day, Z. Li, B. Yuan, Y. Wang, M. Li, Z. Wang, Y. Peng, W. Yu, K. Wong, B. Huang, T. Liang, T. W. B. Lo, *J. Am. Chem. Soc.* 2023, *145*, 8464–8473.

Oral Presentation

Comprehensive evaluation of the urea quantification methods in electrocatalytic experiments

Yan Zhang,[a] Hufei Huang, [b] Zongwei Cai,[b] Minhua Shao [a*]

[a] *Department of Chemical and Biological Engineering, The Hong Kong University of Science and Technology, Hong Kong, People's Republic of China;* [b] *Department of Chemistry, Hong Kong Baptist University, Hong Kong, People's Republic of China.*

E-mail: kezhangyan@ust.hk

Urea is an indispensable fertilizer and raw chemical material in modern society. Electrocatalytic urea synthesis has been a promising alternative to the Haber-Bosch process[1]. Although some advancements have been made in recent years, the urea yield rate over state-of-the-art electrocatalysts is still moderate. Notably, the quantitative detection of urea, especially at a low urea concentration in a complicated electrocatalytic system is error-prone, which brings serious concerns about the rationality and accuracy of catalyst performance evaluation. Herein, the advantages and limitations of the commonly used methods for urea quantification in solution are systematically investigated (for example, diacetyl monoxime method[2], urease method[3], ^{1}H nuclear magnetic resonance spectroscopy[4], and high-performance liquid chromatography). We place particular emphasis on the effect of interferants (for example, C- and N-species byproducts, and dilution ratios) on each detection method. Furthermore, we developed a convenient high-performance liquid chromatography-tandem mass spectrometry (HPLC-MS/MS) method for accurate urea quantitation. This method exhibits a linear response from 0.1 to 5 μg mL^{-1} (R^2>0.9983), the limit of quantitation for urea is 0.1 μg mL^{-1}, and the relative standard deviations of measurements are about 2.94%. Compared with the above methods, the newly established HPLC-MS/MS method has good accuracy, reliability, and anti-interference ability, which can meet the analysis requirements to support urea synthesis studies. In addition, the HPLC-MS/MS method can be used in the qualitative analysis of isotopes-labeled urea and the limit of quantitation for $^{15}N_2$-urea is as low as 10 ppb. We hope that our work provides an easy and reliable analytical method for urea quantification in complicated electrocatalytic systems, which can help the researcher avoid detours in future exploration.

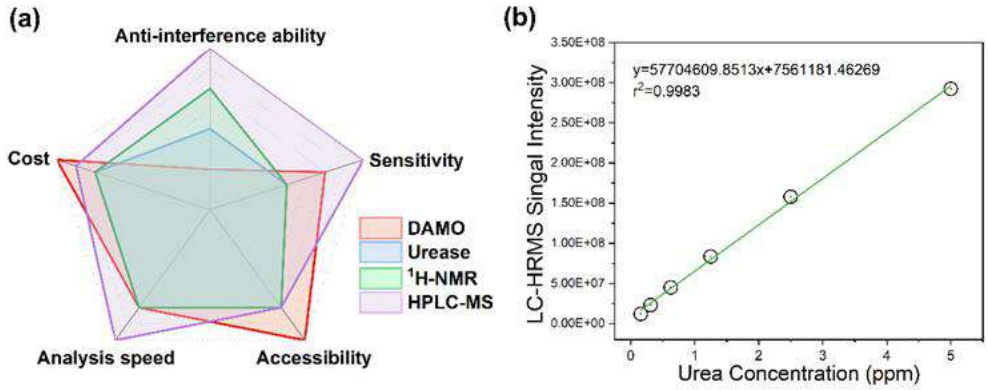

Fig.(a) The comparison of commonly used methods for urea quantification. (b) The calibration curve was used to determine urea in the newly developed HPLC-MS/MS method.

References

[1] Zhang X, Zhu X, Bo S, et al. *Nat. Commun.*, 2022, 13, 5337;

[2] Lv C, Lee C, Zhong L, et al., ACS nano, 2022, 16, 8213-8222;

[3] Wei X, Wen X, Liu Y, et al. *J. Am. Chem. Soc.*, 2022, 144, 11530-11535;

[4] Geng J, Ji S, Jin M, et al. *Angew. Chem. Int. Ed.*, 2023, 62, e202210958.

Oral Presentation

Catalysts Design for Electrochemical CO_2 Reduction to Hydrocarbon

Yi Xie,[a] Ying Wang,[a]

[a] *Department of Chemistry, The Chinese University of Hong Kong, Shatin, New Territories, Hong Kong, China*

E-mail: yixie@cuhk.edu.hk

Electrochemical CO_2 reduction reaction (CO_2RR) is a promising strategy to convert intermittent renewable energy and CO_2 into value-added chemicals and feedstocks. Prior research showed the generation of C_1 (CO, methane, formate) and C_{2+} (ethylene, ethanol, acetate, 1-propanol) products using copper as the catalyst. Among these products, methane is of great interest as the well-established natural gas infrastructure.

In CO_2RR-to-methane, *CO protonation to *CHO is a proposed critical step for methane production, competing with the C–C coupling process on *CO and the hydrogen evolution process on the proton. Our early study showed that introducing a second metal, with stronger[1] or weaker[2] affinity toward *CO, in copper regulates the surface active site and tunes the selectivity. For example, the introduction of Au in Cu lowers *CO and *H coverage[2], efficiently suppresses C–C coupling and HER simultaneously and steers the selectivity toward methane production with Faradaic efficiency (FE) of (56 ± 2) % at a production rate of (112 ± 4) mA cm^{-2}. Inspired by previous research, we further present a strategy wherein we atomically regulate surface adsorption toward crucial intermediates, increasing selectivity and activity simultaneously. $Cu_{40}H_{17}$(2,4-DMBT)$_{24}$(PPh_4), $Cu_{36}H_{10}(PET)_{24}(PPh_3)_6Cl_2$, and $Cu_{15}(PET)_{13}(PPh_3)_6(PF_6)_2$ were designed and synthesised as the well-defined atomic structures and different numbers of highly reactive centres. Using $Cu_{36}H_{10}(PET)_{24}(PPh_3)_6Cl_2$, we produce methane at a production rate of 288 mA cm^{-2} (Fig. 1a and b), improved 2.6× compared with previous research.

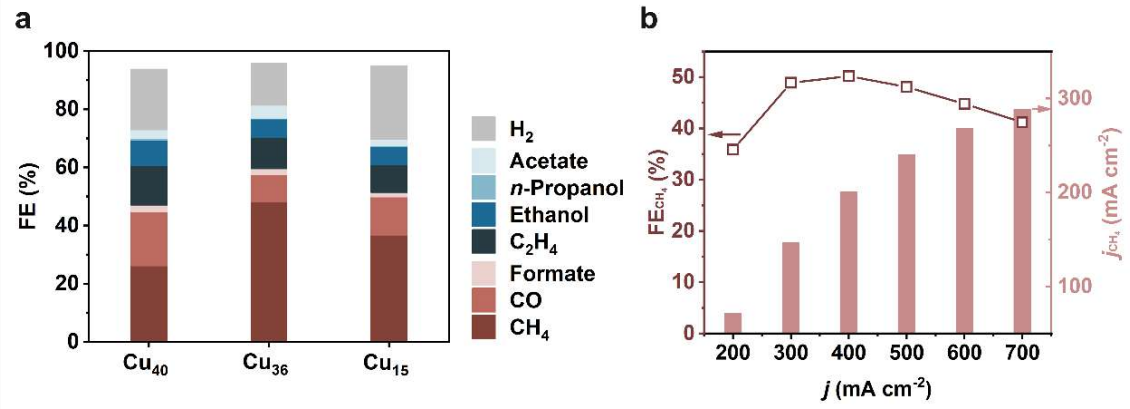

Fig. 1 | CO_2 reduction reaction performance of copper nanoclusters. a, Faradaic efficiencies (FE) of all products on Cu_{40}, Cu_{36} and Cu_{15} nanoclusters under an applied current density of 500 mA cm-2. b, Faradaic efficiency (FE_{CH_4}) and partial current density (j_{CH_4}) of methane under different applied current densities.

References

[1] Y. Xie[1], P. F. Ou[1], X.Wang[1], et al. *Nat. Catal.*, 2022, 5, 564-570.

[2] X. Wang[1], P. Ou[1], J. Wicks[1], Y. Xie[1], Y. Wang[1] et al. *Nat. Commun.*, 2021, 12, 3378

Earth and Energy Transition Session (4 December)

Invited Talk

Ten-year air quality in China

Shixian ZHAI [a]

[a] *Earth and Environmental Sciences Programme*

E-mail: shixianzhai@cuhk.edu.hk

Fine particulate matter ($PM_{2.5}$) and ozone have been causing severe air pollution problems in China. In year 2013, the Chinese government introduced the most stringent ever Clean Air Action to aggressively control anthropogenic emissions. Since then, national observation network shows a dramatic decrease in $PM_{2.5}$ but a significant increase in ozone[1, 2]. $PM_{2.5}$ is a complex mixture of multiple components, among which nitrate is the most difficult to cut down, due both to moderate decrease of nitrogen oxides (NO_x) emissions and chemical and physical feedbacks[3]. $PM_{2.5}$ nitrate at the same time is affected by the presence of anthropogenic fugitive dust[4]. Ozone over industrialized regions is mainly produced by reactions of nitrogen oxides (NO_x) and volatile organic compounds (VOCs) in the presence of sunlight. The formation of ozone is highly nonlinear that a moderate decrease of NO_x emissions and a flattened VOCs emissions can cause an increase in ozone. Meanwhile, changes in $PM_{2.5}$ can affect ozone through heterogeneous reactions[5]. This talk will show the air quality changes in China since around 2013 and how we understand it by integrating observations from satellites[6], aircraft, and surface networks with an atmospheric chemical transport model.

References

[1] Zhai, S.; Jacob, D. J.; Wang, X.; Shen, L.; Li, K.; Zhang, Y.; Gui, K.; Zhao, T.; Liao, H. Fine particulate matter ($PM_{2.5}$) trends in China, 2013-2018: separating contributions from anthropogenic emissions and meteorology. *Atmos. Chem. Phys.* 2019, *19*, 11031-11041 DOI: https://doi.org/10.5194/acp-19-11031-2019.

[2] Li, K.; Jacob, D. J.; Shen, L.; Lu, X.; De Smedt, I.; Liao, H. Increases in surface ozone pollution in China from 2013 to 2019: anthropogenic and meteorological influences. *Atmos. Chem. Phys.* 2020, *20* (19), 11423-11433. DOI: 10.5194/acp-20-11423-2020.

[3] Zhai, S.; Jacob, D. J.; Wang, X.; Liu, Z.; Wen, T.; Shah, V.; Li, K.; Moch, J. M.; Bates, K. H.; Song, S.; et al. Control of particulate nitrate air pollution in China. *Nat. Geosci.* 2021, *14*, 389-395. DOI: https://doi.org/10.1038/s41561-021-00726-z.

[4] Zhai, S.; Jacob, D. J.; Pendergrass, D. C.; Colombi, N. K.; Shah, V.; Yang, L. H.; Zhang, Q.; Wang, S.; Kim, H.; Sun, Y.; et al. Coarse particulate matter air quality in East Asia: implications for fine particulate nitrate. *Atmos. Chem. Phys.* 2023, *23* (7), 4271-4281. DOI: 10.5194/acp-23-4271-2023.

[5] Li, K.; Jacob, D. J.; Liao, H.; Shen, L.; Zhang, Q.; Bates, K. H. Anthropogenic drivers of 2013-2017 trends in summer surface ozone in China. *Proceedings of the National Academy of Sciences* 2019, *116* (2), 422-427.

[6] Zhai, S.; Jacob, D. J.; Brewer, J. F.; Li, K.; Moch, J. M.; Kim, J.; Lee, S.; Lim, H.; Lee, H. C.; Kuk, S. K.; et al. Relating geostationary satellite measurements of aerosol optical depth (AOD) over East Asia to fine particulate matter (PM2.5): insights from the KORUS-AQ aircraft campaign and GEOS-Chem model simulations. *Atmos. Chem. Phys.* 2021, *21* (22), 16775-16791. DOI: 10.5194/acp-21-16775-2021.

International Conference on
Earth, Energy & Environmental Sciences
for Carbon Neutrality

Oral Presentation

Aggravated ozone pollution under the waves of industrialization and urbanization embodies unrecognized agricultural economic inequality in China

Jia Mao,[a] Tai, Amos P. K.[a]

[a] *Graduation Division of Earth and Atmospheric Sciences, Faculty of Science, The Chinese University of Hong Kong, Sha Tin, Hong Kong SAR, China*

E-mail:maojia@link.cuhk.edu.hk

Over the past decades, the urbanization and industrialization processes in China have been fostering rapid economic growth. Meanwhile, the increased anthropogenic emissions lead to prominent ozone pollution, which embodies unrecognized economic inequality for farmers in China due to reduced grain yields. Here, we analyzed the patterns of socio-economic development and industrial restructuring in China between 1980 and 2010, as well as the influence of sector-specific precursor emissions on the deterioration of ozone pollution, which resulted in crop yield reductions and thereby indirect economic losses. In 2015, total ozone-induced annual crop production losses (including rice, wheat and maize) are estimated at ~80.0 million tons, accounting for the economic loss of ~34.5 billion USD, wherein industry department is the dominating contributor to the emission. Taking mitigation action for ozone emission to meet the net-zero target can decrease the annual maximum daily average ozone by ~5.5 ppb in 2060, and reduce the economic losses associated with crop yield reduction by approximately ~31.2 million tons and ~14.1 billion USD, respectively. The findings suggest that carbon reduction and clean air polices can bring indirect economic benefits to farmers, leading to a more equitable development among various social groups in the process of modernization.

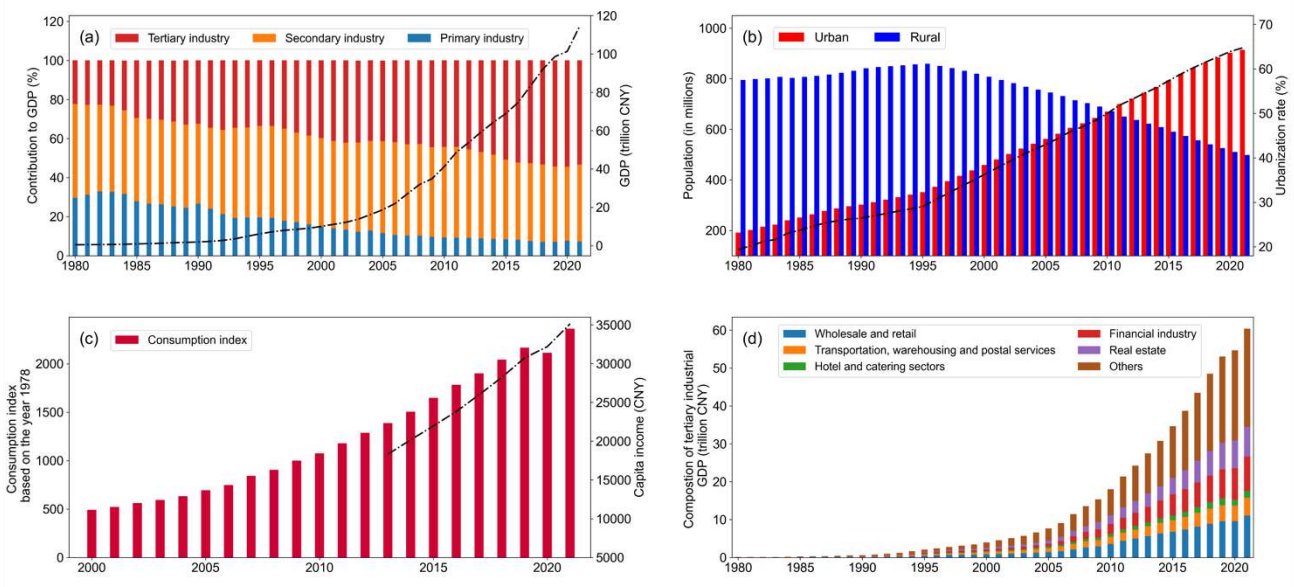

Fig. 1 | The (a) gross domestic product (GDP; CNY; dotted line) and the share of the three major industries (%; bar plot) from 1980 to 2020, (b) urban and rural population (bar plot) with urbanization rates (%; dotted line) from 1980 to 2020, consumption index (bar plot) from 2000 to 2020 based on year 1978, and (d) composition of tertiary industry and the corresponding GDP (CNY).

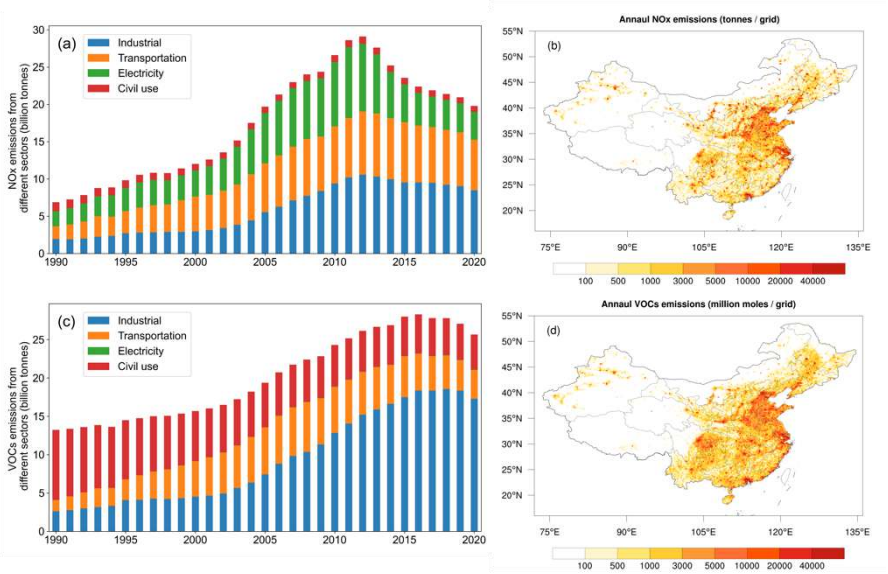

Fig. 2 | The annual emissions of (a) NO_x and (c) VOCs from 1980 to 2021, and the corresponding annual averaged spatial distribution of (b) NO_x and (d) VOCs.

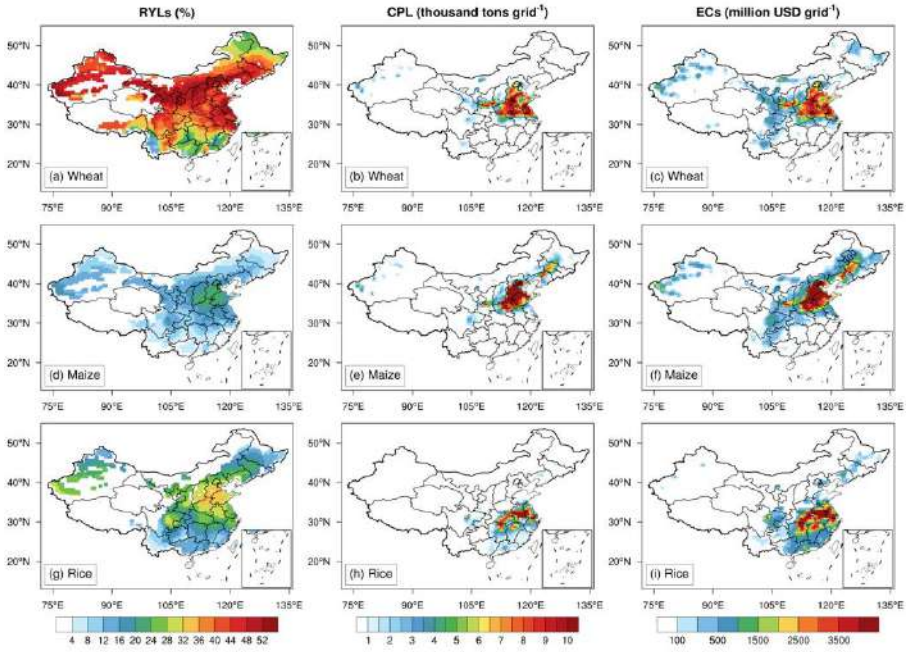

Fig. 3 | The spatial distribution of O_3-induced relative yield losses (RYLs), crop production losses (CPLs), and economic costs (ECs) for wheat, maize and rice.

Oral Presentation

Impacts of agricultural irrigation on regional air quality in China: A modeling study using WRF-GC

Tiangang Yuan,[a] Amos P. K. Tai,[b] Jin Wu[c]

[a] *Earth and Environmental Sciences Programme and Graduation Division of Earth and Atmospheric Sciences, Faculty of Science, The Chinese University of Hong Kong, Sha Tin, Hong Kong SAR, China;* [b] *School of Biological Sciences and Institute for Climate and Carbon Neutrality, The University of Hong Kong, Pok Fu Lam, Hong Kong SAR, China;* [c] *School of Biological Sciences and Institute for Climate and Carbon Neutrality, The University of Hong Kong, Pok Fu Lam, Hong Kong SAR, China*

E-mail: yuantg@link.cuhk.edu.hk

China possesses the largest irrigated area around the world and has witnessed a dramatic increase in irrigated area since the 1950s. Intensive agricultural irrigation has been recognized for its roles in mitigating water stress and altering regional climate. However, little is known about how irrigation influences regional air quality in China. Here we implemented a dynamic irrigation scheme into the Weather Research and Forecasting model coupled with the GEOS-Chem chemical transport model (WRF-GC) to examine the impacts of irrigation on ozone and particulate matter with diameter < 2.5 μm (PM2.5) over the heavily irrigated area in China. Results show that irrigation has a dual effect on regional air quality. On one hand, it increases primary air pollutants such as NOx and CO, because of the weakened turbulent mixing. On the other hand, irrigation alleviates ozone pollution, reducing it by ~4 ppb. This is likely attributable to the elevated NOx, which enhances NO titration and the reaction of NO2+OH. PM2.5, nitrate and ammonium increase by 28%, 70% and 40% when irrigation is included, among which secondary formation contributes by 5–10%, over 60%, and 10–30%, respectively. High humidity and low temperature induced by irrigation promote multiphase chemistry, particularly facilitating the formation of nitrate through the pathways involving the reactions of NO2+OH and N2O5 hydrolysis. The combined reduction of NH3 and NOx emission is the most effective way to mitigate the negative effects of irrigation on PM2.5, but may worsen O3 pollution in NOx-saturated regimes. Besides, it is anticipated that constraints on irrigation in the future may reduce PM2.5 pollution while potentially enhancing ozone pollution. This underscores the complex relationship between land management and air pollution, emphasizing the possible side effects of transition from traditional irrigation methods to water-saving techniques under current anthropogenic emission scenario and the needs for comprehensive emission reduction strategies.

Oral Presentation

Improving Agricultural Nitrogen Use Efficiency to Reduce Air Pollution in China

Biao Luo,[a] Amos P. K. Tai[a]

[a] *Earth System Science Programme and Graduate Division of Earth and Atmospheric Sciences, Faculty of Science, The Chinese University of Hong Kong, Hong Kong SAR, China.*

E-mail: luob@link.cuhk.edu.hk

China has been long characterized by low nitrogen use efficiency (NUE) associated with substantial ammonia (NH_3) loss, which contribute to air pollution. To reduce NH_3 emissions toward cleaner air of China, a series of mitigation strategies need to be realized. However, the knowledge gap in spatial patterns of NH_3 emissions and nitrogen management status of agricultural system would induce uncertainties in policy making. Here we aim to explore the NH_3 mitigation potential and its related $PM_{2.5}$ removal effects, with improving NUE of agricultural system. We use a nitrogen flows model for evaluating NUE of different crop and livestock at province scale in China. We then link bottom-up NH_3 estimates and air quality model to provide an integrated assessment of four improved nitrogen management scenarios: improving NUE of crop system (NUEc), increasing organic fertilizer use (OUR), improving NUE of livestock system (NUEa) and combination measures (Combine). The agricultural NH_3 emissions of China is estimated as 11.18 Tg in 2017, where fertilizer and livestock waste contribute 46.24% and 53.76%, respectively, and emitted hotspots can be identified in North China Plain. Our results show that grain crops have higher NUE than fruits and vegetables, while high livestock NUE can be found in pork and poultry, and NUE for whole crop and livestock system are both better in north China. We also find that agricultural NH_3 emissions can be declined from 11.18 Tg to 9.13 Tg, 9.32 Tg, 9.93 Tg and 6.77 Tg, and consequently annual population weighted $PM_{2.5}$ reductions are estimated as 1.84 $\mu g/m^3$, 1.59 $\mu g/m^3$, 1.29 $\mu g/m^3$ and 4.14 $\mu g/m^3$ under NUEc, OUR, NUEa and Combine scenarios, respectively. Our results are expected to provide decision support for agricultural NH_3 emissions mitigation policy making.

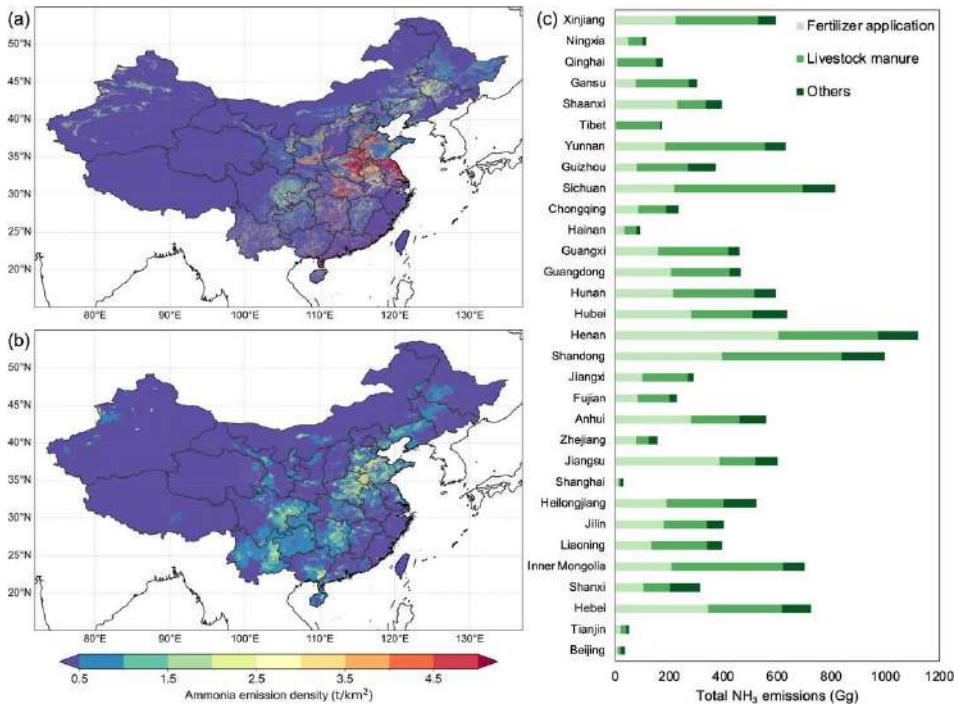

Figure 1. The NH_3 emissions spatial distribution in China of fertilizer application (a), livestock manure (b) and provincial total NH_3 emissions (c) in 2017

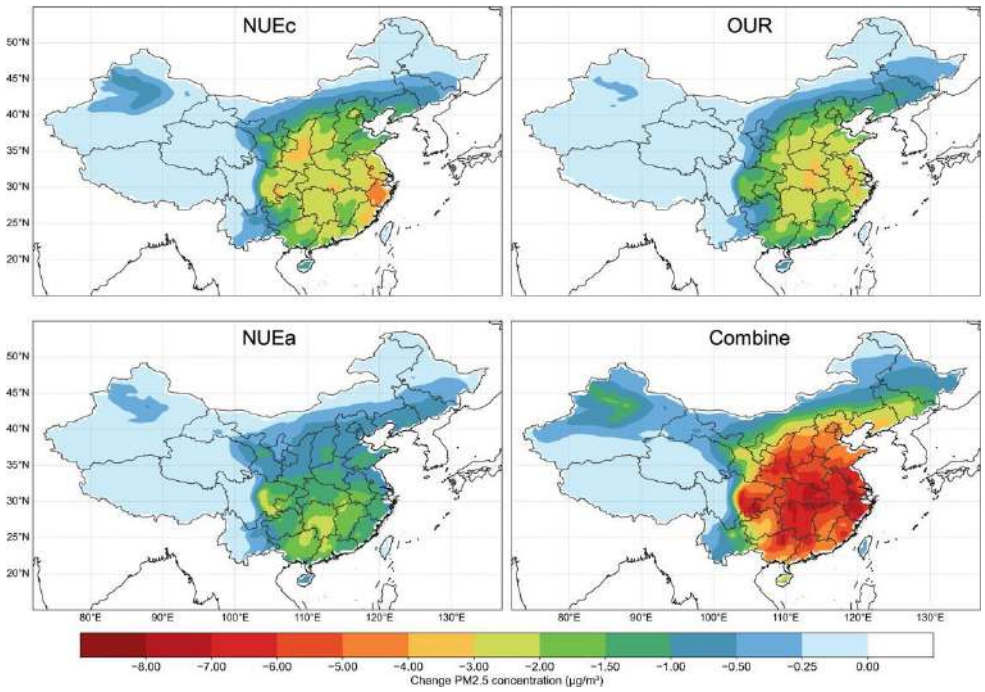

Figure 2. Change of ground-level $PM_{2.5}$ concentration of different mitigation scenarios

Environment Session (4 December)

Invited Talk

The Evolving Concept of Blue Ecosystems and their Role in Carbon Neutrality and Nitrogen Pollution Remediation

Benoit Thibodeau[ab]

[a]*Earth and Environmental Sciences, The Chinese University of Hong Kong, Kong Kong SAR, China;* [b]*School of Life Sciences, The Chinese University of Hong Kong, Kong Kong SAR, China.*

E-mail: benoit.thibodeau@cuhk.edu.hk

Blue ecosystems, including oceans, coasts, and inland waters, play a vital role in supporting human societies and planetary health. Recently, the concept of "blue carbon" has emerged as a means of utilizing these ecosystems for climate change mitigation. Blue carbon recognizes the significant potential of vegetated coastal habitats like mangroves, seagrasses, and salt marshes to sequester and store carbon over the long term. Despite covering only 0.5% of the ocean surface, these blue carbon ecosystems bury carbon at a rate two to four times greater per unit area than terrestrial forests. Additionally, they provide climate regulation by storing carbon, mitigating ocean acidification and sea level rise, and reducing coastal erosion during storms.

Recent research has highlighted the important roles of blue ecosystems in nitrogen cycling and retention. Through processes like nitrification-denitrification, these ecosystems naturally remove reactive nitrogen, countering anthropogenic nitrogen pollution. Enhancing nitrogen removal in blue carbon habitats can provide cost savings compared to relying solely on technological solutions. Understanding the interactions between carbon, nitrogen, sulfur, and oxygen cycles is crucial for preserving carbon in blue ecosystems. Factors like oxygen availability and coupled nitrification-denitrification impact carbon burial efficiency. The role of the open ocean, including phytoplankton, vegetated ocean floors, and marine animals, as blue carbon players is also gaining recognition but requires further quantification.

Unfortunately, human pressures have led to substantial loss of blue carbon ecosystems and their climate and nitrogen regulation benefits. Ongoing degradation and sea level rise further threaten their stability. To mitigate climate change and achieve carbon neutrality goals, integrated conservation and restoration of blue carbon resources, along with decarbonization in other sectors, are urgently needed. Payment for blue carbon ecosystem services is gaining traction as a conservation incentive. However, challenges related to carbon accounting, permanence, and additionality need to be addressed for effective implementation of blue carbon projects.

The evolving blue carbon model provides a comprehensive framework for protecting aquatic systems based on their interconnected values for biodiversity, ecological health, and climate stability. Quantifying and monitoring the intricate connection between the carbon, nitrogen, sulfur and oxygen to produce new knowledge about the sequestration capacities of blue ecosystems will facilitate their integration into national policies, carbon markets, and global climate change mitigation efforts.

Invited Talk

Temperature thresholds of pyrogenic dissolved organic matter

Qiang Zhang,[a,b] Yinghui Wang,[a] Junjian Wang,[a]

[a] *School of Environmental Science and Engineering , Southern University of Science and Technology, Shenzhen, Guandong 518055 China.*

[b] *School of Environment, Harbin Institute of Technology, Harbin, 150090, China*

E-mail: wangjj@sustech.edu.cn

The heating temperature (HT) experienced during forest fires plays a critical role in determining the quantity and quality of pyrogenic soil-derived dissolved organic matter (DOM). However, the temperature thresholds at which maximum DOM production (TT_{max}) occurs or when DOM loss counteracts DOM production (TT_0) remain unclear, especially at a component-specific level. To address this, we conducted an analysis of DOM composition in detritus and soil using solid-state ^{13}C nuclear magnetic resonance, absorbance and fluorescence spectroscopy, and Fourier transform ion cyclotron resonance mass spectrometry. Our study aimed to identify temperature thresholds for DOM components at a structural, fluorophoric, and molecular-formula level.

We found that TT_{max} values were similar for detritus and soil and typically fell within the range of 225–250 °C for bulk dissolved organic carbon (DOC) and most DOM components. However, TT_0 consistently showed lower values in detritus compared to soil. Furthermore, temperature thresholds varied among different DOM components. With increasing HT, we observed an initial net loss in molecular formulae tentatively associated with carbohydrates and aliphatics, followed by proteins, peptides, and polyphenolics, and ultimately condensed aromatics. Notably, even at temperatures below TT_0, particularly at TT_{max}, the burning process increased the DOC quantity, potentially enhancing labile substrates to support the soil microbial community. These composition-specific variations of DOM with temperature suggest that wildfire impacts on soil organic matter properties are non-linear and temperature-dependent. This may help to explain the distinct environmental consequences observed in wildfire cases with varying levels of burning intensity.

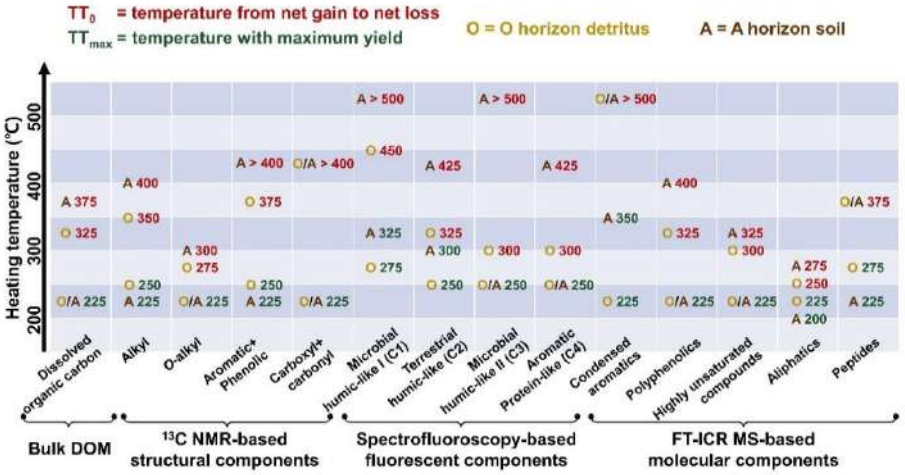

Figure 1. Summary of temperature thresholds of bulk dissolved organic matter (DOM), structural components, fluorescent components, and molecular components.

Oral Presentation

Marine heatwaves and light limitation independently alter the growth and productivity of the tropical seagrass *Halophila ovalis*

Alissa Victoria Bass,[a] Laura Jane Falkenberg,[ab] Haiwei Luo,[acd] Benoit Thibodeau[ae]

[a] *School of Life Sciences, & Simon F.S Li Marine Science Laboratory, The Chinese University of Hong Kong, Hong Kong SAR;* [b] *UniSA STEM, University of South Australia, South Australia, Australia;* [c] *State Key Laboratory of Agrobiotechnology, The Chinese University of Hong Kong, Hong Kong SAR;* [d] *Shenzhen Research Institute, The Chinese University of Hong Kong, Shenzhen, China;* [e] *Earth and Environmental Sciences Programme, The Chinese University of Hong Kong, Hong Kong SAR*

E-mail: alissabass@link.cuhk.edu.hk

Seagrasses are important marine foundation species, which support high coastal biodiversity and provide many socioeconomic benefits[1]. However, seagrasses are threatened by anthropogenic change, both climate and non-climate related, particularly marine heatwaves (MHWs) which are having negative impacts on seagrasses and seagrass ecosystems globally[2]. With the combined impacts of other anthropogenic stressors, such as light limitation from eutrophication or increased sediment load, the growth, productivity, and elemental cycling of the seagrass may be altered. This can be due to underlying shift is the seagrass microbiome.

In this experiment, we exposed the tropical seagrass *Halophila ovalis* to a 10-day MHW and three light intensities to examine the impacts of these two stressors on the growth, productivity elemental cycling and leaf microbiome of the seagrass and to see if there were any interactive effects of the two stressors. We found that both MHW and decreased light negatively impacted the growth of the seagrass, particularly the rhizome elongation rate, and the leaf growth rate, as well as increasing the rate of leaf loss. Similarly, chlorophyll concentration was altered by both stressors, with the normal adaptational responses to reduced light (i.e., increasing chlorophyll concentration) being inhibited by the MHW. Nitrogen assimilation rate also decreased under both MHW temperature and reduced light availability. We found no interactive effects of MHW and light limitation on *Halophila ovalis*.

From the results obtained so far, we show that MHWs can drive decreased productivity of seagrass, particularly when combined with low light availability. Furthermore, MHWs can reduce the ability of *H. ovalis* to adapt to lower light levels. Poor water clarity and habitat health can therefore increase the susceptibility of seagrasses to extreme climatic events.

References

[1] Unsworth, R.K.F., McKenzie, L.J., Collier, C.J. *et al.* Global challenges for seagrass conservation. *Ambio,* 2019, 48, 801–815.

[2] Smale, D.A., Wernberg, T., Oliver, E.C.J. *et al.* Marine heatwaves threaten global biodiversity and the provision of ecosystem services. *Nat. Clim. Chang.,* 2019, 9, 306–312.

Oral Presentation

Dynamics of atmospheric nitrogen in Southern China and its impact on coastal ecosystems

Chenyu LUO,[a] Benoit THIBODEAU,[b]

[a] *School of Life Science, The Chinese University of Hong Kong, China;* [b] *School of Life Sciences and Earth and Environmental Sciences Programme, Chinese University of Hong Kong, China.*

E-mail: 1155205611@link.cuhk.edu.hk

Atmospheric deposition is recognized as an important source of nutrients in the upper ocean, and the nutrients it brings, such as nitrogen (N) and phosphorus (P), can affect the growth of marine phytoplankton and influence marine N cycle. The oligotrophic South China Sea (SCS) is particularly affected by high anthropogenic nitrogen deposition due to the large populations and rapid economic development of neighboring countries. However, little is known about the mechanism of how anthropogenic activities influence the SCS system by interacting with increased landfalling typhoons and winter haze events. It is thus that the main challenges of atmospheric deposition to the ocean are discussed in this research from the aspects of bioavailable N and P as well as response of marine primary production process. Mesocosm experiments in the SCS are planned to conduct to quantify the effects of atmospheric nitrogen deposition on phytoplankton growth and microbiome community changes in February 2024. The additional concentrations of nutrients including N and P that stimulate annual depositing flux will be determined based on field observations and extensive datasets in the SCS according to previous studies. Different atmospheric deposition scenarios will be also evaluated to validate a hypothesis that the phytoplankton biomass over the SCS is found to have increased influenced by the nitrogen deposition in dust or haze events.

Oral Presentation

The sources and behaviour of nitrogen species in hypoxia areas of Hong Kong

Henry C.J. Thomas[a], Benoit Thibodeau[a,b]
[a] *School of Life Sciences, The Chinese University of Hong Kong, Hong Kong SAR*
[b] *Earth and Environmental Sciences Programme, The Chinese University of Hong Kong, Hong Kong SAR*
henrycjthomas@gmail.com

The prevalence of coastal hypoxia and ocean deoxygenation have increased significantly over the past half century, primarily as a result of the influence of anthropogenically produced nitrogen into the marine ecosystems[1–3]. This is an issue, as lower oxygen levels in coastal environments lead to decreases in ecosystem health, primarily as a result of increased species mortality[4,5]. With further increases in the coastal urban population and coastal urbanisation predicted, understanding how incidents of coastal hypoxia develop is paramount to managing and mitigating their negative effects.

Hong Kong is an ideal location to study this as it is a heavily urbanised coastal city, part of the Pearl River greater bay area, and contains two seasonally hypoxic areas, Tolo Harbour and the southern waters between Lantau and Lamma Island[6,7]. The study here aims to look at how nutrient sources and cycling changes on a year-round basis, and how this affects the dissolved oxygen content of the area. This is being carried out using nutrient analysis of key nitrogen species (NH_4^+, NO_3^-, NO_2^-), total carbon and nitrogen levels, chlorophyll-α concentration and dissolved oxygen levels in tandem with stable isotope ($\delta^{15}N\text{-}NO_3^-$, $\delta^{18}O\text{-}\ NO_3^-$) measurements to determine the relative importance of different sources and types of nitrogen within these areas[8].

Using this data, we also hope to be able to answer two more fundamental questions in coastal biogeochemistry. The first of these is how nitrogen fixing bacteria (diazotrophs) continue to fix nitrogen in unfavourable conditions (excess nitrogen), such as those found in hypoxic areas[9]. This will be using a $\delta^{15}N$ tracer (and potentially acetylene reduction assays) to determine the rate of nitrogen fixation as external condition change. The second question is how the oxidation state of organic matter changes as a result of physical and nutrient (particularly nitrogen) stress. As microorganisms adapt to variable conditions, the stoichiometry of their organic matter can change, meaning that during organic matter oxidation the amount of oxygen consumed may change, which could accelerate the rate of ocean deoxygenation[10,11]. This will be carried out studying the organic carbon concentration and chemical oxygen demand of particulate matter, alongside the use of flow cytometry to study the physiology of phytoplankton.

References

[1]Diaz, R.J. & Rosenberg, R. *Science* 321, 926–929 (2008).
[2]Robinson, C. *Front. Mar. Sci.* 5, (2019).
[3]Howarth, R.W. *Harmful Algae* 8, 14–20 (2008).
[4]Gray, J., Wu, R. & Or, Y. *Mar. Ecol. Prog. Ser.* 238, 249–279 (2002).
[5]Steckbauer, A., Duarte, C.M., Carstensen, J., Vaquer-Sunyer, R. & Conley, D.J. *Environ. Res. Lett.* 6, 025003 (2011).
[6]Li, D. et al. *J. Geophys. Res. Oceans* 125, e2020JC016178 (2020).
[7]Liang, W. et al. *Sci. Total Environ.* 905, 167138 (2023).
[8]Archana, A. et al. *Water Res.* 142, 459–470 (2018).
[9]El-Khaled, Y.C. et al. *Mar. Ecol. Prog. Ser.* 645, 55–66 (2020).
[10]Moreno, A.R. et al. *AGU Adv.* 3, e2022AV000679 (2022).
[11]Moreno, A.R. et al. *Proc. Natl. Acad. Sci.* 117, 22866–22872 (2020).

Oral Presentation

Tidal pumping and atmospheric deposition of inorganic nitrogen drive diurnal variation in primary productivity in Mirs Bay, Hong Kong

Ho Wen LO [a], Benoit THIBODEAU [a,b]

[a] *School of Life Sciences, The Chinese University of Hong Kong, Hong Kong*

[b] *Earth and Environmental Sciences Programme, The Chinese University of Hong Kong, Hong Kong*

E-mail: owenhwlo@cuhk.edu.hk

Previous research has shown that Mirs Bay, Hong Kong is a peculiar coastal area in that it exhibits high chlorophyll a concentrations despite low ambient dissolved nutrient levels [1]. It is therefore hypothesised that atmospheric sources of inorganic nitrogen may be important in driving primary productivity in Mirs Bay [2]. We tested this hypothesis by conducting two fieldwork campaigns in the area, one in late summer (September 2022) and another in winter (December 2022). Surface seawater samples were obtained frequently on each day of sampling. Concentrations of chlorophyll a and dissolved inorganic nutrients were determined in the laboratory. During the winter campaign, aerosol samples were also collected and concentrations of inorganic nitrogen were analysed in the field using a newly-developed aerosol nitrogen analyser [3].

During the September campaign, we observed that peaks in dissolved nutrients and chlorophyll a often occurred around one to two hours after the lowest tide. It is suggested that receding tides would have transferred nutrients from the surrounding land into Mirs Bay (tidal pumping). On the other hand, during the December campaign, we found that there were additional peaks in chlorophyll a that could not be attributed to low tides. These anomalous peaks were mostly recorded in the morning and appeared to be responses to overnight accumulations of atmospheric inorganic nitrogen deposits, consumption of which would only be possible under the presence of sunlight. Atmospheric deposition only gained significance in winter, as only the prevailing wind in winter (i.e. northerlies, as opposed to the southerlies in summer) could bring in emissions of anthropogenic nitrogen originating from Mainland China [4]. These findings imply strong diurnal variability in primary productivity in this bay and suggest that existing monitoring and sampling efforts (mostly monthly) may be biased, depending on their timing during the day and/or the season.

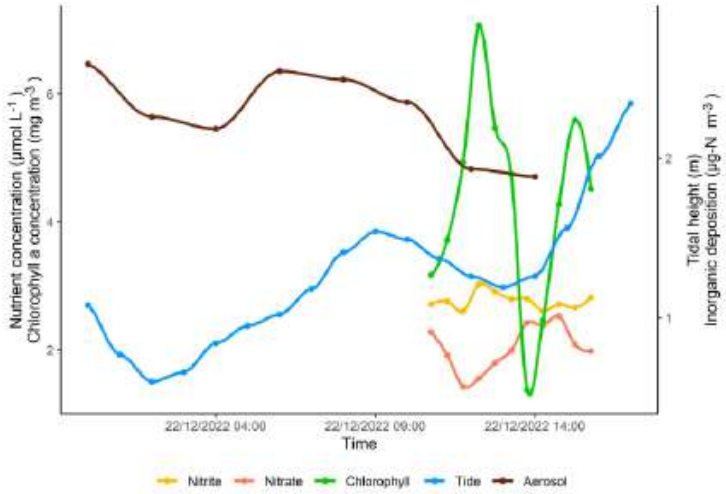

Typical pattern observed in winter: two chlorophyll peaks, one in the morning (likely due to atmospheric inorganic nitrogen) and another in the afternoon (likely due to receding tides)

[1] Archana, A. et al. *Water Research*, **2018**, *142*, 459 – 470.
[2] Yau Y. Y. et al. *Environmental Science & Technology*, **2020**, *54*(7), 3920 – 3928.
[3] Li, J. et al. *Atmospheric Environment*, **2022**, *27*, 118905.
[4] Yau, Y. Y. Y. et al. *Science of the Total Environment*, **2022**, *832*, 154781.

Oral Presentation

Elevational trends in mercury speciation and microbial controls on methylmercury cycling in tropical forest soils

Xizi Yang[a] and Martin Tsz-Ki Tsui

[a] *School of Life Sciences, Earth and Environmental Sciences Programme, The Chinese University of Hong Kong, Hong Kong SAR, China*

E-mail: 1155168394@link.cuhk.edu.hk

The distinct physical and chemical properties of mercury enable its long-distance transport among continents and ecosystems. Its highly toxic organic form, methylmercury, is produced *in situ* in reducing environments such as wetlands, which have been widely identified as hotspots for aquatic sources of methylmercury production. However, our understanding on the production of methylmercury in largely oxic terrestrial landscapes remains relatively limited. Here we investigated mercury and methylmercury distribution in soils along an elevational gradient on Tai Mo Shan, Hong Kong.

As altitude rises in Tai Mo Shan, land cover changes from forests to shrublands, and grasslands. Preliminary data show soil methylmercury positively correlates with altitude and soil pH but negatively correlates with soil organic matter content, while total mercury exhibits the opposite trends. Chemically fractionating soil mercury reveals methylmercury/total mercury correlates with mercury associated with organic matter and metal oxides but negatively correlates with mercury in reducd form.

We hypothesize that methylmercury equilibrates in soil as a result of competition between microbial methylators and demethylators, whose abundance and activities are mainly limited by soil properties and organic inputs. This study aims to determine mercury and methylmercury distribution across altitudes and vegetation zones and decipher ecological and geological factors governing methylmercury levels in soil. Genomic, metabolic, and isotopic studies will unveil interactions between soil, roots, litter, methylators and demethylators on microscopic scale.

International Conference on Earth, Energy & Environmental Sciences for Carbon Neutrality (ICE3SCN)

Conference Abstract

5 December 2023 (Tuesday)

Energy Conversion Session (5 December)

Keynote Lecture

The Promotion of Emerging Energy Materials for Carbon Neutrality through Lithium Bond Chemistry

Qiang Zhang1*

1 Department of Chemical Engineering, Tsinghua University, Beijing 100084, China

zhang-qiang@mails.tsinghua.edu.cn

As one of the most important applications of the element, Li batteries afford emerging opportunities for the exploration of Li bond chemistry. In this talk, the historical development and concept of the Li bond are reviewed, in addition to the application of Li bonds in Li batteries. In this way, a comprehensive understanding of the Li bond in Li batteries and an outlook on its future developments is presented. The Li bond was described in the context of Li batteries, including discussions of sulfur cathodes, liquid electrolytes, and Li metal anodes. Such discourse on the chemistry of the Li bond can provide fruitful insight into the fundamental interactions within Li batteries and thus deliver a deeper understanding of their working mechanism. Nevertheless, further investigations are necessary for a comprehensive understanding of Li bond chemistry, including its clear designation, geometrical and electronic structures, features that differ from other bonds involving Li, and their typical functions in Li batteries.

References

1. Chen X, Bai YK, Zhao CZ, Shen X, Zhang Q. Angew Chem Int Ed 2020, 59, 11192.
2. Hou TZ, Xu WT, Chen X, Peng HJ, Huang JQ, Zhang Q. Angew Chem Int Ed 2017, 56, 8178
3. Zhang R, Chen XR, Chen X, Cheng XB, Zhang XQ, Yan C, Zhang Q. Angew Chem Int Ed 2017, 56, 7764.
4. Li BQ, Peng HJ, Chen X, Zhang SY, Xie J, Zhao CX, Zhang Q. CCS Chem 2019, 1, 128.
5. Chen X, Zhang Q. Acc Chem Res 2020, 53, 1992.
6. Chen X, Bai YK, Shen X, Peng HJ, Zhang Q. J Energy Chem 2020, 51, 1
7. Yao YX, Chen X, Yan C, Zhang XQ, Cai WL, Huang JQ, Zhang Q. Angew Chem Int Ed 2021, 60, 4090.
8. Shi P, Hou LP, Jin CB, Xiao Y, Yao YX, Xie J, Li BQ, Zhang XQ, Zhang Q. J Am Chem Soc 2022, 144, 212.

Invited Talk

Material Design and Device Engineering for Efficient Organic Photovoltaic Cells

Jianhui Hou

Institute of Chemistry, Chinese Academy of Sciences, Beijing, China

E-mail: hjhzlz@iccac.ac.cn

The developments on organic photovoltaic (OPV) materials and device engineering have contributed greatly to the rapid advances in photovoltaic performance of OPV cells. In the past years, we focused on the conjugated polymers based on benzothiophene units and developed a few polymer donors with superior photovoltaic performance, such as PBDB-T and PBDB-TF (also known as PM6). Based on these polymers and the non-fullerene acceptors developed by other research groups, we carried out a series of studies on material design and device engineering. In this presentation, I would like to introduce some interesting and useful strategies related to molecular design and device fabrication. What is more, our recent works including the single-junction cells with over 19% efficiency, the double-junction tandem cells with over 20% efficiency and the efficient OPV cells for indoor applications will be briefly introduced.

Invited Talk

Interface-Driven Stability for Halide Perovskite Photovoltaics: A Fundamental Understanding

Prof. Zonglong Zhu

Associated Professor
Department of Chemistry, City University of Hong Kong
Email：zonglzhu@cityu.edu.hk

Organic-inorganic hybrid perovskite solar cells (PSCs) have shown great progress over the past decade, with power conversion efficiencies (PCEs) of single-junction devices approaching silicon photovoltaics. However, their long-term stability still lags behind silicon-based competitors, which has significantly decelerated their commercialization progress. Faced with this challenge, major efforts have been made to unravel instability mechanisms, develop long-term performance-tracking protocols, and explore various approaches for enhancing the stability of PSCs. Among these strategies, interface manipulation is the most critical as it could simultaneously passivate or anchor the perovskite surface defects and acts as a barrier to protect the bulk of perovskite from the external environment. Recently, the development of diversified interface modification molecules and interfacial regulation strategies has greatly contributed to the improvement of PSC stability. This presentation will elucidate the factors influencing the stability of PSCs, provide an in-depth understanding of device degradation mechanisms, and present advanced approaches to reveal them. Additionally, we will discuss pressing topics on interface manipulation, including low-dimensional perovskite capping layers, interface modification and reaction, and charge transport layer design. Lastly, we will provide insights into the core aspects related to the future development of PSC stability.

Invited Talk

Twisting photons with chiral metal-halide semiconductors

Haipeng LU,[a]

[a] *Department of Chemistry, The Hong Kong University of Science and Technology, Hong Kong, China (SAR)*

E-mail: haipenglu@ust.hk

Chiral metal-halide semiconductors (MHS) have recently developed as promising candidates for spin- and polarization-resolved optoelectronic devices. Although several chiral MHS with rich chemical and structural diversity have been reported lately, the fundamental mechanisms governing their chiroptical activity, namely, circularly polarized absorption and emission, remain elusive. In this talk, I will discuss our recent progress in understanding and tuning the chiroptical activity in chiral MHS. I will first discuss how the chirality is transferred from organic to inorganic component through asymmetric covalent bonding interactions. Their endowed molecular chirality was then studied by circular dichroism (CD). However, we found that the previously reported “apparent” CD in chiral MHS thin films is not an intrinsic chiroptical property, but rather, arising from an interference between the film’s linear birefringence and linear dichroism. We verify the presence of LB and LD effects in both one-dimensional and zero-dimensional chiral MHS thin films. We then establish spectroscopic methods to decouple the genuine CD from other spurious contributions, which allows a quantitative comparison of the intrinsic chiroptical activity across different chiral MHS. The relationship between the structure and the genuine chiroptical activity is then uncovered, which is well described by the chirality-induced spin–orbit coupling in the chiral structures. Meanwhile, we found that high CD signals do not necessarily lead to high circularly polarized luminescence as most of the current chiral MHS display very low photoluminescence quantum yields (PLQY). We will then discuss the reasons of low PLQY in these materials. Finally, we will show our demonstrations of chiral perovskites for spin-LED devices.

References

1. Zhang, Z.; Wang, Z.; Sung, H. Y.; Williams, I. D.; Yu, Z.-G.; Lu, H.* *J. Am. Chem. Soc.*, 2022, *144*, 22242.
2. Wang, Z.; Wang, X.; Chen, Z.; Liu, Y.; Xie, H.; Xue, J.; Mao, L.; Yan, Y.*; Lu, H.* *Angew. Chem. Int. Ed.*, 2023, e202215206.
3. Kim, Y.-H.#; Zhai, Y.#; Lu, H.#; Pan, X.; Xiao, C.; Gaulding, E. A.; Harvey, S. P.; Berry, J. J.; Vardeny, Z. V.; Luther, J. M.*; Beard, M. C.* Chiral Induced Spin Selectivity Enables a Room Temperature Spin-LED. *Science*, 2021, *371*, 1129-1133.

Invited Talk

Efficient e-fuel electrosynthesis from CO_2

Xue Wang[a]

[a] *School of Energy and Environment, City University of Hong Kong.*

E-mail: xue.wang@cityu.edu.hk

The electroreduction of CO_2 (CO_2RR) to chemicals and fuels provides a sustainable avenue to the storage of intermittent renewable electricity. Although a wide range of different products from C_1 to C_3 have been produced, CO_2RR still suffers from low selectivity at commercially relevant current densities (100 mA cm^{-2}). In this talk, I will present our recent progress towards the electrosynthesis of fuels (e.g., methane and ethanol) from CO_2RR (references 1-3), looking both at the catalyst and at the system.

References

[1]X. Wang, Z. Wang, F.P.G. de Arquer, C.-T. Dinh, A. Ozden, Y.C. Li, D.-H. Nam, J. Li, Y.-S. Liu, J. Wicks, Z. Chen, M. Chi, B. Chen, Y. Wang, J. Tam, J.Y. Howe, A. Proppe, P. Todorović, F. Li, T.-T. Zhuang, C.M. Gabardo, A.R. Kirmani, C. McCallum, S.-F. Hung, Y. Lum, M. Luo, Y. Min, A. Xu, C.P. O'Brien, B. Stephen, B. Sun, A.H. Ip, L.J. Richter, S.O. Kelley, D. Sinton and E.H. Sargent. Efficient electrically powered CO_2-to-ethanol via suppression of deoxygenation. *Nature Energy* 2020, *5*, 478;

[2]X. Wang, A. Xu, F. Li, S.-F. Hung, D.-H. Nam, C.M. Gabardo, Z. Wang, Y. Xu, A. Ozden, A.S. Rasouli, A.H. Ip, D. Sinton and E.H. Sargent. Efficient methane electrosynthesis enabled by tuning local CO2 availability. J. Am. Chem. Soc. 2020, *142*, 3525;

[3]X. Wang, X.; P. Ou, J. Wicks, Y. Xie, Y. Wang, J. Li, J. Tam, D. Ren, J. Y. Howe, Z. Wang, A. Ozden, Y. Z. Finfrock, Y. Xu, Y. Li, A. S. Rasouli, K. Bertens, A. H. Ip, M. Graetzel, D. Sinton, E. H. Sargent. Gold-in-copper at low *CO coverage enables efficient electromethanation of CO_2. *Nature Commun.* 2021,*12*, 3387.

Oral Presentation

Interface Engineering for Efficient, Stable and Environmentally Benign Perovskite Solar Cells

Shengfan WU,[a,c] Alex Kwan Yue JEN[a,b,c]

[a] *Department of Materials Science and Engineering, City University of Hong Kong, Kowloon, Hong Kong;*
[b] *Department of Chemistry, City University of Hong Kong, Kowloon, Hong Kong;*
[c] *Hong Kong Institute for Clean Energy, City University of Hong Kong, Kowloon, Hong Kong*

- E-mail: shengfwu2@cityu.edu.hk; alexjen@cityu.edu.hk

Metal halide perovskites (MHPs) have emerged as promising semiconductors within the optoelectronics landscape, owing to their impressive photoelectrical properties, such as high absorption coefficients, high defect tolerance, long carrier diffusion lengths, and low exciton binding energies.[1] Over the past 14 years, the power conversion efficiency (PCE) of single-junction perovskite solar cells (PSCs) has skyrocketed from 3.8% to 26.1%, an unprecedented leap in the photovoltaics (PV) sector. Despite such progress, persistent challenges obstruct further advancement of PSC efficiency. Among these, significant energy losses at the interfaces and below-bandgap optical losses are the two primary concerns. Moreover, the potential impacts of toxic lead-based components in state-of-the-art MHPs present substantial challenges, posing threats to environment, human health, and end-of-life handling of PSCs. In this talk, I will present our recent strides towards realizing high-efficiency, long-term stable, and environmentally benign PSCs, with a particular focus on interface engineering strategies.[1-3]

References

[1] Wu S.F., Zhu, Z.L., Jen, K.Y., et al. *Joule*, 2020, 4, 1248-1262.
[2] Wu S.F., Xu, Z.T., Zhu, Z.L., Jen, K.Y., et al. *Nat. Nanotechnol.*, 2020, 15, 934-940.
[3] Wu S.F., Zhu, Z.L., Jen, K.Y., et al. *Adv. Mater.*, 2021, 33, 2105593.

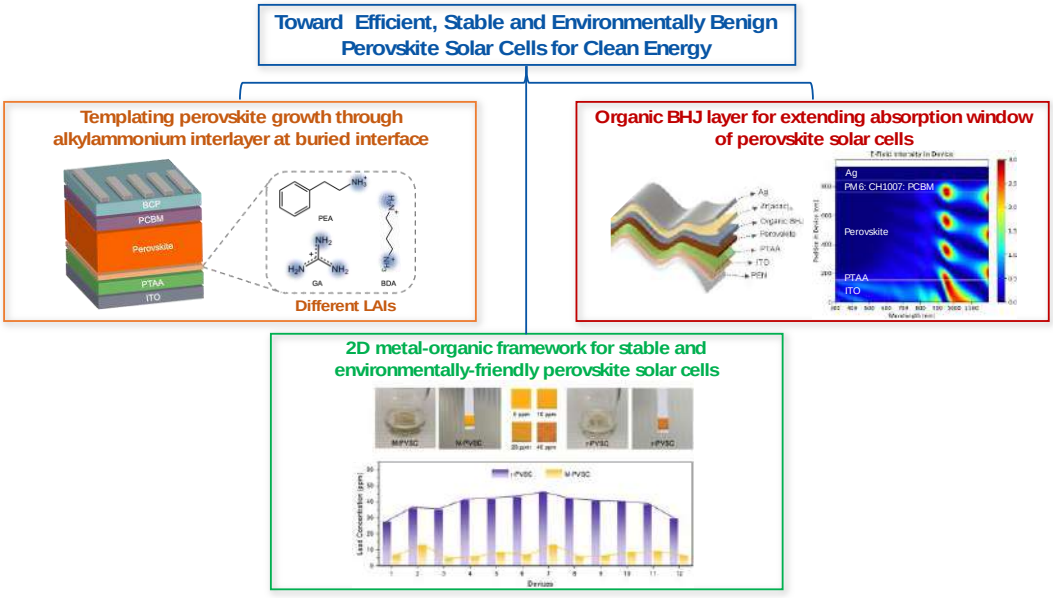

Figure 1. Summary of the interface engineering for efficient, stable and environmentally benign perovskite solar cells

Oral Presentation

Carbon-based Photocatalysts for Efficient Non-sacrificial Synthesis of Hydrogen Peroxide

Liangpang Xu, Jimmy C. Yu

Department of Chemistry, The Chinese University of Hong Kong, Hong Kong, China.

E-mail: liangpangxu@cuhk.edu.hk

Hydrogen peroxide (H_2O_2) is a common and useful eco-friendly oxidant with extensive industrial applications. Photocatalysis is a promising approach for green and sustainable H_2O_2 synthesis from O_2 reduction reaction (ORR). However, the efficiency for photocatalytic H_2O_2 synthesis is still highly restrained by low activity of catalysts, insufficient proton supply, and difficult activation of O_2 molecules, etc. Here, various biomass (glucose, sucrose, starch, cellulose, and paperboard) was converted to hydrothermal carbonaceous carbon (HTCC) photocatalyst for H_2O_2 synthesis in pure water.[1] It was found that the polyfuran structure of HTCC is favorable for adsorption and activation of oxygen and exhibits superior electron transfer property. As such, the H_2O_2 could be efficiently produced in a two-step oxygen reduction reaction with superoxide anions as intermediates. The H_2O_2 synthesis on HTCC could reach a rate of 1.16 mmol g_{cat}^{-1} h^{-1}, together with an apparent quantum yield (Φ_{AQY}) of 18.2% (at 420 nm). To achieve efficient alkaline photocatalytic H_2O_2 synthesis, which is challenging due to limited supply of protons from a sluggish water dissociation, a novel pyrophosphate-based proton shuttle strategy has been proposed.[2] Pyrophosphate-incorporated g-C_3N_4 photocatalyst shows a record-high alkaline H_2O_2 synthesis rate (e.g. 1.07 mmol g_{cat}^{-1} h^{-1} at pH 9) and an Φ_{AQY} of 8.7 % (at 420 nm). Mechanism study demonstrates that the pyrophosphate could serve as a proton shuttle to effectively adsorb and provide protons, and act as advanced active sites for O_2 adsorption and activation to promote O_2 reduction, which greatly benefits the capture of nearby protons by the activated O_2 to form H_2O_2. Taking the advantage of alkaline H_2O_2 generation, on-site treatment of organic pollutants in alkaline waters could be achieved. Furthermore, the introduction of EDTA as functional molecules was found to be effective for further boosting H_2O_2 synthesis efficiency.[3] Such an EDTA-involved system could deliver an outstanding Φ_{AQY} of 27.6 % (at 420 nm), exceeding that of the state-of-the-art ORR photocatalysis. It was found that the EDTA could facilitate ORR in both thermodynamics and kinetics. Mechanism study demonstrates the key role of carboxylic groups in EDTA, whose interaction with O_2 benefits the critical O_2 activation process. Notably, the EDTA is a non-sacrificial agent and could stabilize the H_2O_2 product from decomposition during photocatalysis. The strategies proposed in these works shed light on the development of practical photocatalytic approaches for H_2O_2 synthesis.

References

[1] Xu L, Liu Y, Li L, et al. *ACS Catal.*, 2021, *11*, 14480-14488;
[2] Xu L, Li L, Hu Z, Yu JC. *Appl. Catal. B*, 2023, 122490;
[3] Xu L, Li L, Hu Z, Yu JC. *J. Catal.,* 2023, *418*, 300-311.

International Conference on Earth, Energy & Environmental Sciences for Carbon Neutrality (ICE3SCN)

Poster Presentation

Energy Conversion Session

EC-01

The Role of Anode Porous Transport Layer in Efficient and Durable CO_2 Electrolysis

Xinyuan Chai,[a]Zhanyou Xu,[a] Ying Wang[a]

[a]*Department of Chemistry, The Chinese University of Hong Kong, Shatin, N.T. HK SAR, P. R. China*

E-mail: 1155201355@link.cuhk.edu.hk

Membrane-electrode-assembly (MEA) electrolyser, which eliminates electrolyte usage, is promising to develop energy-efficient and stable electrolysers for electrochemical CO_2 reduction reaction (CO_2RR). While significant progress has been made to optimise the cathodic CO_2RR, less attention is drawn to the anode design, which affects energy efficiency and durability of MEA. Herein, we systematically investigated the effect of anode porous transport layer (PTL) in MEA for CO_2RR. The pore size and roughness of PTL are found to influence the local pressure and mass transport resistance at the membrane-electrode interface. Ti felt PTL exhibits uniformly distributed local pressure and excellent bubble release capacity, giving rise to a low interfacial resistance and stable membrane-electrode interface. The electrolyser with Ti felt PTL shows the highest EE_{CO} ((33.3 ± 1.0)% at 250 mA cm^{-2}) with 7 h electrolysis, nearly double the duration for the one with Ti mesh anode PTL. EIS test reveals that the electrolyser with Ti felt PTL has the lowest charge transfer resistance.

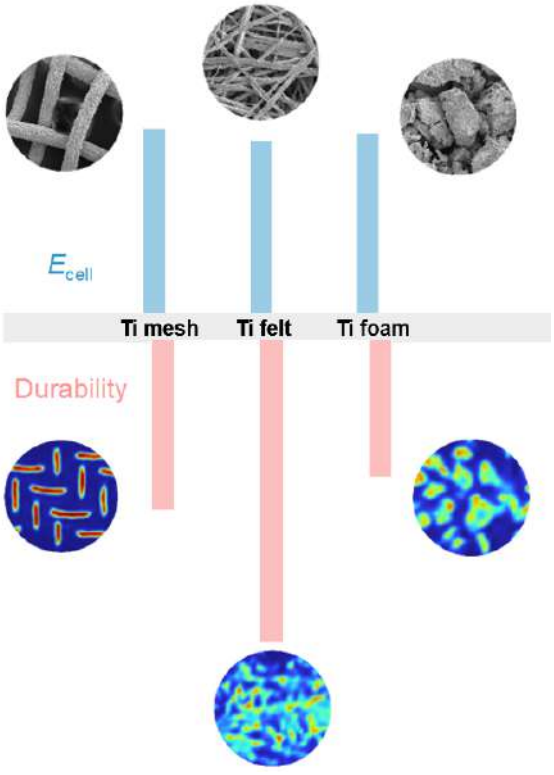

Figure 1. Cell voltage and durability of Ti mesh, Ti felt and Ti foam

EC-02

Surface Recrystallization via careful solvent design for efficient Tin Halide Perovskite Films

Pok Fung Chan[1], Minchao Qin[1], Chun-Jen Su[2], Liping Ye[3], Xuezhou Wang[4], Yunfan Wang[5], Xin Guan[3], To Ngai[3], Sai Wing Tsang[5], Ni Zhao[4], and Xinhui Lu[1,*]

[1]Department of Physics, The Chinese University of Hong Kong, New Territories 999077, Hong Kong SAR, China
[2]National Synchrotron Radiation Research Center, Hsinchu Science Park, Hsinchu 30076, Taiwan
[3]Department of Chemistry, The Chinese University of Hong Kong, New Territories 999077, Hong Kong SAR, China
[4]Department of Electronic Engineering, The Chinese University of Hong Kong, New Territories 999077, Hong Kong SAR, China
[5]Department of Materials Science and Engineering, City University of Hong Kong, Kowloon Tong 999077, Hong Kong, China
*E-mail: xinhui.lu@cuhk.edu.hk

Tin-based perovskite solar cells (PSC) are becoming promising substitutes for their toxic lead counterparts. However, tin-based PSCs are prone to oxidation and thus still exhibit inferior device performance[1]. Owing to the different chemical properties of lead (II) and tin (II) ions, the mechanisms for reliable film preparation processes are still under exploration. Herein, we propose a surface treatment to modify the surface of tin-based perovskite using a commonly used ligand, iso-butylammonium iodide (iso-BAI). We demonstrate that the mechanism of the surface treatment in tin-based perovskite originates from the recrystallization of the surface due to the higher solubility of tin-based perovskite in common solvent, which is different from the lead counterparts. With a carefully designed solvent composition, we successfully modify the perovskite surface (Fig. 1e,f) while keeping the bulk intact. X-ray diffraction measurements reveal that the perovskite surface dissolves and re-crystallizes with the guidance of iso-BAI The resultant films exhibit enhanced surface crystallinity (Fig. 1a,b), released microstrain (Fig. 1c), reduced surface defects, and improved charge transport. With the surface treatment, the power conversion efficiency of the FASnI3 perovskite solar cells increases from 11.8% to 14.2% , which is close to the current record. This work first distinguishes the mechanism of surface treatments in tin-based perovskite from that of the lead counterpart, which is crucial for designing tailor-made strategies for fabricating tin-based PSCs.

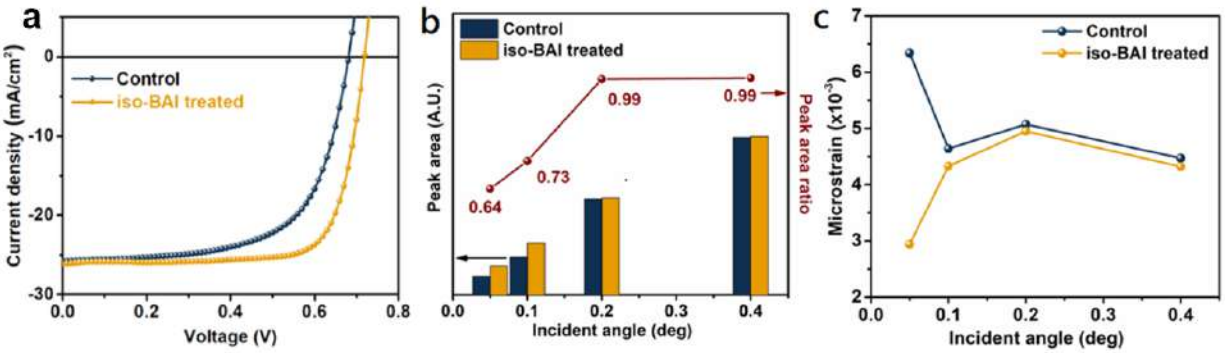

Figure 1. (a) JV curve of the solar cell devices, (b) (100) peak intensity ratio obtained from the GIWAXS measurement of the films, and (c) Estimated microstrain of the control and the iso-BAI treated film.

References

[1] Lanzetta, L., et al., Nat Commun, 2021. 12(1): p. 2853.

EC-03

Passivating deep traps in high-performance organic photovoltaics by improving the connectivity of non-fullerene acceptor domains

Yuang FU,[a] Luhang XU,[a] and Xinhui LU[a]

[a] *Department of Physics, The Chinese University of HONG KONG, New Territories, Hong Kong.*

E-mail: 1155103070@link.cuhk.edu.hk

Organic photovoltaics (OPVs) are promising candidates for building-integrated solar windows and power sources for wearable electronics due to their low cost, tunable energy levels, mechanical robustness, and compatibility with large-scale manufacturing.

The detrimental impact of trap-assisted recombination on high-performance OPVs has been recognized, yet its morphology origin remains unclear[1]. Herein, we studied PM6:Y6-based OPV devices processed using different methods and observed the presence of monomolecular trap-assisted recombination in all devices, especially for those fabricated via sequential deposition. The density of trap states can be effectively suppressed by replacing the liquid additive chloromethane (CN) with solid additive diiodide benzene (DIB). Through multilength scale morphology characterization of blend film morphology using spectroscopic, scanning microscopic as well as X-ray and neutron scattering techniques, we found that CN induces closely-packed H-type aggregates between core units of Y6 molecules that lead to higher crystallinity, but also severe agglomerations in the mesoscale, while DIB enhances the J-type backbone-on packings of Y6 molecules forming polymer-like charge transport networks. As a result, the DIB-processed blend films show much more extended crystalline domains with a lower fractal dimension (*D*) and smaller amorphous intermixed domains compared to the CN-processed films. Based on our results, we propose that both isolated crystalline Y6 domains and poorly connected amorphous Y6 aggregates dispersed within the intermixed domains act as deep electron traps due to the large energetic offset between the lowest unoccupied molecular orbitals (LUMOs) of PM6 and Y6. Therefore, the key for trap passivation is through the formation of extended acceptor networks with low fractal dimensions (*D*) that simultaneously improve inter-domain connectivity and shrink the size of intermixed domains. Our work established a solid correlation between bulk trap density and active layer morphology in high-performance OPVs and provided guidelines for further increasing the efficiency of OPVs through multilength scale morphology control of the less well-connected acceptor components.

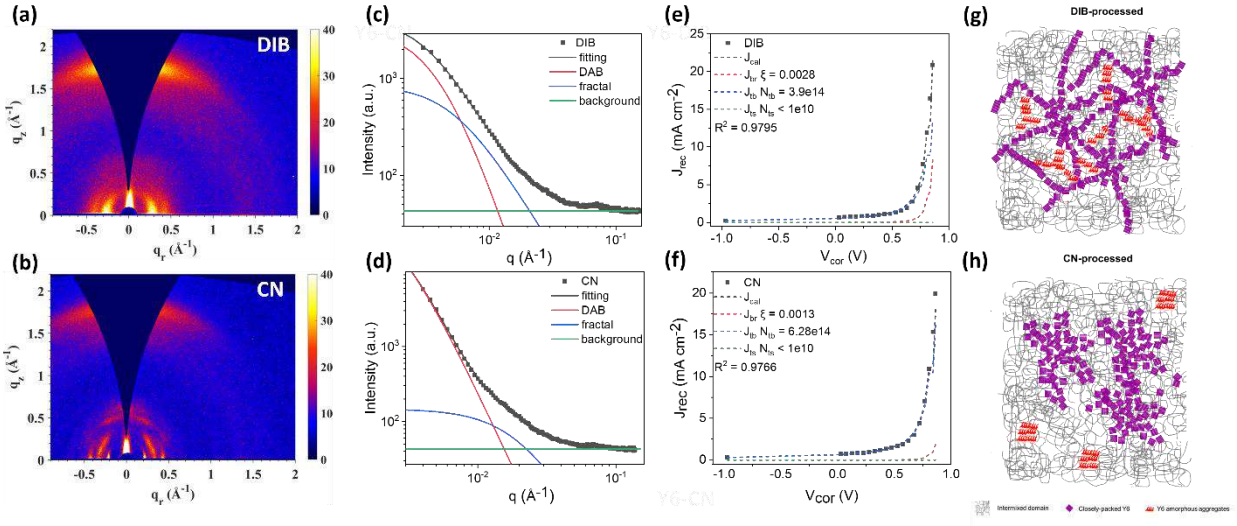

Figure. (a) and (b) The 2-D GIWAXS patterns, (c) and (d) the 1-D inplane GISAXS linecuts and DIB and CN-processed films. The recombination kinetics of the corresponding devices are shown in (e) and (f) while the schematics depicting film morphology are shown in (g) and (h).

References

[1] Zeiske, S. et al. Nat. Commun. 12, 3603 (2021).

EC-04

Understanding ultrafast excited state dynamics in Y6-type acceptors in organic solar cells

Yu Guo, Philip C.Y. Chow*

Department of Mechanical Engineering, The University of Hong Kong, Hong Kong SAR, China

pcyc@hku.hk

Organic solar cells (OSCs) with high mechanical flexibility, light weight, and low-cost solution processability can be a complementary technology to current silicon solar cells. Excitingly, there has been a great improvement in OSC device performance over the past 5 years (from about 13% to over 19% power conversion efficiency). This improvement is largely due to the development of new non-fullerene acceptor materials. The landmark acceptor, Y6, developed in 2019, first enabled OSCs with over 15% efficiency. After that, a series of derivative acceptors based on Y6 have been developed, further promoting the improvement of OSC efficiencies. While extensive research has been conducted to understand the mechanisms behind the outstanding performance of Y6-based OSC devices, a comprehensive understanding of their fundamental excited state dynamics and structure-property relationship is still lacking. In this work, we study the fundamental excited state dynamics in Y6-type acceptors using transient optical spectroscopy techniques. By studying a broad range of Y6-type acceptors, we reveal the precise relationship between molecular structure, film morphology and ultrafast excited state dynamics in these materials. These results help to explain why certain new Y6-type acceptors (such as L8-BO) outperform older systems (such as Y6) in blend devices. Overall, our work sheds light on the fundamental structure-property relationship of Y6-type acceptors and provide guidance for future OSC material development.

EC-05

Self-adaptive and switchable solar heating and radiative cooling system

Senji Li, Dongsheng Li, Philip C.Y. Chow*

Department of Mechanical Engineering, The University of Hong Kong, Hong Kong SAR, China

Radiative cooling has been proven as a highly-promising and scalable technology towards carbon neutrality and energy saving in buildings. By utilizing the mid-infrared (MIR, ~8-13 μm) gap in Earth's atmosphere, thermal radiation can be emitted into outer space on a completely passive and automatic basis without any energy input. However, in many climate zones where ambient temperature varies significantly throughout the year, it is often desirable to switch off the radiative cooling and instead switch on the heating (e.g. during winter). Therefore, the development of a smart, fully self-adaptive thermal management that selectively switch on/off solar heating and radiative cooling in response to the ambient conditions is highly desirable. In this study, we have developed a smart, scalable nanophotonic system with the capability of switching between solar heating and radiative cooling. Through optical and photonic simulation and experimentation, the detailed structure of our smart thermal management system is tested and optimized for tunability in both the solar spectrum and MIR range. We believe that our design will be a valuable reference to studies on smart thermal management, as well as a practicable and scalable solution to energy-efficient buildings, pathing the way towards sustainability.

EC-06

Fostering the Dense Packing of Halide Perovskite Quantum Dots through Binary-Disperse Mixing

Shiang Li,[a] Ziqi Wang,[a] Yuhao Li,[a,b] Chun-Jen Su,[c] Yuang Fu,[a] Yi Wang,[a,*], Xinhui Lu,[a,*]

[a]*Department of Physics, The Chinese University of Hong Kong, Hong Kong SAR, 999077, China*

[b]*Spallation Neutron Source Science Center, Institute of High Energy Physics, Chinese Academy of Sciences, Dongguan, 523803, China*

[c]*National Synchrotron Radiation Research Center, Hsinchu Science Park, Hsinchu, 30076, Taiwan*

*Email: xinhui.lu@cuhk.edu.hk (X. L.)

*Email: yiwang@cuhk.edu.hk (Y. W.)

ABSTRACT: Due to its versatile applications, perovskite quantum dot (PQD)-based optoelectrical devices have garnered significant research attention. However, the fundamental packing behavior of PQDs in thin films and its impact on the device performance remain relatively unexplored. Drawing inspiration from theoretical models concerning packing density with size mixtures, this study presents an effective strategy, namely, binary-disperse mixing, aimed at enhancing the packing density of PQD films. Comprehensive grazing-incidence small-angle X-ray characterization suggested that the PQD film consists of three phases: two mono-size phases and one binary mixing phase. The volume fraction and population of the binary-size phase can be tuned up by mixing an appropriate amount of large and small PQDs. Furthermore, we performed multi-length scale all-atom and coarse-grained molecular dynamics simulations to elucidate the distribution and conformation of organic surface ligands, highlighting their influence on PQD packing. Notably, the mixing of two PQDs of different sizes promotes closer face-to-face contact. The densely packed binary-disperse film exhibited largely suppressed trap-assisted recombination, much longer carrier lifetime and thereby an improved power conversion efficiency. Hence, this study provides fundamental understandings on the packing mechanism of perovskite quantum dots and highlights the significance of packing density for PQD-based solar cells.

References

[1] S. Li, Z. Wang, Y. Li, C. Su, Y. Fu, Y. Wang, and X. Lu. *ACS Nano*, 2023, 17, 20, 20634–20642.

EC-07

Stabilized Heterointerface for High-efficiency and Stable Inverted Perovskite Solar Cells

Zhen Li,[a] Zonglong Zhu [a]

[a] *Department of Chemistry, City University of Hong Kong, Kowloon 999077, Hong Kong*

E-mail: zli269@cityu.edu.hk

Currently, over 85% of global energy is derived from non-renewable fossil fuels, necessitating the development of sustainable energy sources. Metal halide perovskite solar cells (PSCs) have emerged as viable candidates for this purpose. Inverted (p-i-n) PSCs offer improved stability and lifespan due to their un-doped hole-transporting layers (HTLs) and highly crystalline perovskite films. However, their power conversion efficiency (PCE) lags behind conventional (n-i-p) devices. Interfacial engineering to limit non-radiative recombination is one strategy to enhance PSC performance and stability.

To assess the impact of the perovskite/electron-transporting layer interface, we've developed an organometallic interface material ($FcTc_2$). This ferrocene-based compound provides solid Pb-O binding between perovskite and molecule, effectively reducing surface trap states. The electron-rich ferrocene units also accelerate interfacial electron transfer. These effects of FcTc2 lead to a record PCE of 25.0% (certified 24.3%) in inverted PSCs. Devices maintained over 98% of initial efficiency after 1500 hours of operation under simulated AM1.5 illumination and showed satisfactory durability under damp heat conditions, meeting IEC61215:2016 qualifications[1] (Fig. 1a).

In the interface between perovskite and anode, a thermally robust hole-selective layer combined with novel self-assembly monolayer (SAM) and nickel oxide nanoparticles (NiO_x) was developed. The favorable energetic alignment and binding between NiO_x/MeO-4PADBC and perovskite reduced the voltage deficit of PSCs with various perovskite compositions, leading to robust interface toughening effects under thermal stress. The resultant device achieved a certified power conversion efficiency of 25.6% and maintained over 90% of its initial efficiency after continuous operation at 65 ℃ for 1,200 hours under 1 sun illumination. This is the first reported study investigating the degradation mechanism of SAM-based PSCs under thermal stress[2] (Fig. 1b).

Moreover, a simplified PSC fabrication strategy by co-depositing SAM and perovskite absorber, was proposed to iimprove the processability of perovskite solar cells. We observed that phosphonic or carboxylic acids, incorporated into perovskite precursor solutions, self-assemble on the indium tin oxide substrate during perovskite film processing. They form a robust SAM as an excellent hole-selective contact while the perovskite crystallizes. Our approach solves wettability issues and simplifies device fabrication, advancing the manufacturability of PSCs. Our PSC devices show a power conversion efficiency of 24.5% and retain >90% of their initial efficiency after 1,200 h of operating at the maximum power point under continuous illumination. The approach shows good generality as it is compatible with different self-assembled monolayer molecular systems, perovskites, solvents and processing methods[3] (Fig. 1c).

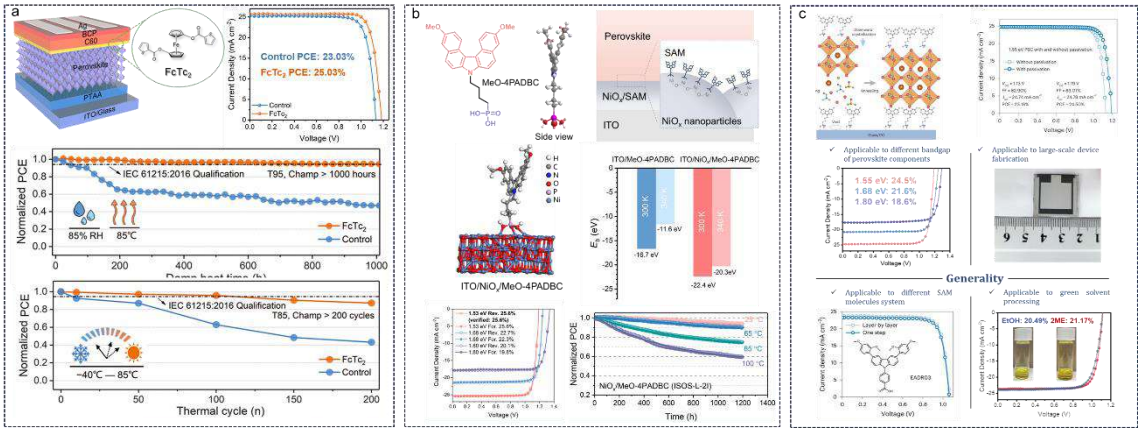

Figure 3 a) Organometallic-functionalized interfaces for highly efficient inverted perovskite solar cells; b) Stabilized hole-selective layer for high-performance inverted pin perovskite solar cells; c) Co-deposition of hole-selective contact and absorber for improving the processability of perovskite solar cells.

References

[1] Li Z, Zhu Z*., et al. *Science*, 2022, *376, 416-420*;

[2] Li Z, Zhu Z*., et al. *Science*, 2023, *382, 284-289;*

[3] Zheng X., Li Z, Zhu Z*., et al. *Nat. Energy*, 2023, *8, 462-472*

EC-08

Dual-additive-driven morphology optimization for solvent-annealing-free all-small-molecule organic solar cells

Heng Liu, Yuang Fu, Zeng Chen, Jiayu Wang, Jiehao Fu, Yuhao Li, Guilong Cai,* Chun-Jen Su, U-Ser Jeng, Haiming Zhu, Gang Li, Xinhui Lu*

Department of Physics, The Chinese University of Hong Kong, New Territories 999077, Hong Kong, China.

E-mail: xinhui.lu@cuhk.edu.hk

All-small-molecule organic solar cells (ASM-OSCs), which consist of small-molecule donor and acceptors, have recently been studied extensively to eliminate the batch-to-batch variation from polymer-based donor or acceptor.[1] On the other hand, the control of their active layer morphology is more challenging than conventional polymer/small molecule based OSCs, due to the similar chemical structure and miscibility of small-molecule donor and small-molecule accepter.[2] Hence, this study developed a dual-additive-driven morphology optimization method for ASM-OSCs based on BTR-Cl:Y6. One solid additive - 1,4-diiodobenzene (DIB) and one liquid additive - diiodomethane (DIM) are added together into the solution of active materials, making use of their distinct interaction mechanisms with Y6 and BTR-Cl. It is found that DIB can form a eutectic phase with Y6, which can increase the intermolecular interactions and modulate the acceptor phase separation, while the simultaneous volatilization of DIM suppresses the over-aggregation of BTR-Cl during the film casting process. As a result of the synergistic morphology tuning, the optimized device delivered a PCE as high as 15.2%, among the highest PCE reported to date for binary ASM-OSCs without solvent annealing treatment. This work demonstrates the potential of morphology tuning via the incorporation of dual additives into ASM-OSCs, enabling them to achieve comparable efficiencies to those of conventional polymer/small-molecule based OSCs.

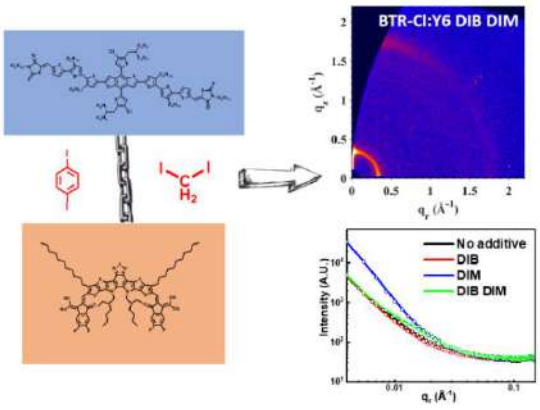

Figure 4. The combination of DIB and DIM can modulate the morphology of blend film

References

[1] J. Qin, Z. Chen, P. Bi, Y. Yang, J. Zhang, Z. Huang, Z. Wei, C. An, H. Yao, X. Hao, *Energy Environ. Sci.* 2021;

[2] K. Sun, Z. Xiao, S. Lu, W. Zajaczkowski, W. Pisula, E. Hanssen, J. M. White, R. M. Williamson, J. Subbiah, J. Ouyang, *Nat. Commun.* 2015, 6, 6013.

EC-09

Dual-atoms induced bifunctional catalytic centers enables highly efficient rechargeable Zn-air batteries

Qian Lu,[a] Ying Wang,[a] Zongping Shao,[b]

[a] *Department of Chemistry, The Chinese University of Hong Kong, Hong Kong, China* [b] *WA School of Mines: Minerals, Energy and Chemical Engineering, Curtin University, Perth, Australia.*

E-mail: qianlu@cuhk.edu.hk

Composite strategies for constructing dual-atom sites at the hetero-interface provide considerable prospects for designing efficient bifunctional oxygen catalysts.[1] Given the insufficient interface site and the instability of the phase interface, we need to develop more efficient strategies for efficiently utilizing the dual-atom site.[2,3] Here, we report a doping strategy to construct abundant dual-atom sites in single-phase oxide catalysts. We first screen a series of transition metal-doped RuO_2 electrocatalysts to extract the optimal metal, considered Mn. The highest bifunctional activity, with an ultra-low overpotential gap of 0.65 V, was achieved when the doping ratio of Mn: Ru was 1: 1. The formation of Ru/Mn dual-atom bonds enables electronic interaction between Ru and Mn, which reduces the oxidation state of Ru^{4+} sites and constructs electron-rich states of Mn^{3+} sites. We further applied DFT calculations to explore the reaction mechanism and found that Mn3+ and Ru^{4+} serve as oxygen reduction and oxygen evolution reaction catalytic sites respectively to facilitate oxygen adsorption and OH* desorption, while co-adsorption of OOH* on Mn/Ru dual sites can greatly enhance the oxygen reduction activity. Rechargeable zinc-air batteries using Mn^{3+}-doped RuO_2 achieve super-durability for 2000 cycles with a final energy efficiency retention of 87.5%. This design concept provides a promising direction for constructing efficient and stable bifunctional oxygen electrocatalysts.

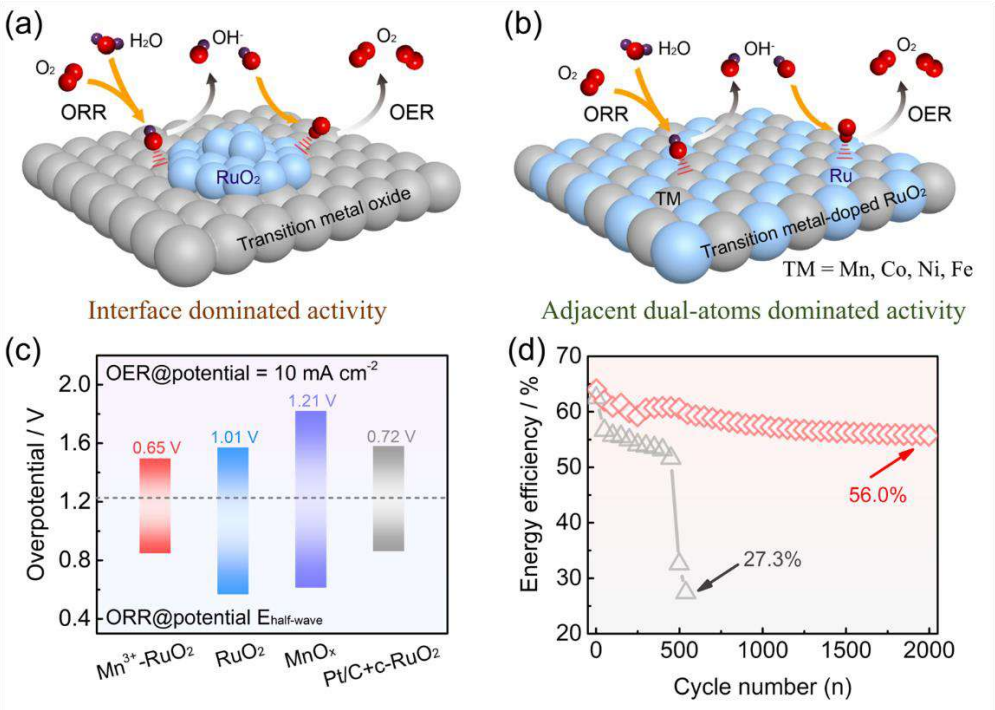

Figure 1. (a) Schematic illustration of composite and single-phase catalysts; (b) Schematic diagram of the synthesis process for transition metal-doped RuO_2; (c) The overpotential gap between the half-wave potential of ORR and the potential of OER at 10 mA cm^{-2}; (d) Energy efficiency of rechargeable Zn-air batteries for Mn^{3+}-RuO_2 and Pt/C-RuO_2 mixture.

References

[1] Q. Lu, X. Zou, Y. Bu, et al. *Energy Storage Mater.*, 2023, 55, 166;

[2] Q. Lu, Y. Guo, P. Mao, et al. *Energy Storage Mater.*, 2020, 32, 20;

[3] Q. Lu, X. Zou, X. Wang, et al. *Appl. Catal. B Environ.*, 2023, 325, 122323;

EC-10

Efficient Electromethanation from CO_2 on Monodisperse Cu-based Catalysts

Jiping Sun,[a,b] Guangchao Li,[b] Zhanyou Xu,[a] Yi Xie,[a] Jiexi Wang,[b] Ying Wang,[a]

[a] *Department of Chemistry, The Chinese University of Hong Kong, Hong Kong 999077, S. A. R., China;*
[b] *School of Metallurgy and Environment, Central South University, Changsha 410083, P. R. China.*
E-mail: jipingsun@cuhk.edu.hk

Electrochemical CO_2 reduction reaction (CO_2RR) is a promising approach to upgrading CO_2 into methane (CH_4) and other high-value-added chemicals, critical for lowering carbon emissions and mitigating the greenhouse effect. However, the selectivity of CO_2RR to methane remains low at the current densities required for commercialization. Herein, we report a simple one-step synthesis of monodisperse copper-based catalysts for efficient electromethanation of CO_2. Through rational regulation of active sites, the selectivity for methane production can reach as high as 57.02% under the current density of 300 mA cm^{-2} due to suppressed C-C coupling for improved *CO hydrogenation. This work offers an effective strategy to regulate Cu-based catalysts to manage the hydrogenation of *CO for CO_2RR toward CH_4 formation.

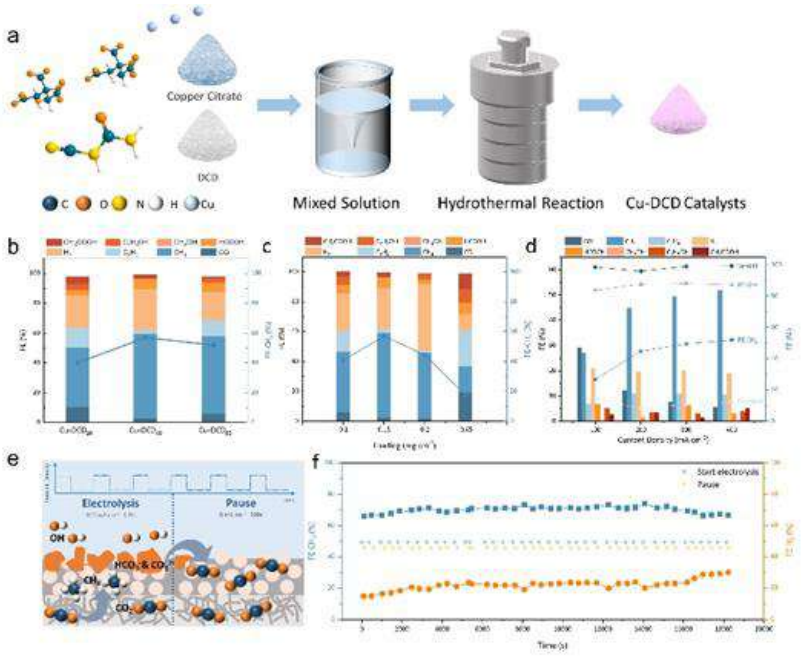

Figure.1. (a) Schematic of the synthesis path of the catalyst; (b) Product distribution; (c) Loading dependence; (d) Current density dependence; (e) Schematic diagram of pulse stability test; (f) Stability test results.

References

[1] J. Sun, Y. Wang*, et al. Efficient methane electrosynthesis from CO_2 over monodisperse Cu-based catalysts. Energy & Fuels, 2023, 37, 12, 8707-8713.

EC-11

Mechanical stability enhancement in lead-halide perovskite solar cells through quasi-2d perovskite buffer layer

Yiran TAO

Flexible solar cells have become one of the most eye-catching photovoltaic devices because of their advantages such as low price and abaundent usage scenarios. Perovskite materials have become strong candidates for manufacturing flexible solar cells due to their excellent optoelectronic properties, low cost and ability to withstand stress accumulation. However, perovskite films still face the problem of limited flexibility and cracks emerging when encountering mechanical movements. Many stratigies have been applied to enhance the mechaincal stability of flexible perovskite solar cells (FPSCs), including compositional engineering, grain boundray crosslinking and interface engineering, etc. It is discovered that by adding a mechaical robust buffer layer on top of the perovskite layer could constrain the tensile strian during convex bending and therefore improving the mechaincal stability of FPSCs. In this work, a quasi-2D perovskite buffer layer which is energy level matching and mechaical demage resisting is intergrated on conventional 3D perovskite solar cells. With the help of the 2D perovskite buffer layer, the inhomogenous strian under convex bending is eliminated to a large extent. The GIWAXS images suggest that cracks exist on the perovskite layer during bending, while the 2D buffer layer could eliminate the cracks to large extent. It is evident by the SEM image that the modified perovskite layer has fewer cracks both on the upper surface and buried interface. The FPSCs exhibit better PCE and anti-fatigue capabilities.

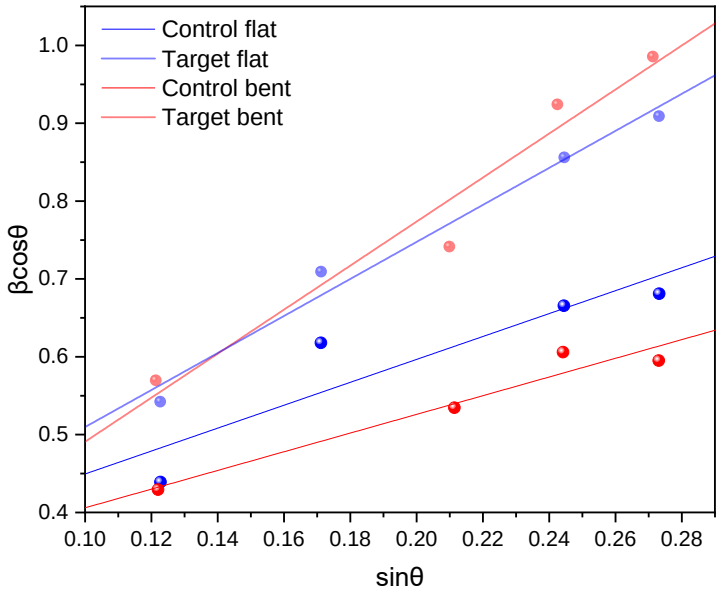
Control flat
Target flat
Control bent
Target bent
βcosθ
sinθ
1.0
0.9
0.8
0.7
0.6
0.5
0.4
0.10
0.12
0.14
0.16
0.18
0.20
0.22
0.24
0.26
0.28

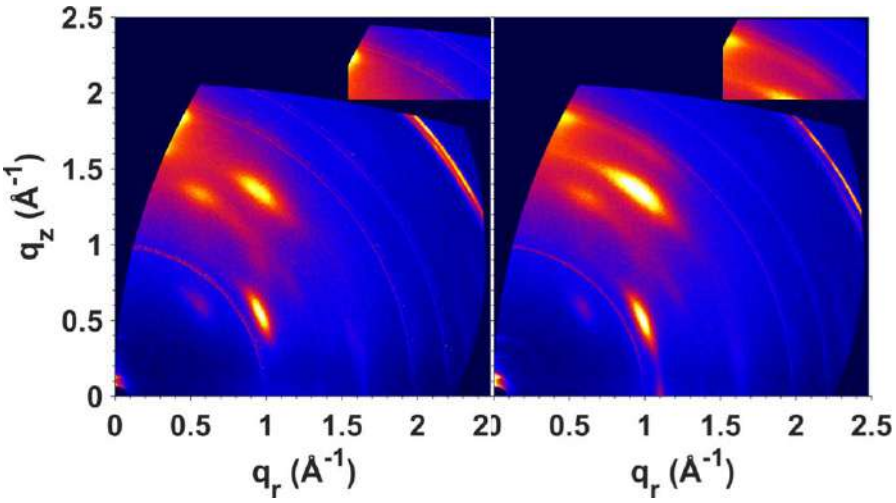
q_z (Å^-1)
q_r (Å^-1)
q_r (Å^-1)
2.5
2
1.5
1
0.5
0
0
0.5
1
1.5
2
0
0.5
1
1.5
2
2.5

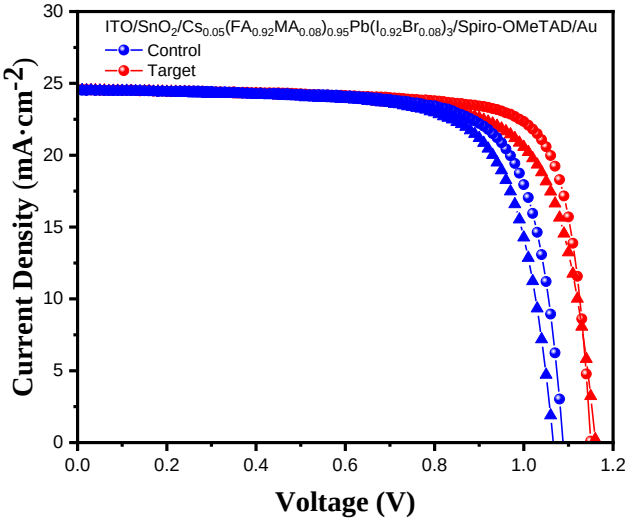
ITO/SnO2/Cs0.05(FA0.92MA0.08)0.95Pb(I0.92Br0.08)3/Spiro-OMeTAD/Au
Control
Target
Current Density (mA·cm-2)
Voltage (V)
30
25
20
15
10
5
0
0.0
0.2
0.4
0.6
0.8
1.0
1.2

EC-12

Porous carbon nanofibers decorated with single Ni atoms for efficient CO_2 electroreduction[1]

Hui Wang [a], Sheng Zhang[a]

[a] *Key Laboratory for Green Chemical Technology of Ministry of Education, Haihe Laboratory of Sustainable Chemical Transformations, School of Chemical Engineering and Technology, Tianjin University, Tianjin, China.*

E-mail: wanghuimm@link.cuhk.edu.hk

In recent years, the reduction of carbon dioxide into other valuable chemicals using electrochemical techniques has become a focus of research. However, most of the catalysts on the market today are powder catalysts, which have the disadvantages of difficult recovery, complicated preparation process, and poor stability. Therefore, it is important to prepare a catalyst with both high selectivity and high stability. Among the transition metals, nickel metal has high selectivity for CO, and electrospinning technology has the advantages of simple processes and large-scale preparation.

A porous single-atom nickel self-supporting electrode with ultra-high selectivity for CO is shown here, which obtained a CO Faraday efficiency of 98.6% and a current density of 7.5 mA cm^{-2} in an H-type cell. This self-supporting electrode was also used as a gas diffusion electrode in a flow cell, obtaining a CO Faraday efficiency of 94.3% and a current density of 170 mA cm^{-2}. It was able to maintain stability for more than 24h in both electrolytic cells. A comparison of a series of catalysts with different porosity showed that the porosity played a decisive role in the catalytic performance, and the porous structure not only provided a large specific surface area but also enhanced mass transfer while increasing the CO_2 adsorption, which together led to the improvement of catalytic performance. Moreover, the porous fibers prepared by this method can be used as self-supporting electrodes to maintain high current density while solving the stability problems of traditional coated electrodes, which provides a new idea for future industrial applications.

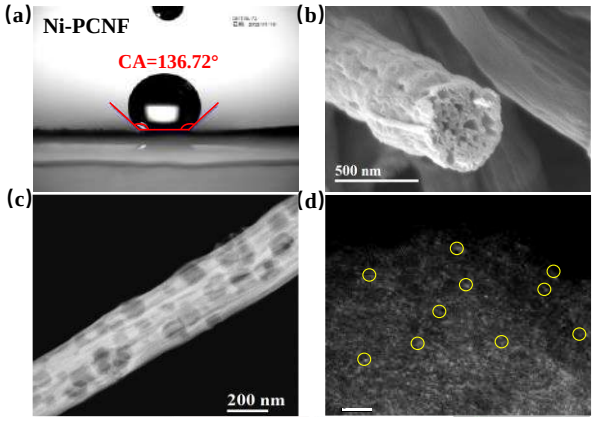

Figure 1 (a) Water contact angle test of Ni-PCNF-0.5PMMA; (b) SEM image of Ni-PCNF-0.5PMMA; (c) TEM image of Ni-PCNF-0.5PMMA; (d)HAADF-STEM images of Ni-PCNF-0.5PMMA those white dots are supposed to be Ni single atoms

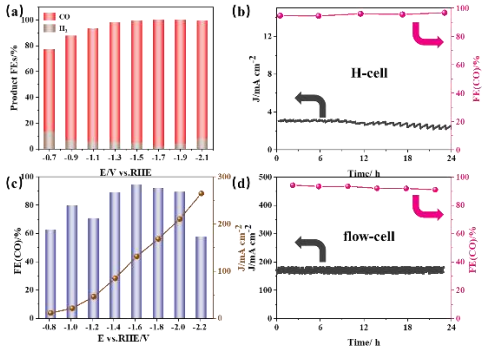

Figure 2 (a) FEs of all products of Ni-PCNF-0.5PMMA in H-cell; (b) Catalytic stability test at −1.3V vs. RHE for 24 h in H-cell; (c) CO FEs and current density of Ni-PCNF-0.5PMMA in flow cell; (d) Catalytic stability at −1.8V vs. RHE for 24 h in the flow cell.

Reference

[1] Wang H , Chuai H , Chen X ,et al. *ACS Appl. Mater. Interfaces 2023, 15, 1, 1376–1383*

EC-13

$CsPbI_3$ perovskite quantum dot-based write-once-read-many-times memory with intrinsic ternary states

Luhang XU,[a] Yuang FU,[a] Xinhui Lu[a]

[a] *Department of Physics, The Chinese University of HONG KONG, New Territories, Hong Kong.*

E-mail: lhxu@link.cuhk.edu.hk

The emergence of the Internet of Things (IoTs) demands the development of novel memory technologies for high-efficiency data storage devices. Non-volatile resistive switching (RS) memory which consists of a metal-semiconductor-metal sandwich-like structure has attracted significant attention due to its fast switching speed, long retention time, and low cost per bit[1]. By applying a proper electric signal, the non-volatile RS memory can switch between a high resistance state (HRS) and a low resistance state (LRS) through the change of conductivity within the semiconductor active layer and retain it after removing the stimulation. Notably, the memory devices that can retain the LRS after transition are referred to as the write-once-read-many-times (WORM) memory, which are widely used in the field of data security and network[2].

Metal halide perovskites (MHPs) with a formula of ABX_3 (A=MA, FA and Cs, B = Pb and Sn, C = Cl, Br and I) are especially promising as they contain a large number of inherent ionic halide vacancies[3,4] with low formation (0.1-0.2 eV) and migration (0.1-0.6 eV) energy[4], allowing them to quickly form or annihilate conductive filaments (CFs) under external bias. Herein, we fabricated a prototypical $CsPbI_3$ perovskite quantum dot (PQD)-based memory device that exhibits intrinsic ternary states without an extra compliance current. This is attributed to the inherent iodide vacancies which efficiently drift under the external electric field and migrate within $CsPbI_3$ PQD film via two different pathways. The growth of the CFs was found to start from the domain boundary of PQDs and gradually extend into the domain interior as directly visualized by the in-situ conductive atomic force microscopy (C-AFM). After two SET operations, a final low resistance state is reached and maintained, resulting in write-once-read-many-times (WORM) effects. Our work demonstrates the potential of $CsPbI_3$ PQDs for WORM devices with a simple device structure and intrinsic multilevel properties achieved by rationally controlling the drift of ionic defects between $CsPbI_3$ PQDs.

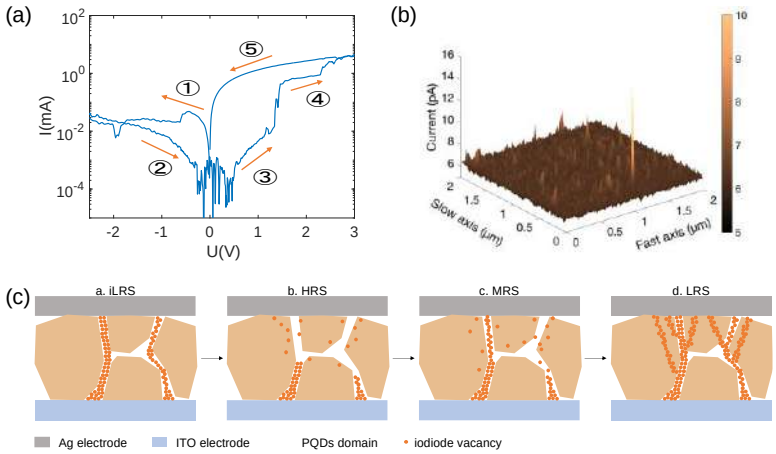

Figure. (a) I-V characteristics of Ag/$CsPbI_3$ PQD/ITO device. (b) 3D views of CAFM images for LRS state. (c) Schematic of CFs formation and annihilation.

References

[1] Chen A. Solid-State Electronics, 2016, 125, 25-38;

[2] Kulkarni SH, Chen Z, He J, Jiang L, Pedersen MB and Zhang K. IEEE journal of solid-state circuits, 2010, 45, 863-868;

[3] Ye J, Byranvand MM, Martínez CO, Hoye RL, Saliba M and Polavarapu L. Angewandte Chemie, 2021, 133, 21804-21828;

[4] Tress W. The journal of physical chemistry letters, 2017, 8, 3106-3114.

EC-14

Post-deposition halide exchange for achieving deep-blue perovskite light-emitting diodes: the role of the organic cations in the chloride source

Hui Yu, Shenghe Zhao, Yongheng Jia, Yang Zhou, Zheng Zhang, Ni Zhao

Department of Electronic Engineering, The Chinese University of Hong Kong, N.T., Hong Kong

E-mail: yuhui@link.cuhk.edu.hk

Metal halide perovskites offer broad spectral tunability, high carrier mobility, excellent color purity and superior photoluminescence quantum yield and are therefore rising as promising candidates for light-emitting diodes (LEDs) and lasers. In the past few years, the performances of perovskite LEDs (PeLEDs) have been improved rapidly, with the maximum external quantum efficiency (EQEmax) already exceeding 20% for green, red, and infrared emission. In contrast, the development of blue PeLEDs has been lagging.[1,2,3] In particular, the EQE_{max} values obtained for deep blue PeLEDs that can meet the requirements of the "blue" standard (e.g., Rec. 2020), with a centered EL wavelength of <465 nm, remain low.[4,5] Post-deposition halide exchange has been a popular strategy for tuning the emission wavelength of metal halide perovskites and is particularly attractive in achieving deep-blue perovskite light-emitting diodes (PeLEDs), where the quality of the emissive layer is largely limited by the low solubility of chlorides in perovskite precursor solution.[6] In this work, we examine the halide exchange strategy for deep-blue PeLEDs, with a focus on understanding the role of the organic cations of the halide salt (i.e., the chloride source for ion exchange) in modifying the properties of the perovskite films and consequently the PeLED performances. By comparatively investigating the treatment effects of two model systems, namely phenethylammonium chloride (PEACl) and 2,2-diphenylethylammonium chloride (DPEACl), we find that although the two chlorides produce highly similar photoluminescence properties of the perovskite films, they create different landscapes for current flow in the PeLEDs. In particular, the bulky branch-structured DPEA cations exhibit minimal disturbance to the perovskite grains while providing highly effective inter-grain void filling and thus leakage current blocking, leading to 3D perovskite based PeLEDs with a record high peak external quantum efficiency of 6.4% at 462 nm. The study highlights the importance of organic cation selection in the halide exchange processes for PeLEDs.

References

[1] D. Ma, K. Lin, Y. Dong, H. Choubisa, A. H. Proppe, D. Wu, Y. K. Wang, et al. *Nature* 2021, *599*, 594.
[2] Y.-K. Wang, F. Yuan, Y. Dong, J.-Y. Li, et al. *Angew. Chem., Int. Ed. Engl.* 2021, *60*, 16164.
[3] L. Zhang, N. Li, D. Liu, G. Tao, et al. *Angew. Chem., Int. Ed. Engl.*, 2022, *61*, e202209337.
[4] G. Zou, Z. Li, Z. Chen, L. Chu, H.-L. Yip and Y. Cao, *Adv. Funct. Mater.,* 2021, 31, 2103219.
[5] C. Wang, G. Dai, J. Wang, M. Cui, Y. Yang, S. Yang, C. Qin, et al. *Nano Lett.*, 2022, 22, 1338.
[6] Y. Jia, R. Li, Y. Zhou, S. Zhao, H. Yu, J. Wang, Z. Lin, H. Su and N. Zhao, *Small Structures*, 2023, 2200393.

International Conference on
Earth, Energy & Environmental Sciences
for Carbon Neutrality

EC-15

Unraveling how local environments impact multicarbon product electrosynthesis in active carbon solutions

Zhongshuo Zhang,[a] Ying Wang[a]

[a] *Department of Chemistry, The Chinese University of Hong Kong, Hong Kong 999077, S. A. R., China.*

E-mail: zhangzhongshuo@link.cuhk.edu.hk

The direct electrochemical conversion of bicarbonate electrolyte, an active carbon solution, presents the potential to produce carbon-neutral chemical commodities without suffering the energy-intensive *ex-situ* carbon dioxide (CO_2) regeneration. However, selectively producing multi-carbon (C_{2+}) products in bicarbonate electrolyzers is challenging. In this work, we developed a continuum model to quantify the complex local environments inside a bicarbonate electrolyzer and its relationship with C_{2+} production. Our model demonstrates that the coexistence of high alkalinity and sufficient CO_2 favors C_{2+} production and a volcano-like relation between the C_{2+} production and the catalyst layer (CL) porosity. The bicarbonate feed concentration and catalyst layer porosity contribute to modulating the local environment and realizing a matching of the buffer capacity, bicarbonate availability, and carbonate transport. Guided by the modeling results, we experimentally improved C_{2+} production through optimizing the bicarbonate feed concentration and CL porosity, which achieved a ~48% C_{2+} Faradaic efficiency (FE) at 60 mA cm^{-2}. These findings unravel the determinative factors and provide guidance on selective C_{2+} products synthesis.

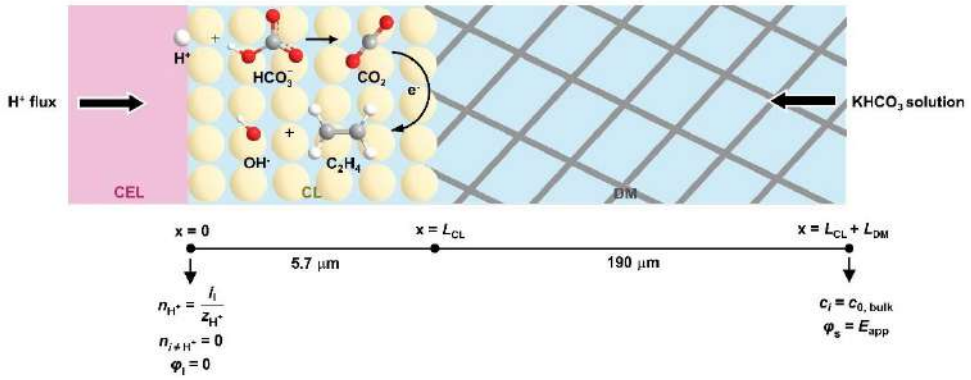

Figure 1. A schematic illustration of the continuum model including the boundary conditions.

EC-16

Bromide-based nonflammable electrolyte for safe and long-life sodium metal batteries

Changjian Zuo, Dejian Dong, Huwei Wang, Yue Sun, and Yi-Chun Lu*

Department of Mechanical and Automation Engineering, The Chinese University of Hong Kong, Shatin, N.T., 999077 Hong Kong, SAR, China..

E-mail: yichunlu@mae.cuhk.edu.hk

Sodium metal batteries (SMBs) are one of the most promising energy storage technologies owing to the rich-abundance of sodium and its high gravimetric capacity. However, safe applications of SMBs are hindered by reactive sodium metal and the highly flammable electrolyte, which leads to dendrite growth, gassing and fire issues. Here we report a new class of bromide-based nonflammable electrolyte for sodium metal batterie using flame-retardant 2-Bromo-1-(2-bromoethoxy) ethane (BBE) solvent. This solvent not only has higher fire retardancy than typical P, Cl, F-based nonflammable solvents owing to lower energy barrier of radical scavenger dissociation, but also derives a solid electrolyte interphase (SEI) containing NaBr with a high ionic conductivity to suppress the dendrite and gassing issues. The BBE-based electrolyte prolongs the cycle life (80% capacity retention) of $Na_3V_2(PO_4)_3$//Na cells from 60 cycles in traditional electrolyte to 1500 cycles and warrants stable cycling of 1400 h in the Na//Na symmetric cells. We further demonstrated a sodium metal pouch cell showing a capacity retention of 88% 240 cycles at 1C. This work provides rational design strategy of improving electrolyte flame retardancy and constructing stable SEI for safe and long-life sodium metal battery applications.

EC-17

Catalytic Graphitization Promotes High-performance Full-carbon Lithium-ion Capacitors

Guangchao Li[a, b], Zhixing Wang[b], Jiexi Wang[b], Ying Wang[a,*]

[a] Department of Chemistry, The Chinese University of Hong Kong, Hong Kong 999077, S. A. R., China; [b] School of Metallurgy and Environment, Central South University, Changsha 410083, China

E-mail: ying.b.wang@cuhk.edu.hk

Lithium-ions capacitors (LICs) have achieved widely attention which can well match the imbalance between lithium-ions batteries of high energy density and supercapacitors of superior power output and long lifespan. Especially, the full-carbon LICs consists of graphite anode and activated carbon cathode deliver excellent electrochemical performance and low cost, being considered as one of the best choices for commercial energy storage fields. However, the mismatch in kinetics of anode and cathode materials restricts the power density and thus impedes their further application. The main problems are the sluggish ions intercalation/de-intercalation of anode cannot compete the fast ions absorption/desorption of cathode during the electrochemical process. It can be work by shorting the ions transport distance, promoting the electrolytes permeation and enhancing the non-faradic reaction behavior. In this way, we employed catalytic graphitization strategy in nano-sized scale in an in-situ way to regulate the graphitization degree, porous structure and functional groups to promote the kinetics behavior of graphite anode. And thus, 2D defective high-graphitic carbon nanosheets were successfully prepared by carbonized 1D nanorods precursor. The effects of defects contained in the as-prepared samples were further explored by the DFT calculations, revealing that carbonylation and N-doping (particularly pyridine N) manifest synergistic effect on improving the electronic conductivity and regulating the microstructure. The high reversible capacity accompanied with large plateau capacity and superior rate capability in the half-cell test implies that GNS can be a promised candidate as negative electrode for LICs. When assembled into full-carbon LICs devices, high energy density of 112 Wh kg^{-1} and excellent power density of 19,600 W kg^{-1}, together with outstanding energy density retention of 96.5% after 5,000 cycles at 5 A g^{-1} were achieved.

References

[1] Li G, Yin Z, Guo H, et al, Adv Energy Mater., 2019, 9, 1802878;

[2] Li G, Huang Y, Yin Z, et al, Energy Storage Mater., 2020, 24, 304-311;

[3] Sun J, Li, G, Wang Z, et al, Carbon 2022, 200, 28-37.

EC-18

Interface engineering of polymeric molecular catalysts for acidic CO_2 reduction

LI Geng

City University of Hong Kong

E-mail: ligengchn@foxmail.com

[BLANK]

EC-19

The role of proton donor in electrochemical CO_2 reduction reaction in acid

Weixing WU,[a] Ying WANG[a]

[a] *Department of Chemistry, the Chinese University of Hong Kong, Hong Kong, China;*

E-mail: 1155165527@link.cuhk.edu.hk

Electrochemical CO_2 redution reaction (CO_2RR) is a promising technique for CO_2 conversionand utilization. Currently, its major bottleneck is the “carbonate issue” — the inevitable reaction between CO_2 and the neutral/alkaline electrolyte[1]. Acidic CO_2RR is proposed as a attractive strategy, but most reported results is still under psudo-acidic condition — the local environment is alkaline due to the rapid generation of OH^- from the electrode[1-3]. To understand if authentic acidic CO_2RR is possible, identifying the proton donor of CO_2RR is crucial

Considering the proton-coupled electron transfer (PCET) nature of CO_2RR, identifying proton donor is in fact a kinetic problem. We postulate that when the proton donor switches (H^+-CO_2RR and H_2O-CO_2RR), differences in the reaction coordination will lead to changes in the transfer coefficient, which is a kinetic parameter connecting the macroscopic kinetics — the empirical Bulter-Volmer equation to the molecular level mechanism (the Marcus-Hush theory, M-H)[4]. Benefiting from the established methodology to extract transfer coefficient from the potential-catalytic current response, insight into the proton donor identity of CO_2RR could be obtained[5].

Herein, we report the observation of H^+-CO2RR pathway in mild acidic media based on both conventional kinetic experiments and M-H analysis. The adopted Au-Au rotating ring disk electrode platform (RRDE)[6] provides a high product detection sensitivity and a sufficient mass transport condition in unbuffered electrolyte, enabling the observation of the unprecedentedly early CO_2RR onset at -0.2 V vs RHE. The direct transfer of proton to CO_2 is observed at low overpotential region before H_2O-HER onset, according to the positive reaction order in proton (Fig. 1a) and larger-than-one KIE. After *ca*. -0.9V, CO_2RR becomes insensitive to pH, indicating H_2O-CO_2RR. Based on M-H theory, we further extracted the transer coefficient (Fig. 1b) and converted it into reorganisation energy (Fig. 1c). M-H analysis reveals two kinetic regions, corresponding to the pH-dependent and pH-independent region in Fig. 1a. A higher reorganisation energy is observed for H_2O-CO_2RR region than H^+-CO_2RR, indicating feasibility of H^+-CO_2RR pathway and its lower kinetic barrier. This work completes the missing puzzle of the reaction mechanism of CO_2RR under acidic local condition and supports the further development of acidic CO_2 electrolyzer.

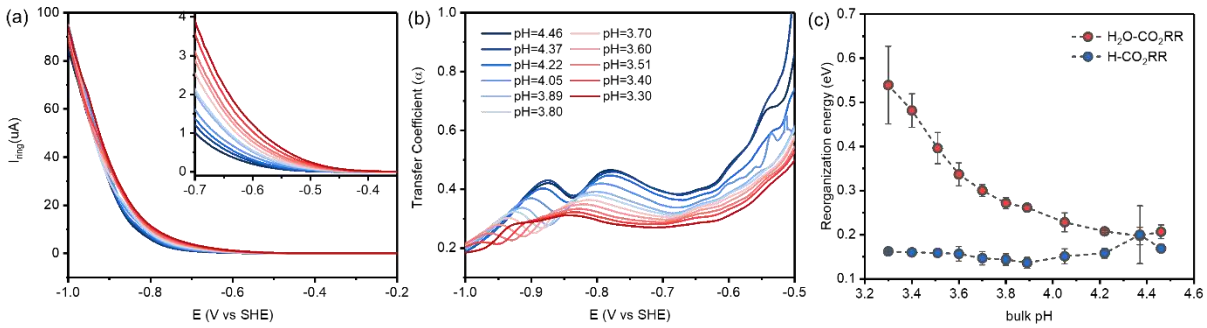

Fig.1 (a) Ring electrode current during LSV at different pH, representing CO_2-to-CO partial current density. Inset shows the zoom-in figure at low overpotential region. (b) Potential dependency of transfer coefficient derived from (a). (c) The extracted reorganisation energy under different bulk pH.

References

[1] Huang J, Li F, Ozden A, et al. *Science* 2021, *372*, 1074-1078.

[2] Xie Y, Ou P, Wang X, et al. *Nat. Catal.,* 2022, *5*, 564-570.

[3] Zhao Y, Hao L, Ozden A, et al. *Nature Synth.,* 2023, *2*, 403-412.

[4] Batchelor C, Kätelhön E, Barnes O, et al. *ChemistryOpen* 2015, *4*, 224-260.

[5] Laborda E, Henstridge C, Batchelor C, et al. *Chem. Soc. Rev.,* 2013, *42*, 4894-4905.

[6] Goyal A, Marcandalli G, Mints A, et al. *J. Am. Chem. Soc*., 2020, *142*, 4154-4161.

Earth and Energy Transition Session

ET-01

Dynamic simulations on September 5, 2022 Luding M_S 6.8 earthquake at the Moxi fault zone in southwest China

Di Deng,[a] Suli Yao,[a] Hongfeng Yang,[a]*

[a] *Earth and Environmental Sciences Program, The Chinese University of Hong Kong*

E-mail: di.deng@link.cuhk.edu.hk

Understanding earthquake dynamics is critical for seismic hazard assessment and mitigation. On September 5th, 2022, an Ms 6.8 earthquake occurred in the Luding County, Sichuan Province, resulting in tens of casualties and enormous economic loss. This event occurred on the Moxi segment of the seismically active Xianshuihe fault, located in the eastern periphery of the Tibet plateau. Here, we conduct dynamic simulations to probe the dynamic rupture process of the Ms 6.8 Luding earthquake using the finite element tool PyLith. We first construct a 3-D strike-slip fault in a elastic domain. Then we use a geodetic-data-based slip model to calculate the stress strop and prescribe the initial stress on the fault and use a linear slip-weakening law as the governing constitutive law on the fault. Our simulation results recover the first-order characteristics of the Luding earthquake, including the slip distribution and moment magnitude, and successfully capture the first peak in the fault parallel direction at Moxi station which is located ~2 km from the fault. Moreover, we have observed potential stopping phase near the northern end of the rupture. To fully comprehend the complex rupture process of this earthquake, further analysis on seismic data and refinement on the model are required.

ET-02

A high-resolution earthquake catalog built by machine learning- based phase pickers in Weiyuan Shale Gas Field

Yukai Hu[a], Jinping Zi[a], Hongfeng Yang[a]*

[a] *Earth and Environmental Sciences Programme, The Chinese University of Hong Kong*

yukai.hu@link.cuhk.edu.hk

Since the shale gas exploitation in the Weiyuan Shale Gas Filed, the number of the earthquakes has dramatically increased and 8 Mw4.0 events have occurred, which not only caused substantial economic loss but also casualties. In order to mitigate seismic hazard, understanding the triggering mechanism of those earthquakes is of vital importance, which heavily relies on a comprehensive high-resolution earthquake catalog while not available for the Weiyuan Shale Gas Field yet. We use a machine learning-based method, PhaseNet, to pick the arrival time starting from January 1, 2014 to February 28, 2019. The GaMMA method is then applied for the phase association. After that, 36327 events are detected, which is more than three times the number of the events detected by the local earthquake agency. Their absolute location is determined by the VELEST, and the relative location is further obtained by the hypoDD. The high-resolution catalog reveals clear spatiotemporal evolution of earthquakes and illustrates several clusters that are not included in the agency catalog. The emergence of these earthquakes is in agreement with the hydraulic fracturing activities both in time and space, showing their tight causative relationship.

International Conference on
Earth, Energy & Environmental Sciences
for Carbon Neutrality

ET-03

Evaluating the Utility of b-Value for Discriminating Foreshocks and Mainshocks in the Yunnan Region

Tsz Lam Lau[a], Hongfeng Yang[a]

[a] Earth and Enviormental Sciences Programme, The Chinese University of Hong Kong

E-mail: lamlam3041@link.cuhk.edu.hk

Yunnan province, located in southwestern China, is prone to frequent earthquakes due to the convergence of the Indian and Eurasian tectonic plates, along with its complex subsurface geological structure and active fault zones. Over the years, notable seismic events have impacted the region, such as the 2014 M 6.1 Yingjiang earthquake, the 2014 M 6.9 Jinggu earthquake, and the 2021 M 6.5 Yangbi earthquake. These large earthquakes resulted in significant socioeconomic losses. Distinguishing mainshocks from subsequent seismic activity following significant earthquakes poses a challenge for real-time seismic hazard assessment. This study aims to address this issue by utilizing temporal variations in the b-value, derived from the Gutenberg-Richter law, to differentiate mainshocks from other earthquakes in Yunnan. It also seeks to evaluate the predictive power of precursory signals and enhance accuracy in earthquake forecasting and hazard assessment for Yunnan. We employ ZMAP software to compute b-value time series and compare them to the reference b-value for the region. By analyzing seismic events above magnitude 5 using China's national catalog, this research examines the existence and reliability of precursory signals prior to large quakes. The findings have the potential to strengthen preparedness and resilience against seismic activity through refined forecasting methodologies and effective mitigation strategies that could help reduce future socioeconomic losses.

ET-04

Mapping and Inventorying rock glaciers on the Tibetan Plateau using Planet Basemaps and deep learning

Zhangyu Sun[a], Yan Hu[a,b], Lin Liu[a,b], Adina Racoviteanu[c,d], Stephan Harrison[c]

[a]*Earth System Science Programme, The Chinese University of Hong Kong, Hong Kong, China;* [b]*Institute of Environment, Energy and Sustainability, The Chinese University of Hong Kong, Hong Kong, China;* [c]*College of Life and Environmental Sciences, University of Exeter, Exeter, United Kingdom;* [d]*Laboratoire de Glaciologie et Géophysique de l'Environnement, Saint-Martin-d'Hères, France*

E-mail: sunzhangyu@link.cuhk.edu.hk

Rock glaciers, periglacial landforms commonly found in high mountain systems, are of great scientific value for assessing the presence of permafrost, understanding mountain hydrology, and assessing the climate impacts on high mountain environments. However, understanding of their global occurrence and distribution is patchy, and on the Tibetan Plateau they have remained poorly understood due to the lack of a comprehensive inventory. To address this gap, we propose an innovative deep learning-based mapping method that utilizes a powerful neural network, DeepLabv3+, to help develop an inventory. By training the model with visually consistent image mosaics from the Planet Basemaps and leveraging existing rock glacier inventories from different regions, we have detected and delineated numerous rock glaciers on the plateau. Building upon these deep learning mapped results, we created an inventory consisting of a total of 43,442 rock glaciers. These rock glaciers cover approximately 6,000 km^2, with a mean area of 0.14 km^2. They are predominantly situated at elevations ranging from 4,000 m to 5,500 m above sea level, with a mean elevation of 4,728 m. They tend to occur on slopes with gradients between 10° and 25°, with a mean slope angle of 17.7°. Notably, we found that rock glaciers are widespread in the northwestern and southeastern areas of the plateau with dense concentrations in the Western Pamir and Nyainqentanglha, while they are sparsely distributed in the inner plateau. Furthermore, rock glaciers in the western plateau exhibit larger areas, with a mean area of 0.21 km^2. Our inventory serves as a benchmark dataset that can contribute significantly to the future monitoring and assessment of permafrost on the Tibetan Plateau in the context of a warming climate.

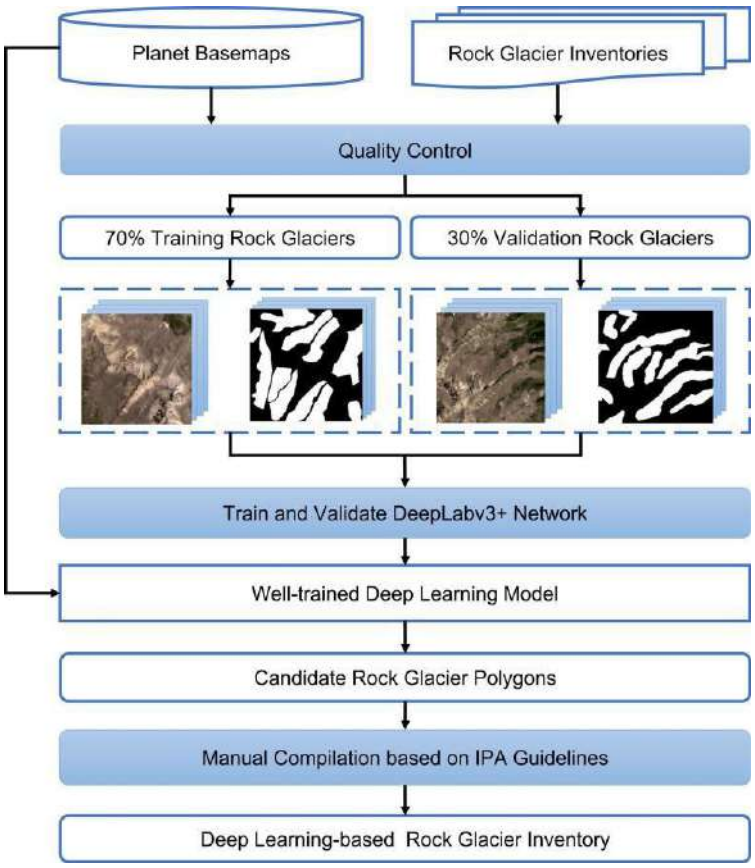

Figure 1. Flowchart of deep learning-based approach for mapping rock glaciers.

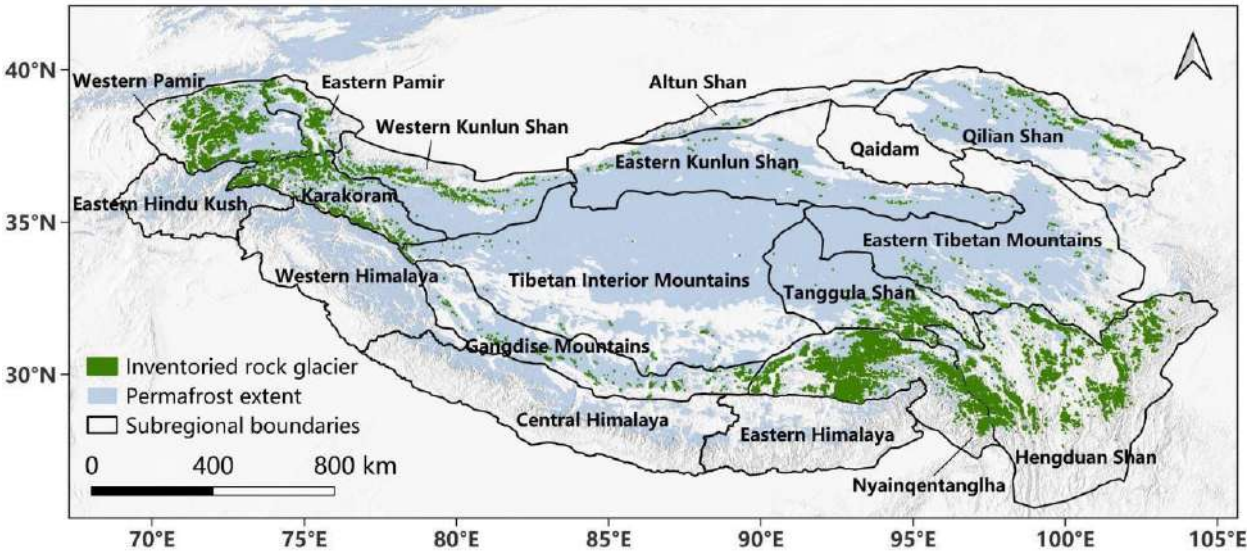

Figure 2. Deep learning-based rock glacier inventory on the Tibetan Plateau.

ET-05

Physics-Based Ground Motion Modeling Using Heterogeneous Parallel Technique: Design, Implementation and Optimization of Algorithms

Wenqiang Wang[a,b]

[a]*Earth and Environmental Sciences Programme, The Chinese University of Hong Kong, Hong Kong, China;* [b]*Shenzhen Research Institute, The Chinese University of Hong Kong, Shenzhen, Guangdong, China.*

E-mail: wangwq2018@mail.sustech.edu.cn

Earthquakes present an immeasurable threat to human lives and property. To gain a scientific understanding of earthquakes is significant to reduce the losses caused by earthquake disasters. Physics-based ground motion modeling is one of the crucial methods in achieving this objective. Efficient earthquake modeling techniques, coupled with advanced highperformance computing platforms, can aid researchers in expediting ground motion modeling. This, in turn, allows for timely analysis of earthquake events and enables swift decision-making for emergency response efforts. The curvilinear grid finite difference method stands out for its exceptional flexibility and efficiency. By harnessing the power of heterogeneous parallel platforms like GPUs and Sunway, the performance of CGFDM can be greatly enhanced. Therefore, in our study, we have devised and implemented heterogeneous parallel algorithms for CGFDM, leveraging a CPU-GPU cluster and the Sunway master-slave architecture. Furthermore, we have developed two seismic modeling solvers based on CGFDM: CGFDM3DEQR (multi-GPU solver) and SW-CGFDM3D (Sunway master-slave solver). These solvers have achieved significant speed-ups, enabling the completion of ground motion simulations within a short timeframe. Additionally, we have introduced an optimized seismic modeling method that utilizes half-precision floats (FP16) and low-storage Runge-Kutta (LSRK) techniques. This optimization approach drastically reduces memory usage and substantially improves computational efficiency compared to the original CGFDM. Our developed seismic modeling tool has been successfully applied to several real-world earthquake ground motion simulations, notably contributing to earthquake hazard evaluation, such as the Luding earthquake. Looking ahead, our modeling tools will play a crucial role in facilitating fast physicsbased ground motion simulations, timely earthquake hazard assessment, and post-earthquake emergency response efforts.

ET-06

Investigating global warming controls on tropical cyclone rainfall using convection-resolving model experiments

Maiqian Xiao [a], Francis Tam [a] and Leo Chow [a,b]

[a] *Earth System Science Programme, The Chinese University of Hong Kong, Hong Kong, China;*

[b] *Department of Mathematics, The Chinese University of Hong Kong, Hong Kong, China.*

E-mail: maiqianxiao@link.cuhk.edu.hk

As shown in numerous studies, the impact of tropical cyclones (TC) on coastal regions is expected to become stronger as the climate becomes warmer[1,2,3,4]. However, large uncertainties exist in future projected storm intensity and rain rate under various warming scenarios[2]. In this study, using the Weather and Research Forecasting model (WRF), pseudo global warming (PGW) experiments for SSP2-45 and SSP5-85 targeted at the end of this century were conducted for 25 historical TC cases. These storm cases were selected due to their great impacts over the Pearl River Delta (PRD) region in South China. It was found that, averaged over all storm cases, the percentage change in extreme rain rate exceeds that given by the Clausius-Clapeyron (CC) relation. Moreover, TC rainfall increments can vary from one storm case to another, even due to the same PGW forcing. Further inspection revealed that such rainfall response fluctuation which cannot be explained by the CC relation can be attributed to the dynamical component in the increased moisture flux and its convergence, which in turn is related to enhanced TC inflow in the planetary boundary layer when storm intensity increases. In other words, stronger projected TCs will lead to super-CC rainfall anomalies under global warming, with variations of storm response controlling TC rainfall fluctuations from case to case. Implications of our results to estimating climate risks of and uncertainties in extreme rainfall due to future TCs will be discussed.

References

[1]Emanuel KA. *Proceedings of the National Academy of Sciences*., 2013, *110, 12219-12224*;

[2]Knutson T, Camargo SJ, Chan JC, et al. *Bulletin of the American Meteorological Society.*, 2020, *101*, E303-E322;

[3]Patricola CM and Wehner MF. *Nature.*, 2018, *563*, 339-346;

[4]Zhang L, Karnauskas KB, Donnelly JP and Emanuel KA. *Journal of Climate.*, 2017, *30*, 1233-1243.

ET-07

Unzip rupture propagation from near-fault rupture phases of the 2023 Kahramanmaraş, Turkey Mw 7.8 earthquake

Suli Yao[a] and Hongfeng Yang[a]

[a] *Earth and Environmental Sciences Programme, Chinese University of Hong Kong, Hong Kong, China*

E-mail: suliyao@cuhk.edu.hk , hyang@cuhk.edu.hk

Understanding and deciphering wiggles from seismograms has been a long endeavor to understand the internal structure of the Earth and to explore earthquake source properties. However, coherent phases directly associated with natural earthquake rupture propagation have not been available, due to the lack of continuous near-fault observations during large earthquakes. Here we report the continuous phases directly associated with rupture propagation as large near-fault velocity pulses along the southern segment of the 2023 Mw 7.8 Kahramanmaraş, Turkey earthquake. The pulses reveal an overall subshear rupture speed of ~ 3.2 km/s. However, unlike the predictions of velocity field in homogeneous rupture, the real records show complexities with multiple peaks. Through particle-motion analysis and dynamic rupture simulations, we isolate the contribution from the geometry change and slip heterogeneities and then identify the rupture phases. Our results prove the efficiency of rupture phases in tracking the rupture propagation and suggest a transient supershear propagation in this event which ends at a geometrical irregularity. Our study highlights the complexity and superior application of near-fault data in studying earthquake source dynamics.

ET-08

Application of local scattered-wave gradiometry for subsurface structure delineation beneath the Chenghai fault zone

Jia Zhang,[a] Hongfeng Yang,[a,b]

[a] *Shenzhen Research Institute, the Chinese University of Hong Kong, Shenzhen, China;*

[b] *Earth System Science Programme, the Chinese University of Hong Kong, Hong Kong, China.*

E-mail: jiazhang@cuhk.edu.hk

The dense array-based wave gradiometry technique has been demonstrated as an efficient tool to invert phase velocity and geometrical spreading festures of the Earth's interior using well-recodred surface waves. However, the seismic data recorded by small-aerture yet highly dense arrays usually show complicated waveforms due to a stong wavefield interference caused by shallow velocity heterogeneities, posing challenges to imaging reliable, detailed shallow structures with the use of wave gradiometry method. In this study, we develop a novel data processing procedure of utilizing dense array datasets to derive shallow velocity structures based on local scattered-wave gradiometry analysis. A wavelet-based wave decomposition method is exploited to separate the local scattered wavefields out prior to computing the gradiometry coefficients. Applying our method to dense linear arrays deployed beneath the Chenghai fault zone, southwest China, we invert the velocity structures down to a 2-3 km depth in this region. The results display a relatively low-velocity beneath the fault zone. The cross-section along the southern segment of Chenghai fault exhibits a ~2 km deep low velocity zone with Rayleigh wave velocity varing from 0.5 to 1.0 km/s, which are basically consistent with seismic reflection observations and tomography studies. Our results suggest that the wave gradiometry, integrated with wave decomposition technique are applicable for small-aperture dense array datasets to delineate high-resolution subsurface velocity structures.

ET-09

Using S/P amplitude ratio and stress drop to differentiate mechanisms of induced earthquakes from injection activities in Weiyuan Shale Gas Field

Jiewen Zhang [ab], Hongfeng Yang [abc], Jinping Zi [a]

[a] *Earth and Environmental Sciences Programme, The Chinese University of Hong Kong, Hong Kong S.A.R., China;*

[b] *Shenzhen Research Institute, The Chinese University of Hong Kong, Shenzhen, Guangdong, China,*

[c] *Institute of Environment, Energy and Sustainability, The Chinese University of Hong Kong, Hong Kong S.A.R., China.*

E-mail: jwzhang@cuhk.edu.hk

Injection activities during unconventional oil & gas exploration have the potential of inducing large earthquakes. The induced earthquakes, the footprints of injection activities, are either on new fractures from fluid injection near the operation well, or coupled with nearby pre-existing faults hydrated during fluid migration; differentiating the two mechanisms is important as the latter may be the precursor of seismic hazard. Stress drop is found varying with the proximity of induced seismicity to the injection point, though it remains unclear whether the variability is due to different mechanisms. The S/P wave amplitude ratio can potentially differentiate tensile-dominant and shear-dominant mechanisms, as the two stimulates different portion of S-wave radiated energy; an earthquake at over-pressured spot near an injection point may be associated with stronger fault expansion and more tensile components, and on nearby faults vice versa. Therefore, we introduce both stress drop and S/P ratio to trace the induced earthquakes and investigate their relationship with large induced earthquakes.

The increasing seismicity and M>5 deadly earthquake in the Weiyuan Shale Gas Field enable large-scale analysis of stress drop and S/P ratio. We included nearly 12000 earthquakes from early 2019 to late 2020 with solid seismic records at local stations, finding an average stress drop of 2.29MPa and S/P ratio of 3.58 from spectra. We also use a pure tensile and a pure shear moment tensor for theoretical S/P ratio calculation, and obtain a maximum of around 3 for pure-tensile and an average of 5 for pure-shear. This is consistent with an observation near an injection well above an M5 earthquake fault, where the S/P ratio (<3.5) and stress drop are both lower near the injection spot, and both high closer to the fault. This may tell that combining stress drop and S/P ratio could help detect different mechanisms of induced earthquakes.

References

[1] Liang W, Xu H, Carraro F, et al. *J. Am. Chem. Soc*., 2020, *In Press*;

[2] Konkankit CC, Lovett J, Harris HH and Wilson JJ. *Chem. Commun.*, 2020, *56*, 6515-6518.

International Conference on
Earth, Energy & Environmental Sciences
for Carbon Neutrality

ET-10

Data-Driven Immediate Foreshock Detection: Using Dense Seismic Array to Uncover Hidden Precursors

Fengjiang Ju, Haoran Meng, Xiaofei Chen

Department of Earth and Space Sciences, Southern University of Science and Technology, Shenzhen, China

E-mail: jufj2022@mail.sustech.edu.cn

Advancing our understanding of earthquake nucleation process can shed lights on earthquake prediction, early warning, and hazard assessment[1]. Foreshocks, which usually refer to smaller earthquakes that occur before an earthquake, exhibit good temporal and spatial correlations with the mainshock. Investigating the relationship between foreshocks and mainshocks can therefore help elucidate earthquake nucleation mechanisms and lead to enhancements in earthquake prediction and early warning capabilities.

A recent study on the 2019 Mw 7.1 Ridgecrest earthquake sequence indicates that immediate foreshocks often have similar waveforms to the P-waves of the following earthquakes, differing only in amplitude[2]. This phenomenon is considered to result from the fractal nature of the fault fracture process. Consequently, there might be many immediate foreshocks with similar waveforms hidden in ambient noise that have gone undetected. However, existing detection techniques rely on waveform cross-correlations, which struggles to identify weak immediate foreshocks when Signal-to-Noise Ratios (SNR) are extremely low (e.g., SNR ~ 1). To address this challenge, we propose an advanced method combining the advantages of cross-correlation and beamforming analyses using dense array data[3,4]. We first compute the cross-correlation functions of the contentious records with the P-waves of the target earthquake. We then grid searches around the hypocenter using N-th root stacking to detect and locate the immediate foreshocks (Fig. 1). With numerous immediate foreshocks detected, we can statistically quantify the earthquake nucleation process.

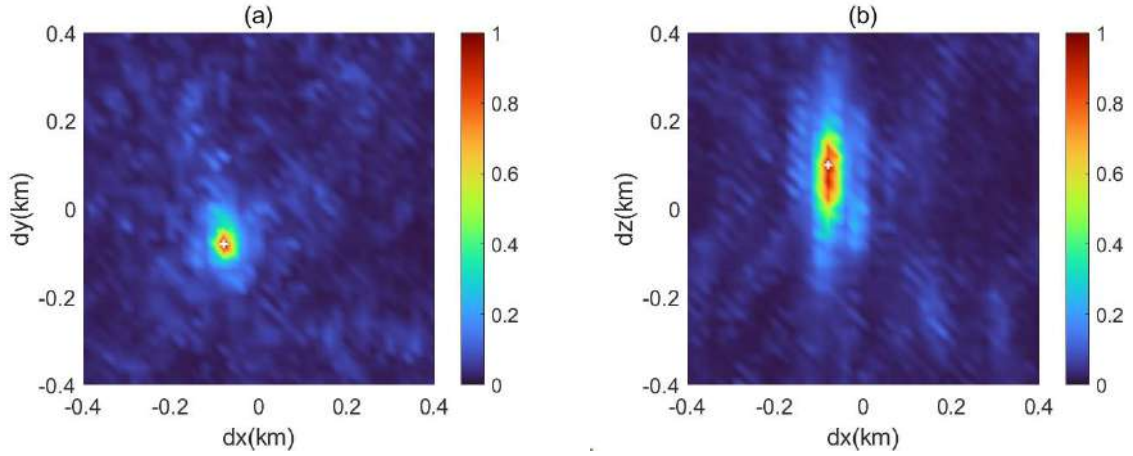

Figure 1. Beamforming diagram showing the energy of slant-stacked waveforms. (a) The white cross marks the maximum energy, and it corresponds relative distances dx and dy of the immediate foreshock with respect

to the target earthquake. (b) The white cross corresponds relative distances dx and dz of the immediate foreshock with respect to the target earthquake.

References

[1] Ellsworth, W. L., & Beroza, G. C. (1995). Seismic evidence for an earthquake nucleation phase. *Science*, *268*(5212), 851-855.

[2] Meng, H., & Fan, W. (2021). Immediate foreshocks indicating cascading rupture developments for 527 M 0.9 to 5.4 Ridgecrest earthquakes. *Geophysical Research Letters*, *48*(19), e2021GL095704.

[3] Waldhauser, F., & Ellsworth, W. L. (2000). A double-difference earthquake location algorithm: Method and application to the northern Hayward fault, California. *Bulletin of the seismological society of America*, *90*(6), 1353-1368.

[4] Rost, S., & Thomas, C. (2002). Array seismology: Methods and applications. *Reviews of geophysics*, *40*(3), 2-1.

Environment Session

EN-01

Marine heatwaves and light limitation independently alter the growth and productivity of the tropical seagrass *Halophila ovalis*

Alissa Victoria Bass,[a] Laura Jane Falkenberg,[ab] Haiwei Luo,[acd] Benoit Thibodeau[ae]

[a] *School of Life Sciences, & Simon F.S Li Marine Science Laboratory, The Chinese University of Hong Kong, Hong Kong SAR;* [b] *UniSA STEM, University of South Australia, South Australia, Australia;* [c] *State Key Laboratory of Agrobiotechnology, The Chinese University of Hong Kong, Hong Kong SAR;* [d] *Shenzhen Research Institute, The Chinese University of Hong Kong, Shenzhen, China;* [e] *Earth and Environmental Sciences Programme, The Chinese University of Hong Kong, Hong Kong SAR*

E-mail: alissabass@link.cuhk.edu.hk

Seagrasses are important marine foundation species, which support high coastal biodiversity and provide many socioeconomic benefits[1]. However, seagrasses are threatened by anthropogenic change, both climate and non-climate related, particularly marine heatwaves (MHWs) which are having negative impacts on seagrasses and seagrass ecosystems globally[2]. With the combined impacts of other anthropogenic stressors, such as light limitation from eutrophication or increased sediment load, the growth, productivity, and elemental cycling of the seagrass may be altered. This can be due to underlying shift is the seagrass microbiome.

In this experiment, we exposed the tropical seagrass *Halophila ovalis* to a 10-day MHW and three light intensities to examine the impacts of these two stressors on the growth, productivity elemental cycling and leaf microbiome of the seagrass and to see if there were any interactive effects of the two stressors. We found that both MHW and decreased light negatively impacted the growth of the seagrass, particularly the rhizome elongation rate, and the leaf growth rate, as well as increasing the rate of leaf loss. Similarly, chlorophyll concentration was altered by both stressors, with the normal adaptational responses to reduced light (i.e., increasing chlorophyll concentration) being inhibited by the MHW. Nitrogen assimilation rate also decreased under both MHW temperature and reduced light availability. We found no interactive effects of MHW and light limitation on *Halophila ovalis*.

From the results obtained so far, we show that MHWs can drive decreased productivity of seagrass, particularly when combined with low light availability. Furthermore, MHWs can reduce the ability of *H. ovalis* to adapt to lower light levels. Poor water clarity and habitat health can therefore increase the susceptibility of seagrasses to extreme climatic events.

References

[1] Unsworth, R.K.F., McKenzie, L.J., Collier, C.J. *et al.* Global challenges for seagrass conservation. *Ambio,* 2019, 48, 801–815.

[2] Smale, D.A., Wernberg, T., Oliver, E.C.J. *et al.* Marine heatwaves threaten global biodiversity and the provision of ecosystem services. *Nat. Clim. Chang.,* 2019, 9, 306–312.

EN-02

Methylmercury biomagnification in subtropical forest food webs

Matthew Long-Hei Cheng [a], Martin Tsz-Ki Tsui [a, b], Ken Ming-Yin Yau [a], Jack Tsun-Hung Cheung [a]

[a] School of Life Sciences, The Chinese University of Hong Kong, Shatin, N.T., Hong Kong SAR, China; [b] Earth and Environmental Sciences Programme, The Chinese University of Hong Kong, Shatin, N.T., Hong Kong SAR, China

E-mail: matthewcheng@link.cuhk.edu.hk

Mercury (Hg), especially its organic form methylmercury (MeHg), is highly toxic and found to biomagnify in food webs, where its concentration increases with trophic position of organisms. Basal resources (e.g., litter) and terrestrial invertebrates were collected and their MeHg concentrations were determinated. Stable carbon ($\delta^{13}C$) and nitrogen ($\delta^{15}N$) isotope ratios were also used as indicators of energy flow and trophic structure respectively[1]. In contrast to aquatic ecoystems, such investigation is limited in terrestrial environment, particularly in subtropical biome.

Here we show that biomagnification exists in the three studied forests of Hong Kong as revealed by positive trophic magnification slopes (TMS) (0.1347 - 0.2383; $p < 0.05$), which is the slope of $\log_{10}$ [MeHg] vs $\delta^{15}N$. Such trend is consistent with relevant forset studies in other regions (e.g. USA[2] and Southwest China[3], etc.). The TMS value is similar to previous study on tropical freshwater and marine ecosystems (0.15 ± 0.07, n=9) under similar climatic conditions[4]. The percentage of total mercury (THg) as MeHg is found to have an significant increase with $\delta^{15}N$ ($p < 0.05$), confirming that MeHg mainly drives the Hg bioaccumulation within the food webs.

The three studied sites could be classified as mature secondary forests, fung shui wood and montane shrubland with a variety on elevation (~100m, ~200m and ~700m). Based on previous study[5] and official meteorological record[6], temperature is the lowest at the highest points. Our study suggests a warmer environment would facilate the productivity of organisms in the forest, therefore, the TMS value is lowered as a result of Hg dilution inside their faster growing biomass[4]. Previous studies on aquatic food webs also support such trend[4]. The current study emphasises the biomagnifying effect of MeHg in terrestrial ecosystems and how the TMS in various forest food webs were affected needs further investigation.

References

[1] Peterson, B. J., & Fry, B. (1987). Stable isotopes in ecosystem studies. *Annual review of ecology and systematics*, *18*(1), 293-320.

[2] Tsui, M. T. K., Liu, S., Brasso, R. L., Blum, J. D., Kwon, S. Y., Ulus, Y., ... & Finlay, J. C. (2019). Controls of methylmercury bioaccumulation in forest floor food webs. *Environmental science & technology*, *53*(5), 2434-2440.

[3] Li, C., Xu, Z., Luo, K., Chen, Z., Xu, X., Xu, C., & Qiu, G. (2021). Biomagnification and trophic transfer of total mercury and methylmercury in a sub-tropical montane forest food web, southwest China. *Chemosphere*, *277*, 130371.

[4] Lavoie, R. A., Jardine, T. D., Chumchal, M. M., Kidd, K. A., & Campbell, L. M. (2013). Biomagnification of mercury in aquatic food webs: a worldwide meta-analysis. *Environmental science & technology*, *47*(23), 13385-13394.

[5] Hao, J., & Chu, L. M. (2021). Vegetation Types Attributed to Deforestation and Secondary Succession Drive the Elevational Changes in Diversity and Distribution of Terrestrial Mosses in a Tropical Mountain Forest in Southern China. *Forests*, *12*(8), 961.

[6] Hong Kong Observatory, 2022: The Year's Weather 2022. *Monthly Weather Summary Dec 2022*.

EN-03

Mercury Biomagnification in Temperate Grassland Food Web (Kansas, USA)

Jack Tsun-Hung Cheung [a], Martin Tsz-Ki Tsui [a,b], Yener Ulus [b], Peijia Ku [b], Kristina Morales [b], Paul Nyarko [b], Hon-Ming Lam [a]

[a] *School of Life Sciences, Earth and Environmental Sciences Programme, State Key Laboratory of Agrobiotechnology, The Chinese University of Hong Kong, Hong Kong*

[b] *Department of Biology, University of North Carolina at Greensboro, Greensboro, North Carolina 27402, USA*

E-mail: 1155125230@link.cuhk.edu.hk

Mercury (Hg) is a pollutant of global concern, and Hg can be converted into methylmercury (MeHg), a highly toxic and persistent form risking the health of human and wildlife. Many studies on Hg cycling have been conducted in aquatic ecosystems, and to a lesser extent on forest ecosystems. To our knowledge, little is known regarding Hg cycling and bioaccumulation in grassland ecosystems. In this study, vegetation, animal and soil samples were collected in the Konza Prairie Biological Station (KPBS) dedicated to research in various locations in 2019. KPBS is a grassland divided into different zones, which are subject to different treatments, such as burning and cattle grazing. Analysis for total mercury (THg), MeHg and stable isotope ratios for carbon ($\delta^{13}C$) and nitrogen ($\delta^{15}N$) were performed on the biota samples. The mean THg concentration in the animal samples was 42.70±59.63 ng/g dry weight (n = 147) while the mean MeHg concentration was 15.55±31.96 ng/g dry weight (n = 155). By comparing $\delta^{15}N$, an indicator of trophic level [1] (n = 96) and $\log_{10}$MeHg, the evidence of MeHg biomagnification can be obtained when the slope of $\log_{10}$MeHg concentration against $\delta^{15}N$ was shown to be greater than 0 [1]. The slope of the terrestrial food web was found to be 0.201, which is similar to that in terrestrial forest food web in the temperate ecosystems [2]. The percentage of THg as MeHg, i.e., %MeHg, increased along trophic levels. Overall, %MeHg in vegetation had an average of 7.8% (THg concentration was 7.55±3.34 ng/g dry weight, MeHg concentration was 0.53±0.44 ng/g dry weight, n = 11), as compared to 18.0% in herbivore (n = 74), 29.8% in detritivore (n = 14), 50.4% in omnivore (n = 16), and 61.5% in carnivore (n = 32). Evidence shows that bioaccumulation and biomagnification occurs in a similar manner in terrestrial grassland and forest ecosystems.

References

[1] Rodenhouse NL, Lowe WH, Gebauer RLE et al. *Science of the Total Environment*, 2019, *665*, 1125 -1134.

[2] Tsui TK, Liu S, Brasso RL, et al. *Environ. Sci. Technol.,* 2019, *53*, 2434−2440.

EN-04

Tracking circulation change in the western North Atlantic during the Little Ice Age using a multi-proxy approach

Wai Ching Chu [a], Anne de Vernal [b], Andre Poirier [b], Christelle Not [c], Benoit Thibodeau [a,d]

[a] *School of Life Sciences, The Chinese University of Hong Kong, Hong Kong SAR,*
[b] *Geotop, University of Quebec at Montreal, Quebec, Canada,*
[c] *Department of Earth Sciences, The University of Hong Kong, Hong Kong SAR,*
[d] *Earth and Environmental Sciences Programme,The Chinese University of Hong Kong, Hong Kong SAR.*
E-mail: wcrachel@link.cuhk.edu.hk

Atlantic Meridional Circulation is hypothesized to be at a weak state in present days and is predicted to be further weakened in the future[1]. While ocean circulation is often suggested to be a climate driver for past climatic events, there have been on-going debates on the role of a weakened circulation to the onset of the Little Ice Age (LIA). Previous studies have observed a weaker Labrador Current during LIA[2,3], suggesting a linkage between changes in the western North Atlantic circulation and the abnormal cooling during that period[3]. However, the mentioned shift in oxygen isotopic signals could infer to a change in circulation and/ or a change in water temperature. To deduce the actual cause of the shift, this study incorporates an additional temperature proxy, Mg/Ca ratio, to constrain the data from the oxygen isotopic analysis, such that a concise ocean circulation during LIA in the western North Atlantic can be reconstructed.

To acquire the Mg/Ca ratio in foraminifera, results acquired from a novel technique called Laser Ablation Inductively Coupled Plasma Mass Spectrometry (LA-ICPMS)[4] are compared against the results from the conventional solution-based ICPMS method. This comparison aims to verify both the accuracy of the results and the effectiveness of the method used.

Two cores from the Laurentian Channel are selected for this study: 1) CR02-23 (48°42.008'N, 68°38.894'W, water depth = 345cm), is used to establish a Mg/Ca calibration curve against instrumental temperature from 1903 to 2001 CE; 2) The sections covering the LIA are analysed in high-resolution in MD99-2220 (48°38.32'N, 68°37.93'W, water depth = 320m). The benthic foraminifera species, Globobulimina auriculata., is selected for the Mg/Ca ratio paleo-temperature reconstruction because of its high temperature sensitivity[5].

All in all, this study aims to provide new knowledge about the potential role of ocean circulation and its linkages with cooler condition during the LIA. Also, the use of a multi-proxy approach will be validated, enhancing the methodologies used in paleoceanography. With a better understanding of the mechanism of climate drivers in the past, better predictions and preparations for future climatic scenarios can be done.

References

6. Ditlevsen P and Ditlevsen S. *Nat. Commun.,* 2023*, 14*, 4254.
7. Thornalley DJR. *et al. Nature* 2018, *556*, 227–230.
8. Thibodeau, B. *et al. Geophys. Res. Lett.* 2018, *45*, 12,376-12,385.
9. Fehrenbacher, J., Marchitto, T. & Spero, H. J. *Geochem. Geophys. Geosystems* 2020, *21*.
10. Weldeab, S., Arce, A. & Kasten, S. *Earth Planet. Sci. Lett.* 2016, *438*, 95–102

EN-05

The sources and behaviour of nitrogen species in hypoxia areas of Hong Kong

Henry C.J. Thomas[a], Benoit Thibodeau[a,b]
[a] *School of Life Sciences, The Chinese University of Hong Kong, Hong Kong SAR*
[b] *Earth and Environmental Sciences Programme, The Chinese University of Hong Kong, Hong Kong SAR*
henrycjthomas@gmail.com

The prevalence of coastal hypoxia and ocean deoxygenation have increased significantly over the past half century, primarily as a result of the influence of anthropogenically produced nitrogen into the marine ecosystems[1–3]. This is an issue, as lower oxygen levels in coastal environments lead to decreases in ecosystem health, primarily as a result of increased species mortality[4,5]. With further increases in the coastal urban population and coastal urbanisation predicted, understanding how incidents of coastal hypoxia develop is paramount to managing and mitigating their negative effects.

Hong Kong is an ideal location to study this as it is a heavily urbanised coastal city, part of the Pearl River greater bay area, and contains two seasonally hypoxic areas, Tolo Harbour and the southern waters between Lantau and Lamma Island[6,7]. The study here aims to look at how nutrient sources and cycling changes on a year-round basis, and how this affects the dissolved oxygen content of the area. This is being carried out using nutrient analysis of key nitrogen species (NH_4^+, NO_3^-, NO_2^-), total carbon and nitrogen levels, chlorophyll-α concentration and dissolved oxygen levels in tandem with stable isotope ($\delta^{15}N\text{-}NO_3^-$, $\delta^{18}O\text{-}\ NO_3^-$) measurements to determine the relative importance of different sources and types of nitrogen within these areas[8].

Using this data, we also hope to be able to answer two more fundamental questions in coastal biogeochemistry. The first of these is how nitrogen fixing bacteria (diazotrophs) continue to fix nitrogen in unfavourable conditions (excess nitrogen), such as those found in hypoxic areas[9]. This will be using a $\delta^{15}N$ tracer (and potentially acetylene reduction assays) to determine the rate of nitrogen fixation as external condition change. The second question is how the oxidation state of organic matter changes as a result of physical and nutrient (particularly nitrogen) stress. As microorganisms adapt to variable conditions, the stoichiometry of their organic matter can change, meaning that during organic matter oxidation the amount of oxygen consumed may change, which could accelerate the rate of ocean deoxygenation[10,11]. This will be carried out studying the organic carbon concentration and chemical oxygen demand of particulate matter, alongside the use of flow cytometry to study the physiology of phytoplankton.

References

[1]Diaz, R.J. & Rosenberg, R. *Science* 321, 926–929 (2008).
[2]Robinson, C. *Front. Mar. Sci.* 5, (2019).
[3]Howarth, R.W. *Harmful Algae* 8, 14–20 (2008).
[4]Gray, J., Wu, R. & Or, Y. *Mar. Ecol. Prog. Ser.* 238, 249–279 (2002).
[5]Steckbauer, A., Duarte, C.M., Carstensen, J., Vaquer-Sunyer, R. & Conley, D.J. *Environ. Res. Lett.* 6, 025003 (2011).
[6]Li, D. et al. *J. Geophys. Res. Oceans* 125, e2020JC016178 (2020).
[7]Liang, W. et al. *Sci. Total Environ.* 905, 167138 (2023).
[8]Archana, A. et al. *Water Res.* 142, 459–470 (2018).
[9]El-Khaled, Y.C. et al. *Mar. Ecol. Prog. Ser.* 645, 55–66 (2020).
[10]Moreno, A.R. et al. *AGU Adv.* 3, e2022AV000679 (2022).
[11]Moreno, A.R. et al. *Proc. Natl. Acad. Sci.* 117, 22866–22872 (2020).

EN-06

Tidal pumping and atmospheric deposition of inorganic nitrogen drive diurnal variation in primary productivity in Mirs Bay, Hong Kong

Ho Wen LO [a], Benoit THIBODEAU [a,b]

[a] *School of Life Sciences, The Chinese University of Hong Kong, Hong Kong*

[b] *Earth and Environmental Sciences Programme, The Chinese University of Hong Kong, Hong Kong*

E-mail: owenhwlo@cuhk.edu.hk

Previous research has shown that Mirs Bay, Hong Kong is a peculiar coastal area in that it exhibits high chlorophyll a concentrations despite low ambient dissolved nutrient levels [1]. It is therefore hypothesised that atmospheric sources of inorganic nitrogen may be important in driving primary productivity in Mirs Bay [2]. We tested this hypothesis by conducting two fieldwork campaigns in the area, one in late summer (September 2022) and another in winter (December 2022). Surface seawater samples were obtained frequently on each day of sampling. Concentrations of chlorophyll a and dissolved inorganic nutrients were determined in the laboratory. During the winter campaign, aerosol samples were also collected and concentrations of inorganic nitrogen were analysed in the field using a newly-developed aerosol nitrogen analyser [3].

During the September campaign, we observed that peaks in dissolved nutrients and chlorophyll a often occurred around one to two hours after the lowest tide. It is suggested that receding tides would have transferred nutrients from the surrounding land into Mirs Bay (tidal pumping). On the other hand, during the December campaign, we found that there were additional peaks in chlorophyll a that could not be attributed to low tides. These anomalous peaks were mostly recorded in the morning and appeared to be responses to overnight accumulations of atmospheric inorganic nitrogen deposits, consumption of which would only be possible under the presence of sunlight. Atmospheric deposition only gained significance in winter, as only the prevailing wind in winter (i.e. northerlies, as opposed to the southerlies in summer) could bring in emissions of anthropogenic nitrogen originating from Mainland China [4]. These findings imply strong diurnal variability in primary productivity in this bay and suggest that existing monitoring and sampling efforts (mostly monthly) may be biased, depending on their timing during the day and/or the season.

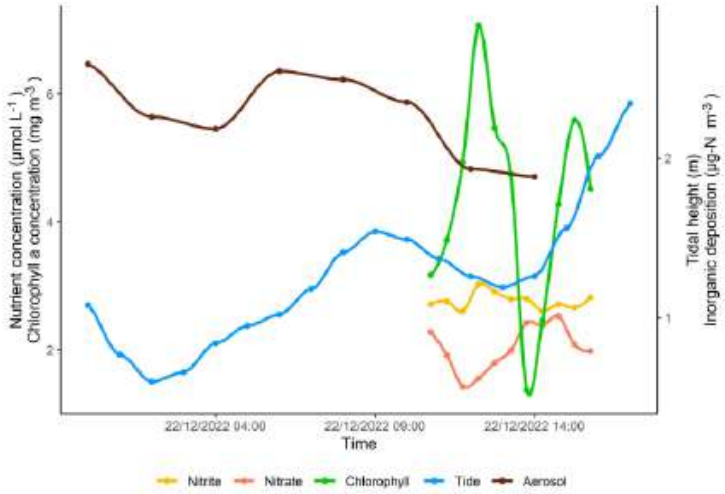

Typical pattern observed in winter: two chlorophyll peaks, one in the morning (likely due to atmospheric inorganic nitrogen) and another in the afternoon (likely due to receding tides)

[1] Archana, A. et al. *Water Research*, **2018**, *142*, 459 – 470.
[2] Yau Y. Y. et al. *Environmental Science & Technology*, **2020**, *54*(7), 3920 – 3928.
[3] Li, J. et al. *Atmospheric Environment*, **2022**, *27*, 118905.
[4] Yau, Y. Y. Y. et al. *Science of the Total Environment*, **2022**, *832*, 154781.

EN-07

Dynamics of atmospheric nitrogen in Southern China and its impact on coastal ecosystems

Chenyu LUO,[a] Benoit THIBODEAU,[b]

[a] *School of Life Science, The Chinese University of Hong Kong, China;* [b] *School of Life Sciences and Earth and Environmental Sciences Programme, Chinese*

University of Hong Kong, China.

E-mail: 1155205611@link.cuhk.edu.hk

Atmospheric deposition is recognized as an important source of nutrients in the upper ocean, and the nutrients it brings, such as nitrogen (N) and phosphorus (P), can affect the growth of marine phytoplankton and influence marine N cycle. The oligotrophic South China Sea (SCS) is particularly affected by high anthropogenic nitrogen deposition due to the large populations and rapid economic development of neighboring countries. However, little is known about the mechanism of how anthropogenic activities influence the SCS system by interacting with increased landfalling typhoons and winter haze events. It is thus that the main challenges of atmospheric deposition to the ocean are discussed in this research from the aspects of bioavailable N and P as well as response of marine primary production process. Mesocosm experiments in the SCS are planned to conduct to quantify the effects of atmospheric nitrogen deposition on phytoplankton growth and microbiome community changes in February 2024. The additional concentrations of nutrients including N and P that stimulate annual depositing flux will be determined based on field observations and extensive datasets in the SCS according to previous studies. Different atmospheric deposition scenarios will be also evaluated to validate a hypothesis that the phytoplankton biomass over the SCS is found to have increased influenced by the nitrogen deposition in dust or haze events.

References

[1]Bernhardt, J. R., & Leslie, H. M. (2013). Resilience to climate change in coastal marine ecosystems. *Annual Review of Marine Science*, *34*(6), 933-940.

[2]Chen, B., & Smith, S. L. (2018). Optimality-based approach for computationally efficient modeling of phytoplankton growth, chlorophyll-to-carbon, and nitrogen-to-carbon ratios. *Annual review of earth and planetary sciences*, *7*, 443-472.

[3]Dagenais-Bellefeuille, S., & Morse, D. (2013). Putting the N in dinoflagellates. *Frontiers in Microbiology*, *109*(D18).

[4]Gao, P., Wang, P., Chen, S., Bi, W., Lu, S., He, J., et al. (2020). Effect of ambient nitrogen on the growth of phytoplankton in the Bohai Sea: Kinetics and parameters. Journal of Geophysical Research: Biogeosciences, *25*(8), 1661-1678.

[5]Jankowiak, J., Hattenrath-Lehmann, T., Kramer, B. J., Ladds, M., & Gobler, C. J. (2019). Deciphering the effects of nitrogen, phosphorus, and temperature on cyanobacterial bloom intensification, diversity, and toxicity in Western Lake Erie. *Journal of Geophysical Research: Atmospheres*, *99*(D10), 21033-21041.

[6]Liu, T., Chen, G., Chen, J., Xu, L., Li, M., Hong, Y., Chen, Y., Ji, X., Yang, C., & Chen, Y. (2022). Seasonal characteristics of atmospheric peroxyacetyl nitrate in a coastal city of Southeast China: Explanatory factors and photochemical effects. *Atmospheric Chemistry and Physics*, *22*(7), 4339-4353.

[7]Marsh, D. R., Mills, M. J., Kinnison, D. E., Lamarque, J.-F., Calvo, N., & Polvani, L. M. (2013). Climate change from 1850 to 2005 simulated in CESM1 (WACCM). *Journal of climate*, *26*(19), 7372-7391.

[8]Marshall, H. G., Lane, M. F., Nesius, K. K., & Burchardt, L. (2009). Assessment and significance of phytoplankton species composition within Chesapeake Bay and Virginia tributaries through a long-term monitoring program. *Environmental Monitoring and Assessment*, 150(1), 143–155.

[9]Melosi, M. V. (1979). Urban pollution: historical perspective needed. *Environmental review*, *3*(3), 37-45.

[10]Qiu, Y., Ma, Z., & Li, K. (2018). A modeling study of the peroxyacetyl nitrate during a wintertime haze event in Beijing, China. *Science of the Total Environment*, *650*, 1944-1953.

[11]Qiu, Y., Ma, Z., Li, K., Lin, W., Tang, Y., Dong, F., & Liao, H. (2020). Markedly enhanced levels of peroxyacetyl nitrate (PAN) during COVID-19 in Beijing. *Geophysical Research Letters*, *47*(19), e2020GL089623.

[12]Wang, Y., Sun, Y., Wang, C., & Hu, X. (2019). Distribution of the net-phytoplankton community and chlorophyll-a in the Bohai Sea in summer and its impacts on fishery resources. Progress in Fishery Sciences, *318*(6044), 347-349.

International Conference on
Earth, Energy & Environmental Sciences
for Carbon Neutrality

EN-08

Agroecosystem Modeling of Reactive Nitrogen Emissions from U.S. Agricultural Soils with Biochar Amendments

Lina Luo,[a] Daniel S. Cohan,[b] Caroline A. Masiello,[c] Taras E. Lychuk,[d] Amos P. K. Tai[a]

[a]*Earth and Environmental Sciences Programme, The Chinese University of Hong Kong, Hong Kong SAR, China;* [b]*Department of Civil and Environmental Engineering, Rice University, Texas, United States;* [c]*Department of Earth, Environmental, and Planetary Sciences, Rice University, Texas, United States;* [d]*Agriculture and Agri-Food Canada, Manitoba, Canada*

E-mail: linaluo@cuhk.edu.hk

Fertilizer-intensive agriculture is a leading source of reactive nitrogen (Nr) emissions in the United States, including the potent greenhouse gas nitrous oxide (N_2O), and the air pollutants nitric oxide (NO) and ammonia (NH_3) which contribute to most health-damaging air pollution fine particulate matter (PM) and ozone (O_3). Biochar, a carbonaceous soil amendment produced from biomass, has potential for boosting crop yields, enabling carbon sequestration, and possibly reducing Nr emissions. However, the impacts of biochar on Nr emissions vary significantly with soil properties, climate conditions, and the properties of the biochar itself, ranging from positive to negative and even neutral. Previous studies have relied on field measurements or field-scale agroecosystem models, which are inadequate to characterize such complex variations across U.S. agricultural lands.

In this study, we incorporated biochar algorithms[1] into a regional-scale agroecosystem model, the Fertilizer Emission Scenario Tool for CMAQ (FEST-C)[2,3], to simulate changes in Nr emissions following biochar applications. Unlike typical field-scale process-based models, FEST-C, with its built-in databases for sites, soils, and crops, allows for simulations across U.S. agricultural lands at a fine-scale (12km by 12km) spatial resolution. Our previous work[2] enhanced FEST-C's nitrogen schemes to include emissions of NO and N_2O from nitrification, as well as NO from denitrification, enabling a consistent and mechanistic prediction of Nr emissions from U.S. agricultural soils. Model performance evaluations against published field studies in the United States showed that the enhanced FEST-C, with biochar algorithms, could capture the trends of Nr emission changes upon biochar applications. Scenario analyses were then performed with biochar application rates of 5 and 20 ton ha^{-1} on U.S. fertilized soils. Our results demonstrated that the responses of Nr emissions to biochar amendments vary significantly across different agricultural areas and are influenced by the amount of biochar applied. High-dose biochar applications in acidic soils with low organic carbon and inorganic nitrogen content exhibited the most favorable impacts on Nr emissions. Our analyses suggest that the net effects of biochar amendments on Nr emissions depend mostly on how nitrification rate is affected.

Our study is the first to model spatial variability in the impacts of biochar amendments on emissions of three crucial Nr species.[4] These simulations could inform the identification of field study sites where the application of soil carbon amendments would be most likely to mitigate emissions and their associated adverse impacts on air quality, human health, and climate.

References

[1] Lychuk TE, Izaurralde RC, Hill RL, McGill WB, Williams JR. *Mitig Adapt Strateg Glob Change* 2015, *20* (8), 1437–1458.

[2] Luo LL, Ran LM, Rasool QZ, Cohan DS. Integrated Modeling of U.S. *Environ. Sci. Technol.* 2022, acs.est.1c08660.

[3] Ran LM, Yuan YP, Cooter E, Benson V, Yang DM, Pleim J, Wang RY, Williams J. *J. Adv. Model. Earth Syst.* 2019, *11* (12), 4645–4668.

[4] Luo LL, Cohan DS, Masiello CA, Lychuk TE, Gao XD. *Biochar* 2023, *5* (1), 72.

EN-09

[Withdrawn]

EN-10

Baseline lithium-ion concentrations in sediments and soils in a rural area of Hong Kong

Norah Muisa[a#], Tsz Ki Martin Tsui[b],

[ab]School of Life Sciences, Earth and Environmental Sciences Programme, The Chinese University of Hong Kong, Shatin, Hong Kong

E.mail: norahmuisa@gmail.com/mtktsui@cuhk.edu.hk

Lithium (Li) is possibly an environmental contaminant of elevating concern due to its increasing global use, while it is neither regulated nor monitored in the environment. The major driver of the increasing demand is the use of Li-ion batteries (LIBs) in electric vehicles since electric vehicles are regarded as a panacea to achieve carbon neutrality in the transport sector. However, spent Li-ion batteries may pose a potential source of Li and associated metals in the environment. To monitor and assess this potential future impact, reference levels of lithium in diverse environments are critical. Numerous studies have been conducted on metals in various environmental compartments in Hong Kong, but only one study performed between 2002 and 2003 on assessment of groundwater quality in and around the Mid-Levels area in Hong Kong examined twenty elements including lithium. Nevertheless, a more recent examination is warranted amid the increasing global use of Li. Outside Hong Kong, detailed studies on lithium distribution in diverse environmental compartments are still relatively scarce.

This study determined baseline lithium distribution in sediments and soils from a rural area in northeastern Hong Kong called Kuk Po Village, as a case study of unimpacted sites. Sediment samples were collected twice in each of four seasons from April to February 2022 in a freshwater stream and marshland at Kuk Po Village. Soil composite samples were collected from five accessible sites adjacent to sediment sampling sites along the stream and marshland, and the soil cores were separated as 0-10 cm, 10-20 cm and 20-30 cm depths. General water quality of the stream was also assessed.

All soil and sediment samples were microwave-digested at 180 ^{o}C using a modified aqua regia method, and analyzed using the Inductively Coupled Plasma-Mass Spectrometer (ICP-MS). In this presentation, lithium levels in Kuk Po Village will be reported. Our ongoing study is assessing the distribution of Li in other areas of Hong Kong and more diverse land uses to get a holistic view. Also, speciation and isotope studies are critical to establish the mobility, source, and potential for trophic transfer in the food chain.

References

[1] Bolan, N., et. al. From mine to mind and mobiles- Lithium contamination and its risk management. Environ. Pollut., 2021, 290: 118067.

[2] Chow, A. T. Proactive approach to minimize lithium pollution. *J. Environ. Qual*., 2022.

[3] Leung, C.-M., & Jiao, J. J. Heavy metal and trace element distributions in groundwater in natural slopes and highly urbanized spaces in Mid-Levels area, Hong Kong. *Water Res.*, 2006, 40(4): 753-767.

[4]Robinson, B. H., Yalamanchali, R., Reiser, R., & Dickinson, N. M. Lithium as an emerging environmental contaminant: Mobility in the soil-plant system. *Chemosphere*, 2018,197: 1-6.

[5] Shakoor, N., Adeel, M., Azeem, I., Ahmad, M. A., Zain, M., Abbas, A., Hussain, M., Jiang, Y., Zhou, P., & Li, Y. Interplay of higher plants with lithium pollution: Global trends, meta-analysis, and perspectives. *Chemosphere*, 2022,136663.

[6] Thibon, F., Weppe, L., Vigier, N., Churlaud, C., Lacoue-Labarthe, T., Metian, M., Cherel, Y., & Bustamante, P. Large-scale survey of lithium concentrations in marine organisms. *Sci. Total Environ.*, 2021,751, 141453.

EN-11

Candidatus Accumulibacter use fermentation products for enhanced biological phosphorus removal

Guanglei Qiu, Liping Chen, Gengrui Wei, Yushen Zhang, Kaiying Wang, Cenchao Wang, Xuhan Deng, Yaqian Li, Xiaojing Xie, Jinling Chen, Fu Huang, Hang Chen, Bin Zhang, Chaohai Wei.

School of Environment and Energy, South China University of Technology, Guangzhou 510006, China.

qiugl@scut.edu.cn

Abstract: Previous research suggested that two major groups of polyphosphate-accumulating organisms (PAOs), i.e., *Ca.* Accumulibacter and *Tetrasphaera*, play cooperative roles in enhanced biological phosphorus removal (EBPR). The fermentation of complex organic compounds by Tetrasphaera provides carbon sources for *Ca.* Accumulibacter. However, the viability of the fermentation products (e.g., lactate, succinate, alanine) as carbon sources for *Ca.* Accumulibacter and their potential effects on the metabolism of Ca. Accumulibacter were largely unknown. This work for the first time investigated the capability and metabolic details of *Ca.* Accumulibacter clade IIC strain SCUT-2 (enriched in a lab-scale reactor with a relative abundance of 42.8 %) in using these fermentation products for EBPR. *Ca.* Accumulibacter clade IIC strain SCUT-2 (with a relative abundance of 42.8 %) was enriched in a lab-scale reactor. The enrichment culture was able to assimilate lactate and succinate with the anaerobic P release to carbon uptake ratios of 0.28 and 0.36 P mol/C mol, respectively. In the co-presence of acetate, the uptake of lactate was strongly inhibited, since two substrates shared the same transporter as suggested by the carbon uptake bioenergetic analysis. When acetate and succinate were fed at the same time, *Ca.* Accumulibacter assimilated these two carbon sources simultaneously. Proton motive force (PMF) was the key driving force (up to 90%) for the uptake of lactate and succinate by *Ca.* Accumulibacter. Apart from the efflux of protons in symport with phosphate via the inorganic phosphate transport system, translocation of proton via the activity of fumarate reductase contributed to the generation of PMF, which agreed with the fact that PHV was a major component of PHA when lactate and succinate were used as carbon sources, involving the succinate-propionate pathway. Metabolic models for the usage of lactate and succinate by *Ca.* Accumulibacter for EBPR were built based on the combined physiological, biochemical, metagenomic, and metatranscriptomic analyses. Alanine was shown as an invalid carbon source for *Ca.* Accumulibacter. Instead, it significantly and adversely affected *Ca.* Accumulibacter-mediated EBPR. Phosphate release was observed without alanine uptake. Significant inhibitions on the aerobic phosphate uptake of *Ca.* Accumulibacter was also evident. Overall, this study suggested that there might not be a simply synergic relationship between *Ca.* Accumulibacter and *Tetrasphaera*. Their interactions would largely be determined by the kind of fermentation products released by the latter.

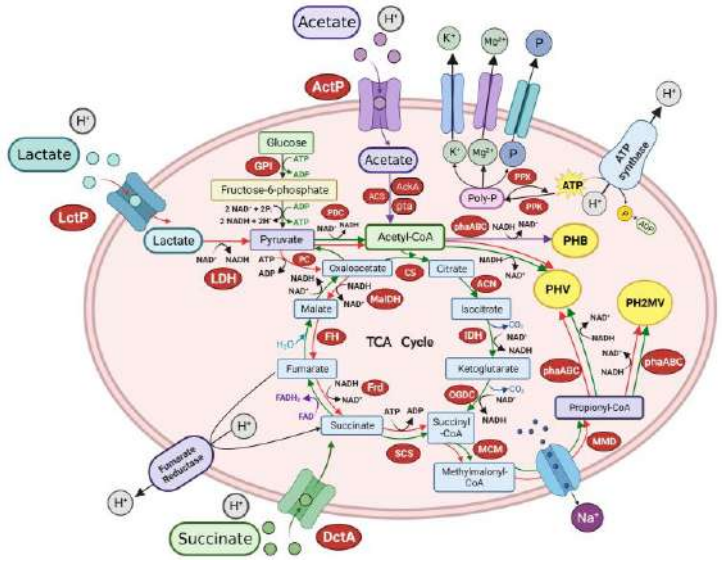

Fig. 1 Metabolic models for *Ca.* Accumulibacter with acetate, lactate, and succinate as carbon sources for EBPR.

EN-12

Study on photocatalytic degradation to eliminate microplastic pollution in water environment under carbon neutral background

Huixue Ren,[a] Shengyun Jiang,[a] Yaping Qin [a]
[a] *School of Municipal and Environmental Engineering , Shandong Jianzhu University , Shandong Province ,P.R.China.*
E-mail: renhx138@163.com

The microplastics (MPs) in the water system could easily enter the human body and pose potential threat, so finding a green and effective solution remains a great challenge[1]. At present, the advanced oxidation technology represented by photocatalysis has been proven to be effective in the removal of organic pollutants, making it a feasible method to solve the problem of MP pollution[2]. In this study, the photocatalytic degradation of typical MP polystyrene (PS) and polyethylene (PE) by a new quaternary layered double hydroxide composite photomaterial CuMgAlTi-R400 was tested under visible-light irradiation. After 300 h of visible-light irradiation, the average particle size of PS decreased by 54.2% compared with the initial average particle size. The smaller the particle size, the higher the degradation efficiency. The degradation pathway and mechanism of MPs were also studied by GC-MS, which showed that PS and PE produced hydroxyl and carbonyl intermediates in the process of photodegradation. This study demonstrated a green, economical, and effective strategy for the control of MPs in water.

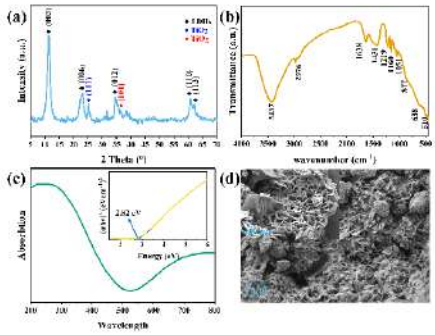

Fig. 1 (a)XRD patterns, (b)FTIR spectra, (c) Diffuse reflectance spectra and Tauc plot, and (d) SEM image of CuMgAlTi-R400.

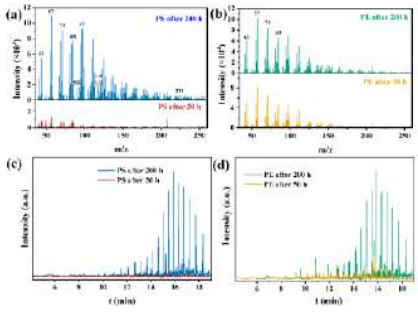

Fig. 2 GC/MS spectrum of PS(a,c) and PE(b,d).

References

[1]Shen M, Zhang Y, Zhu Y, et al. *Environ. Pollut.* 2019, *252*, 511–521.
[2]Xu Q, Huang Q.S, Luo T.Y,et al. *Chem. Eng. J.* 2021, *416*, 129123.

EN-13

Variations of Methylmercury in a Mangrove Wetland Sediments: Insights from Subtropical Ecosystems in Hong Kong

Shaoyi Wang[a,b] Martin Tsz-Ki Tsui[a,b]

[a]*School of Life Sciences, Earth and Environmental Sciences Programme, The Chinese University of Hong Kong, Shatin, Hong Kong SAR, China*

[b]*State Key Laboratory of Marine Pollution, The City University of Hong Kong, Shatin, Hong Kong SAR, China*

E-mail: 1155168642@link.cuhk.edu.hk

Tropical and subtropical coastal wetland ecosystems serve vital bridging functions between offshore and inland environments. Most tropical and subtropical wetland areas, estimated to be between 60% and 75%, is mangrove forest. Mangroves are considered to have significant ecological and economic value, however, mangrove sediments with strong reducing conditions may play a potentially important, yet not well understood, role in converting inorganic mercury (Hg) into highly toxic methylmercury (MeHg). In this study, multiple 15-cm sediment cores were collected over different seasons from Mai Po Nature Reserve in Hong Kong along a transect: from within mangrove stands, water-land interface (margin), middle of the water channel to open water area. Sediment cores were sliced every centimeter for total mercury (THg), MeHg, and organic matter content analysis. We found that THg in sediments ranged narrowly between 90.32 and 225.81 ng/g and did not show a positive correlation with MeHg, which have been shown in many other aquatic studies. Interestingly, elevated MeHg concentrations were found at surface sediment near the root zones of mangrove trees. The percentage of THg as MeHg, i.e., %MeHg, was significantly correlated with loss-on-ignition (LOI), a proxy of organic matter content ($p<0.0001$), which suggests that sedimentary organic matter could serve as a crucial factor mediating Hg methylation in mangrove sediment. Over different seasons, a significantly higher MeHg ($p<0.05$) was observed during summertime, e.g., June & August. During summertime, the water would have lower salinity and higher temperature, which we suggest to be important factors promoting Hg methylation in sediments. All these results are now examined in other mangrove forests around Hong Kong, including one site at Futian Mangrove Reserve, Shenzhen), in which we will perform analyses for THg, MeHg, LOI, and Hg methylation related genes (*hgcAB* and *merAB*). Our current work will provide new insights into the key factors influencing Hg methylation in mangrove wetlands, where the resident food webs can extensively bioaccumulate and biomagnify.

EN-14

A microcosm of nitrogen removal and carbon mineralization under salinity gradients: an insight into coastal salinity intrusion

Ziyan Wang[a], Benoit Thibodeau[a,b]

[a] *School of Life Sciences, the Chinese University of Hong Kong, Hong Kong, China;* [b] *Earth and Environmental Sciences Programme, the Chinese University of Hong Kong, Hong Kong, China.*

E-mail: 1155186101@link.cuhk.edu.hk

Nitrogen loading in aquatic environments has been identified as far exceeding the threshold for a stable Earth[1]. Human activities like agriculture and industrial processes majorly contribute to excessive nitrogen levels and ecological crises (e.g. eutrophication, hypoxia) in natural water. Coastal wetlands, as a transition between lands and seas, play a vital role in reducing this nitrogen overload through natural processes, including denitrification and anaerobic ammonium oxidation (anammox)[2,3]. Considering denitrification's potential risk of producing nitrous oxide—a potent greenhouse gas—and anammox's efficient co-removal of ammonium and nitrite, it's crucial to identify what controls the balance between these two processes. However, the mechanisms that determine the predominance of anammox and its interplay with carbon and sulfur cycles in coastal wetlands are not well-documented.

Herein, our study investigated salinity's role in anammox's contribution to nitrogen loss in response to coastal salinity intrusion. We hypothesized that higher salinity could enhance the ratio of anammox to denitrification. Slurry incubation of air-dried mangrove sediments and artificial seawater with different salinities is set for 28 days (n=80). Nitrogen transformation was monitored by NH4+, NO2-, and NO3- variance. Carbon mineralization was monitored by dissolved inorganic carbon (DIC) and total alkalinity. 15N-paring isotope technique was applied to quantify the potential of nitrogen loss pathways[4].

Results showed that effective nitrogen removal began after a week. Interestingly, while salt ions generally slowed the process, we observed faster nitrogen removal at higher salinities. The turnover rates of NH4+ and NO3- showed the same pattern, while the releasing rates of DIC were the reverse. The data suggests source differences between DIC and nitrogen species. Namely, autotrophic anammox could be more active than heterotrophic denitrification. The ratio of total alkalinity to DIC (~1) supports that sulfate reduction contributes more to carbon mineralization instead of denitrification[5]. Further isotope and molecular analysis will provide more information for intertwined nitrogen, carbon, and sulfur cycles.

References

[1] Richardson, K. et al. Earth beyond six of nine planetary boundaries. Sci. Adv., 2023, 9 (37), eadh2458.
[2] Cao, W., Guan, Q., Li, Y., Wang, M. & Liu, B. The contribution of denitrification and anaerobic ammonium oxidation to N2 production in mangrove sediments in Southeast China. J. Soils Sediments., 2017, 17 (6), 1767–1776.
[3] Salk, K. R., Erler, D. V., Eyre, B. D., Carlson-Perret, N. & Ostrom, N. E. Unexpectedly high degree of anammox and DNRA in seagrass sediments: Description and application of a revised isotope pairing technique. Geochim. Cosmochim. Acta., 2017, 211, 64–78.
[4] Thamdrup, B. & Dalsgaard, T. Production of N2 through Anaerobic Ammonium Oxidation Coupled to Nitrate Reduction in Marine Sediments. Appl. Environ. Microbiol. 2002, 68 (3), 1312–1318.
[5] Santos, I. R. et al. The renaissance of Odum's outwelling hypothesis in 'Blue Carbon' science. Estuar. Coast. Shelf Sci., 2021, 255, 107361.

EN-15

[Withdrawn]

EN-16

Two new clades recovered at high temperatures provide new phylogenetic and genomic insights into Ca. Accumulibacter

Xiaojing Xie,[a] Xuhan Deng,[a] Jinling Chen[a], , Liping Chen[a], Jing Yuan[a], Hang Chen[a], Chaohai Wei [a,c], Xianghui Liu[b], Guanglei Qiu[a,b,c,d*]

[a] *School of Environment and Energy, South China University of Technology, Guangzhou 510006, China., ;* [b] Singapore *Centre for Environmental Life Sciences Engineering, Nanyang Technological University, Singapore 637551, Singapore.* [c] *Guangdong Provincial Key Laboratory of Solid Wastes Pollution Control and Recycling, Guangzhou 510006, China.* [d] *The Key Lab of Pollution Control and Ecosystem Restoration in Industry Clusters, Ministry of Education, Guangzhou 510006, China.*

E-mail: 1030472309@qq.com

Candidatus Accumulibacter, a key genus of polyphosphate-accumulating organisms playing key roles in enhanced biological phosphorus removal (EBPR) systems, can be divided into two major clades based on the gene polyphosphokinase 1. The genomic studies have deepened understanding of *Ca*. Accumulibacter over the years, but some metabolic aspects remain controversial. Controversies include P uptake coupled with nitrate/nitrite reduction and novel carbon source utilization. It is not clear if these capabilities are widely preserved within the genus, or clade/species specific. Additionally, in high-temperature EBPR systems, clade I members were scarcely detected while Clade IIF and IIC were observed as predominant community members, suggesting potential differences in their ability to survive in warmer environment. The genetic basis for this potential remains unexplored owing to the absence of high-quality genomes or limited genome integrity recovered at high-temperature systems.

A reliable phylogeny and clade classification is a prerequisite for understanding metabolic diversities of microorganisms. Some members, not adhere to ppk1-based population structure, highlight classification based on ppk1 may not sufficiently represent the evolutionary relationships. Modern evolutionary studies employ multiple genes and whole-genome data, aided by machine learning, for more accurate classification. Re-evaluating the phylogenetic structure through machine learning and pangenomics, in addition to ppk1-based classification, is necessary.

In this study, we used ten high-quality *Ca*. Accumulibacter genomes were recovered from high-temperatures reactors with available high-quality genomes in NCBI to perform a systematic pangenomic analysis. Clade IIF members SCELSE-3, SCELSE-4, and SCELSE-6 encoded a complete denitrification pathway, suggesting that Ca. Accumulibacter alone could achieve complete denitrification. All *Ca*. Accumulibacter likely has the potential to use dicarboxylic amino acids. AALB seemed to be the only one capable of glucose usage. A heat shock protein Hsp20 encoding gene was found exclusively in genomes recovered at high temperatures, which was absent in clades IA, IC, IIA, IIB, and IID members. High transcription of this gene in SCUT-2 suggested its role in surviving high temperatures. Ambiguous clade identity was observed for newly recovered genomes (SCELSE-9 and SCELSE-10). Five machine learning models, using orthogroups as input features, suggested that these two genomes belong to a new clade (IIJ). The phylogeny of *Ca*. Accumulibacter was re-evaluated based on the horizontally transferred polyphosphokinase 2 gene which showed effectiveness in differentiating and defining different clades.This study provide renovative understandings of nitrogen and carbon metabolisms, heat stress adaption and the phylogenic characteristics, resulting in an improved understanding of genomic differences within and among clades.

EN-17

Elevational trends in mercury speciation and microbial controls on methylmercury cycling in tropical forest soils

Xizi Yang[a] and Martin Tsz-Ki Tsui

[a] *School of Life Sciences, Earth and Environmental Sciences Programme, The Chinese University of Hong Kong, Hong Kong SAR, China*

E-mail: 1155168394@link.cuhk.edu.hk

The distinct physical and chemical properties of mercury enable its long-distance transport among continents and ecosystems. Its highly toxic organic form, methylmercury, is produced *in situ* in reducing environments such as wetlands, which have been widely identified as hotspots for aquatic sources of methylmercury production. However, our understanding on the production of methylmercury in largely oxic terrestrial landscapes remains relatively limited. Here we investigated mercury and methylmercury distribution in soils along an elevational gradient on Tai Mo Shan, Hong Kong.

As altitude rises in Tai Mo Shan, land cover changes from forests to shrublands, and grasslands. Preliminary data show soil methylmercury positively correlates with altitude and soil pH but negatively correlates with soil organic matter content, while total mercury exhibits the opposite trends. Chemically fractionating soil mercury reveals methylmercury/total mercury correlates with mercury associated with organic matter and metal oxides but negatively correlates with mercury in reducd form.

We hypothesize that methylmercury equilibrates in soil as a result of competition between microbial methylators and demethylators, whose abundance and activities are mainly limited by soil properties and organic inputs. This study aims to determine mercury and methylmercury distribution across altitudes and vegetation zones and decipher ecological and geological factors governing methylmercury levels in soil. Genomic, metabolic, and isotopic studies will unveil interactions between soil, roots, litter, methylators and demethylators on microscopic scale.

EN-18

Influences of microplastics on mercury cycling in forested ecosystems

Ming Yin Yau[a], Martin Tsz-Ki Tsui[a], Aijun Miao[b]

[a] *School of Life Sciences, Earth and Environmental Sciences Programme, The Chinese University of Hong Kong, Hong Kong SAR, China*

[b] *School of the Environment, Nanjing University, Nanjing, Jiangsu Province 210023, China*

E-mail: kenyau0422@link.cuhk.edu.hk

Owing to the high toxicity and long-distance atmospheric transport, mercury (Hg) is widely considered as a global environmental pollutant, which is capable of being converted into highly toxic methylmercury (MeHg) by certain anaerobic microbes. Once produced, MeHg can be extensively bioaccumulated and biomagnified within natural food webs, resulting in elevated MeHg levels in top predators which can pose a health threat to wildlife and human[1]. There have already been plenty of studies regarding MeHg production in the aquatic environment. Both Hg methylation and demethylation processes determine the net MeHg concentrations, and potentially control the elevated MeHg contamination in forested ecosystems.

Global concerns of microplastic (MP) pollution are rising. Recent studies have found extensive MP contamination not just in aquatic ecosystems, but also terrestrial forested environments, and thus the roles of MP on transforming contaminant such as Hg/MeHg should be better clarified in the environments because MP can accumulate and interact with MeHgCl[2]. Some recent studies have already revealed that the ability of MP to reduce the agricultural soils' bioavailable MeHg concentration by modifying the soils' dissolved organic matter composition and microbial communities[3,4]. Meanwhile, a recent study has revealed the high Hg methylation potential in the plastisphere, leading to increasing MeHg production[5].

Therefore, this study is aimed to investigate the relationship between the presence of MP and the rate of MeHg production in forested environments, an experimental study demonstrating the process of litter decomposition with MP addition has been designed. Different types of MPs including polystyrene (PS) and polyvinyl chloride (PVC) of different sizes, i.e. 10, 100 and 1000 μm have been incubated with fresh streamwater and leaf litter from local forest over several weeks. Each bottle was kept sealed to provide an anaerobic environment which can elevate the MeHg production by Hg methylating micro-organisms. In this presentation, findings of the MP-litter incubation experiments will be shown regarding the MeHg levels. The preliminary data has provided us with insights into the suppression of MeHg production due to the presence of MPs, which may offer extra surface area to promote establishment of biofilm communities, which we hypothesize can adsorb MeHg or even degrade MeHg.

References

[1] Tsui MTK, Liu S, Brasso RL, et al. *Environ. Sci. Technol.*, 2019, *53*, 5, 2434–2440;
[2] Zhu J, Zhang Y, Xu Y, et al. *Mar. Environ. Res.*, 2022, *176*, 105615;
[3] Allouzi MMA, Tang DYY, Chew KW, et al. *Sci. Total Environ.*, 2021, *788*, 147815;
[4] Yang X, Li Z, Ma C, et al. *J. Hazard. Mater.*, 2022, *423*, 126895;

EN-19

Mercury in Human Health: Effects on Sperm Dysfunction and Maternal-Fetal Blood Systems

Mengwei Yuan, [a] Martin Tsz-Ki Tsui, [a] Chi-Chiu Wang, [b] David Yiu-Leung Chan, [b] Tak-Yeung Leung, [b]

[a] School of Life Science, The Chinese University of Hong Kong, Hong Kong, China; [b] Department of Obstetrics and Gynaecology, The Chinese University of Hong Kong & Prince of Wales Hospital, Hong Kong, China

E-mail: mengweiyuan@link.cuhk.edu.hk

In recent decades, a global decline in birth rates has been observed, with notable instances such as Hong Kong recording fewer than 40,000 births last year for the first time in over half a century. Besides social and economic factors, an increasing concern has been raised about impact of environmental contaminant on the reproductive health in human.

As a prevalent environmental toxin, mercury (Hg) poses significant reproductive risks. Its detrimental effects encompass direct cellular injury, endocrine disruption, and neural modifications. Animal studies indicated that exposure to Hg can induce DNA rupture in sperm and leads to a decrement in sperm motility and their dysfunction[1]. However, the exact mechanisms by which various Hg forms influence sperm morphology and fertilizing capacity remain uncertain. Methylmercury (MeHg), an organic form of Hg, can readily cross placenta and blood-brain barrier[2], potentially harming the fetal brain during pregnancy, while the selective transport mechanisms at the placental barrier are still unidentified. Examining the impact of Hg on human reproductive health could offer valuable insights for medical interventions.

In our preliminary study, we analyzed 28 semen samples from patients undergoing semen analysis in Hong Kong. The average concentrations of total mercury (THg) and MeHg in the seminal plasma were 0.34±0.47 and 0.008±0.04 μg/L respectively. In sperm cells THg and MeHg were found to be 9.12±19.94 and 1.57±3.38 *p*g/10^6 cells, respectively. When grouped by median, it was observed that samples with higher THg had 12% and 11% higher sperm motility and progressive motility compared to the men with lower THg concentrations. Samples with higher THg displayed better normal morphology compared to those with lower THg concentration when grouped by the top 30% ($p < 0.03$). Additionally, we also test maternal blood from Hong Kong patients, the levels of THg and MeHg were 2.69 μg/L and 1.59 μg/L respectively. In cord blood, 4.59 μg/L of THg and 1.90 μg/L of MeHg were observed. The ratios of cord to maternal blood concentrations were 1.71 for THg and 1.19 for MeHg, our results are in agreement with earlier studies indicating active transport of Hg from mothers to fetuses[3], while the mechanism remains unclear. It's important to note while the current sample size is limited, and further investigation is required to validate our hypotheses.

References

[1] Henriques, Magda Carvalho et al. *Reproductive toxicology (Elmsford, N.Y.)* vol. 85 (2019): 93-103.

[2] Sakamoto M, Haraguchi K, Tatsuta N, et al. Environ Res. 2021;196:110896.

[3] Sakamoto M, Tatsuta N, Izumo K, et al. Toxics. 2018 Aug 3;6(3):45.

EN-20

Changes of dissolved organic matter from roots to soils and their relationships with microbial community in a grassland

Xiaohan Mo,[a, b] Hui Zeng,[a] Junjian Wang[b]

[a] *School of Urban Planning and Design, Peking University Shenzhen Graduate School, Peking University, Shenzhen 518055, China.* [b] *School of Environmental Science and Engineering, Southern University of Science and Technology, Shenzhen 518055, China.*

E-mail: moxh@stu.pku.edu.cn

Dissolved organic matter (DOM) derived from plant litter is widely recognized as a highly labile and biodegradable resource for heterotrophic microorganisms[1,2]. However, confusion remains regarding the extent to which litter-derived DOM is incorporated into soils. While some studies suggested that DOM leaching from litter made minor contributions to soil DOM due to rapid biodegradation[3], others considered that DOM flux from aboveground to belowground contributes to the formation of mineral-associated organic matter in soils[4,5]. Noted, most studies focused on aboveground litter or bulk soil. In grasslands, where aboveground detritus layer is usually absent, belowground biomass can account for over 80% of the total biomass, making carbon inputs from roots to soil the dominant pathway. Yet, there is limited knowledge regarding how DOM derived from root litter changes in the soil environment. Hereby, this study aims to focus specifically on DOM derived from roots and rhizosphere soils. We sampled roots and rhizosphere soils of eight herbaceous plants from a semiarid grassland in Inner Mongolia, China. We employed fluorescent spectroscopy and Fourier transform ion cyclotron resonance mass spectrometer to determine DOM composition and characteristics. Moreover, we employed metagenomics and ecological network approach to assess the DOM-microbe associations.

Our results showed that, while bulk dissolved organic carbon, chromophoric DOM, fluorescent DOM, lipids, and peptides exhibited a significant decrease from roots to rhizosphere soils, the contents of these DOM components derived from roots did not show significant linear relationships with those from rhizosphere soils. Instead, they showed significant correlations with the percentage variations of each DOM component. This suggests that the 'lost' root-derived DOM components did not contribute to the quantity of rhizosphere soil DOM; rather, they regulated changes in DOM within the rhizosphere. Furthermore, we observed lower DOM molecular diversity and a higher degree of DOM-microbe specialization in roots than in rhizosphere soils. This indicates that DOM derived from roots interacts with a limited range of microbial communities, whereas that derived from rhizosphere soils interacts with a broader range of microbial communities. Overall, our findings suggest that the quantities of DOM derived from roots and rhizosphere soils are not comparable and lack direct causal linkages, and these two sources of DOM in the rhizosphere environment interact with microbial communities in distinct ways.

References

[1] Qualls R, et al. *Environ. Sci. Technol.*, 2005, *39*, 1616–1622;
[2] Chow AT, Ulus Y, Huang G, et al. *J. Environ. Qual.*, 2022, *51*, 837–871;
[3] Yano Y, McDowell WH, Aber JD, *Soil Biol. Biochem.*, 2000, *32*, 1743–1751;
[4] Cotrufo MF, Soong J, Horton A, et al. *Nat. Geosci.*, 2015, *8*, 776–779;
[5] Bai YF, Cotrufo MF, *Science*, 2022, *377*, 603–608.

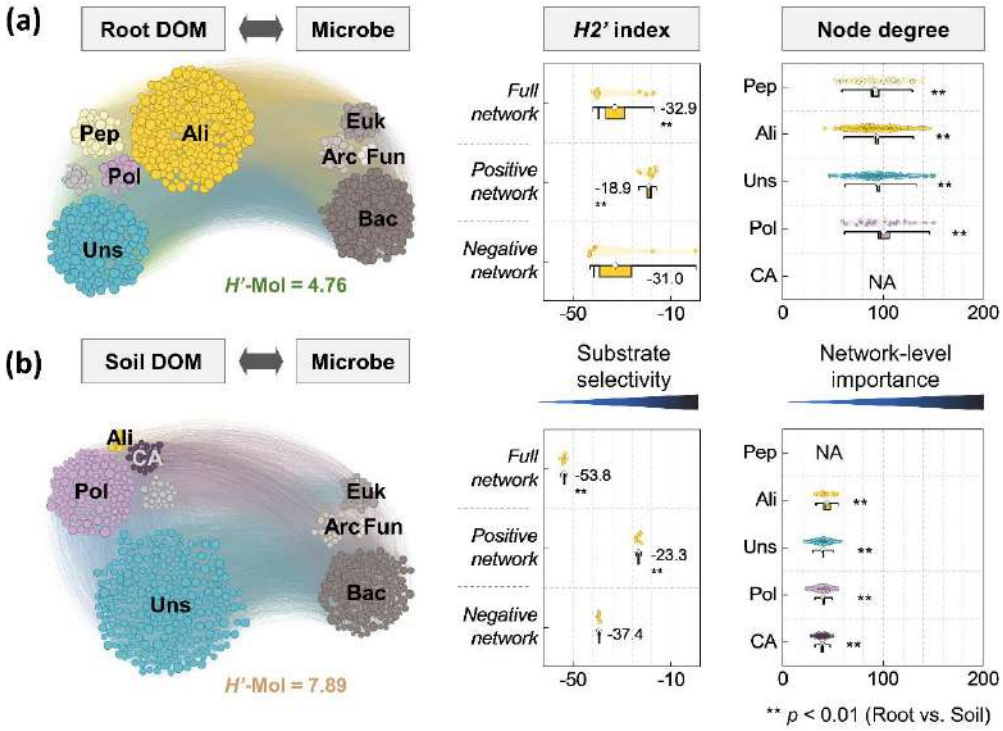

Figure 1. DOM-microbe network in (a) roots and (b) rhizosphere soils and their network properties. Pep: peptides; Ali: aliphatics; Uns: highly unsaturated compounds; Pol: polyphenolics; CA: condensed aromatics. *H'*-Mol: DOM molecular diversity calculated by R package *vegan*; *H2'*: the degree of DOM- microbe specialization calculated by R package *iDOM*; Node degree: one of the network topological properties calculated by R package *igraph.*

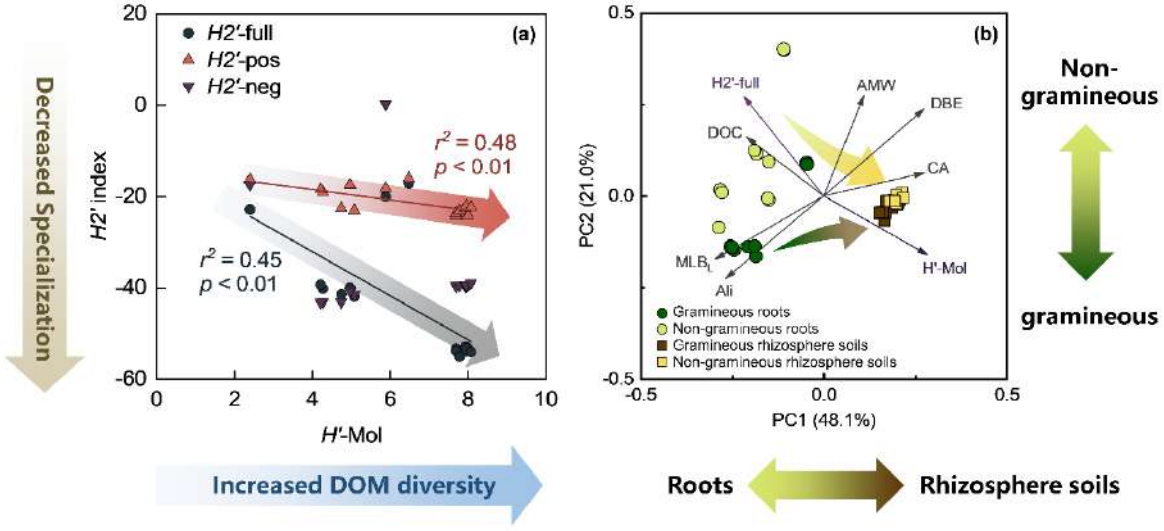

Figure 2. (a) Linear regression between DOM molecular diversity (*H'-Mol*) and the degree of DOM-microbe specialization (*H2'*); (b) principal component analysis, only indices with the absolute values of loadings in either one of the axes larger than 0.2 were shown in the biplot figure.

Empowers Your Dreams

Faculty of Science, The Chinese University of Hong Kong

Room G43, Charles Kuen Kao Building, Science Centre
The Chinese University of Hong Kong
Shatin, N.T., HKSAR
T: (+852) 3943 6327
Email: sfo@cuhk.edu.hk